

UNIVERSAL  
LIBRARY

**OU\_148712**

UNIVERSAL  
LIBRARY









# **ADVANCED MECHANICS OF MATERIALS**



# ADVANCED MECHANICS OF MATERIALS

---

by GLENN MURPHY, C.E., Ph.D.  
*Professor of Theoretical and Applied Mechanics  
Iowa State College*

---

FIRST EDITION

NEW YORK AND LONDON  
McGRAW-HILL BOOK COMPANY, INC.  
1946

ADVANCED MECHANICS OF MATERIALS

COPYRIGHT, 1946, BY THE  
MCGRAW-HILL BOOK COMPANY, INC.

PRINTED IN THE UNITED STATES OF AMERICA

*All rights reserved. This book, or  
parts thereof, may not be reproduced  
in any form without permission of  
the publishers.*

THE MAPLE PRESS COMPANY, YORK, PA.

## PREFACE

Among the several objectives of a second course in mechanics of materials the three that merit special attention are (a) to guide the student in a critical analysis of the knowledge obtained in the first course, (b) to extend the boundaries of his factual information, and (c) to assist him in developing that understanding of the field which will most effectively enable him to apply and to extend his knowledge in the future.

This book is directed toward these objectives. The derivations of the standard formulas of mechanics of materials are analyzed with particular reference to the limiting assumptions involved in their development. Exceptions to the assumptions are considered, to give the student some perspective concerning the importance of the various limitations and a means of evaluating stresses in members for which some of the assumptions are violated, thereby extending his fund of factual information. Throughout the text emphasis is placed upon the three fundamental tools of stress analysis—statics, geometry, and the properties of the material—for these tools are among the most powerful ones at the disposal of the analyst or designer. Their limitations are indicated, and attention is directed toward the more advanced and involved tools of the theory of elasticity and the theory of elastic stability. Because of the effectiveness of problems as teaching aids, an extensive list of problems of a wide range of difficulty is included.

In compiling the material contained in the text, the author has made extensive use of the works of Cross, Seely, Timoshenko, and a number of others who have published in this and allied fields. To them grateful acknowledgment is given. The footnote references are not intended to be inclusive but rather to be indicative of sources and to provide a starting place for the reader who wishes to pursue some topic further.

Photographs were made available through the courtesy of the Society for Experimental Stress Analysis and Messrs. C. P.

O'Haven and J. F. Harding, and through the courtesy of John Wiley & Sons, Inc., and Prof. M. M. Frocht.

The author is indebted to his colleagues and former students for valuable suggestions made during the use of preliminary editions of the material contained herein, and to Joyce Day Fisher, Frances Murphy, Betty Grimes, and Pat Harrington for their assistance in the preparation and proof reading of the manuscript.

GLENN MURPHY.

AMES, IOWA,  
*August, 1946.*

# CONTENTS

<b>Preface . . . . .</b>	<b>PAGE V</b>
--------------------------	-------------------

## *Chapter I*

<b>RELATIONSHIP OF MATERIALS TO DESIGN. . . . .</b>	<b>1</b>
Structural Design Problem. Significance of Stress. Significance of Failure. Types of Failure. Types of Loading. Criteria of Failure. Factor of Safety. Stiffness. Other Properties.	

## *Chapter II*

<b>STRESSES AND STRAINS AT A POINT . . . . .</b>	<b>19</b>
General Problem. STRESSES AT A POINT: General Relationships. Principal Stresses. Maximum Shearing Stresses. Graphical Evaluation of Principal Stresses. Evaluation of Other Stresses from Principal Stresses. Graphical Solution by the Mohr Circle. The Mohr-Land Circle. Tri-axial Stresses at a Point. Stress Trajectories and Isoclinics. STRAINS AT A POINT: General Considerations. Evaluation of Normal Strain. Principal Strains. Shearing Strains. Evaluation of Principal Strains. Strain-measuring Equipment. Graphical Evaluation of Principal Strains.	

## *Chapter III*

<b>STRESS-STRAIN RELATIONSHIPS . . . . .</b>	<b>59</b>
Need for Relationships. Relationships under Axial Stress. Relationships under Triaxial Stress. Shearing Strains. Principal Stresses from Principal Strains. Evaluation of Principal Stresses from Strains Measured on a Rosette.	

## *Chapter IV*

<b>THEORIES OF FAILURE . . . . .</b>	<b>70</b>
Purpose of Theories. Maximum-normal-stress Theory. Maximum-normal-strain Theory. Maximum-shearing-stress Theory. Internal-friction Theory and Mohr Theory. Maximum-strain-energy Theory. Hencky-von Mises Theory. Comparisons of Theories. Interaction Curves.	

## *Chapter V*

<b>AXIAL LOADING . . . . .</b>	<b>87</b>
Definition and Loading Requirements. Distribution of Stress in Axially Loaded Members. Axial Compressive Loads. Nonuniform Axially	

Loaded Members. Stress-concentration Factor. Values of Stress-concentration Factor. Stress Concentration under Repeated Loading. Reduction of Stress-concentration Factor. Significance of Stress-concentration Factor.

### *Chapter VI*

CYLINDERS, SPHERES, AND DISKS UNDER RADIALLY SYMMETRICAL LOADS. . . . . 112

Thin-walled Pressure Vessels. Thick-walled Pressure Vessels. Variation of Stress in a Thick-walled Cylinder. Increasing the Effectiveness of the Material. External Loading by a Shrink Fit. Plastic Prestressing. Displacements Due to a Uniform Temperature Change. Stresses in a Thick-walled Sphere. Shrink-fit Assemblies. Stresses in Rotating Disks of Constant Thickness. Specific Solutions. Stresses in Disks of Variable Thickness.

### *Chapter VII*

TORSION. . . . . 143

General Considerations. Solutions for Noncircular Members. Approximate Solution for a Rectangular Cross Section. Torsional Stresses in an Elliptical Shaft. The Saint Venant Theory. The Membrane Analogy. Application of the Membrane Analogy. Hollow Sections. Torsional Stresses in Thin-walled Open Sections. Torsional Stresses in Thin-walled Closed Sections. Multicelled Thin-walled Sections. Effect of End Restraint. Stress Concentration in Torsional Members. Plastic Yielding in Circular Shafts. The Sand-heap Analogy.

### *Chapter VIII*

FLEXURE. . . . . 192

STRESSES: General Considerations. Derivation of Elementary Formula for Flexural Stresses. Direction of the Neutral Axis. General Solution. Evaluation of Stresses. Direction of Deflection. Flexural Stresses beyond the Proportional Limit. Stress Concentration in Beams. Beams of Two Materials. Curved Beams. Winkler-Bach Theory for Curved Beams. Location of Neutral Axis in Curved Beams. Modification of Stress Formula. Stresses in Curved Beams by the Transformed Cross Section. DEFLECTIONS: General Considerations. Double Integration. Area Moments. Conjugate Beams. Castigliano's Theorem. Virtual Work. Comparison of Methods.

### *Chapter IX*

CROSS SHEAR . . . . . 236

General Considerations. Evaluation of Stresses Due to Cross Shear. Bending without Twisting. The Shear Center. Shear Center of a Chan-



nel. Shear Flow. Shearing Stresses and Shear Center in Thin-webbed Beams. Secondary Effects.

### Chapter X

## INTRODUCTION TO PHOTOELASTIC ANALYSIS . . 254

The Photoelastic Method. Analytical Representation of Light. Polarized Light. Refraction of Polarized Light. Application of Stress Analysis. Evaluation of Principal Stresses. Extension to Triaxial Stress Situations.

### Chapter XI

## COMPRESSIVE LOADS AND BUCKLING . . . . . 269

General Considerations. CONCENTRATED LOADS: Point Loads. Line Loads. Distributed Loads. Contact Stresses. GENERAL BUCKLING: Buckling of a Bar under Axial Compression. Beam Columns. Buckling of Strips by End Moments. Buckling of Sheets and Panels. Curved Panels in Shear. LOCALIZED BUCKLING: Thin-walled Cylinders in Axial Compression. Thin-walled Cylinders under Uniform External Pressure. Thin-walled Cylinders in Torsion. Thin-walled Cylinders in Bending. Noncircular Closed Sections in Axial Compression. Noncircular Open Sections in Axial Compression. TORSIONAL INSTABILITY OF COLUMNS: Torsional Failure. Critical Stress for Torsional Instability.

Answers to Problems . . . . . 297

Author Index. . . . . 299

Subject Index. . . . . 303



# ADVANCED MECHANICS OF MATERIALS

## CHAPTER I

### RELATIONSHIP OF MATERIALS TO DESIGN

**1. Structural Design Problem.**—The general problem of designing a structural member or a machine part to carry load without failure may be resolved into several component problems.

1. The determination of the general shape or form of the member.

2. The evaluation of the loads that the member will be expected to carry during its useful life.

3. The selection of a suitable material and determination of maximum allowable stresses.

4. The expression of the maximum stress (or other criterion of condition) in terms of the loads and dimensions.

5. The adjustment of the dimensions to meet strength, space, and fabrication requirements.

Definite, logical procedures based upon natural laws have been developed for the solution of each of the component problems, but in general the problems are interdependent, the complete solution of any one involving consideration of the others. Hence, the judgment and experience of the designer contribute greatly to the evolution of a satisfactory design.

The function of the member and its appearance, as well as its necessary thermal, electrical, chemical, and acoustical characteristics, must be considered during the designing operation. The availability of the material and cost of the final product are important considerations. The member must have sufficient hardness and stiffness to function properly. In addition, the strength of the member must be adequate but should not be excessive because excessive strength usually means wasted

material and unnecessary weight. The determination of the adequate strength involves a consideration of the relationships among load, stress, and dimensions, which topic is known as "mechanics of materials." Elementary mechanics of materials usually includes a study of axially loaded members, thin-walled pressure vessels, straight shafts and beams of constant cross section, and columns. However, many members and machine parts are subjected to biaxial or triaxial stress or are of more complex shape than those considered in a first course in mechanics of materials. The determination of the stresses in some of the more commonly used of these complex members is the function of advanced mechanics of materials.

As a step preliminary to the actual determination of stress-load relationships, it is desirable to consider the adequacy of stress, or any other pertinent characteristic of the material, in predicting mechanical failure and in establishing criteria of safety or satisfactory performance.

**2. Significance of Stress.**—The relationship between the load and the corresponding stresses in a structural member is considered to be important because design procedures in engineering have developed around the idea that the stress,<sup>1</sup> or intensity of loading, developed within a material is a highly significant quantity.<sup>2</sup> Values of so-called "allowable working stresses" are stipulated for various materials, often rather arbitrarily, by specification or by building code, and the designer manipulates the size, shape, and arrangement of the members to keep the maximum stress below, but usually as close as possible to, the allowable working stress.

Justification for the use of an allowable working stress as a basis of design is usually founded on the observation that, within limits, standard specimens of a given class of material will fail within a relatively small range of values of stress when tested under standard conditions. The allowable working stress is then obtained by dividing the stress at failure by an arbitrary number

<sup>1</sup> The term "stress" will be used throughout to denote intensity of loading measured as force per unit area (usually p.s.i.). In structural engineering practice the term "stress" is also used to denote the total axial force transmitted by a member.

<sup>2</sup> The use of stress as a criterion of condition probably dates back to early builders who observed that the load-carrying capacity of a tensile or short compressive member is proportional to its cross-sectional area.

ranging from slightly more than 1 to over 20, depending upon the material and conditions of usage. The arbitrary number, or factor of safety, is introduced to allow for (1) uncertainties of loading, (2) approximations in the stress calculations, and (3) uncertainties in the characteristics of the material as actually used.

Thus, the allowable working stress upon which the design is based depends upon

1. The relative hazards and uncertainties that are involved in the use of the given material in the given type of construction.
2. The magnitude of the stress that the material is capable of developing before failure.

The term "failure" may denote any one of several conditions.

**3. Significance of Failure.**—In the broad sense of the word a material is said to have failed when it no longer functions properly in its intended use. Improper functioning is relative—action that may be considered satisfactory in one use may be entirely unsatisfactory in another use. A close-fitting machine part may be entirely unsatisfactory if its length changes more than 0.001 in. under load, while a cable used in a hoist may elongate several inches without being considered unfit for use. In practically all structural members a value of limiting distortion for satisfactory service may be established. Then the member must be so designed that failure will not occur as a result of either excessive distortion of the member or cracking or rupture of the material selected. It is evident, therefore, that the strain developed within the material is highly significant in predicting failure of the member.

**4. Types of Failure.**—Qualitatively there are four types of failure, each manifested by a specific type of excessive deformation. They are

1. Excessive elastic deformation.
2. Slip.
3. Fracture.
4. Creep.

1. *Excessive elastic deformation* involves no change in the properties of the material and, consequently, no damage to the material. The failure is fundamentally one of design. There may be ample material to carry the load without collapse but insufficient material to prevent objectionable displacements. For

example, a light rope bridge across a deep canyon may be amply strong to carry the required loads, but it may be quite unpleasant to use, especially in a high wind. Another example is the "knee-action" spring which, when first installed on one of the popular makes of automobiles, was so flexible that it was impossible to lift the front wheels with an ordinary jack.

When a member fails owing to excessive elastic deformation, the design may be improved by using a different material, by using more material, or by reportioning the member to use the material more effectively in increasing the rigidity of the member.

2. *Slip* denotes failure by inelastic, or plastic, action. Most materials have the characteristic of returning to their original dimensions after a cycle of loading and unloading if the strain developed during loading is relatively small. The material is then said to be elastic. However, if a sufficient amount of strain is developed during loading, the material will not resume its original dimensions upon unloading, but will exhibit a more or less permanent change in dimensions, which is an indication of inelastic, or plastic, action. The change in dimensions may be sufficient, particularly in the case of close-fitting machine parts, to render the part unfit for further use, even though the part has not "broken" or separated into two pieces.

In metals, at least, the permanent strain is the cumulative result of a large number of displacements on parallel planes of weakness within individual crystals. The atomic readjustments effected by the inelastic action accompany even a very small load on the member. Practically, inelastic action is not considered to have begun until an appreciable portion of the member becomes plastic, or until sufficient inelastic deformation has occurred to render the member unfit for further use.

3. *Fracture* denotes complete separation of the material into two or more portions, thereby rendering the original part unfit for further use. Materials requiring relatively large axial deformations (0.20 or more) to cause fracture are often called "ductile materials"; those which fracture at a comparatively low axial strain (0.0001 to 0.0040) are called "brittle materials."<sup>1</sup>

4. *Creep* denotes a continuing deformation over a period of time in a material subjected to a constant load. Creep is dis-

<sup>1</sup> A ductile material is relatively strong in tension compared with shear, while a brittle material is comparatively weak in tension.

tinguished from slip in that the deformation accompanying the latter does not continue for more than a few minutes under constant load. The tendency of a material to creep usually increases with an increase in pressure (stress) or temperature. Structural steel at ordinary temperature does not creep at stresses below about 50,000 or 60,000 p.s.i. but will creep at low stresses at temperatures near the melting point. Lead creeps at room tempera-

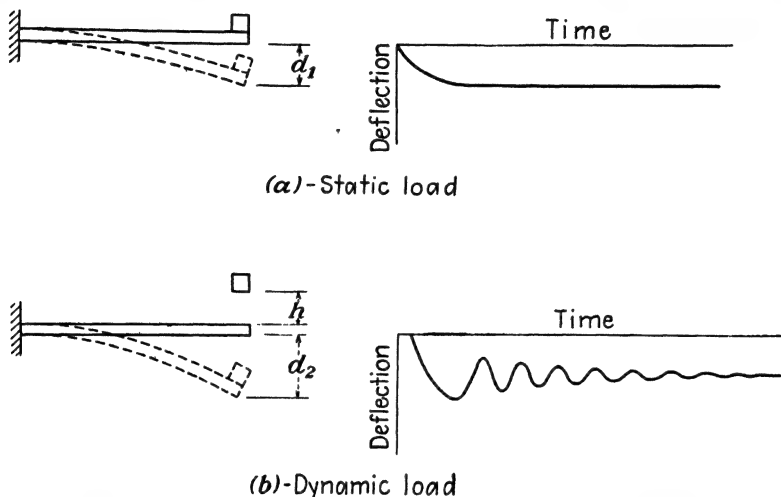


FIG. 1.—Static and dynamic loads.

ture under very low stresses. The mechanical behavior of a material showing creep may be likened to the slow flow of a viscous liquid.

**5. Types of Loading.**—Investigations have shown consistently that the magnitude of the load required to cause failure of a member of specified dimensions and a specified material depends upon the manner and frequency of the application of the load. A member that will safely carry a given load if it is applied slowly may fail if the same magnitude of load is applied suddenly or applied a large number of times. There are three principal types of loading.

1. *Steady or static loads* are those which remain on the member without fluctuation or which are applied sufficiently slowly that the stresses and deflections are gradually built up to their maximum values. For example, a load applied slowly at the end of the cantilever beam of Fig. 1a will cause a deflection  $d_1$  as

indicated, which remains constant as long as the load remains on the beam, unless slip, creep, or fracture occurs. Dead loads due to the weight of the structure are static loads.

2. *Impact or dynamic loads* are those which are applied with sufficient rapidity to cause a fluctuating stress and deflection in the member. If they are not sufficiently great to produce fracture immediately, they usually induce vibration in the member, resulting in stresses much greater than those produced by a load of the same magnitude slowly applied. For example, a load dropped on the end of a cantilever beam, as indicated in Fig. 1b, constitutes an impact load. Even though the load has the same weight as that applied in Fig. 1a, it will cause the beam to deflect a maximum distance  $d_2$ , which is greater than  $d_1$ . The increased deflection, which is accompanied by an increased strain, may be sufficiently great to cause failure of the beam. If not, vibration will be set up in the beam, and continued vibration may result in failure of the material.

A static load is usually evaluated in pounds, but a dynamic load, such as that due to a weight dropped on a beam, may be evaluated in either of two ways.

- a. The dynamic load may be evaluated in terms of the amount of energy (inch-pounds or foot-pounds) that the member must absorb in stopping the load or bringing it to equilibrium. To determine whether or not the dynamic load will cause failure the maximum concentration of energy absorbed by the member is compared with the maximum amount of energy that a unit volume of the material will absorb without failure.
- b. The dynamic load may be evaluated in terms of an *equivalent static load* or static load that would have the same effect upon the member. The ratio of the equivalent static load to the magnitude of the dynamic load (usually the weight of the dynamic load) is known as the "load factor." The load factor may be determined algebraically or experimentally.

3. *Repeated loads* are loads that are applied a large number of times. Recoil springs, connecting rods, and crankshafts are examples of members subjected to repeated loading. A repeated load may be applied with or without impact. This type of loading must be considered separately from static loading because a



load that would not even cause inelastic action if applied once may result in fracture if applied many times. A single application of load will invariably cause some localized inelastic action even though the member as a whole is considered to be acting elastically. If the member is metal, the embrittling effect of the inelastic action, or cold working, makes the material more sensitive to stress concentration, and further application of the load may cause a crack to form. Continued application of the load extends the crack until it finally progresses entirely across the member. Failure by a progressive cracking is also characteristic of nonmetallic materials subjected to repeated loading even though the strain hardening is not a factor.

**6. Criteria of Failure.**—Although failure is definitely a phenomenon of excessive strain rather than stress, it is customary to use stresses as indexes of the nearness of a material or a member to failure. While the use of stresses as indexes is traditional, it offers no fundamental advantage over the use of strains since the interrelationships among load, stress, and strain must all be taken into account in design.

TABLE I.—PROPERTIES MEASURING RESISTANCE TO FAILURE\*

Type of failure	Type of loading		
	Steady	Impact	Repeated
Fracture	Ultimate strength, $S_u$ , p.s.i. or percentage elongation, $\epsilon_u$	Modulus of toughness, $U_u$ , in.-lb. per cu. in. $U_u = f(S_u, \epsilon_u)$	Endurance limit, $S_e$ , p.s.i.
Slip	Elastic strength, $S_p$ , p.s.i. or elasticity, $\epsilon_p$	Modulus of resilience, $U_p$ , in.-lb. per cu. in. $U_p = \frac{1}{2}S_p\epsilon_p$	
Creep	Creep limit, $S_{cr}$ , p.s.i.		

\* Adapted from "Properties of Engineering Materials," International Textbook Company, Scranton, Pa., 1939.

The criteria commonly used to indicate the resistance of a material to failure under the various combinations of loadings and

types of failure are indicated in Table I. The criteria are stresses, strains, or combinations of stresses and strains.

The properties as defined and evaluated from tensile or compressive test data of a specimen of the material are as follows:

1. *Ultimate strength* is the maximum load that the specimen is capable of developing under axial loading divided by the original cross-sectional area. It is the ordinate of the highest point on a stress-strain diagram for the material. It does not usually represent the maximum unit stress developed within the material since the stress is, in general, not uniformly distributed and since the area resisting the maximum load is less than the original area. The ultimate tensile strength of both ductile and brittle materials is usually regarded as being significant, while the ultimate compressive strength of a ductile material is largely dependent upon the amount of plastic deformation that may occur. Shearing stresses are not uniformly distributed across the cross section of a test specimen subjected to cross shear, so shearing tests are used only in a few special cases such as in evaluating the shearing strength of timber parallel to the grain. The shearing resistance of a metal is most accurately evaluated from a torsional test of a thin-walled specimen of the material.

The maximum load-carrying capacity of a material in torsion or bending may be evaluated by the modulus of rupture, which is defined as the maximum stress computed using the torsion ( $S = Tc/J$ ) or beam ( $S = Mc/I$ ) formula. The modulus of rupture is not an actual stress since the formulas are not valid above the proportional limit, but it gives a satisfactory basis for the comparison of different materials provided that the test specimens of the materials are geometrically similar.

2. *Percentage elongation* is the unit strain at fracture under axial tensile loading. Since the magnitude of the percentage elongation is dependent upon the gage length, standard lengths of 2 or 8 in. are used.

The percentage elongation is commonly used as an index of the amount of plastic strain to which the material may be subjected without failure and as an index of the capacity of the material for being bent, twisted, or otherwise deformed without failure during fabrication.

3. *Modulus of toughness* is the maximum amount of energy load per unit volume that the material will withstand. It may

be evaluated approximately as the area under the entire stress-strain diagram.

4. *Endurance limit* is the maximum stress to which a material may be subjected an infinite (or  $500 \times 10^6$  for some materials) number of times without failure. It cannot be determined from the stress-strain diagram. The endurance limit is usually evaluated for completely reversed stress, *i.e.*, equal maximum stresses in tension and compression. However, machine parts may be subjected to fluctuating stresses that do not vary from compression to an equal value in tension. Such stresses are usually considered to be the resultant of an average stress  $S_a$  and a completely reversed stress  $S_r$  as indicated in Fig. 2a. The

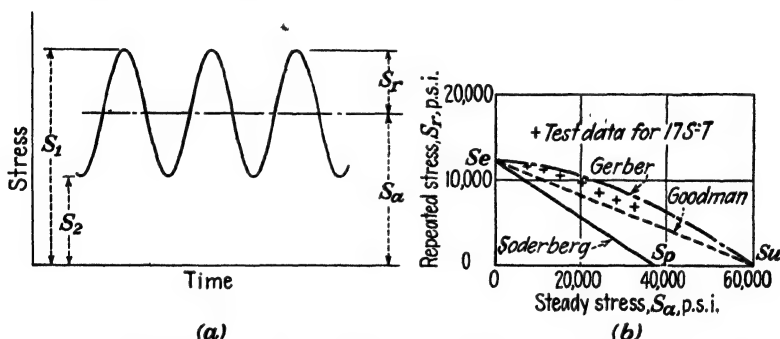


FIG. 2.—Analysis of fluctuating stresses. (Test data for aluminum alloy 17S-T from "Structural Aluminum Handbook," Aluminum Company of America, 1940.)

magnitude of the maximum  $S_r$  that may be superimposed on a given  $S_a$  must be determined by test. The test results may be plotted in the form indicated in Fig. 2b, which shows results for the aluminum alloy 17S-T. Values of  $S_r$  are plotted as ordinates against values of  $S_a$  as abscissae. The intersection of the curve with the vertical axis denotes the endurance limit for completely reversed stress, in this case axial tension and compression. A similar diagram could be drawn for fluctuating stresses in flexure or in torsion.

Points near the vertical axis (for small values of  $S_a$ ) correspond to failure by progressive fracture, or "fatigue," while points to the right may correspond to failure by slip or by fracture. Two limiting curves may be developed for a material: one, extending from the endurance limit on the vertical axis to the elastic strength on the horizontal axis and corresponding to failure by

fatigue or by slip; the other, extending from the endurance limit to the ultimate strength and corresponding to failure by fatigue or by fracture.

Several theories have been evolved in an attempt to obtain a direct relationship between the limiting values of  $S_a$  and  $S_r$  and standard properties of the material such as the endurance limit  $S_e$ , the ultimate tensile strength  $S_u$ , and the elastic strength in tension  $S_p$ . Among these, the three to which most frequent reference is made are the generalized Goodman theory expressed as<sup>1</sup>

$$\frac{S_r}{S_e} = 1 - \frac{S_a}{S_u}$$

the Gerber theory

$$\frac{S_r}{S_e} = 1 - \left( \frac{S_a}{S_u} \right)^2$$

and the straight-line theory, expressed by the Soderberg<sup>2</sup> formula

$$\frac{S_r}{S_e} = 1 - \frac{S_a}{S_p}$$

The three formulas are plotted to the same axes in Fig. 2*b* for comparison with the test data. It is evident that for this material the Goodman theory is the best. The Gerber theory gives results on the unsafe side, and the Soderberg theory is ultraconservative. Test results indicate that, in general, the modified Goodman theory is satisfactory for ductile materials in tension. For brittle materials in tension or torsion, the Soderberg formula gives results in best agreement with test data. Ductile materials in torsion and either ductile or brittle metals in which the steady stress is compression may have a repeated stress equal to the endurance limit  $S_e$  superimposed upon the steady stress without damage so long as the steady stress is below the elastic strength. All evidence indicates that if accurate data for a material are lacking the Soderberg theory may be expected to yield safe results.

5. *Elastic strength* may be evaluated from the stress-strain diagram as

<sup>1</sup> SMITH, JAMES O., The Effect of Range of Stress on the Fatigue Strength of Metals, *Univ. Illinois Eng. Expt. Sta. Bull.* 334, 1942.

<sup>2</sup> SODERBERG, C. R., Working Stresses, *Trans. Am. Soc. Mech. Engrs.*, Vol. 55, p. 131, 1933.

- a. **Proportional limit**—the unit stress at the upper end of the straight-line portion of the stress-strain diagram.
  - b. **Yield strength**—the maximum unit stress to which a material may be subjected without having more than a specified (often 0.002) residual strain upon the removal of the load.
  - c. **Yield point**—the unit stress at which there is an increase in strain with no increase in stress. Mild steel is the only important engineering material that has a yield point.
  - d. **Johnson's apparent elastic limit, proof stress, and several others of less importance.**
6. **Elasticity** is the unit strain at the elastic limit or at the proportional limit and measures the limiting strain that may be developed without an appreciable amount of slip occurring.
7. **Modulus of resilience** is the maximum amount of energy load per unit volume that the material will absorb without inelastic action. It may be evaluated as the area under the straight-line portion of the stress-strain diagram.
8. **Creep limit** is the maximum unit stress that the material will withstand at a specified temperature without the rate of creep exceeding a specified amount. A maximum rate of 0.01 in 100,000 hr. is sometimes specified for machine parts. The creep limit cannot be evaluated from the stress-strain diagram.
7. **Factor of Safety.**—The factor of safety of a structural element is defined as the strength of a material divided by the maximum computed unit stress in the element. When energy loads are involved, the factor of safety may be expressed as the strength of the material divided by the maximum concentration of energy per unit volume. The term "factor of safety" is a misnomer, since in no sense does it mean that the structural element could safely carry that many times the given load without failure. In most cases (1) the loadings used in computing the stresses are only estimated, (2) the stress calculations involve assumptions and approximations that are not necessarily valid, and (3) the properties of the material actually used in the structural element are seldom known but are assumed to be equal to those in a similar piece of the material that has been tested. For those reasons, the term "factor of safety" really denotes a "factor of ignorance."
- In aeronautical engineering practice the "limit loads" or maximum loads that are anticipated during maneuvers are

multiplied by the factor of safety (usually 1.5) to obtain the "design loads." The criterion used for evaluating the "safety" of the member is the so-called "margin of safety," defined as

$$\text{M.S.} = \frac{\text{ultimate strength of material}}{\text{maximum stress due to design load}} - 1$$

**8. Stiffness.**—Since the criterion of proper functioning of a structural element is primarily geometrical—*i.e.*, related to the deformation or distortion of the piece in use—it is necessary to define measures of stiffness to assist in comparing the behavior of different materials and in predicting the change in dimensions of a structural element under given conditions. While several such measures have been defined, three are needed most frequently.

1. *Modulus of Elasticity.*—The modulus of elasticity, or Young's modulus, is defined as the ratio of the change in axial stress to the corresponding change in axial strain for axial loading below the proportional limit. It is therefore equal to the slope of the stress-strain diagram.

Similarly, the modulus of elasticity in shear (modulus of rigidity) is equal to the ratio of the change in the unit shearing stress to the corresponding change in the unit shearing strain under a condition of pure shear below the proportional limit.

2. *Poisson's Ratio.*—Poisson's ratio is the ratio of the lateral strain to the axial strain under a condition of axial loading below the proportional limit. It serves as a measure of lateral stiffness.

3. *Coefficient of Thermal Expansion.*—The coefficient of thermal expansion is the unit strain produced by a 1° temperature change. It is an inverse measure of resistance to deformation under thermal loading.

**9. Other Properties.**—The importance of the strength properties in relationship to design may easily be overemphasized. Obviously, the member or machine part must have sufficient strength to prevent failure during its life, but the primary objective of design is to proportion a member of suitable material that can be fabricated and assembled readily and that will do the job for which it is intended, all at the lowest possible cost. In other words, stress analysis is only a tool, but a very important tool, which the engineer utilizes in the process of design.

Some of the more important properties with which the designer may be concerned are listed in Table III. Their significance is

self-evident. Numerical values are given for a few of them for some representative materials, but many of the important qualities such as workability, appearance, and resistance to

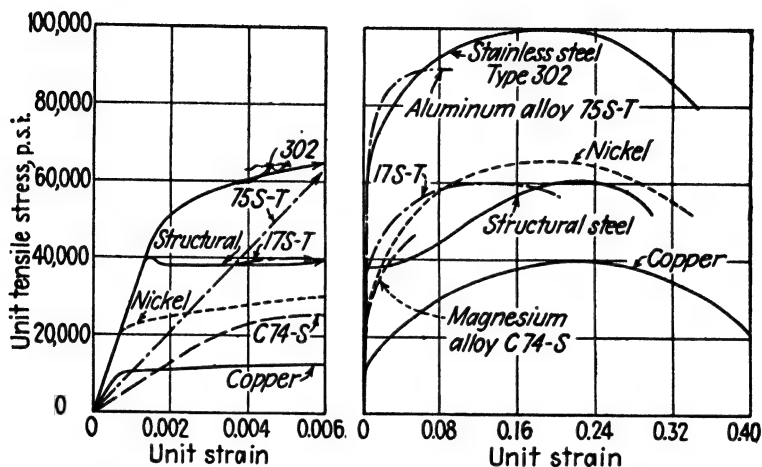


FIG. 3.—Typical stress-strain diagrams for metals in tension.

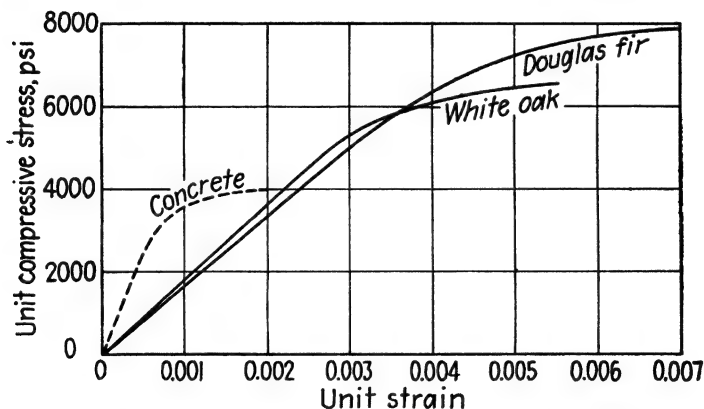


FIG. 4.—Typical stress-strain diagrams for materials loaded in compression—medium strength concrete; small clear timber specimens.

corrosion have no numerical measure, and, in addition, many, such as chemical characteristics, are dependent upon environmental factors.

Values of strength properties are given in Table II and may be evaluated from Figs. 3 and 4 for a few of the more common materials.

TABLE II.—AVERAGE VALUES OF PROPERTIES OF A FEW MATERIALS

Material	Tensile strength, p.s.i.		Shearing strength, p.s.i.		Endur- ance limit, p.s.i.	Creep limit, p.s.i.*	Percent- age elon- gation in 2 in.	Modulus of elas- ticity p.s.i. $\times 10^6$	Modulus of rigidity, p.s.i. $\times 10^6$	Poisson's ratio	Specific weight, p.c.f.
	Elastic	Ultimate	Elastic	Ultimate							
Wrought iron.....	30,000	47,000	20,000	60,000	25,000	2,200(B)	30	29.0	11.0	0.30	490
Structural steel.....	40,000	60,000	20,000	60,000	28,000	.....	34	29.0	11.0	0.30	490
S.A.E. 2315, annealed.....	58,000	80,000	.....	.....	.....	.....	30	29.0	11.0	0.30	490
S.A.E. 2315, hardened.....	132,000	160,000	.....	.....	.....	.....	14	29.0	11.0	0.30	490
S.A.E. X4130, annealed.....	55,000	90,000	40,000	55,000	45,000	.....	30	29.0	11.0	0.30	490
S.A.E. X4130, drawn.....	180,000	205,000	.....	.....	110,000	.....	13	29.0	11.0	0.30	490
Stainless steel†.....	60,000	100,000	.....	.....	47,000	11,000(B)	60	29.0	11.9	0.30	490
Gray cast iron No. 20.....	.....	20,000	.....	.....	.....	.....	..	15.0	.....	.....	450
Gray cast iron No. 60.....	.....	60,000	.....	.....	.....	.....	..	15.0	.....	.....	450
Aluminum, annealed.....	6,000	16,000	4,000	9,600	5,000	9,000(C)	23	10.3	3.8	0.33	169
Al alloy 17S-T.....	37,000	60,000	22,000	36,000	15,000	.....	22	10.5	3.9	0.33	175
Al alloy 24S-T.....	44,000	60,000	24,000	37,000	18,000	.....	12	10.5	3.9	0.33	173
Al alloy 75S-T.....	80,000	88,000	.....	47,000	22,500	.....	10	10.4	.....	0.33	.....
Copper, annealed.....	10,000	40,000	.....	.....	10,000	.....	40	16.5	6.1	0.33	557
Brass, 30 per cent Zn, soft.....	15,000	45,000	.....	.....	16,500	.....	50	15.0	5.6	0.33	532
Brass, 30 per cent Zn, hard.....	65,000	86,000	.....	.....	20,500	12,700(A)	4	15.0	5.6	0.33	532
Mg alloy, 26S-C†.....	11,000	27,000	.....	.....	11,000	.....	6	6.5	2.4	0.34	113
Mg alloy, C74S‡.....	27,000	42,000	.....	.....	17,000	.....	18	30.0	2.4	0.34	112
Nickel, annealed.....	20,000	70,000	.....	.....	33,000	38,000(C)	50	30.0	11.0	0.31	555
Monel metal, forged  .....	125,000	165,000	57,000	98,000	58,000	8,500(B)	20	26.0	9.5	0.32	528
Zn die-casting alloy¶.....	.....	34,400	.....	31,000	.....	.....	8	4.0	.....	0.20	415
Concrete.....	.....	250	.....	.....	.....	.....	..	.....	.....	.....	150
White oak.....	.....	.....	.....	2,000	.....	.....	..	.....	.....	.....	48
Douglas fir.....	.....	.....	.....	1,130	.....	.....	..	.....	.....	.....	31

\* (A) 1 per cent in 100,000 hr. at 400°F. (B) 1 per cent in 100,000 hr. at 1,000°F. (C) 1 per cent in 10 yr at 360°C.

† Stainless steel type 302. 18 per cent Cr, 8 per cent Ni, 0.1 per cent C.

‡ Mg alloy, 26S-C, Dowmetal H. Cast. 6.0 per cent Al, 3.0 per cent Zn, 0.2 per cent Mn, 0.5 per cent Si, remainder Mg.

§ Mg alloy, C74S, Dowmetal X. Extruded. 3.0 per cent Al, 3.0 per cent Zn, 0.2 per cent Mn, 0.5 per cent Si, remainder Mg.

|| K Monel. Age hardened. 66 per cent Ni, 29 per cent Cu, 2.75 per cent Al, 0.9 per cent Fe, 0.85 per cent Mn, 0.5 per cent Si, 0.15 per cent C.

¶ Die-casting alloy, Zamak-3. A.S.T.M. 23, S.A.E. 903. 3.5 to 4.3 per cent Al, 0.10 max per cent Cu, 0.10 max per cent Fe, remainder Zn



TABLE III.—PROPERTIES OTHER THAN STRENGTH

Name of property	Structural steel, (S.A.E. 1015)	Cast iron	S.A.E. X4130 steel, drawn 700°F.	Aluminum alloy, 24S-T	Brass, (30% Zn) hard	Magnesium alloy, C74-S	Copper, soft
<b>Stiffness:</b>							
Modulus of elasticity (p.s.i. $\times 10^6$ ).....	29.0	15.0	29.0	10.5	15.0	6.5	16.5
Modulus of rigidity (p.s.i. $\times 10^6$ ).....	11.0	.....	11.0	3.9	5.6	2.4	6.1
Poisson's ratio.....	0.30	.....	0.30	0.33	0.33	0.34	0.33
<b>Weight:</b>							
Specific weight, p.c.f.	490	450	490	173	532	112	557
Specific gravity.....	7.85	7.21	7.85	2.77	8.53	1.79	8.93
<b>Workability:</b>							
Ductility, % elong. 2 in.....	35	.....	13	22	4	17	40
Malleability.....							
Plasticity.....							
Machinability.....	.....	.....	.....	.....	Fair	.....	Fair
Weldability.....	.....	.....	.....	.....	Good		
<b>Hardness:</b>							
Percentage wear....							
Rockwell no. ....	-5 (C)	.....	.....	.....	87 (B)	.....	40 (F)
Brinell no. (kg. per sq. mm.).....	128	.....	429	.....	.....	50	
<b>Thermal characteristics:</b>							
Specific heat (B.t.u. per lb. per degree F.).....	.....	.....	.....	.....	0.089	0.249	0.0942
Thermal conductivity (B.t.u. per hr. per ft. per sq. ft. per deg. F.).....	26	26	26	68	70	48	227
Coefficient of linear expansion (per degree F. $\times 10^{-6}$ )	6.50	5.50	.....	12.2	11.1	16.0	9.8
<b>Electrical characteristics:</b>							
Conductivity (% I.A.C.S.).....	.....	.....	.....	30.0	27.6	14.4	101.6
<b>Acoustical characteristics:</b>							
Coefficient of absorption.....							
Coefficient of reflection.....							
<b>Vibration characteristics:</b>							
Damping capacity..	.....	Good					
<b>Chemical characteristics:</b>							
Electrolytic action..							
Resistance to corrosion.....							

## PROBLEMS

1. Name the factors that should be taken into consideration in selecting a suitable shape of cross section for the connecting rod of an automobile engine.

2. How are the magnitudes and distributions of loading established for each of the following units?

- a. Floor beam in a building.
- b. Rudder of an airplane.
- c. Locomotive draw bar.

3. A weight  $W$  dropping through a free distance  $h$  is snubbed by a steel rod of length  $L$  and diameter  $d$ . Determine the equivalent static load for the rod, assuming that it absorbs one-half of the total energy.

4. Determine the equivalent static load for a weight dropped on the end of a cantilever beam.

5. Determine the load factor for the wings of an airplane coming out of a dive at 700 m.p.h. on a 2,000-ft. radius.

6. Tabulate values of the ultimate strength, proportional limit, yield strength for an offset of 0.002, and modulus of elasticity for the materials indicated on the stress-strain diagrams of Fig. 3.

7. An annealed aluminum rod with an effective length of 18 in. is to carry a slowly applied axial tensile load of 8,000 lb. Determine the minimum required cross-sectional area of the rod if it is not to fail by

- a. Slip at ordinary temperature.
- b. Fracture at ordinary temperature.
- c. Creep at 360°C.

8. Compare the resistance of annealed aluminum and duralumin (17S-T) to failure by

- a. Slip under static load.
- b. Fracture under impact load.

9. Compare the impact resistance with respect to failure (a) by slip, and (b) by fracture of Douglas fir in compression with that of structural steel in tension.

10. A Douglas fir beam of constant cross section is to support a uniform load of 480 lb. per ft. on a 12-ft. span. The fiber stress is not to exceed 800 p.s.i., and the deflection is not to exceed  $\frac{1}{360}$  of the span. Determine a suitable cross section for the beam.

11. A Douglas fir beam is to carry a concentrated load of 1,000 lb. at the center of a 12-ft. span. The depth of the beam is to be one-half of its width. Determine the minimum depth and width for each of the following conditions:

- a. The maximum deflection is not to exceed  $\frac{1}{2}$  in.
- b. The maximum flexural stress is not to exceed the proportional limit.
- c. The maximum shearing stress is not to exceed 400 p.s.i.

- d. The maximum flexural stress is not to exceed one-half of the modulus of rupture.

12. A machine part is to carry an axial load that fluctuates from 10,000 lb. tension to 4,000 lb. compression 120 times per minute. If the part is to be made of aluminum alloy 17S-T, determine the minimum permissible cross-sectional area.

13. A stainless-steel member is to carry a load that fluctuates from 20,000 lb. tension to 4,000 lb. tension. Specify a working stress for the member if other factors indicate a factor of safety of 2.00 to be desirable.

14. A member made of magnesium alloy C74S carries a load that produces a tensile stress of 2,000 p.s.i. What maximum magnitude of reversed stress may be superimposed on the steady stress without causing failure?

15. The following maximum allowable stresses are stipulated by the Wisconsin State Building Code (1934). Determine the approximate nominal factor of safety with respect to failure by (a) slip, (b) fracture.

- a. Structural steel in tension—18,000 p.s.i.
- b. Douglas fir in compression parallel to the grain—800 p.s.i.
- c. Oak in compression parallel to the grain—1,000 p.s.i.

16. A structural-steel tie rod with an effective length of 14 ft. is to carry a total static load of 12,000 lb.

- a. Determine the required area if the rod is to have a factor of safety of 2.5 with respect to failure by slip.
- b. If the minimum permissible stock diameter (multiples of  $\frac{1}{16}$  in.) is used, how much will the rod elongate when loaded?

17. Solve Probs. 16a and 16b if the rod is to withstand an impact load of 12,000 in.-lb.

18. The allowable working stress for a certain structural-steel member is 18,000 p.s.i. Determine the nominal minimum factor of safety with respect to failure by

- a. Slip under a steady load.
- b. Fracture under a steady load.
- c. Slip under an impact load.
- d. Fracture under an impact load.

19. A round structural-steel rod, for which the allowable working stress is 18,000 p.s.i., is to carry a static axial tensile load of 10,000 lb. If the diameters of available rods are in multiples of  $\frac{1}{8}$  in. determine

- a. The most economical size of rod.
- b. The nominal factor of safety with respect to failure by slip.
- c. The factor of safety with respect to failure by slip.
- d. If the allowable working stress were 17,000 p.s.i., what would the factor of safety become?
- e. If the allowable working stress were 19,000 p.s.i., what would the factor of safety become?

20. A  $\frac{3}{8}$ - by  $1\frac{1}{2}$ -in. structural-steel strap is to be subjected to a static axial tensile load with a factor of safety of 2.00. Determine the magnitude of the maximum permissible load if an 18-in. length of the strap is not to elongate more than

- a. 0.010 in.
- b. 0.020 in.
- c. 0.030 in.

21. The limit load for a certain  $\frac{3}{16}$ -in.-diameter-24S-T rivet is 600 lb. Determine the margin of safety.

22. If the minimum permissible margin of safety is 0.05 determine the maximum permissible limit load which an 84-in. length of 24S-T tubing will carry

- a. In axial tension.
- b. In axial compression.

The outside diameter is 1.000 in., and the wall thickness is 0.035 in.

23. A structural-steel tension member with an effective length of 15 in. was designed to carry a static load with a factor of safety of 2.00 with respect to failure by slip. After installation it was found that vibration caused a repeated change of  $\pm 0.0075$  in. in length (in addition to the stretch due to the static load) of the member. Determine the actual factor of safety with respect to failure by slip.

24. A duralumin rod with an effective length of 10 in. is used as a machine part to support a slowly applied axial tensile load of 4,000 lb.

- a. Determine the minimum required diameter of the rod if it is to have a factor of safety of 2.50 with respect to failure by slip.
- b. Assume that the rod has the diameter determined in *a* and that subsequent wear of the machine causes the 4,000-lb. load to drop through a distance of 0.01 in. as it is applied to the rod. What will the factor of safety be?

25. A steel rod 12 in. long and 1 in. in diameter is turned down to a  $\frac{1}{2}$ -in. diameter for one-half of its length. Compare its resistance to failure by slip under axial load with that of a  $\frac{1}{2}$ -in.-diameter-rod 12 in. long if the load is

- a. Static.
- b. Dynamic.
- c. Repeated.

Neglect stress concentration in the rod.

## CHAPTER II

### STRESSES AND STRAINS AT A POINT

**10. General Problem.**—As has been indicated, the maximum load that a structural element of given dimensions can carry without failure is limited by the magnitude of the strain that is developed in the material. Traditionally, the limiting unit

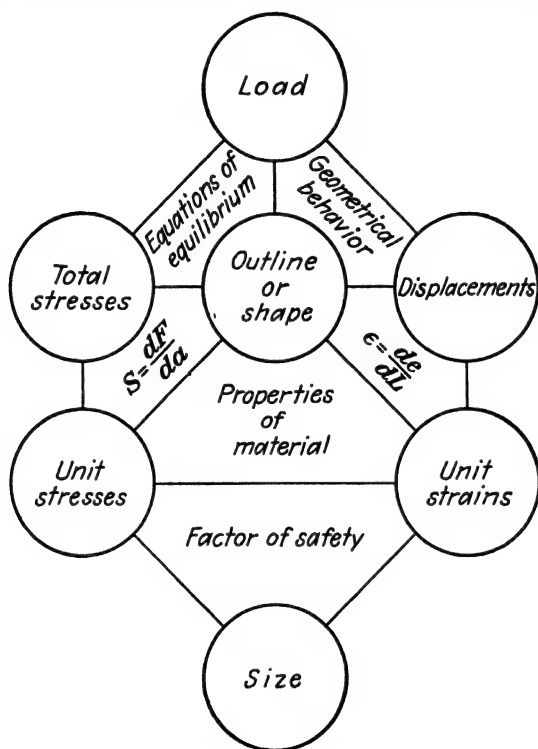


FIG. 5.—Interrelationships among some factors involved in design.

strain is expressed in terms of the corresponding limiting unit stress because the stress may be evaluated in terms of the load by means of the equations of equilibrium (or the equations of motion if the member is experiencing an acceleration) after the

stress distribution is known. However, the distribution of stress throughout a member cannot be expressed completely until something is known about the geometrical behavior of the member or how it deforms under the load.<sup>1</sup>

Interrelationships among the various factors involved in the general design procedure are indicated in Fig. 5. Usually the shape or general outline of the member is established by its function, and the loads to which it will be subjected can be estimated. The problem is then one of determining the requisite size. However, the size cannot be determined directly from the loads and shape but can be evaluated only after consideration of the total stresses and displacements, and the unit stresses and unit strains, relationships among which are found with the aid of *statics, geometry, and the properties of the material*.

As the first step in establishing a design procedure there will be developed (1) the statical relationships among the stresses on various planes at a point, (2) the geometrical relationships among the strains in different directions at a point, and (3) the relationships between stress and strain as governed by the properties of the material. Then the relationships among load, stress, displacement, and size may be set up for various typical shapes of members and typical systems of applied forces.

### STRESSES AT A POINT

**11. General Relationships.**—In a fluid at rest the stress situation at a given point can be expressed completely by a single number, the unit pressure, since the pressure or compressive stress has the same magnitude on all planes through the point. However, in a solid at rest the state of stress at a given point cannot be described fully by a single number because the stress, in general, is not the same on all planes passing through the point. Additional information is required to give an adequate description of the state of stress at the point.

Fortunately it is not necessary to state the magnitude of the stress on every plane through the point in order to describe completely the stress situation. In fact, if the stresses on three orthogonal planes through the point are known, the stress on any plane may be determined by using the equations of equilibrium.

Stress is a vector quantity. Hence, in order to describe the

<sup>1</sup> If plastic action is involved, time also may become an important factor.

stress acting on any plane through a point, both the magnitude and the direction of the stress must be specified. For convenience, the force acting on a given plane at a point is usually resolved into a normal component and one or more shearing components, from which the corresponding normal and shearing stresses may be computed.

For example, the three forces  $F_1$ ,  $F_2$ , and  $F_3$  acting on the three sides of the element in Fig. 6a may each be resolved into a normal and two shearing components as indicated in Fig. 6b. Each

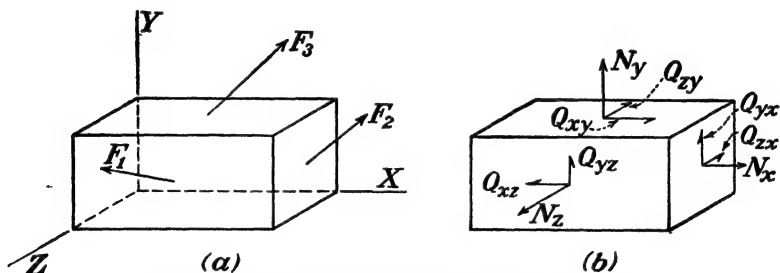


FIG. 6.—Normal and shearing components of forces.

component is distinguished by a standardized notation that indicates direction by means of subscripts. The normal forces are designated as  $N_x$ ,  $N_y$ , and  $N_z$ , in which the subscript denotes the coordinate axis to which the force is parallel. The shearing forces are designated by the letter  $Q$  with two subscript letters. The first letter of the subscript denotes the direction of the shearing force, and the second letter indicates the plane in which the force lies. For example,  $Q_{xy}$  denotes a shearing force in the  $x$  direction lying in a plane perpendicular to the  $y$  axis, while  $Q_{zx}$  denotes a shearing force in the  $z$  direction lying in a plane perpendicular to the  $x$  axis. The same system applies to the stresses.  $S_y$  indicates<sup>1</sup> a normal stress in the  $y$  direction (acting on a plane perpendicular to the  $y$  axis), while  $S_{xz}$  is used to indicate a shearing stress in the  $x$  direction and lying in a plane perpendicular to the  $z$  axis.

The relationships among the stresses on various planes passing through a point may be determined by applying the equations of

<sup>1</sup> Some writers use the Greek small sigma to denote normal stress, as  $\sigma_y$ , and small tau to denote shearing stress, as  $\tau_{xz}$ . The symbol  $f$  with appropriate subscripts is frequently used to denote stress.

equilibrium to a free-body diagram of an element of the material at the point.

For the condition of biaxial stress<sup>1</sup> the most convenient free-body diagram is a triangular wedge as indicated in Fig. 7a. The

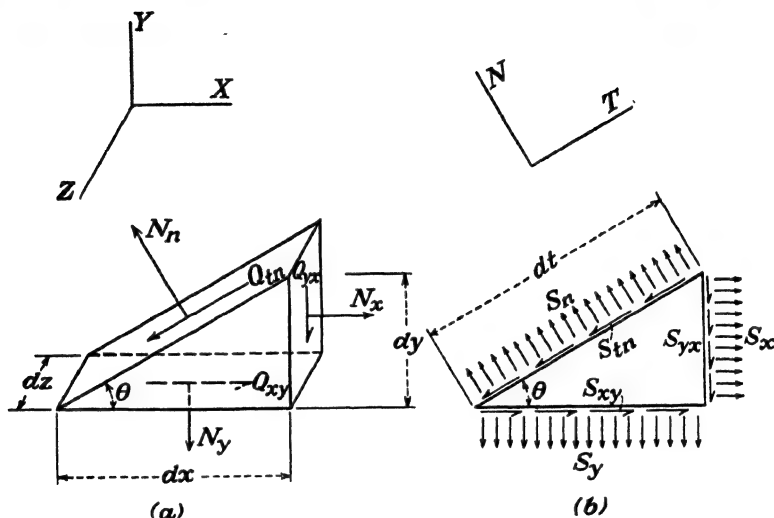


FIG. 7.—Free-body diagram and stress diagram for biaxial-stress condition.

three orthogonal planes used for reference are those formed by the  $x$ ,  $y$ , and  $z$  axes. The normal and shearing stresses on those planes are assumed to be known. Since it is a biaxial stress situation, the axes may be selected so that

$$N_z = Q_{xz} = Q_{zx} = Q_{yz} = Q_{zy} = 0$$

The other forces are assumed to be positive when acting in the directions shown. That is, tensile forces (and stresses) are positive, compressive forces (and stresses) are negative, and the sign convention for shearing forces (and stresses) is identical with the one used to designate vertical shear in a beam. The  $tz$  plane is selected arbitrarily, the angle that it makes with the  $xz$

<sup>1</sup> If the components of stress parallel to one of the three coordinate axes are zero, the stress situation is said to be biaxial. If the normal stresses and the components of shearing stress parallel to any two of the coordinate axes are zero, the stress situation is axial, while if none of the normal stresses is zero, a triaxial stress situation exists. The biaxial condition is of the most importance to the engineer, since it is the common condition on the surface of a member, where stresses are a maximum.



plane being designated as  $\theta$ , and the forces acting on it are assumed to be unknown. The  $n$  direction is normal to the  $tz$  plane. If the equation of equilibrium is written in the  $n$  direction, there results

$$N_n = N_x \sin \theta + Q_{yx} \cos \theta + N_y \cos \theta + Q_{xy} \sin \theta \quad (1)$$

For convenience, let  $dy dz = a$ ,  $dx dz = b$ , and  $dt dz = c$ . If these areas are small, so that the stress is constant over the area, Eq. (1) may be rewritten in terms of the stresses as

$$S_n c = S_x a \sin \theta + S_{yx} a \cos \theta + S_y b \cos \theta + S_{xy} b \sin \theta \quad (2)$$

or

$$S_n = S_x \sin^2 \theta + S_{yx} \sin \theta \cos \theta + S_y \cos^2 \theta + S_{xy} \sin \theta \cos \theta \quad (3)$$

However

$$S_{xy} = S_{yx}$$

Hence

$$S_n = S_x \sin^2 \theta + S_y \cos^2 \theta + S_{xy} \sin 2\theta \quad (4)$$

In a like manner, the shearing stress on the  $tz$  plane may be found by writing the equation of equilibrium in the  $t$  direction

$$\begin{aligned} S_{tn} &= S_x \sin \theta \cos \theta - S_y \sin \theta \cos \theta + S_{xy}(\cos^2 \theta - \sin^2 \theta) \\ &= \frac{S_x - S_y}{2} \sin 2\theta + S_{xy} \cos 2\theta \end{aligned} \quad (5a)$$

Equations (4) and (5) are based upon the assumptions that the weight and other body forces acting on the material are negligible and that the material is in equilibrium, without regard to elastic or plastic condition. The equations are valid so long as the material can develop the stresses. If the material is a fluid at rest, it cannot develop shearing stresses and Eq. (5a) yields

$$S_x = S_y \quad (5b)$$

Then Eq. (4) reduces to

$$S_n = S_x \quad (4a)$$

Hence

$$S_n = S_x = S_y \quad (4b)$$

which is the mathematical statement of Pascal's law. Consideration of the free-body diagram of Fig. 7a shows that the stresses  $S_n$  and  $S_{tn}$  as given by Eqs. (4) and (5a) are independent of any normal stresses on the  $xy$  plane. They are also independent of

shearing stresses on the  $xy$  plane ( $S_{xz}$  and  $S_{yz}$ ) provided that the magnitude of the shearing stress does not vary with  $z$ , i.e., if a condition of *plane stress* exists.

If the normal stresses in the  $x$  and  $y$  directions are zero, i.e., if the material is subjected to pure shear on the  $xz$  and  $yz$  planes, Eq. (4) reduces to

$$S_n = S_{xy} \sin 2\theta \quad (4c)$$

and Eq. (5a) yields

$$S_{tn} = S_{xy} \cos 2\theta \quad (5c)$$

Then

$$S_n = S_{tn} \tan 2\theta \quad (4d)$$

**12. Principal Stresses.**—The evaluation of the maximum normal stress is of considerable practical importance. The direction of the plane on which the normal stress becomes a maximum or minimum may be determined by differentiating Eq. (4) with respect to  $\theta$  and equating the derivative to 0.

$$\frac{dS_n}{d\theta} = 2S_x \sin \theta \cos \theta - 2S_y \sin \theta \cos \theta + 2S_{xy} \cos 2\theta = 0 \quad (6)$$

from which

$$\tan 2\theta = \frac{-2S_{xy}}{S_x - S_y} \quad (7)$$

Equation (7) defines two planes, at right angles to each other. The normal stress is a maximum on one of the planes and a minimum on the other. From Eq. (7)

$$\sin 2\theta = \frac{-2S_{xy}}{\pm \sqrt{(S_x - S_y)^2 + 4S_{xy}^2}} = \frac{\mp 2S_{xy}}{\sqrt{(S_x - S_y)^2 + 4S_{xy}^2}} \quad (8)$$

and

$$\cos 2\theta = \frac{(S_x - S_y)}{\pm \sqrt{(S_x - S_y)^2 + 4S_{xy}^2}} = \frac{\pm (S_x - S_y)}{\sqrt{(S_x - S_y)^2 + 4S_{xy}^2}} \quad (9)$$

If Eqs. (8) and (9) are used to evaluate the functions of  $2\theta$ , Eq. (5a) becomes

$$S_{tn} = \frac{\pm (S_x - S_y)(-S_{xy})}{\sqrt{(S_x - S_y)^2 + 4S_{xy}^2}} + \frac{\pm S_{xy}(S_x - S_y)}{\sqrt{(S_x - S_y)^2 + 4S_{xy}^2}} = 0 \quad (10)$$

Therefore, the shearing stress is equal to zero on the plane on which the normal stress is a maximum (or minimum). In a similar manner it may be shown that no shear exists on a third plane that is normal to the two planes defined by Eq. (7).

The maximum and minimum normal stresses may be calculated from Eqs. (4), (8), and (9).

$$S_n = \frac{S_x + S_y}{2} \pm \sqrt{\left(\frac{S_x - S_y}{2}\right)^2 + S_{xy}^2} \quad (11)$$

The stresses calculated from Eq. (11) are known as "principal stresses." They are the maximum (and the minimum) normal stresses that occur on any plane (perpendicular to the  $xy$  plane) through the point and are developed on the planes on which there is no shearing stress. *The directions of the principal stresses will be designated as the  $u$  and  $v$  directions, and the angle that the  $u$  direction makes with the  $x$  direction will be designated as  $\theta_{xu}$ .*

Principal stresses are important because they represent the maximum and minimum values of stress that exist at a point and also because they afford one of the most convenient ways of completely describing the stress situation at a point. If the principal stresses are known, the stresses on all other planes through the point may be determined.

**13. Maximum Shearing Stresses.**—The direction of the planes on which the shearing stress is a maximum may be found by differentiating Eq. (5a) and equating the derivative to zero.

$$\frac{\partial S_{tn}}{\partial \theta} = (S_x - S_y) \cos 2\theta - 2S_{xy} \sin 2\theta = 0 \quad (12a)$$

from which

$$\tan 2\theta = \frac{S_x - S_y}{2S_{xy}} \quad (12b)$$

Equation (12b) defines a pair of planes that make angles of 45 deg. with those defined by Eq. (7). Hence, the maximum shearing stresses occur on planes at 45 deg. with the planes on which the principal stresses act. The axes formed by the intersections of the  $xy$  plane with the planes on which the shearing stresses are maximum (or minimum) will be designated as the  $i$  and  $j$  axes.

The magnitude of the maximum shearing stress  $S_{ij}$  may be found by substituting the functions of  $2\theta$ , which may be determined from Eq. (12b) into Eq. (5a).

$$S_{ij} = \pm \frac{1}{2} \sqrt{(S_x - S_y)^2 + 4S_{xy}^2} = \pm \sqrt{\left(\frac{S_x - S_y}{2}\right)^2 + S_{xy}^2} \quad (13a)$$

Equation (13a) shows that the two maximum shearing stresses are equal in magnitude. Hence,  $S_{ij} = S_{ji}$  as may be verified from the equilibrium of an elementary cube with sides in the  $i$  and  $j$  directions.

Furthermore, the maximum shearing stress is equal to the second term in the expression for the principal stress, Eq. (11). Therefore Eq. (11) may be written as

$$S_{u,v} = \frac{1}{2}(S_x + S_y) \pm S_{ij} \quad (11a)$$

*Illustrative Problem.*—At a point on the vertical side of a beam  $S_x = 1,200$  p.s.i. tension,  $S_y = 600$  p.s.i. compression, and the shearing stress is 800 p.s.i. due to a positive vertical shear. Determine the principal stresses and the maximum shearing stress.

*Solution.*—Since the point under consideration is on the surface of the beam, a biaxial stress situation prevails. The axes may be taken as in Fig. 7. Then  $S_x$  and  $S_{xy}$  are positive, and  $S_y$  is negative. From Eq. (13b) the maximum shearing stress is

$$\begin{aligned} S_{ij} &= \frac{1}{2} \sqrt{(1,200 + 600)^2 + 4(800)^2} \\ &= 1,204 \text{ p.s.i.} \end{aligned}$$

The principal stresses are, from Eq. (11a),

$$S_{u,v} = \frac{1}{2}(1,200 - 600) \pm 1,204$$

from which

$$\begin{aligned} S_u &= 1,504 \text{ p.s.i.} \\ S_v &= -904 \text{ p.s.i.} \end{aligned}$$

The angle  $\theta$  between the  $x$  axis and the directions of the principal stresses is, from Eq. (7),

$$\begin{aligned} \tan 2\theta &= \frac{-1,600}{1,200 + 600} = -0.8889 \\ \theta &= -20^\circ 49' \text{ or } +69^\circ 11' \end{aligned}$$

Since  $\theta$  is multiple-valued, one of these angles is  $\theta_{xu}$  or the angle that the  $u$  axis makes with the  $x$  axis, and the other angle is  $\theta_{xv}$ . The  $u$  direction and the  $v$  direction were assigned arbitrarily when the stresses were evaluated, and the angles  $\theta_{xu}$  and  $\theta_{xv}$  are identified most readily by inspection as indicated in Fig. 8. If the original block, Fig. 8a, is cut along the line  $OA$  (at an angle of  $69^\circ 11'$  with the  $x$  direction), the free-body diagram of one portion of it is as represented in Fig. 8b. Five forces  $N_x$ ,  $N_y$ ,  $Q_{yx}$ ,  $Q_{xy}$ , and  $N_z$  are acting on the block, and the directions of the first four are known. By inspection it is evident that the resultant of  $N_x$  and  $Q_{xy}$  is a force to the right that must be balanced by the horizontal

component of the force on the inclined face. Hence, the stress acting on the inclined face is tension and, therefore,  $S_u$ . It follows that the  $u$  axis is perpendicular to  $OA$  and that

$$\theta_{zu} = -20^\circ 49'.$$

This result may be checked by means of the free body shown in Fig. 8c, the inclined face of which makes an angle of  $-20^\circ 49'$  with the  $x$  axis. In this diagram the vertical forces  $N'_y$  and  $Q'_{yz}$

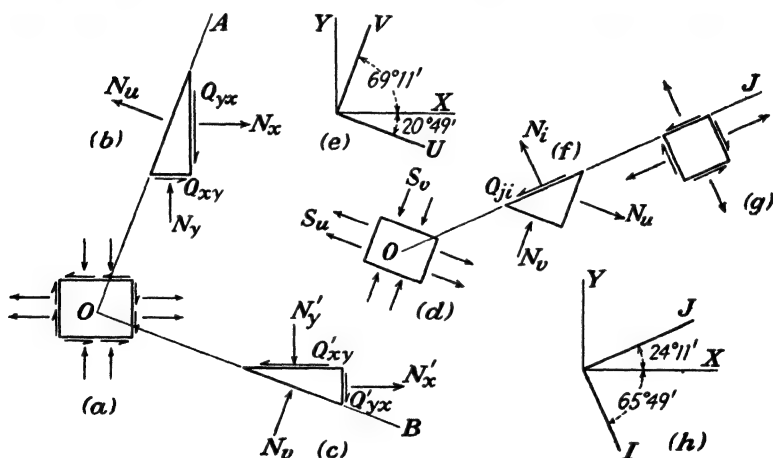


FIG. 8.—Identification of directions of principal stresses and maximum shearing stresses.

add to give a downward force that must be balanced by compression on the inclined face. Since the compressive stress was arbitrarily called  $S_v$ , the  $v$  direction must be at right angles to  $OB$ , and  $\theta_{zv} = +69^\circ 11'$ . Hence, the principal stresses act in the directions indicated in Fig. 8d, and the  $u$  and  $v$  axes are as shown in Fig. 8e.

In a like manner the sense of the maximum shearing stresses (which are at  $45^\circ$  with the principal stresses) may be found from a free-body diagram, Fig. 8f, cut along the plane  $OJ$  at  $45^\circ$  with the direction of the principal stresses. The  $j$  components of  $N_u$  and  $N_v$  add. Therefore, the force  $Q_{ji}$  must be to the left to hold the block in equilibrium. The maximum shearing stresses will be as indicated in Fig. 8g.

**14. Graphical Evaluation of Principal Stresses.**—The principal stresses and maximum shearing stress may also be determined

from the normal and shearing stresses on orthogonal planes by a graphical construction known as the "stress circle." The construction is outlined in Fig. 9b for a point at which the stresses are as shown in Fig. 9a, which is identical to the situation in Fig. 7. From an origin  $O$ , Fig. 9b, one normal stress  $S_x$  is laid off to scale as the vector  $OX$ , and the other normal stress is laid off along the same line as  $OY$ . Tensile stresses are plotted to the right and compressive stresses to the left. At  $X$  and  $Y$  the perpen-

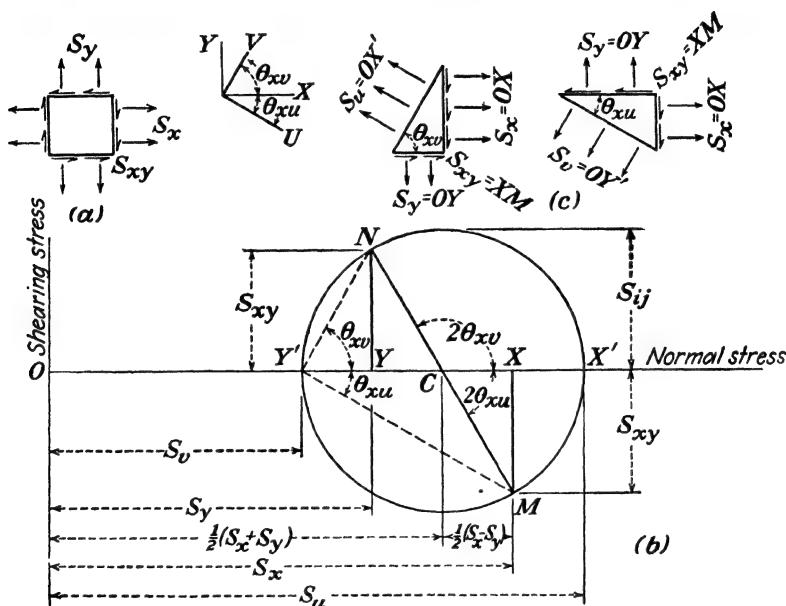


FIG. 9.—The stress circle.

diculars  $XM$  and  $YN$  are erected, their lengths being  $S_{xy}$  to scale. The vector  $XM$  is laid off downward if the shearing stress on the right hand side of the differential element is downward as shown in Fig. 9a. With  $C$ , the intersection of  $OX$  and  $MN$ , as a center a circle is drawn through  $M$  and  $N$ . The points  $X'$  and  $Y'$  are determined as the intersection of the circle with the line  $OX$  or its extension. The magnitudes of the principal stresses are given as the distances  $OX'$  and  $OY'$  while the maximum shearing stress is equal to the radius of the circle. The angle  $XY'M$  is  $\theta_{xu}$  or the angle between the  $x$  direction and the direction of the principal stress  $OX'$ . The angle  $\theta_{yu}$  is the angle  $XY'N$ .

The validity of the construction is evident from the following relationships:

$$CX = \frac{OX - OY}{2} = \frac{S_x - S_y}{2} \quad (14a)$$

$$CM = \sqrt{CX^2 + MX^2} = \sqrt{\left(\frac{S_x - S_y}{2}\right)^2 + S_{xy}^2}$$

$$CX' = OC + CM = \frac{S_x + S_y}{2} + \sqrt{\left(\frac{S_x - S_y}{2}\right)^2 + S_{xy}^2} \quad (14b)$$

$$OY' = OC - CM = \frac{S_x + S_y}{2} - \sqrt{\left(\frac{S_x - S_y}{2}\right)^2 + S_{xy}^2} \quad (14c)$$

$$\tan 2\theta = \frac{-MX}{CX} = \frac{-S_{xy}}{\frac{1}{2}(S_x - S_y)} \quad (14d)$$

A slightly different graphical construction, which may also be used for the evaluation of the principal stresses from a pair of normal stresses and the accompanying shearing stress, is shown in Fig. 10.

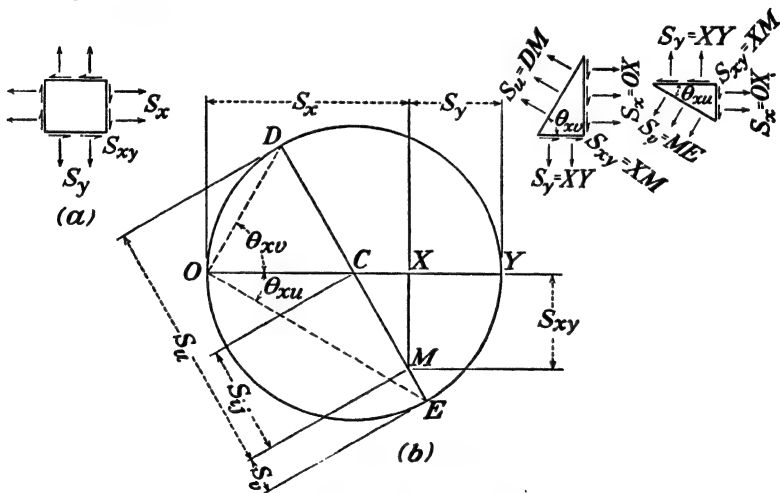


FIG. 10.—Alternative stress circle.

From the origin  $O$  the normal stresses  $S_x$  and  $S_y$ , which are acting as shown in Fig. 10a, are laid off vectorially as  $OX$  and  $OY$  respectively. With  $C$ , the mid-point of  $OY$ , as a center and  $OC$  as a radius the circle is drawn through  $O$  and  $Y$ . From point  $X$  the shearing stress  $S_{xy}$  is plotted perpendicular to  $OY$  as  $XM$ . The diameter  $DCE$  is drawn through  $C$  and  $M$ .

Then one principal stress is equal to  $DM$ , the other is equal to  $ME$ , and the angle  $\theta$ , which the planes of the principal stresses make with the  $x$  and  $y$  direction, may be obtained from the angle  $ECY$ , which is  $2\theta$ .

From the construction it is evident that

$$\begin{aligned} DM &= DC + CM = DC + \sqrt{CX^2 + XM^2} \\ &= \frac{S_x + S_y}{2} + \sqrt{\left(\frac{S_x - S_y}{2}\right)^2 + S_{xy}^2} \end{aligned} \quad (15a)$$

$$ME = CE - CM = \frac{S_x + S_y}{2} - \sqrt{\left(\frac{S_x - S_y}{2}\right)^2 + S_{xy}^2} \quad (15b)$$

It is also evident that  $CM$  is the maximum shearing stress and

$$\tan 2\theta = \frac{-XM}{CX} = \frac{-S_{xy}}{\frac{1}{2}(S_x - S_y)} \quad (15c)$$

The signs of the principal stresses may be determined by inspection.

In addition to being evaluated algebraically or graphically from two normal stresses and a shearing stress, principal stresses may be evaluated from measured strains as outlined in Art. 26.

### 15. Evaluation of Other Stresses from Principal Stresses.—

Once the principal stresses at a point are known, the stresses acting on any plane at the point may be evaluated from a free-body diagram of a triangular wedge at the point or from Eqs. (4) and (5), which were developed from such a wedge. If  $S_u$  and  $S_v$  are the principal stresses at a point, the shearing stress  $S_{uv}$  is equal to zero, and the normal stress  $S_n$  on any plane that makes an angle  $\theta_{ut}$  with the  $uv$  plane and is perpendicular to the  $uv$  plane may be evaluated by substituting  $S_u$  and  $S_v$  into Eq. (4), which reduces to

$$S_n = S_u \sin^2 \theta_{ut} + S_v \cos^2 \theta_{ut} \quad (16)$$

Equation (16) may also be written in the form

$$S_n = \frac{S_u + S_v}{2} - \frac{S_u - S_v}{2} \cos 2\theta_{ut} \quad (16a)$$

The normal stress  $S_t$  acting on a plane at right angles to the stress defined in Eq. (14a) may be evaluated by replacing  $\theta_{ut}$  with  $\theta_{un}$  or  $\theta_{ut} + 90$  deg. and is

$$S_t = S_u \cos^2 \theta_{ut} + S_v \sin^2 \theta_{ut} \quad (16b)$$



or

$$S_t = \frac{S_u + S_v}{2} + \frac{S_u - S_v}{2} \cos 2\theta_{ut} \quad (16c)$$

The shearing stress  $S_{tn}$  acting on the pair of inclined planes is from Eq. (5a)

$$S_{tn} = \frac{S_u - S_v}{2} \sin 2\theta_{ut} \quad (17)$$

It will be noted that if Eq. (16a) is added to Eq. (16b) there results

$$S_n + S_t = S_u + S_v \quad (18)$$

That is, the algebraic sum of the normal stresses on any pair of mutually perpendicular planes through a point is a constant, independent of the angles that the planes make with the coordinate axes.

The direction of the maximum shearing stress with reference to the direction of the principal stresses may be found by differentiating Eq. (17) with respect to  $\theta_{ut}$  and equating the derivative to zero.

$$\frac{dS_{tn}}{d\theta_{ut}} = (S_u - S_v) \cos 2\theta_{ut} = 0 \quad (19)$$

Equation (19) is satisfied for the special case in which

$$S_u = S_v \quad (19a)$$

If the principal stresses are equal, Eq. (17) indicates that  $S_{tn} = 0$ . That is, no shearing stresses are developed on any plane at the point. This corresponds to the condition of hydrostatic pressure. Equation (19) is also satisfied if

$$\cos 2\theta_{ut} = 0$$

or

$$\theta_{ut} = 45^\circ, 135^\circ, \dots (2n - 1) \frac{\pi}{4} \quad (19b)$$

which indicates that the maximum shearing stresses are developed on planes that are at 45 deg. with the planes on which the principal stresses act. This is in agreement with the results obtained in Art. 13. The magnitude of the maximum shearing stress on any of the planes perpendicular to the  $uv$  plane may be found from Eq. (17) as well as from Eq. (13b)

$$S_{tn(\max)} = \frac{S_u - S_v}{2} = S_{ij} \quad (20a)$$

However,  $S_{ij}$  is not necessarily the maximum shearing stress at the point. For certain combinations of  $S_u$ ,  $S_v$ , and  $S_w$  (the third principal stress, perpendicular to  $S_u$  and  $S_v$ ) the maximum shearing stress may occur on planes that make angles of 45 deg. with the  $uv$  plane. It is evident that either of two other shearing stresses,  $S_{kl}$  or  $S_{mp}$ , may be critical.

$$S_{kl} = \frac{S_v - S_w}{2} \quad (20b)$$

and

$$S_{mp} = \frac{S_w - S_u}{2} \quad (20c)$$

For example, if the principal stresses at a point are  $S_u = 10,000$  p.s.i.,  $S_v = 4,000$  p.s.i., and  $S_w = 0$  as indicated in Fig. 11a the

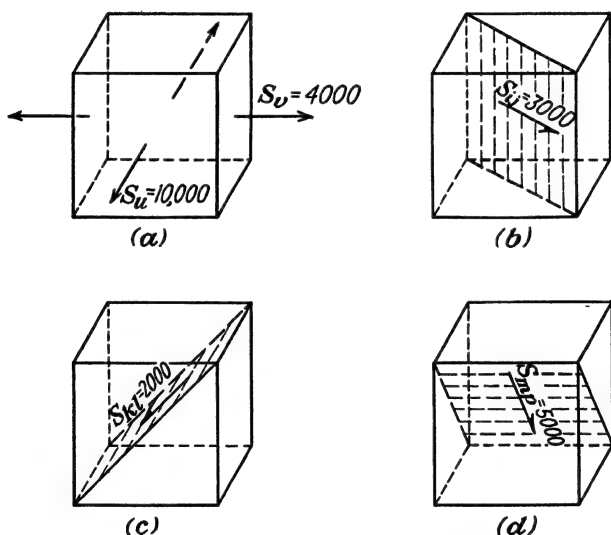


FIG. 11.—Maximum shearing stresses.

maximum shearing stress on any plane perpendicular to the  $uv$  plane is  $S_{ij} = 3,000$  p.s.i. as shown in Fig. 11b. A shearing stress  $S_{kl} = 2,000$  p.s.i. as shown in Fig. 11c, is the maximum on any plane perpendicular to the  $vw$  plane, while the maximum on any plane perpendicular to the  $uv$  plane is  $S_{mp} = 5,000$  p.s.i. as shown in Fig. 11d. The stress  $S_{mp}$  is the maximum shearing stress on any plane through the point.

**16. Graphical Solution by the Mohr Circle.**—A convenient graphical determination of the stresses on any plane when the principal biaxial stresses are known is that of the Mohr circle<sup>1</sup> and is indicated in Fig. 12. From an origin  $O$  one of the principal stresses  $S_u$  is laid off as a horizontal vector (to some convenient scale)  $OA$ , and the other principal stress  $S_v$  is laid off horizontally from the same origin as  $OB$ . Tensile stresses are plotted to the

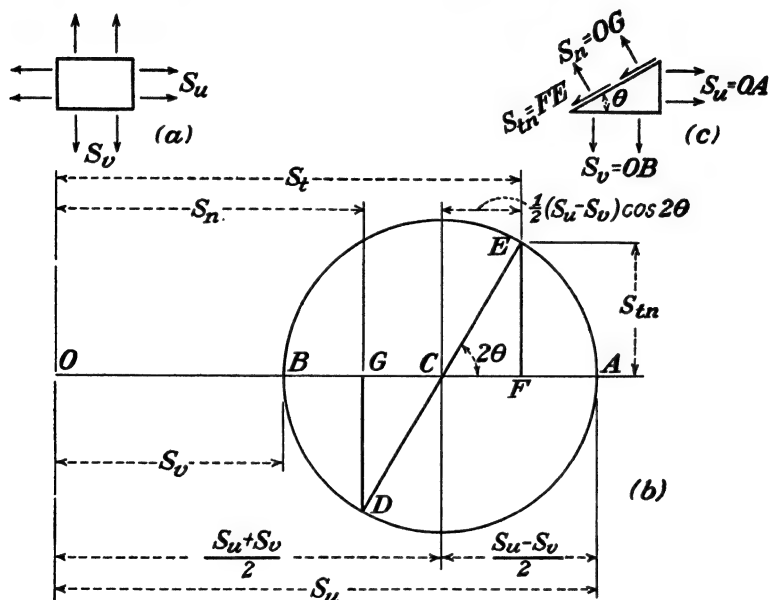


FIG. 12.—The Mohr circle for stresses.

right and compressive stresses to the left. With  $C$ , the mid-point between  $A$  and  $B$ , as a center a circle is drawn through  $A$  and  $B$ . To determine the stresses on a plane that makes an angle  $\theta$  with the  $u$  direction a diameter  $DCE$ , making an angle  $2\theta$  with the  $u$  direction, is drawn through  $C$ . Lines  $EF$  and  $DG$  are drawn from  $D$  and  $E$  perpendicular to  $OA$ .

From the geometry of Fig. 12 it is evident that

$$OG = \frac{S_u + S_v}{2} - \frac{S_u - S_v}{2} \cos 2\theta \quad (21)$$

Therefore, from the similarity of Eqs. (21) and (16a), it is

<sup>1</sup> MOHR, O., *Zivilingenieur*, p. 113, 1882.

MOHR, O., "Technische Mechanik," 2d ed., 1914.

apparent that the normal stress on a plane that makes an angle  $\theta$  with the  $u$  direction is determined as the distance  $OG$ . Similarly, the distance  $OF$  indicates the normal stress on a plane that makes an angle of 90 deg. with the stress given by the distance  $OG$ .

It is also evident from Fig. 12 that

$$EF = GD = \frac{S_u - S_v}{2} \sin 2\theta \quad (22)$$

Therefore, from Eq. (17), the shearing stress on a plane that makes an angle  $\theta$  with the  $u$  direction is determined as the distance  $EF$ .

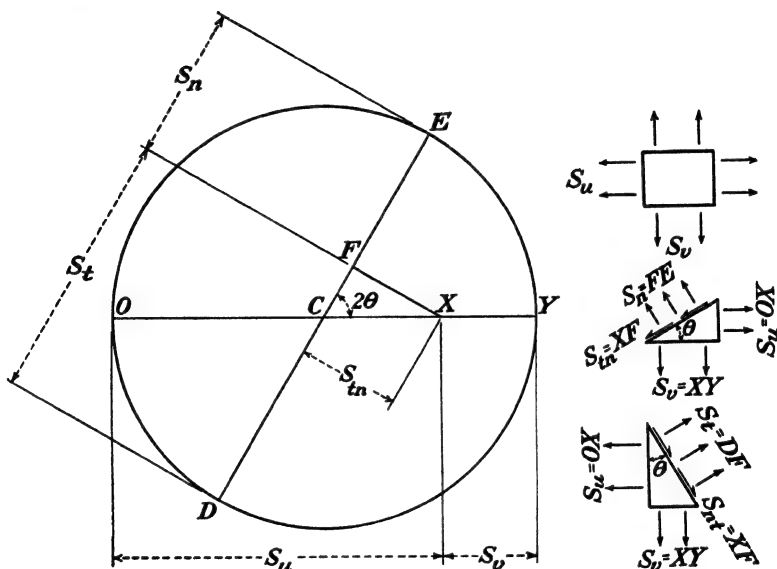


FIG. 13.—The Mohr-Land circle.

Complete information concerning the state of stress on any plane through the point is available from the Mohr circle.

The construction of Fig. 12 parallels that of Fig. 9.

**17. The Mohr-Land Circle.**—An alternate graphical solution known as “the Mohr-Land circle” is also available for use in determining biaxial stresses on any plane from given principal stresses. The construction is indicated in Fig. 13.

From the origin  $O$  the principal stress  $S_u$  is laid off as a vector  $OX$  and the other principal stress  $S_v$  as the vector  $XY$ . With the mid-point of  $OY$  as a center  $C$  a circle of radius  $CO$  is drawn.

To determine the stresses on a plane making an angle  $\theta$  with the  $u$  direction the diameter  $DCE$  is drawn making an angle  $2\theta$  with  $CY$ , and the line  $XF$  is drawn from  $X$  perpendicular to  $DCE$ .

The magnitude of the normal stress that acts on the plane making an angle  $\theta$  with the  $u$  direction is given by  $FE$ , and the shearing stress that acts on that plane is given by  $XF$ . The normal stress on a perpendicular plane is given by the distance  $DF$ .

From the construction of the circle it is evident that

$$DC = OC = \frac{OY}{2} = \frac{OX + XY}{2} = \frac{S_u + S_v}{2} \quad (23)$$

$$\begin{aligned} CF &= CX \cos 2\theta = (OX - OC) \cos 2\theta \\ &= \left( S_u - \frac{S_u + S_v}{2} \right) \cos 2\theta \\ &= \frac{S_u - S_v}{2} \cos 2\theta \end{aligned} \quad (24)$$

$$FE = CE - CF = \frac{S_u + S_v}{2} - \frac{S_u - S_v}{2} \cos 2\theta \quad (25a)$$

$$DF = DC + CF = \frac{S_u + S_v}{2} + \frac{S_u - S_v}{2} \cos 2\theta \quad (25b)$$

Equations (25a) and (25b) agree with Eqs. (16a) and (16c); hence,  $EF$  and  $DF$  give the pair of normal stresses. Also

$$XF = CX \sin 2\theta = \frac{S_u - S_v}{2} \sin 2\theta \quad (26)$$

which agrees with Eq. (17). Therefore, the shearing stress is given by  $XF$ .

The Mohr-Land construction gives visual evidence of the relationships indicated in Eq. (18)—that the sum of the orthogonal normal stresses at a point is a constant, in this case the diameter of the circle.

The Mohr-Land construction is essentially the reverse of that outlined in Fig. 10 for determining principal stresses.

**18. Triaxial Stresses at a Point.**—If the point under consideration is subjected to stresses in three directions, three principal stresses  $S_u$ ,  $S_v$ , and  $S_w$  and their directions are required to define the state of stress. If the principal stresses are not known, three normal stress components ( $S_x$ ,  $S_y$ , and  $S_z$ ) and three sets of shearing stresses ( $S_{xy} = S_{yx}$ ,  $S_{yz} = S_{zy}$ , and  $S_{zx} = S_{xz}$ ) are required. The stresses on any plane may be evaluated in terms of the orthogonal stress components by use of the equations of equilib-

rium applied to a tetrahedron, three sides of which are the planes on which the known stresses act, and the fourth side of which is the plane on which the stresses are to be determined. The normal stress on the fourth plane may be evaluated in terms of the stress components on the three orthogonal planes formed by the  $x$ ,  $y$ , and  $z$  axes as

$$S_n = r_1^2 S_x + r_2^2 S_y + r_3^2 S_z + 2r_1 r_2 S_{xy} + 2r_2 r_3 S_{yz} + 2r_3 r_1 S_{zx} \quad (27)$$

in which  $r_1$ ,  $r_2$ , and  $r_3$  are the cosines of the angles between the direction of the stress  $S_n$  and the  $x$ ,  $y$ , and  $z$  axes respectively.

It may also be shown that

$$S_{in}^2 = r_1^2 r_2^2 (S_u - S_v)^2 + r_2^2 r_3^2 (S_v - S_w)^2 + r_3^2 r_1^2 (S_w - S_u)^2 \quad (28)$$

in which the  $r$  terms are the cosines of the angles between the normal to the plane on which the shearing stress acts and the directions of the principal stresses. As before, the shearing stress is zero on the planes on which the principal stresses act.

Equations (27) and (28) reduce to the equivalent of Eqs. (4) and (5a) for the condition of biaxial stress. Graphical methods have been developed for the evaluation of triaxial stresses.<sup>1</sup>

In general, the triaxial stress condition is less important than the biaxial condition because for most structural members such as beams, columns, and torsional members the maximum stresses occur at an outside edge or a surface where a biaxial stress condition exists.

**19. Stress Trajectories and Isoclinics.**—The algebraic and graphical techniques that have been described permit the evaluation of principal stresses at any given point on the surface of a member if two normal stresses and the accompanying shearing stress are known. In many cases it is desirable to have a picture of the variation of principal stresses throughout the member. Such a picture may be prepared by calculating the principal stresses at a number of points and plotting stress contours or lines that pass through points of equal principal stress. A set of stress contours for a short cantilever beam of rectangular cross section

<sup>1</sup> MOHR, O., "Abhandlungen aus dem Gebiete der technischen Mechanik," 2d ed., p. 192, Berlin, 1914.

FÖPPL, A., "Technische Mechanik," Vol. 5, 2d ed., p. 13, Leipzig, 1918.

FÖPPL, A., and L. FÖPPL, "Drang and Zwang," p. 11, Oldenbourg, Munchen, 1920.

WESTERGAARD, H. M., *Z. ang. Math. Mech.*, Vol. 4, p. 520, 1924.

carrying a concentrated load at the end is indicated in Fig. 14a. Stress concentration at the load point is neglected in this sketch.

Similarly a set of lines, each connecting points having identical directions of principal stress, may be drawn as shown in Fig. 14b. These lines are called "isoclinics." The directions of the principal

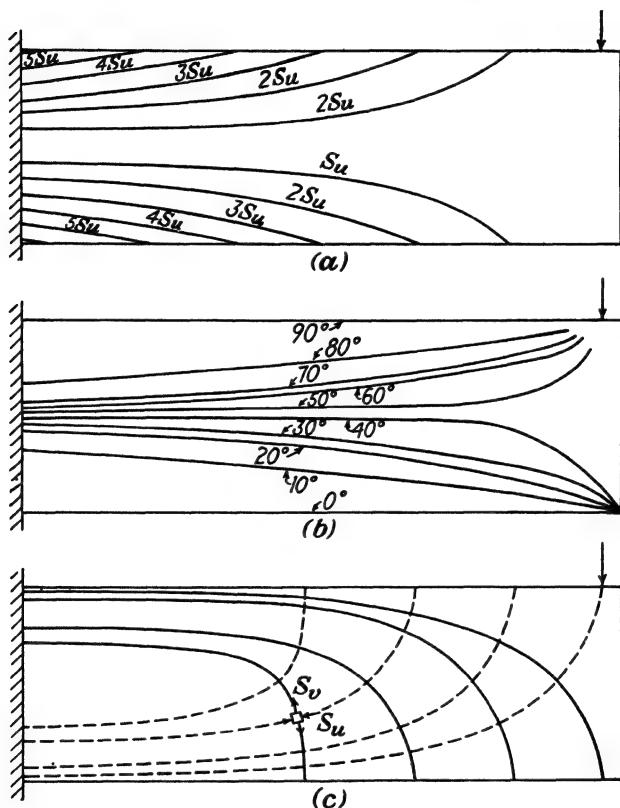


FIG. 14.—Stress contours, isoclinics, and stress trajectories.

stresses may also be indicated by *stress trajectories* or lines so drawn that their tangents at every point are in the direction of the principal stress. It is evident that the stress trajectories for a member consist of two sets of orthogonal lines. Stress trajectories for the beam are shown in Fig. 14c.

In indicating the direction of the principal stresses, stress trajectories also indicate the direction of maximum weakness in the member, which may be an important factor in design.

For example, if the beam of Fig. 14 were made of concrete, which is weak in tension, failure perpendicular to the solid set of trajectories would be expected, and to be most effective, reinforcement should be placed in the direction of the trajectories. Similarly, if the beam were metal, with a thin web, the trajectories in the compression area of the beam would indicate the directions in which stiffeners should be placed to prevent buckling of the web.

Isoclinics and stress trajectories may also be obtained experimentally from photoelastic studies as described in Chap. 10. It is evident that stress trajectories are analogous to the streamlines of fluid flow.

### STRAINS AT A POINT

**20. General Considerations.**—The relationships among the stresses acting on various planes through a point were built up using the equations of equilibrium as applied to a free-body diagram of a differential block at the point. In a somewhat similar manner the relationships among the strains in different directions at a point will be developed on the basis of the geometrical relationships involved in the distortion of the differential block at the point.

In developing the stress relationships a differential block was used so that the stress could be assumed uniformly distributed over the sides of the block. In developing the strain relationships a differential block is used so that the strains in parallel directions may be assumed constant throughout the block. Then the sides of the block will remain plane and the edges remain straight lines.

Since the biaxial stress condition, or condition existing at the surface of a member, was considered to be the most important, the analysis of strains will also be made for a point on the surface of a member, although the techniques employed may be extended to the consideration of interior points as well.

The sides of the differential block are assumed to remain plane; the intersections of the sides with the plane of the surface remain straight lines. Hence, the movement of any side may be resolved into a movement of translation and a movement of rotation, and the *relative* motion of two opposite or adjacent sides may be resolved into components of translation and rotation. The rela-



tive translation of two opposite sides constitutes *normal*, or *axial*, strains while the relative rotation of two adjacent sides constitutes *shearing strain*. For example, if a rectangle  $OABC$ , Fig. 15a, is scribed on the surface of a member, it will be displaced to some position such as  $O'A'B'C'$  when the member is strained. Since the block is a differential block, the strain is uniform in parallel directions throughout the block, and the rectangle becomes a parallelogram. However, strains are measured by the relative displacements of two sides rather than the absolute displacement

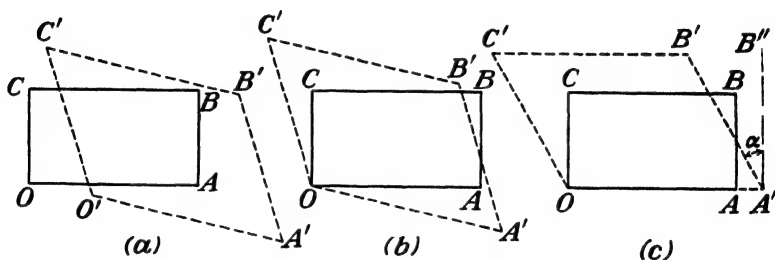


FIG. 15.—Distortion of a rectangle due to strain.

of one point or side; hence, point  $O$  may be assumed to remain fixed, and the two blocks may be superimposed as shown in Fig. 15b. In addition, the side  $OA$  may be assumed fixed in direction, and the strained block superimposed on the unstrained block as indicated in Fig. 15c. The movement of the side  $AB$  to  $A'B'$  consists of a translation  $AA'$  and a rotation through the angle  $\alpha$ . The translation of  $AA'$  relative to the opposite side constitutes the normal, or axial, strain, and the rotation is a shearing strain.

The *unit axial strain*  $\epsilon_x$  is equal, by definition, to the displacement  $AA'$  divided by the length  $OA$  over which it occurs. The unit shearing strain, by definition, is the displacement  $B''B'$  (at right angles to the reference length  $A'B''$ ) divided by the length  $A'B''$  over which the displacement occurs. The unit shearing strain is designated as  $\gamma_{xy}$ , and it is evident that  $\gamma_{xy} = \tan \alpha$ .

It is apparent that the displacements of the two pairs of opposite sides are independent; hence  $\epsilon_x$  and  $\epsilon_y$  are independent. However, the relative angular displacement of any pair of adjacent sides is the same, so  $\gamma_{xy}$  could be measured at any corner of the block, but  $\gamma_{xy}$  is independent of both  $\epsilon_x$  and  $\epsilon_y$ . The strains as indicated in Fig. 15 are assumed to be positive

since they correspond to the strains that would be expected to accompany positive normal and shearing stresses, Fig. 7.

**21. Evaluation of Normal Strain.**—The normal strain developed in the  $t$  direction at an angle  $\theta$  with the  $x$  direction is dependent upon  $\epsilon_x$ ,  $\epsilon_y$ , and  $\gamma_{xy}$ . It may be evaluated by considering the geometry of a differential triangle with sides in the  $x$ ,  $y$ , and  $t$  directions as indicated in Fig. 16a. The triangle is one-half of the basic differential rectangle, stressed as indicated

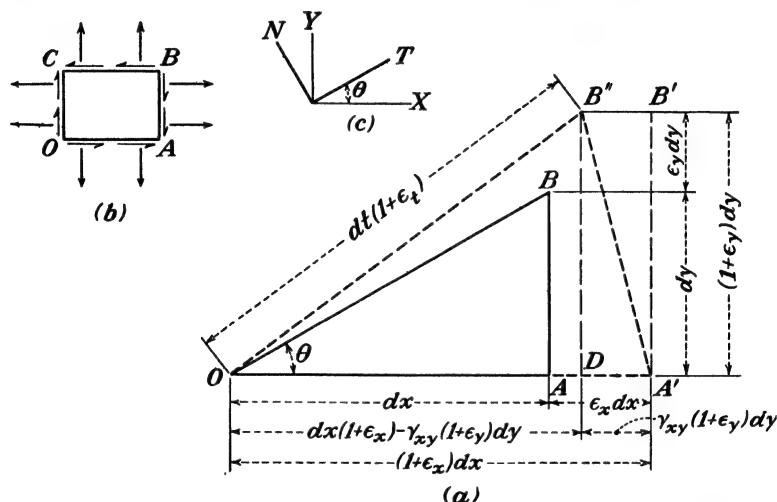


FIG. 16.—Distortion of a block subjected to normal and shearing strains.

in Fig. 16b so that the strains  $\epsilon_x$ ,  $\epsilon_y$ , and  $\gamma_{xy}$  are all positive. If the corner  $O$  is assumed to remain fixed and the lower edge  $OA$  to remain along the  $x$  axis, point  $A$  will be displaced to  $A'$ , a distance of  $\epsilon_x dx$ , in which  $\epsilon_x$  is the resultant unit strain in the  $x$  direction. Point  $B$  will be displaced to  $B''$ , a distance

$$\gamma_{xy}(1 + \epsilon_y) dy$$

from  $B'$ , by the action of the shearing stresses. Thus, the side  $OB$  in the  $t$  direction is changed in length to  $OB''$ .

The resultant normal unit strain in the  $t$  direction is  $\epsilon_t$ , and if the original length of the side  $OB$  is designated as  $dt$ , the new length  $OB''$  is  $dt + \epsilon_t dt$ .

From the right triangle  $ODB''$

$$\begin{aligned} (OB'')^2 &= (OD)^2 + (DB'')^2 \\ [dt(1 + \epsilon_t)]^2 &= [dx(1 + \epsilon_x) - \gamma_{xy}(1 + \epsilon_y) dy]^2 + [dy(1 + \epsilon_y)]^2 \end{aligned}$$

or

$$(1 + \epsilon_t)^2 = [(1 + \epsilon_x) \cos \theta - \gamma_{xy}(1 + \epsilon_y) \sin \theta]^2 + (1 + \epsilon_y)^2 \sin^2 \theta$$

since

$$\begin{aligned} dx &= dt \cos \theta \\ dy &= dt \sin \theta \end{aligned}$$

Then

$$(1 + \epsilon_t)^2 = (1 + \epsilon_x)^2 \cos^2 \theta - 2\gamma_{xy}(1 + \epsilon_x)(1 + \epsilon_y) \sin \theta \cos \theta + (1 + \epsilon_y)^2 \sin^2 \theta$$

which reduces to

$$1 + 2\epsilon_t = 2\epsilon_x \cos^2 \theta + 1 - 2\gamma_{xy} \sin \theta \cos \theta + 2\epsilon_y \sin^2 \theta$$

if differentials of higher order are dropped.

Then

$$\epsilon_t = \epsilon_x \cos^2 \theta + \epsilon_y \sin^2 \theta - \gamma_{xy} \sin \theta \cos \theta \quad (29)$$

$$= \epsilon_x \cos^2 \theta + \epsilon_y \sin^2 \theta - \frac{1}{2}\gamma_{xy} \sin 2\theta \quad (29a)$$

Similarly, the unit strain in the  $n$  direction, which is normal to the  $t$  direction, may be determined as

$$\epsilon_n = \epsilon_x \sin^2 \theta + \epsilon_y \cos^2 \theta + \frac{1}{2}\gamma_{xy} \sin 2\theta \quad (29b)$$

in which  $\theta$  is the angle which the  $t$  plane, or the plane perpendicular to  $\epsilon_n$ , makes with the  $x$  axis. Equation (29b) is similar in form to Eq. (4) for stresses.

The sum of Eqs. (29a) and (29b) gives

$$\epsilon_t + \epsilon_n = \epsilon_x + \epsilon_y \quad (30)$$

indicating that the sum of the orthogonal strains at a point is constant, regardless of the orientation of the pair in the plane. Equation (29a) may also be written in the form

$$\epsilon_t = \frac{\epsilon_x + \epsilon_y}{2} + \frac{\epsilon_x - \epsilon_y}{2} \cos 2\theta - \frac{\gamma_{xy}}{2} \sin 2\theta \quad (29c)$$

**22. Principal Strains.**—The directions of the principal strains, or maximum (and minimum) normal strains, may be found by differentiating Eq. (29a) with respect to  $\theta$  and equating the derivative to zero, which gives

$$\tan 2\theta = \frac{-\gamma_{xy}}{\epsilon_x - \epsilon_y} \quad (31)$$

The principal strain, therefore, is found to be

$$\epsilon_{u,v} = \frac{\epsilon_x + \epsilon_y}{2} \pm \frac{1}{2} \sqrt{(\epsilon_x - \epsilon_y)^2 + \gamma_{xy}^2} \quad (32)$$

Since the angle  $2\theta$  as given in Eq. (31) is multiple valued, and since the subscripts  $u$  and  $v$  may be assigned arbitrarily in Eq. (32), there remains the problem of identifying each of the principal strains with the proper direction. This may be done

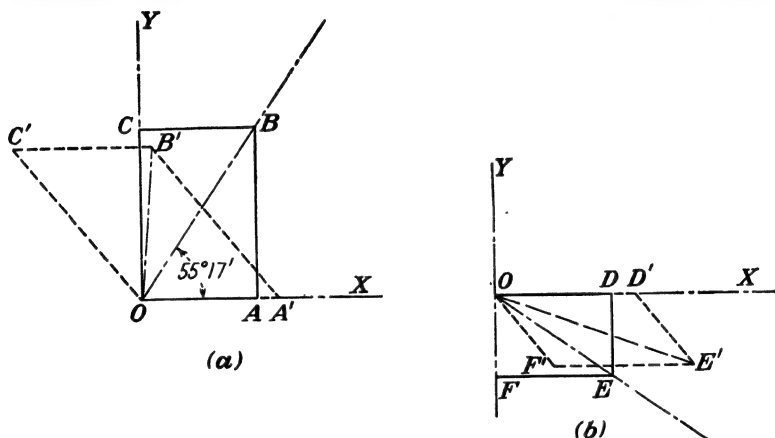


FIG. 17.—Sketches to identify axes of principal strains.

conveniently with the aid of a sketch as shown in Fig. 17. For example, assume  $\epsilon_x = +0.2$ ,  $\epsilon_y = -0.1$ ,  $\gamma_{xy} = +0.8$ . Then from Eq. (32)  $\epsilon_{u,v} = 0.050 \pm 0.427$ . Arbitrarily, let

$$\epsilon_u = +0.477,$$

$\epsilon_v = -0.377$ . From Eq. (31),  $\theta = -34^\circ 43'$  or  $+55^\circ 17'$ . In Fig. 17a one of the principal directions,  $55^\circ 17'$ , is sketched with reference to the  $x$  axis. From a point  $B$  on the diagonal axis perpendiculars are dropped to the  $x$  and  $y$  axes, forming the block  $OABC$  having a diagonal in one of the principal directions. If the given strains are applied to the block, it will take the position  $OA'B'C'$ . By inspection, the new diagonal  $OB'$  is shorter than the original  $OB$ ; hence, the direction  $OB$  is the direction of the compressive strain, or the  $v$  direction. This conclusion may be checked by a similar sketch using the other axis as the diagonal of the block as shown in Fig. 17b. In this block the diagonal  $OE$  lengthens, so  $OE$  is the direction of the maximum tensile strain, or the  $u$  direction.

**23. Shearing Strains.**—The shearing strains that are developed in different directions on the surface of a member may likewise be evaluated in terms of the strains in two orthogonal directions. The relationship between any shearing strain  $\gamma_{nt}$  in the plane and the shearing strain  $\gamma_{xy}$  will be developed first. This may be done by considering the geometry of a strained element such as the rectangular section  $OABC$  in Fig. 18. The sides  $OA$  and  $OC$  are in the directions of the known shearing strain  $\gamma_{xy}$  and the diagonal  $OB$  is taken in the  $t$  direction. The  $n$  direction is identified by dropping a perpendicular  $CD$  from  $C$  to  $OB$ . If

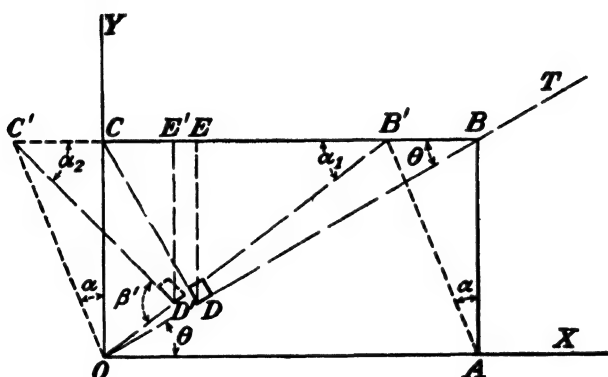


FIG. 18.—Resolution of shearing strain.

one side ( $BC$ ) of the element is slid with respect to the opposite side in such a way that the two sides remain parallel and at the same distance apart (the condition of shearing strain but no normal strain), the element takes the shape  $OAB'C'$ , and shearing strains are developed throughout it.

Point  $D$  is taken as one corner of an element inclined at an angle  $\theta$  with the  $x$  axis. When the element is strained, the point  $D$  moves parallel to the  $x$  axis to  $D'$ , on the new diagonal  $OB'$ . The side  $DC$  moves to  $D'C'$  and is no longer perpendicular to the diagonal but makes an angle  $\beta$  with it.

The change in angle at the corner of the block  $D$  is a measure of the shearing strain  $\gamma_{nt}$  occurring at an angle  $\theta$  with the  $x$  axis.

$$\gamma_{nt} = \tan (90^\circ - \beta) \quad (33)$$

$$= \cot \beta \quad (33a)$$

$$= \cot (\alpha_1 + \alpha_2)$$

From Fig. 18

$$\begin{aligned}\tan \alpha_1 &= \frac{OC}{CB'} = \frac{OB \sin \theta}{CB - BB'} = \frac{OB \sin \theta}{OB \cos \theta - OB \sin \theta \tan \alpha} \\ &= \frac{\sin \theta}{\cos \theta - \sin \theta \tan \alpha}\end{aligned}\quad (34a)$$

$$\begin{aligned}\tan \alpha_2 &= \frac{DE}{C'E'} = \frac{DE}{CE + OC \tan \alpha - EE'} \\ &= \frac{DE}{DE \tan \theta + OC \tan \alpha - OD \sin \theta \tan \alpha} \\ &= \frac{1}{\tan \theta + \tan \alpha} \\ &= \frac{\cos \theta}{\sin \theta + \cos \theta \tan \alpha}\end{aligned}\quad (34b)$$

Then from Eqs. (33a), (34a), and (34b)

$$\begin{aligned}\gamma_{nt} &= \frac{1 - \tan \alpha_1 \tan \alpha_2}{\tan \alpha_1 + \tan \alpha_2} \\ &= \tan \alpha \cos 2\theta - \frac{1}{2} \tan^2 \alpha \sin 2\theta\end{aligned}\quad (34c)$$

However

$$\tan \alpha = \gamma_{xy}$$

Hence, Eq. (34c) reduces to

$$\gamma_{nt} = \gamma_{xy} \cos 2\theta - \frac{1}{2} \gamma_{xy}^2 \sin 2\theta \quad (35)$$

$$= \gamma_{xy} \cos 2\theta \quad (35a)$$

when  $\gamma_{xy}$  is small.

It is evident that the maximum shearing strain developed in the element is  $\gamma_{xy}$  and that the shearing strain at 45 deg. with the  $x$  and  $y$  axes is zero.

Equation (35a) gives the value of the shearing strain developed in any direction due to an applied shearing strain  $\gamma_{xy}$ . Shearing strains are also developed when an element is subjected to normal strains. Their magnitudes may be determined by again considering the geometry of a deformed rectangular element.

If the original rectangular differential element  $OABC$  is subjected to the axial strains  $\epsilon_x$  and  $\epsilon_y$ , it will deform to the rectangle  $OA'B'C'$  as indicated in Fig. 19. The axes are selected as before in Fig. 18. The point  $D$  on the diagonal will move to  $D'$ , and the shearing strain  $\gamma_{nt}$  of the element that makes an angle  $\theta$  with the  $x$  axis may be expressed by Eq. (33) as before. From Fig. 18

$$\tan \alpha_1 = \frac{OC'}{C'B'} = \frac{(1 + \epsilon_y) dy}{(1 + \epsilon_x) dx} = \frac{(1 + \epsilon_y) \tan \theta}{1 + \epsilon_x} \quad (36a)$$

$$\tan \alpha_2 = \frac{EC'}{ED'} = \frac{(1 + \epsilon_y) dy \cos^2 \theta}{(1 + \epsilon_x) dx \sin^2 \theta} = \frac{(1 + \epsilon_y)}{(1 + \epsilon_x) \tan \theta} \quad (36b)$$

Then

$$\tan \beta = \frac{\frac{(1 + \epsilon_y)}{(1 + \epsilon_x)} (\tan \theta + \cot \theta)}{1 - \frac{(1 + \epsilon_y)^2}{(1 + \epsilon_x)^2}} \quad (36c)$$

$$= \frac{1 + \epsilon_y + \epsilon_x + \epsilon_y \epsilon_x}{(2\epsilon_x + \epsilon_x^2 - 2\epsilon_y - \epsilon_y^2) \sin \theta \cos \theta} \quad (36d)$$

$$\cot \beta = \frac{[2(\epsilon_x - \epsilon_y) + \epsilon_x^2 - \epsilon_y^2] \sin \theta \cos \theta}{1 + \epsilon_x + \epsilon_y + \epsilon_x \epsilon_y} \quad (36e)$$

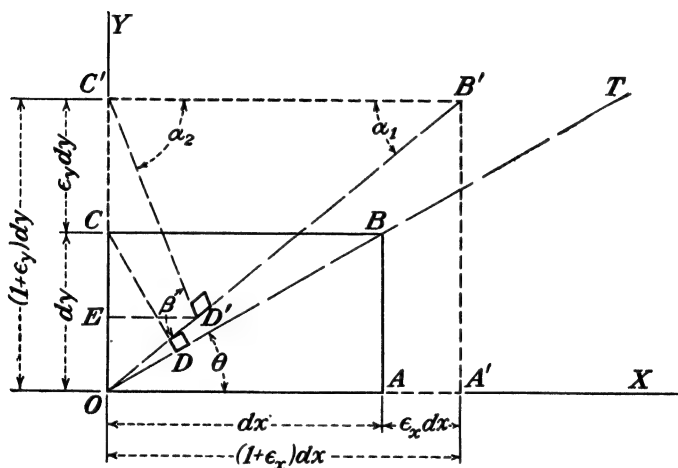


FIG. 19.—Shearing strain resulting from normal strains.

However,  $\epsilon_x^2$  and  $\epsilon_y^2$  may be dropped from the numerator and  $\epsilon_x$ ,  $\epsilon_y$ , and  $\epsilon_x \epsilon_y$  are usually small in comparison with unity in the denominator, so

$$\gamma_{nt} = (\epsilon_x - \epsilon_y) \sin 2\theta$$

The shearing strains in all directions are equal to zero when  $\epsilon_x = \epsilon_y$ . For example, no shearing strain is produced by a temperature change in an isotropic material if the material is not restrained. If  $\epsilon_x$  and  $\epsilon_y$  are not equal, the maximum shearing strain occurs at an angle of 45 deg. with the  $x$  and  $y$  axes.

If the original element is subjected to both normal and shearing

strains in the  $x$  and  $y$  directions, the resultant shearing strain at an angle  $\theta$  with the  $x$  direction may be found by adding the results of Eqs. (35a) and (37).

$$\gamma_{nt} = (\epsilon_x - \epsilon_y) \sin 2\theta + \gamma_{xy} \cos 2\theta \quad (38)$$

Equation (38) is similar in general form to Eq. (5a) for shearing stresses.

The direction of the maximum shearing strain may be determined by differentiating Eq. (38) with respect to  $\theta$  and equating the derivative to zero.

$$\frac{\partial \gamma_{nt}}{\partial \theta} = 2(\epsilon_x - \epsilon_y) \cos 2\theta - 2\gamma_{xy} \sin 2\theta = 0 \quad (39)$$

from which

$$\tan 2\theta = \frac{\epsilon_x - \epsilon_y}{\gamma_{xy}} \quad (39a)$$

A comparison of Eq. (39a) with Eq. (31) shows that the maximum shearing strain occurs at an angle of 45 deg. with the principal strain.

The magnitude of the maximum shearing strain  $\gamma_{ij}$  may be determined by substituting in Eq. (38) values of  $\sin 2\theta$  and  $\cos 2\theta$  which may be determined from Eq. (39a). Equation (38) then reduces to

$$\gamma_{ij} = \sqrt{(\epsilon_x - \epsilon_y)^2 + \gamma_{xy}^2} \quad (40)$$

The shearing strain in the directions of the maximum normal strains may be found by substituting the values of the angle from Eq. (31) in Eq. (38).

$$\begin{aligned} \gamma_{nt} &= \frac{(\epsilon_x - \epsilon_y)(-\gamma_{xy})}{\sqrt{(\epsilon_x - \epsilon_y)^2 + \gamma_{xy}^2}} + \frac{\gamma_{xy}(\epsilon_x - \epsilon_y)}{\sqrt{(\epsilon_x - \epsilon_y)^2 + \gamma_{xy}^2}} \\ &= 0 \end{aligned} \quad (41)$$

That is, there is no shearing strain in the direction of the principal strains. Therefore, the state of strain on the surface of a member may be described completely by the magnitudes and directions of the principal strains just as the state of stress may be described completely by the magnitudes and directions of the principal stresses.

If  $\epsilon_u$  and  $\epsilon_v$  are used to designate the values of the principal strains, the normal strain in a direction making an angle  $\theta_{ut}$



with the  $u$  axis is, from Eq. (29),

$$\epsilon_t = \epsilon_u \cos \theta_{ut} + \epsilon_v \sin \theta_{ut} \quad (42a)$$

$$= \frac{\epsilon_u + \epsilon_v}{2} + \frac{(\epsilon_u - \epsilon_v)}{2} \cos 2\theta_{ut} \quad (42b)$$

and the shearing strain on planes making an angle  $\theta_{ut}$  with the direction of the principal strains is, from Eq. (37),

$$\gamma_{nt} = 2(\epsilon_u - \epsilon_v) \sin \theta_{ut} \cos \theta_{ut} \quad (42c)$$

$$= (\epsilon_u - \epsilon_v) \sin 2\theta_{ut} \quad (42d)$$

From either Eq. (40) or from Eq. (42d) it is evident that the maximum shearing strain on the surface of a member is

$$\gamma_{ij} = \epsilon_u - \epsilon_v \quad (43)$$

This result is similar to that given in Eq. (20), which shows that the maximum shearing stress is equal to *one-half* the difference of the principal stresses.

**24. Evaluation of Principal Strains.**—As is indicated in Eq. (32) the principal strains may be evaluated from two orthogonal normal strains and the accompanying shearing strain. However, from the practical standpoint a means of evaluating the principal strains at a point from normal strains alone at the point is essential because strain-measuring equipment has been designed to measure normal rather than shearing strains.<sup>1</sup>

From the mathematical standpoint it is relatively easy to evaluate the principal strains in terms of three normal strains at the point instead of two normal strains and a shearing strain. The three normal strains may be designated as  $\epsilon_1$ ,  $\epsilon_2$ , and  $\epsilon_3$  and may be assumed to be oriented as indicated in Fig. 20, with  $\alpha$  and  $\beta$  denoting the angles<sup>2</sup> that  $\epsilon_2$  and  $\epsilon_3$  make with  $\epsilon_1$ .

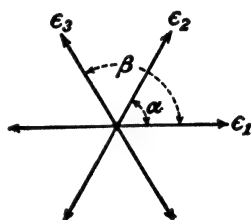


FIG. 20.—Designation of strains for Eq. 44.

<sup>1</sup> The measurement of a shearing strain involves the measurement of the change in angle between two reference lines, whereas the measurement of a normal strain requires only the determination of the change in distance between two reference points.

<sup>2</sup> From the laboratory standpoint, best results are obtained when the angles  $\alpha$  and  $\beta$  are 60 and 120 deg. Frequently, strains are measured on four intersecting gage lines at the point giving one "check" reading. The analysis of this special situation is outlined in Art. 29.

If the  $x$  direction is taken as the direction of  $\epsilon_1$ , two equations patterned after Eq. (29) may be written expressing  $\epsilon_2$  and  $\epsilon_3$  in terms of the three known quantities  $\epsilon_x$ ,  $\alpha$ , and  $\beta$ , and the two unknown strains  $\epsilon_y$  (at right angles to  $\epsilon_x$ ) and  $\gamma_{xy}$ .

$$\epsilon_2 = \epsilon_x \cos^2 \alpha + \epsilon_y \sin^2 \alpha - \gamma_{xy} \sin \alpha \cos \alpha \quad (44a)$$

$$\epsilon_3 = \epsilon_x \cos^2 \beta + \epsilon_y \sin^2 \beta - \gamma_{xy} \sin \beta \cos \beta \quad (44b)$$

The resulting equations may be solved simultaneously for  $\epsilon_y$  and  $\gamma_{xy}$ , after which the principal strains may be evaluated by Eqs. (30) and (32). An illustrative problem using this method is given in Art. 32.

Another procedure is to assume that the strain  $\epsilon_1$  makes an angle  $\theta$  with the direction of one of the principal strains (as yet unknown). Three equations of the type of Eq. (42b) may be written.

$$\epsilon_1 = \frac{\epsilon_u + \epsilon_v}{2} + \frac{(\epsilon_u - \epsilon_v)}{2} \cos 2\theta \quad (45a)$$

$$\epsilon_2 = \frac{\epsilon_u + \epsilon_v}{2} + \frac{(\epsilon_u - \epsilon_v)}{2} \cos 2\theta \cos 2\alpha - \frac{(\epsilon_u - \epsilon_v)}{2} \sin 2\theta \sin 2\alpha \quad (45b)$$

$$\epsilon_3 = \frac{\epsilon_u + \epsilon_v}{2} + \frac{(\epsilon_u - \epsilon_v)}{2} \cos 2\theta \cos 2\beta - \frac{(\epsilon_u - \epsilon_v)}{2} \sin 2\theta \sin 2\beta \quad (45c)$$

Since the quantities  $\epsilon_1$ ,  $\epsilon_2$ ,  $\epsilon_3$ ,  $\alpha$ , and  $\beta$  are known, the three equations may be solved simultaneously for the three unknowns  $\epsilon_u$ ,  $\epsilon_v$ , and  $\theta$ . The angle  $\theta$  is the angle that gage line 1 makes with the principal strains. The principal strains may be identified with their directions by inspection.

Several mechanical and electrical devices have been developed to determine automatically the directions and magnitudes of the principal strains from readings on a rosette at a point.<sup>1</sup>

<sup>1</sup> MURRAY, W. M., An Adjunct to the Strain Rosette, *Proc. Soc. Exptl. Stress Analysis*, Vol. 1, No. 1, pp. 128-133, 1943.

HOSKINS, E. E., and R. C. OLESON, An Electrical Computer for the Evaluation of Strain Rosette Data, *Proc. Soc. Exptl. Stress Analysis*, Vol. 2, No. 1, pp. 67-77, 1944.

MEIER, J. H., and W. R. MEHAFFEY, Electronic Computing Apparatus for Rectangular and Equiangular Strain Rosettes, *Proc. Soc. Exptl. Stress Analysis*, Vol. 2, No. 1, pp. 78-105, 1944.

MURRAY, W. M., Machine Solution of the Strain Rosette Equations, *Proc. Soc. Exptl. Stress Analysis*, Vol. 2, No. 1, pp. 106-112, 1944.

**25. Strain-measuring Equipment.**—Recognition of the importance of obtaining measurements of strain in structural members and machine parts under load has led to the development of a number of strain-measuring devices. Since the strains involved in the majority of structural materials are small within the working range (usually less than 0.002), some means of magnifying the change in distance between the reference points must be used. Among the techniques that have been developed<sup>1</sup>

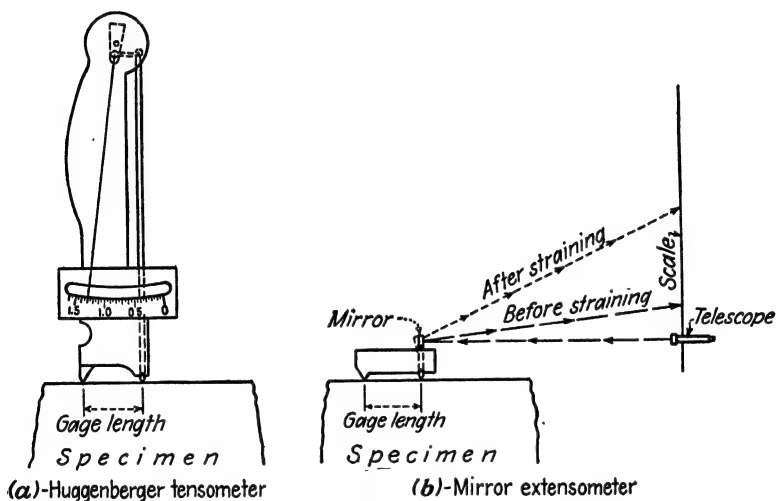


FIG. 21.—Examples of strain-measuring devices.

are (a) mechanical-lever systems, (b) optical levers, (c) electrical systems, (d) direct magnification by a microscope, and (e) use of a model constructed of a material having a lower modulus of elasticity.

**1. Mechanical-lever Systems.**—The standard strain gages such as the Berry and Whittemore make use of the mechanical magnification embodied in a dial indicator but are restricted to relatively long (2 in. or more) gage lengths. The Huggenberger tensometer<sup>2</sup> is a light-weight instrument with a  $\frac{1}{2}$ - or 1-in. gage

<sup>1</sup> Probably the most sensitive device available is the interferometer, which is sensitive to a change in a distance equal to one-half the wave length of light. The instrument is described by Houstoun in "A Treatise on Light" 7th ed., 1938.

<sup>2</sup> Voss, R. W., Characteristics of the Huggenberger Tensometer, *Proc. Am. Soc. Testing Materials*, Part 2, Vol. 34, p. 862, 1934.

length and a multiplication ratio of approximately 1,200. The principle upon which it is based is evident in Fig. 21a.

2. *Optical Levers*.—A beam of light is used as the magnifying lever in the Martens mirror extensometer<sup>1</sup> indicated in Fig. 21b and in the Tuckerman optical strain gage.<sup>2</sup>

3. *Electrical Systems*.—Several strain gages have been developed utilizing the fact that the electrical resistance of a wire is dependent upon the stress in the wire. One example of this type is the popular SR-4 Bonded Metaelectric strain gage, which may be cemented to the surface of the member. The change in gage length is indicated by a sensitive galvanometer in a Wheatstone bridge circuit. Since the gage weighs only a few grams, it is well adapted for measuring strain in rapidly moving parts such as propeller blades. A range of sensitivities and types, including rosettes, is available.

4. *Magnification by a Microscope*.—In the de Forest scratch extensometer, which is a light-weight instrument cemented in place, a stylus scratches a permanent record of the strain on a target, which can later be examined under a microscope.

A process known as the "photogrid process" has been developed<sup>3</sup> for photographing an accurate grid of closely spaced lines on the surface of a member. The load is applied to the member and the grid examined by a cathometer or under a microscope, or photographed and enlarged. Both axial and shearing strains may be evaluated by comparing the size and shape of the distorted grid with the original. Figure 22 shows photographs of a photogrid tensile specimen containing a pair of semicircular notches. The unequal distribution of strain across the reduced section is clearly visible in the bottom photograph.

<sup>1</sup> MARTENS, A., "Handbook of Testing Materials," trans. by G. C. Henning.

<sup>2</sup> TUCKERMAN, L. B., Optical Strain Gages and Extensometers, *Proc. Am. Soc. Testing Materials*, Part 2, Vol. 23, p. 602, 1923.

<sup>3</sup> CORNELL, K., Photogrid Printing, *Am. Phot.*, November, 1942.

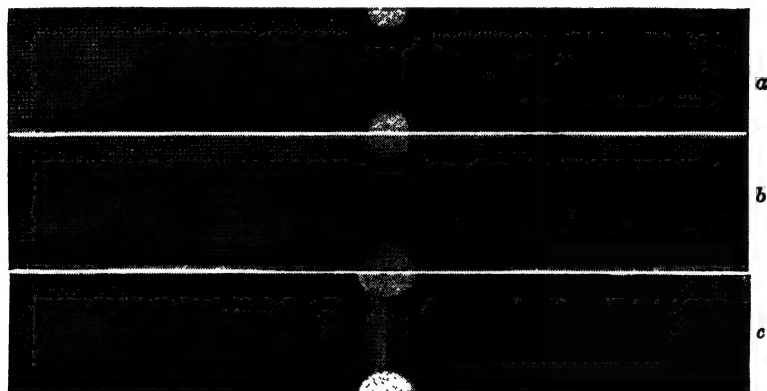
BREWER, G. A., and R. B. GLASSCO, Determination of Strain Distribution by the Photogrid Process, *J. Aeronaut. Science*, Vol. 9, pp. 1-7, November, 1941.

BREWER, G. A., Measurement of Strain in the Plastic Range, *Proc. Soc. Exptl. Stress Analysis*, Vol. 1, No. 2, pp. 105-115, 1944.

O'HAVEN, C. P., and J. F. HARDING, Studies of Plastic Flow Problems by Photogrid Methods, *Proc. Soc. Exptl. Stress Analysis*, Vol. 2, No. 2, p. 59, 1945.

The method has also been applied to the evaluation of plastic and residual strains. Studies of strains induced in metal by rolling have been made by simply scribing a grid on the surface of the material before rolling and examining the grid after rolling.<sup>1</sup>

5. *Flexible Model*.—An indication of the strains induced in a member may be obtained by marking a series of lines on the surface of a model made of rubber, or other material having a



(a) Before straining.  
(b) After start of plastic strain.  
(c) Near failure.

FIG. 22.—Strains in a notched bar indicated by photogrid process. (From *Studies of Plastic Flow Problems by Photogrid Methods*, C. P. O'Haven and J. F. Harding, *Proc. Soc. Exptl. Stress Analysis*, Vol. 2, No. 2, 1945.)

low modulus of elasticity, and noting the distortion of the original squares or rectangles when the member is loaded.

26. *Graphical Evaluation of Principal Strains*.—Under some conditions a graphical procedure for the evaluation of principal strains may be advantageous. Several graphical methods have been developed for the special cases of strains measured along gage lines that make angles of 45 or 60 deg. with each other,<sup>2</sup>

<sup>1</sup> MAC GREGOR, C. W., and L. F. COFFIN, JR., The Distribution of Strains in the Rolling Process, *Trans. Am. Soc. Mech. Engrs.*, Vol. 65, p. A-13, 1943.

<sup>2</sup> WISE, J. A., Circles of Strain, *J. Aeronaut. Science*, Vol. 7, pp. 438-440, August, 1940. CONTINI, R., A Graphic Solution for Strains and Stresses from Strain Rosette Data, *J. Aeronaut. Science*, Vol. 12, p. 47, January, 1945.

HILL, H. N., A Semi-graphical Method for Analyzing Strains Measured on Three or Four Gage Lines Intersecting at 45°, *Nat. Advisory Comm. Aeronaut. Tech. Note* 709, May, 1939. OSGOOD, W. R., and R. G. STURM,

and general graphical methods have been described by Westergaard and by Hansen.<sup>1</sup> A more convenient graphical method for strains,<sup>2</sup> which involves the construction of the Mohr circle, is as follows.

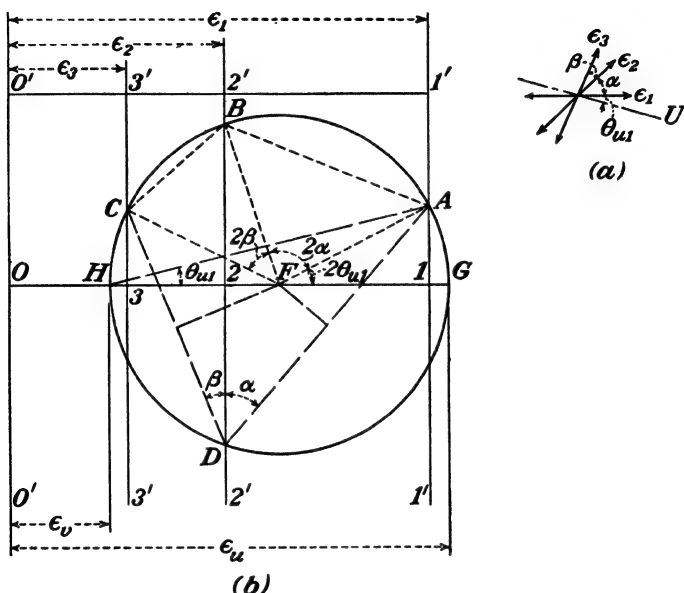


FIG. 23.—Construction of Mohr circle for strains.

The strains  $\epsilon_1$ ,  $\epsilon_2$ , and  $\epsilon_3$  are assumed to be measured along gage lines oriented with respect to each other as shown in Fig. 23a. From an origin  $O'$  the three strains are laid off to scale as  $O'-1'$ ,  $O'-2'$ , and  $O'-3'$  respectively. Tensile strains are laid off to the right and compressive strains to the left of  $O'$ . The lines  $O'00'$ ,  $1'1'1'$ ,  $2'2'2'$  and  $3'3'3'$  are drawn through  $O'$ ,  $1'$ ,  $2'$ , and  $3'$  perpendicular to  $O'-1'$  as shown in Fig. 23b. From an arbitrary

The Determination of Stresses from Strains on Three Intersecting Gage Lines and Its Application to Actual Tests, *Bur. Standards J. Research Paper No. 559*, 1933.

<sup>1</sup> WESTERGAARD, H. M., *Anwendung der Statik auf die Ausgleichungsrechnung*.

HANSEN, H. M., Discussion of paper entitled "An Adjunct to the Strain Rosette," *Proc. Soc. Exptl. Stress Analysis*, Vol. 1, No. 1, p. 138, 1943.

<sup>2</sup> MURPHY, GLENN, A Graphical Method for the Evaluation of Principal Strains from Normal Strains, *J. Applied Mech.*, Vol. 12, No. 4, p. A-209, 1945.

point  $D$  on the line  $2'22'$  lines making angles of  $\alpha$  and  $\beta$  with  $2'22'$  are drawn to intersect  $1'11'$  and  $3'33'$  in points  $A$  and  $C$  respectively. The intersection of the perpendicular bisectors of  $AD$  and  $CD$  determines a point  $F$ . With  $F$  as a center a circle having a radius  $FA = FC = FD$  is drawn. This is the Mohr circle for strains. The intersection of a horizontal line through the center  $F$  with the line  $0'00'$  locates  $O$ , the new origin for the Mohr circle, and the intersection of the circle with  $OF$  locates points  $G$  and  $H$ .

The two principal strains are equal to  $OG$  and  $OH$ , and the maximum shearing strain is equal to  $GH$ , the diameter of the circle. The angle that gage line 1 makes with the direction of the principal strain is the angle  $GHA$  or one-half of the angle  $GFA$ .

To prove the validity of the construction, point  $B$  is located as the intersection of the circle and the line  $2'22'$ . Since the arc  $AB$  in the circle of Fig. 23b is common to both triangles  $ADB$  and  $AFB$  with point  $F$  at the center and  $D$  on the circumference of the circle, the angle  $AFB$  is equal to  $2\alpha$ . Similarly the angle  $BFC$  is equal to  $2\beta$ .

An equation of the type of Eq. (42b) may be written for each of the strains. For example

$$\epsilon_1 = \frac{\epsilon_u + \epsilon_v}{2} + \frac{(\epsilon_u - \epsilon_v)}{2} \cos 2\theta \quad (42b)$$

From the construction it is evident that

$$OF = \frac{\epsilon_u + \epsilon_v}{2}$$

$$FA = \frac{\epsilon_u - \epsilon_v}{2} = \text{radius of the circle}$$

The horizontal projection of the radius  $FA$  on the diameter is

$$F1 = \left( \frac{\epsilon_u - \epsilon_v}{2} \right) \cos 2\theta$$

Therefore

$$\epsilon_1 = OF + F1 = O1$$

which checks the original construction.

Similarly

$$\begin{aligned} \epsilon_2 &= \frac{\epsilon_u + \epsilon_v}{2} + \frac{(\epsilon_u - \epsilon_v)}{2} \cos 2(\theta + \alpha) \\ &= OF + F2 = O2 \end{aligned}$$

and

$$\begin{aligned}\epsilon_3 &= \frac{\epsilon_u + \epsilon_v}{2} + \frac{(\epsilon_u - \epsilon_v)}{2} \cos 2(\theta + \alpha + \beta) \\ &= OF + F3 = O3\end{aligned}$$

The diameter of the circle is  $GH$

$$\begin{aligned}GH &= OG - OH \\ &= \epsilon_u - \epsilon_v \\ &= \gamma_{ij}\end{aligned}$$

from Eq. (43).

### PROBLEMS

26. In the derivation of Eq. (4) the condition  $S_{xy} = S_{yz}$  was used. Prove that the relationship is valid.

27. Is Eq. (11) valid above the proportional limit? Explain.

28. In a structural member  $S_x = 3,000$  p.s.i.,  $S_y = -5,000$  p.s.i., and  $S_{xy} = 4,000$  p.s.i. Determine the stresses on a plane that makes an angle of 30 deg. with the  $x$  direction. Solve using a free-body diagram and check using Eqs. (4) and (5).

29. At a point on the surface of a structural member,  $S_x$  is 8,660 p.s.i. tension,  $S_y$  is 2,890 p.s.i. tension, and  $S_{xy} = -5,000$  p.s.i. Determine the normal and shearing stresses on a plane that makes an angle of 30 deg. with the  $x$  direction.

30. A triangular wedge, similar to Fig. 7, for which  $\theta = 60$  deg. is subjected to the stresses  $S_n = -3,330$  p.s.i.,  $S_{xy} = 5,000$  p.s.i., and  $S_{tn} = 7,700$  p.s.i. (up the plane). Determine  $S_x$  and  $S_y$ .

31. At a point on the surface of a machine part,  $S_x = 4,000$  p.s.i.,  $S_y = -6,000$  p.s.i., and  $S_{xy} = -3,000$  p.s.i. In what direction is the normal stress zero?

32. At a point,  $S_x = 24,000$  p.s.i.,  $S_y = -12,000$  p.s.i., and  $S_{xy} = 15,000$  p.s.i. On what plane is  $S_n$  equal to 10,000 p.s.i., and what is the shearing stress on that plane?

33. A wedge-shaped free body, similar to that in Fig. 7, is 4 units long in the  $x$  direction and 3 units long in the  $y$  direction.  $S_x = 3,000$  p.s.i.,  $S_y = 4,000$  p.s.i., and  $S_n = 5,000$  p.s.i. Determine the shearing stresses  $S_{xy}$  and  $S_{tn}$ , if any.

34. If  $S_x$  and  $S_y$  are both tension at a point, can a compressive stress exist on any plane through the point? Explain.

35. A cylindrical tank 6 ft. in diameter is made of plates  $\frac{1}{4}$  in. thick. The tank is built with a spiral seam that makes an angle of 30 deg. with a transverse plane normal to the axis of the tank. Determine the magnitude of normal force and shearing force per inch of joint when the pressure in the tank is 140 p.s.i.

36. The Wood Handbook of the Forest Products Laboratory, U.S. Department of Agriculture, specifies that the allowable compressive stress for a post in which the grain has a slope of 1 horizontal to 6 vertical shall



not exceed about 53 per cent of the allowable stress in compression parallel to the grain. What ratio of shearing strength along the grain to compressive strength does this imply?

**37.** A timber beam 6 in. wide and 12 in. deep carries a concentrated load at the center of a 16-ft. span. At a point 3 in. above the bottom of the beam at the center the grain has a slope of 1 vertical to 2.4 horizontal. Determine the ratio of the critical shearing stress (along the grain) to the horizontal tensile stress at the point.

**38.** Evaluate  $S_n$  and  $S_{tn}$  at intervals of  $\theta = 15$  deg. from 0 to 360 deg. for  $S_x = 10,000$  p.s.i.,  $S_y = 20,000$  p.s.i., and  $S_{xy} = 0$ . Plot the results using polar coordinates.

**39.** Using polar coordinates, plot a pair of curves showing the variation in the normal and shearing stress with  $\theta$  from 0 to 360 deg., if  $S_x = 10,000$  p.s.i.,  $S_y = 2,000$  p.s.i., and  $S_{xy} = 3,000$  p.s.i.

**40.** Solve Prob. 39 for  $S_x = 10,000$  p.s.i.,  $S_y = -2,000$  p.s.i., and

$$S_{xy} = 3,000 \text{ p.s.i.}$$

**41-47.** For the following combinations of stresses determine the principal stresses and the maximum shearing stress. Show the directions on a sketch.

Prob. no.	$S_x$ p.s.i.	$S_y$ p.s.i.	$S_{xy}$ p.s.i.
<b>41</b>	6,000	4,000	3,000
<b>42</b>	6,000	-4,000	3,000
<b>43</b>	6,000	-4,000	-3,000
<b>44</b>	6,000	10,000	2,000
<b>45</b>	-6,000	10,000	-2,000
<b>46</b>	1,000	3,000	12,000
<b>47</b>	1,000	-1,000	8,000

**48.** A timber beam 6 in. wide and 12 in. deep carries a concentrated load of 14,400 lb. at the center of a 48-in. span. Determine the magnitude and direction of the principal stresses and the maximum shearing stress at a point 6 in. from one end and 2 in. above the bottom of the beam.

**49.** Show on a sketch the directions of the principal stresses throughout the beam of Prob. 48.

**50.** A cantilever beam 6 in. wide, 12 in. deep, and 8 ft. long carries a concentrated load of 3,000 lb. at the free end. Sketch three sets of stress contours, one for tension, one for compression, and one for maximum shearing stresses.

**51.** A cylindrical boiler 6 ft. in diameter has a wall thickness of 1 in. If the internal pressure is 5,000 p.s.i., determine the principal stresses and the maximum shearing stress at a point.

- a. On the inside of the shell.
- b. On the outside of the shell.

52. A 1.250-in.-diameter shaft is used to transmit 100 hp. at 1,800 r.p.m. Determine the maximum tensile, compressive, and shearing stresses developed at a section of the shaft that is not near the end connections.

53. An airplane engine transmits 2,000 hp. at 1,800 r.p.m. through a shaft having an external diameter of 4 in. The maximum thrust developed is 8,000 lb. Determine the maximum internal diameter of the shaft if the maximum tensile stress is not to exceed 10,000 p.s.i.

54. Solve Prob. 41 graphically.

55. Solve Prob. 42 graphically.

56. Solve Prob. 43 graphically.

57. Solve Prob. 44 graphically.

58. Solve Prob. 45 graphically.

59. Solve Prob. 46 graphically.

60. Solve Prob. 47 graphically.

61. A conical vessel with a base diameter of 4 ft., an altitude of 6 ft., and a wall thickness of  $\frac{1}{4}$  in., is suspended with the apex down and filled with water. Determine the principal stresses and maximum shearing stress at a point on the inside of the wall midway between the base and the apex.

62. At a point in a structural member  $S_x = 10,000$  p.s.i.,  $S_y = 6,000$  p.s.i.,  $S_z = 8,000$  p.s.i.,  $S_{xy} = S_{yz} = 4,000$  p.s.i., and  $S_{xz} = S_{yz} = S_{xy} = 0$ . Determine the principal stresses and the maximum shearing stress.

63. In a certain structural member  $S_u = 12,000$  p.s.i.,  $S_v = 16,000$  p.s.i., and  $S_w = 0$ . Determine the stresses on a plane that makes an angle of 30 deg. with the  $uv$  plane and is perpendicular to the  $w$  plane.

64. For each of the following combinations of principal stresses, determine by means of the Mohr circle the maximum shearing stress and the stresses on the plane which makes the indicated angle with the  $u$  axis. Show directions by means of a sketch of a triangular element of the material.

	$S_u$	$S_v$	$\theta$
a	+8,000	+4,000	30°
b	+8,000	-4,000	-30°
c	+8,000	00	60°
d	-4,000	-4,000	60°

65. A cylinder 10 ft. in diameter has a wall thickness of  $\frac{3}{4}$  in.

a. Construct a Mohr circle for a point on the outside surface, and from it determine the maximum shearing stress when the internal pressure is 200 p.s.i.

b. Will the maximum shearing stress at a point on the inside of the shell be the same? Explain.

66. Solve Prob. 65 if the container is spherical instead of cylindrical.

67. Derive Eq. (27).

68. Derive Eq. (28).

69. Develop the general equation for any stress contour for the beam of Fig. 14.

70. A simple beam of rectangular cross section carries a concentrated load at the center. Develop the general equation for the isoclinics. Neglect stress concentration.

71. Derive an equation for the stress trajectories for a cantilever beam of rectangular cross section carrying a concentrated load at the end.

72. A horizontal member having a width of 6 in. and a depth of 12 in. is simply supported at two points 4 ft. apart and carries a uniformly distributed load of 1,200 lb. per linear inch on the top surface between supports.

a. Sketch the contours for maximum shearing stress.

b. Construct the isoclinics at 10-deg. intervals.

c. Sketch a set of stress trajectories.

73. If  $\epsilon_x = +0.00060$ ,  $\epsilon_y = -0.00040$ , and  $\gamma_{xy} = +0.00025$ , determine the normal strain along a line that makes an angle with the  $x$  direction of (a)  $+30$  deg., (b)  $-30$  deg.

74. A rectangle 1.5000 by 0.5000 in. was laid out on the surface of a member. After the member was loaded the long sides of the rectangle had rotated through an angle of  $+0^\circ 4' 25''$  and had lengthened 0.0009 in., while the short sides had rotated through an angle of  $-0^\circ 2' 11''$  and had shortened 0.0002 in. Determine the normal strain along each diagonal of the rectangle.

75. From the data given in Prob. 73 determine the principal strains at the point.

76. Determine the principal strains in the rectangle of Prob. 74.

77. At a point in a structural member  $\epsilon_x = +0.00100$ ,  $\epsilon_y = -0.00060$ , and  $\gamma_{xy} = +0.00050$ . Determine the shearing strain developed on a rectangular block the sides of which make an angle of 30 deg. with the  $x$  and  $y$  directions respectively. Show the directions on a sketch of the block.

78. Circles 0.5000 in. in diameter were scribed on the surface of billets that were to be cold rolled. After the cold rolling the circles were found to be ellipses with major axes of 0.5048 in. and minor axes of 0.4972 in. Determine the maximum residual unit shearing strain.

79. Determine the maximum shearing strain at the point in Prob. 77.

80. Determine the maximum shearing strains in the rectangle of Prob. 74 and show their directions on a sketch.

81. Outline the procedure for constructing a Mohr circle for strains from given values of two normal strains and the accompanying shearing strains.

82. Develop an expression for the multiplication ratio of an optical lever of the type shown in Fig. 21b.

83. At a point on the surface of a flat plate,  $\epsilon_x$  is measured as  $+0.00100$ , and the strains along lines making angles of  $+60$  deg. and  $-60$  deg. with the  $x$  direction are  $-0.00030$  and  $+0.00040$  respectively. Determine the magnitudes and directions of the principal strains using both methods outlined in Art. 24.

84-88. In each of the following problems  $\epsilon_1$  is measured in the  $x$  direction,  $\epsilon_2$  at an angle of 60 deg. with the  $x$  direction, and  $\epsilon_3$  at an angle of 120 deg. with the  $x$  direction. Determine the principal strains.

Prob. No.	$\epsilon_1$	$\epsilon_2$	$\epsilon_3$
<b>84</b>	+0.00100	+0.00100	+0.00100
<b>85</b>	+0.00100	-0.00100	+0.00100
<b>86</b>	+0.00020	+0.00040	-0.00060
<b>87</b>	+0.00020	-0.00040	+0.00060
<b>88</b>	+0.00020	+0.00040	+0.00060

**89-93.** The strains indicated in the following problems were measured on rosettes in which the gage lines were at intervals of 45 deg. Determine the principal strains.

Prob. No.	$\epsilon_1$	$\epsilon_2$	$\epsilon_3$	$\epsilon_4$
<b>89</b>	+0.00080	-0.00040	+0.00020	+0.00140
<b>90</b>	+0.00074	+0.00035	-0.00012	+0.00027
<b>91</b>	+0.00036	+0.00012	+0.00007	+0.00031
<b>92</b>	+0.00050	+0.00080	+0.00024	-0.00002
<b>93</b>	+0.00043	+0.00013	-0.00012	+0.00014

**94.** Strains were measured along 4 gage lines at 45 deg. with each other at a point on the surface of a bulkhead. The values obtained were +0.00100, -0.00070, -0.00040, and +0.00130 in sequence. Determine the magnitudes and directions of the principal strains and of the maximum shearing strain.

**95.** Solve Prob. 83 graphically.

**96.** Solve Prob. 94 graphically.

**97.** Are Eqs. (31) and (32) valid above the proportional limit? Explain.

**98.** How large may  $\gamma_{xy}$  become before Eq. (32a) is 10 per cent in error?

**99.** If  $\epsilon_x = -\epsilon_y$ , what magnitude must they have to result in a 10 per cent error in Eq. (37)?

**100.** If the principal strains are known, can strains in other directions be determined graphically? Explain.

### CHAPTER III

#### STRESS-STRAIN RELATIONSHIPS

**27. Need for Relationships.**—As has been indicated, one step in the process of evaluating the load-carrying capacity of a structural member involves the determination of the distribution of stress throughout the member, or at least evaluating the stress at the critical sections in the member. The maximum, or critical, stresses are then compared with the stresses associated with failure of the material as evidenced by excessive strain (slip, creep, or fracture). Because of the uncertainties of assumptions involved in analytical determinations or because of the mathematical difficulties often encountered in analytical solutions, it frequently is desirable to obtain information regarding load-carrying capacity by direct observation of actual loaded members. Since stresses cannot be measured or observed directly, the stress distribution must be evaluated through observation of strains (or displacements that may be converted to strains) combined with a knowledge of the stress-strain behavior of the material. Therefore, the determination of the stress-strain relationships is of primary importance. These basic relationships can be established only by direct observation in the laboratory.

As a matter of convenience, most laboratory tests conducted for the purpose of establishing the relationship between stress and strain in a given material are made by subjecting a standardized specimen of the material to axial loading, *i.e.*, to a direct tensile or compressive test, or to torsion, and measuring the strains that occur in a standard length. Then, in analyzing a member of complex shape or loading, each element of the material is assumed to have the same characteristics as those which were observed in the simple specimen tested in the laboratory.

**28. Relationships under Axial Stress.**—From the axial test of a material a stress-strain diagram of the type shown in Fig. 3 or 4 may be obtained, which shows graphically the relationship between the principal stress and the principal strain. If the

proportional limit is not exceeded the relationship may be expressed analytically as

$$S_u = E\epsilon_u \quad (46)$$

in which the constant  $E$  is the quantity known as the "modulus of elasticity." For stresses above the proportional limit the relationship becomes more involved, the general equation being expressed as

$$S_u = f(\epsilon_u) \quad (46a)$$

or, if creep can occur,

$$S_u = f(\epsilon_u, t) \quad (46b)$$

A parabola has been used to approximate the diagram for some concretes.<sup>1</sup> While, in general, the stress-strain relationship is a function of the chemical composition of the material, the techniques used in shaping it, and the environment in which it is tested, certain factors affecting the strength of concrete and timber do not alter the basic shape of the stress-strain diagram.<sup>2</sup>

Even when the load is axial, strains are produced in directions other than the direction of the load. Below the proportional limit a definite relationship exists between the strain at right angles to the load and the strain (and hence, the stress) in the direction of the load. If the stress is applied in the  $u$  direction

$$\epsilon_v = -\mu\epsilon_u \quad (47)$$

in which  $\mu$  is Poisson's ratio.

From Eq. (46)

$$\epsilon_v = -\frac{\mu S_u}{E} \quad (47a)$$

The minus sign indicates that the strain in the  $v$  direction is compressive when the strain in the  $u$  direction is tensile, and vice versa. If the stresses are above the proportional limit, neither  $E$  nor  $\mu$  are constant but depend upon  $\epsilon_u$ .

**29. Relationships under Triaxial Stress.**—If a material is subjected to the principal stresses  $S_u$ ,  $S_v$ , and  $S_w$ , the unit strain in

<sup>1</sup> TALBOT, A. N., Tests of Reinforced Concrete Beams, Series of 1905, *Univ. Illinois Eng. Expt. Sta. Bull.* 4, 1906.

<sup>2</sup> GILKEY, H. J., and GLENN MURPHY, The Percentage Stress-strain Diagram as an Index to the Comparative Behavior of Materials under Load, *Iowa Eng. Expt. Sta. Bull.* 159, 1943.

each direction is a function of the three stresses and the properties of the material. If it is assumed that the individual effects of each stress are additive (*i.e.*, that superposition is valid), the expressions for the unit strains in the principal directions are

$$\epsilon_u = f_1(S_u) + f_2(S_v) + f_3(S_w) \quad (48a)$$

$$\epsilon_v = f_4(S_u) + f_5(S_v) + f_6(S_w) \quad (48b)$$

$$\epsilon_w = f_7(S_u) + f_8(S_v) + f_9(S_w) \quad (48c)$$

If the proportional limit of the material in each direction is not exceeded, and if Poisson's ratio is constant

$$\epsilon_u = C_1 S_u + C_2 S_v + C_3 S_w \quad (49a)$$

$$\epsilon_v = C_4 S_u + C_5 S_v + C_6 S_w \quad (49b)$$

$$\epsilon_w = C_7 S_u + C_8 S_v + C_9 S_w \quad (49c)$$

The constants  $C_1$ ,  $C_5$ , and  $C_9$  are the reciprocals of the moduli of elasticity while the remainder of the constants are equal to the respective Poisson's ratios divided by the appropriate moduli of elasticity.

$$\epsilon_u = \frac{S_u}{E_u} - \frac{\mu_{uv}}{E_v} S_v - \frac{\mu_{uw}}{E_w} S_w \quad (50a)$$

$$\epsilon_v = \frac{-\mu_{vu}}{E_u} S_u + \frac{S_v}{E_v} - \frac{\mu_{vw}}{E_w} S_w \quad (50b)$$

$$\epsilon_w = \frac{-\mu_{wu}}{E_u} S_u - \frac{\mu_{wv}}{E_v} S_v + \frac{S_w}{E_w} \quad (50c)$$

Minus signs have been introduced into Eq. (50) to take care of the reversal of strain in the Poisson effect, *i.e.*, each  $\mu$  indicates only the magnitude of Poisson's ratio.

From Eq. (50) it is evident that nine constants—three moduli of elasticity and six Poisson's ratios—are required to define the geometrical behavior of the material below the proportional limit. However, if the material is isotropic, two constants, one modulus of elasticity and one Poisson's ratio, are sufficient. Then

$$E\epsilon_u = S_u - \mu(S_v + S_w) \quad (51a)$$

$$E\epsilon_v = S_v - \mu(S_w + S_u) \quad (51b)$$

$$E\epsilon_w = S_w - \mu(S_u + S_v) \quad (51c)$$

**30. Shearing Strains.**—The resultant strains in the direction of the principal stresses are the principal strains. A change in dimensions of a material usually involves shearing strains as well as normal strains. If the shearing stresses are known,

the shearing strains may be evaluated directly from the stress-strain relationships of the material in shear. For example, if the shearing stresses are below the proportional limit, the definition of the modulus of rigidity (modulus of elasticity in shear)  $G$  gives

$$G_{uv} = \frac{S_{uv}}{\gamma_{uv}} \quad (52)$$

or

$$\gamma_{uv} = \frac{S_{uv}}{G_{uv}} \quad (52a)$$

$$\gamma_{vw} = \frac{S_{vw}}{G_{vw}} \quad (52b)$$

$$\gamma_{wu} = \frac{S_{wu}}{G_{wu}} \quad (52c)$$

For stresses below the proportional limit a definite relationship exists among the modulus of elasticity, the modulus of rigidity, and Poisson's ratio. The relationship may be developed by considering the strain  $\epsilon_t$  along the diagonal of a block subjected to a shearing strain  $\gamma_{xy}$ , as in Fig. 18. From Eq. (29)

$$\begin{aligned} \epsilon_t &= -\frac{1}{2}\gamma_{xy} \sin 2\theta \\ &= -\frac{1}{2} \frac{S_{xy}}{G} \sin 2\theta \end{aligned} \quad (53a)$$

The strain in the  $t$  direction may also be evaluated in terms of the stresses in the  $t$  and  $n$  directions by Eq. (51a)

$$E\epsilon_t = S_t - \mu S_n$$

The stresses  $S_t$  and  $S_n$  may be expressed in terms of  $S_{xy}$  by Eq. (4c)

$$\begin{aligned} E\epsilon_t &= S_{xy} \sin 2(\theta + 90^\circ) - \mu S_{xy} \sin 2\theta \\ &= -S_{xy}(1 + \mu) \sin 2\theta \end{aligned} \quad (53b)$$

Equation (53b) divided by Eq. (53a) gives

$$E = 2(1 + \mu)G \quad (54)$$

Since Eq. (54) is developed using Eqs. (51a) and (53a) it is subject to the limitations that the material is homogeneous and isotropic and that neither the proportional limit for normal stress nor for shearing stress is exceeded.

**31. Principal Stresses from Principal Strains.**—The principal stresses may be evaluated from the principal strains or strains



in the direction of the principal stresses. If Eqs. (51a), (51b), and (51c) are solved simultaneously for the principal stress  $S_u$ , there results

$$S_u = \frac{E[\epsilon_u + \mu(-\epsilon_u + \epsilon_v + \epsilon_w)]}{1 - \mu - 2\mu^2} \quad (55a)$$

$$= E \left[ \frac{\epsilon_u}{1 + \mu} + \frac{\mu(\epsilon_u + \epsilon_v + \epsilon_w)}{(1 + \mu)(1 - 2\mu)} \right] \quad (55b)$$

This may be simplified by introducing a quantity  $e$  called the cubical dilatation and defined by

$$e = \epsilon_u + \epsilon_v + \epsilon_w \quad (55c)$$

Then

$$S_u = \frac{E}{1 + \mu} \left[ \epsilon_u + \frac{\mu e}{1 - 2\mu} \right] \quad (55d)$$

Similarly, the principal stresses in the  $v$  and  $w$  directions are determined as

$$S_v = \frac{E}{1 + \mu} \left[ \epsilon_v + \frac{\mu e}{1 - 2\mu} \right] \quad (55e)$$

$$S_w = \frac{E}{1 + \mu} \left[ \epsilon_w + \frac{\mu e}{1 - 2\mu} \right] \quad (55f)$$

If the principal strains are not known, the principal stresses may still be evaluated from strains, but for the triaxial stress condition three normal and three shearing strains are required. In any event, six quantities—three principal strains and their three directions, or three normal strains and the accompanying three shearing strains—are required for the evaluation of principal stresses at a point subjected to triaxial stress.

For the two-dimensional stress condition  $S_w = 0$  and Eqs. (51a) and (51b) for an isotropic material reduce to

$$E\epsilon_u = S_u - \mu S_v \quad (56a)$$

$$E\epsilon_v = -\mu S_u + S_v \quad (56b)$$

from which

$$S_u = \frac{E(\epsilon_u + \mu\epsilon_v)}{1 - \mu^2} = E'(\epsilon_u + \mu\epsilon_v) \quad (57a)$$

$$S_v = \frac{E(\mu\epsilon_u + \epsilon_v)}{1 - \mu^2} = E'(\epsilon_v + \mu\epsilon_u) \quad (57b)$$

in which the term  $E'$  is an "effective modulus of elasticity."

$$E' = \frac{E}{1 - \mu^2} \quad (58)$$

Therefore, if the principal directions are known, the principal stresses at a point in a biaxial stress situation may be evaluated from the two normal strains in the corresponding directions. If the principal directions are not known, the principal stresses may be evaluated from two normal strains and the accompanying shearing strain or from three normal strains.

**32. Evaluation of Principal Stresses from Strains Measured on a Rosette.**—In many situations where the evaluation of stresses by the usual mathematical processes is difficult or impossible, valuable information concerning the stresses may be obtained by measuring the strains developed in a model or a trial design of the prototype and converting the strains into stresses. The usual procedure involves the measurement of the normal strains on a rosette of three or four intersecting gage lines at the point.<sup>1</sup> A few more or less standard rosettes have come into general use. They include

1. The “delta” rosette—3 gage lines at 60 deg.
2. The “fan” rosette—4 gage lines at 45 deg.
3. The “tee-delta” rosette—4 gage lines, 0, 60, 90, 120 deg.

After the normal strains have been determined, there are several slightly different analytical procedures, as well as the graphical procedure outlined in Art. 26, for evaluating the principal biaxial strains from measured tensile or compressive strains, all being based upon the equations expressing the relationships among the strains at a point.

After the principal strains have been determined, the principal stresses may be evaluated by Eq. (57).

Two solutions based on the procedures outlined in Art. 24 follow.

#### METHOD A

If the  $x$  direction is taken in the direction of one of the measured strains, an equation of the form of Eq. (44) may be written for each of the other measured strains. The resulting set of simultaneous equations will contain only  $\epsilon_y$  and  $\gamma_{xy}$  as unknowns and may be solved for  $\epsilon_y$  and  $\gamma_{xy}$ , after which Eqs. (31) and (32)

<sup>1</sup> A minimum of three normal strains is required, but a reading on an additional gage line is frequently taken as a check. Of course, two normal strains and the corresponding shearing strain could theoretically be used, but techniques for measuring shearing strains are not developed so well as techniques for measuring normal strains.

may be applied to determine the magnitude and direction of the principal strains. The principal stresses may then be found from Eq. (57).

*Illustrative Problem.*—Strains observed along three gage lines of a delta rosette at a point on the surface of a steel member are  $\epsilon_1 = +0.00060$ ,  $\epsilon_2 = -0.00010$ ,  $\epsilon_3 = +0.00040$ . Determine the principal stresses.

*Solution.*—Assume the  $x$  direction to be in the direction of  $\epsilon_1$  and apply Eq. (44a)

$$\begin{aligned}\epsilon_2 &= 0.00060 \cos^2 60^\circ + \epsilon_y \sin^2 60^\circ - \gamma_{xy} \sin 60^\circ \cos 60^\circ \\ -0.00010 &= 0.00015 + \frac{3}{4}\epsilon_y - \sqrt{\frac{3}{4}}\gamma_{xy}\end{aligned}$$

or

$$\epsilon_y - \sqrt{\frac{3}{4}}\gamma_{xy} = -0.000333 \quad (a)$$

Then from Eq. (44b)

$$\begin{aligned}\epsilon_3 &= 0.00060 \cos^2 120^\circ + \epsilon_y \sin^2 120^\circ - \gamma_{xy} \sin 120^\circ \cos 120^\circ \\ 0.00040 &= 0.00015 + \frac{3}{4}\epsilon_y + \sqrt{\frac{3}{4}}\gamma_{xy}\end{aligned}$$

or

$$\epsilon_y + \sqrt{\frac{3}{4}}\gamma_{xy} = +0.000333 \quad (b)$$

The solution of (a) and (b) as simultaneous equations gives<sup>1</sup>

$$\begin{aligned}\epsilon_y &= 0 \\ \gamma_{xy} &= 0.000577\end{aligned}$$

The magnitudes of the principal strains are, from Eq. (32),

$$\begin{aligned}\epsilon_{u,v} &= 0.00001(30 \pm \frac{1}{2}\sqrt{60^2 + 57.7^2}) \\ &= 0.00001(30 \pm 41.6) \\ \epsilon_u &= 0.000716 \\ \epsilon_v &= -0.000116\end{aligned}$$

The directions of the principal strains may be determined from Eq. (31)

$$\begin{aligned}\tan 2\theta &= \frac{-0.000577}{0.00060} = -0.962 \\ \theta_{xu} &= -21^\circ 57' \\ \theta_{xv} &= 68^\circ 3'\end{aligned}$$

The minus sign of  $\theta_{xu}$  designates a line in the fourth (and second) quadrants. The second principal strain is normal to the

<sup>1</sup> It will be noted that when  $\alpha = 60$  deg. and  $\beta = 120$  deg. the difference of Eqs. (a) and (b) gives  $\gamma_{xy} = \frac{\epsilon_3 - \epsilon_2}{0.866}$ . When  $\alpha = 45$  deg., and  $\beta = 90$  deg.

$$\gamma_{xy} = 2\epsilon_2 = (\epsilon_1 + \epsilon_3)$$

first. The angles are paired with the proper strains by inspection. The magnitudes of the principal stresses may be found from the principal strains by applying Eq. (57). If

$$\begin{aligned} E &= 30 \times 10^6 \text{ p.s.i.} & \text{and} & \mu = 0.30 \\ S_u &= 22,500 \text{ p.s.i. tension} \\ S_v &= 3,260 \text{ p.s.i. tension} \end{aligned}$$

The directions of the principal stresses are the same as the directions of the principal strains.

### METHOD B

Values of each of the three measured strains may be substituted as the left-hand side of Eq. (42b), giving three simultaneous equations in the three unknowns  $\epsilon_u$ ,  $\epsilon_v$ , and  $\theta$ . The principal strains may then be evaluated from the solution of the set of equations, and the principal stresses evaluated using Eq. (57). Both Bergman<sup>1</sup> and Osgood<sup>2</sup> have presented a standardized procedure for the special case of four normal strains measured on gage lines 45 deg. apart. When the gage lines are at 45 deg. ( $\epsilon_2$ ,  $\epsilon_3$ , and  $\epsilon_4$  making angles of 45, 90, and 135 deg. respectively with  $\epsilon_1$ ), the four measured strains may be checked for consistency by applying Eq. (30).

$$\begin{aligned} \epsilon_t + \epsilon_n &= \epsilon_x + \epsilon_y & (30) \\ &= \epsilon_1 + \epsilon_3 = \epsilon_2 + \epsilon_4 & (59) \end{aligned}$$

If the algebraic sums of the two sets of orthogonal strains are not equal the data are not valid, and the experimental work should be checked. A slight discrepancy may be balanced out by adjusting the strains to satisfy Eq. (59). In any event Eq. (59) should be satisfied before proceeding further.

If the direction of the strain  $\epsilon_1$  is assumed to make an angle  $\theta$  with one of the principal strains, it may be expressed in terms of  $\epsilon_u$ ,  $\epsilon_v$ , and  $\theta$  by Eq. (42b) or (45a)

$$\epsilon_1 = \frac{1}{2}(\epsilon_u + \epsilon_v) + \frac{1}{2}(\epsilon_u - \epsilon_v) \cos 2\theta \quad (60a)$$

<sup>1</sup> BERGMAN, E. O., Calculation of Stress Data from Strain Measurements, *Tech. Mem. No. 542, U. S. Bur. Reclamation*, 1936.

<sup>2</sup> OSGOOD, W. R., Determination of Principal Stresses from Strains on Four Intersecting Gage Lines 45 Degrees Apart, *J. Research Nat. Bur. Standards*, Vol. 15, pp. 579-581, December, 1935.

Then

$$\epsilon_2 = \frac{1}{2}(\epsilon_u + \epsilon_v) + \frac{1}{2}(\epsilon_u - \epsilon_v) \cos 2(\theta + 45^\circ)$$

or

$$\epsilon_2 = \frac{1}{2}(\epsilon_u + \epsilon_v) - \frac{1}{2}(\epsilon_u - \epsilon_v) \sin 2\theta \quad (60b)$$

Similarly

$$\epsilon_3 = \frac{1}{2}(\epsilon_u + \epsilon_v) - \frac{1}{2}(\epsilon_u - \epsilon_v) \cos 2\theta \quad (60c)$$

$$\epsilon_4 = \frac{1}{2}(\epsilon_u + \epsilon_v) + \frac{1}{2}(\epsilon_u - \epsilon_v) \sin 2\theta \quad (60d)$$

from Eqs. (60a) and (60c)

$$\epsilon_1 - \epsilon_3 = (\epsilon_u - \epsilon_v) \cos 2\theta$$

or

$$\epsilon_u - \epsilon_v = \frac{\epsilon_1 - \epsilon_3}{\cos 2\theta} \quad (61a)$$

Similarly, from Eqs. (60b) and (60d)

$$\epsilon_u - \epsilon_v = \frac{-(\epsilon_2 - \epsilon_4)}{\sin 2\theta} \quad (61b)$$

also

$$\tan 2\theta = \frac{-(\epsilon_2 - \epsilon_4)}{\epsilon_1 - \epsilon_3} \quad (62)$$

Equations (59), (61), and (62) suffice to evaluate the principal strains and to determine their directions. Then the principal stresses may be evaluated from Eq. (57), and if the shearing stresses are desired, they may be obtained from Eq. (5).

*Illustrative Problem.*—At a point on the surface of a steel member the strains observed along four successive (counterclockwise) gage lines 45 deg. apart are  $\epsilon_1 = +0.00060$ ,  $\epsilon_2 = +0.00001$ ,  $\epsilon_3 = 0$ ,  $\epsilon_4 = +0.00059$ . Determine the principal stresses.

*Solution.*—From Eq. (59)

$$0.00060 = 0.00001 + 0.00059$$

which checks, indicating that the measured strains are compatible. From Eq. (62)

$$\begin{aligned} \tan 2\theta &= \frac{5}{60} = 0.0833 \\ \theta &= 22^\circ 1' \end{aligned}$$

Since the angle  $\theta$  is positive, the gage line 1 makes a positive angle of  $22^\circ 1'$  with the direction of one of the principal strains.

From Eq. (59)

$$\epsilon_u + \epsilon_v = +0.00060$$

and from Eq. (61a)

$$\epsilon_u - \epsilon_v = \frac{+0.00060}{0.719} = +0.000835$$

or from Eq. (61b)

$$\epsilon_u - \epsilon_v = \frac{+0.00058}{0.695} = +0.000835$$

Then

$$\epsilon_u = +0.000717$$

$$\epsilon_v = -0.000117$$

By inspection it is evident that the angle of  $22^\circ 1'$  is  $\theta_{u1}$ . The principal stresses are evaluated from the principal strains and Eq. (57), using  $E = 30 \times 10^6$  p.s.i. and  $\mu = 0.30$  as

$$S_u = 22,500 \text{ p.s.i. tension}$$

$$S_v = 3,260 \text{ p.s.i. tension}$$

In either of the preceding problems the principal strains could have been evaluated graphically by the method of Art. 26.

### PROBLEMS

**101.** A duralumin rod 8 in. long and  $1\frac{1}{4}$  in. in diameter is subjected to an axial compressive load of 9,000 lb. Determine the change in all dimensions of the rod and the change in volume.

**102.** Solve Prob. 101 if the rod is replaced by a duralumin tube with an inside diameter of 1 in. and an outside diameter of  $1\frac{1}{4}$  in.

**103.** A 2- by 2- by 8-in. block of steel is placed with the longitudinal axis in the  $z$  direction and a load of 48,000 lb. applied at the ends in the  $z$  direction. Determine  $S_x$ ,  $S_y$ ,  $S_z$ ,  $\epsilon_x$ ,  $\epsilon_y$ , and  $\epsilon_z$ .

**104.** If the steel block of Prob. 103 is subjected to a unit strain of 0.00100 in the  $z$  direction, determine  $S_x$ ,  $S_y$ ,  $S_z$ ,  $\epsilon_x$ , and  $\epsilon_y$ .

**105.** The steel block of Prob. 103 is placed between two rigid bearings, one at each end of the longitudinal axis, and is then heated  $200^\circ$  F. Determine  $S_x$ ,  $S_y$ ,  $S_z$ ,  $\epsilon_x$ ,  $\epsilon_y$ , and  $\epsilon_z$ .

**106.** What value of Poisson's ratio must a material have if it is to undergo no volume change under

- a. Axial stress,
- b. Equal biaxial stresses,
- c. Equal triaxial stresses?

**107.** An isotropic body is held rigidly to prevent straining in the  $x$  and  $y$  directions. What is the relationship between stress and strain in the  $z$  direction?

**108.** A tensile test specimen is subjected to a longitudinal strain. In what direction or directions, if any, will the normal strain be zero?

**109.** Under what loading conditions, if any, will the cubical dilatation of a specimen become zero? Does this have any physical significance?

**110.** Develop the equations for the principal strains in terms of the principal stresses for a homogeneous material that has a stress-strain relationship of the form  $S = C\epsilon^{1/2}$ . Assume that Poisson's ratio is constant.

**111.** Develop the stress-strain relationships for biaxial loading of an idealized mild steel that has a straight-line stress-strain diagram to the yield point and then develops constant stress with increasing strain.

**112.** Is it possible to evaluate the principal strains in a steel bar that has been stressed to the yield point? Explain.

**113.** What relationships must exist in an anisotropic material if Maxwell's principle is to apply with respect to stresses and strains?

**114.** Many metals have a value of Poisson's ratio of 0.33. What is the relationship between the modulus of elasticity and the modulus of rigidity for them?

**115.** In a certain structural-steel member the principal stresses are  $S_u = -12,000$  p.s.i.,  $S_v = +10,000$  p.s.i. and  $S_w = -6,000$  p.s.i. If  $S_w$  is increased in magnitude

a. Will the maximum principal strain be increased or decreased?

b. How will the maximum shearing strain be affected?

**116.** Develop Eq. (57a) from Eq. (55b).

**117.** At a point on the vertical surface of a steel beam  $S_u = -8,000$  p.s.i. and  $S_v = -2,000$  p.s.i. Determine  $\epsilon_u$ ,  $\epsilon_v$ , and  $\epsilon_w$ .

**118.** Discuss the conditions under which the superposition assumed in Eq. (48) is valid.

**119.** What will Eq. (51) become if creep occurs in the material?

**120.** Determine the maximum normal and shearing strains in the steel boiler of Prob. 51.

**121.** If the strains indicated in Prob. 83 were measured on the surface of a stainless-steel plate, determine the principal stresses.

**122.** The strains indicated in Prob. 94 were measured on the surface of a 24S-T aluminum-alloy bulkhead. Determine the principal stresses and the maximum shearing stress.

**123.** If in a biaxial stress situation one principal strain is tensile and one compressive, what is known about the signs of the principal stresses?

## CHAPTER IV

### THEORIES OF FAILURE

**33. Purpose of Theories.**—The numerical values of the stresses and strains in a structural member or machine part have little significance as such. The chief reason for determining the magnitudes and the directions of the principal stresses and strains and of the maximum shearing stresses in a member is to use them in evaluating the maximum load that the member can carry satisfactorily or in finding the optimum dimensions of the member if it is to carry a specified load. That is, the stresses and strains are used as criteria of the possibility of failure within the material under the expected loading conditions.

In a member that is subjected to axial loading, either stress or strain may be used as an index of impending failure once the condition that constitutes failure is known and the pertinent characteristics of the material have been established in a direct tensile or compressive test.

For example, if a tie rod is to carry a static tensile load of 20,000 lb. without slip, a  $\frac{7}{8}$ -in. diameter structural-steel rod might be suggested as satisfactory. The adequacy of the rod could be investigated by comparing the tensile stress in the rod with the elastic strength of the material in tension. The stress in the rod is

$$S = \frac{P}{A} = \frac{20,000}{0.601} = 33,300 \text{ p.s.i.}$$

while the elastic strength, or stress that will result in failure by slip, is, from Fig. 3, about 38,000 p.s.i. It may, therefore, be concluded that the proposed rod would be safe, having a factor of safety of  $38,000/33,300 = 1.14$ .

The proposed rod could also be checked by comparing the maximum unit strain in the rod with the unit strain that would result in failure by slip.

$$\epsilon = \frac{33,300}{30 \times 10^6} = 0.00111$$



From Fig. 3, the elasticity, or maximum strain that may be applied without failure by slip, is 0.00127. Since the maximum strain is less than the strain causing failure, the rod would be considered adequate. The factor of safety may be evaluated as  $0.00127/0.00111 = 1.14$ , which checks the value found by using stress as the criterion of failure.

In general, the use of stress is somewhat more convenient than the use of strain unless the criterion of failure is given as a limiting value of deformation, such as  $\frac{1}{16}$  in. in a length of 50 in. Nevertheless, the two methods will give identical results for axial loading.

However, if the member is subjected to biaxial loading instead of axial loading, a comparison of the maximum normal stress with the normal stress causing failure in the standard test specimen subjected to axial loading is not satisfactory. Sometimes failure will occur when the maximum principal stress developed in the member is less than the critical stress for the material as determined from a test specimen subjected to axial loading, and in other situations the maximum normal stress may exceed the critical stress appreciably before failure occurs. Furthermore, comparisons made on the basis of strains may give results very different from those obtained if the comparisons are made on the basis of stresses.

That is, whether or not failure occurs depends on the relationship among the stresses (or strains) developed at the critical point and not on the magnitude of the maximum normal stress alone.

In an attempt to avoid having to make experimental determinations for all of the infinite number of combinations of stress, several theories<sup>1</sup> have been advanced to aid in predicting the maximum load that may be applied to a member without causing a critical condition in the member if the load results in a biaxial or triaxial stress situation. Each theory is based on the assumption that a specific stress, a specific strain, or a specific combination of stresses or strains constitutes the limiting condition. The safety of a member is then predicted by comparing the stress, the strain, or combinations of stress and strain with the corresponding factors as evaluated from results of axial loading

<sup>1</sup> These theories are known as the "theories of failure" and are in general based on the premise that slip, rather than fracture, constitutes failure.

tests of the material. The accuracy of a given theory may be checked by a relatively few careful tests for a group of selected combinations of stresses.

**34. Maximum-normal-stress Theory.**—The maximum-normal-stress theory, which is also known as the Rankine theory, is based on the assumption that the material will fail under any condition of loading when the *maximum normal stress* at any point reaches the value of the limiting stress, as determined from an axial test in tension or in compression regardless of what the stresses may be on other planes through the point. The theory may be expressed mathematically by saying that the condition of failure is

$$S_u = S_m \quad (63)$$

in which  $S_u$  is the maximum principal stress at the critical point  
 $S_m$  is the critical stress as determined in an axial test.

The maximum-normal-stress theory appears to give satisfactory results for some brittle materials, like gray cast iron, but is inadequate for ductile materials.

**35. Maximum-normal-strain Theory.**—The maximum-normal-strain theory, which is also known as the Saint Venant theory,<sup>1</sup> is based on the assumption that the material will fail at a point under any condition of loading when the *maximum normal strain* at that point reaches the value of the limiting strain as determined from an axial test in tension or compression, regardless of what the stresses or strains may be on any other planes in the member.

The limiting condition as given by the maximum-normal-strain theory may be expressed in equation form as

$$\epsilon_u = \epsilon_m \quad (64)$$

in which  $\epsilon_u$  is the maximum principal strain at the point

$\epsilon_m$  is the critical strain as determined in an axial test.

If  $\epsilon_m$  does not exceed the elasticity of the material, Eq. (64) may be written in terms of stress as

$$\frac{S_u}{E} - \mu \frac{S_v}{E} = \frac{S_m}{E}$$

or

$$S_u - \mu S_v = S_m \quad (64a)$$

<sup>1</sup> SAINT VENANT, B. DE, *Historique abrégé* in C. L. NAVIER, "Résumé des leçons . . .," Carilian-Goeury, Paris, 1833.

A comparison of Eqs. (64a) and (63) indicates that if  $S_u$  and  $S_v$  are of like sign, the maximum-normal-strain theory will permit a higher stress in the material than will the maximum-normal-stress theory. If  $S_u$  and  $S_v$  are of unlike sign, the reverse is true.

The maximum-normal-strain theory is in better agreement with test results of ductile materials than is the maximum-normal-stress theory.

**36. Maximum-shearing-stress Theory.**—The maximum-shearing-stress theory, which is a special case of Coulomb's theory,<sup>1</sup> was proposed by Guest<sup>2</sup> and is based on the assumption that under any condition of loading the material will fail when the *maximum shearing stress* reaches the value of the limiting shearing stress as determined under a condition of pure shear.

The limiting condition as expressed by the maximum-shearing-stress theory is

$$S_{ij} = S_{mp} \quad (65)$$

in which  $S_{ij}$  is the maximum shearing stress developed in the material

$S_{mp}$  is the critical shearing stress as determined from a test in shear or from an axial test.

The theory may also be expressed in terms of principal stresses. For example, if the material is subjected to biaxial stresses of like sign with  $S_u > S_v$ , and  $S_w = 0$

$$S_{ij} = \frac{1}{2}(S_u - 0)$$

The critical shearing stress  $S_{mp}$  may be determined by loading the material axially until slip occurs. Then

$$S_{mp} = \frac{1}{2}S_m$$

in which  $S_m$  is the critical axial stress as before. Therefore, Eq. (65) reduces to

$$S_u = S_m$$

which is identical with Eq. (63), or the maximum-normal-stress

<sup>1</sup> NAVIER, C. L., "Résumé des leçons . . . , 1<sup>re</sup> partie, Sur la resistance des matériaux," p. 126, Paris, 1833.

<sup>2</sup> GUEST, J. J., On the Strength of Ductile Materials under Combined Stress, *Phil. Mag.*, Vol. 216, p. 69, 1900.

theory. However, if  $S_u$  and  $S_v$  are of opposite sign, Eq. (65) becomes

$$S_u - S_v = S_m \quad (65a)$$

A comparison of Eqs. (64a) and (65a) indicates that the maximum-shearing-stress theory gives even lower allowable values of  $S_u$  than does the maximum-normal-strain theory for stresses of unlike sign. In general, the maximum-shearing-stress theory gives conservative results for both ductile and brittle materials. Its use is specified in several design codes.

**37. Internal-friction Theory and Mohr Theory.**—The internal-friction theory, formulated by Coulomb, is based on the concept of failure occurring by a sliding action within the material. The resistance to sliding is considered to be a combination of shearing strength and resistance similar to frictional resistance, and failure is assumed to occur whenever the maximum shearing stress on any plane exceeds this combined resistance to sliding. It is evident that the maximum-shearing-stress theory discussed in the preceding article is a special case of the Coulomb theory in which the influence of the internal friction is neglected. The Coulomb theory was generalized by Mohr,<sup>1</sup> who assumed that the limiting shearing stress on the plane along which failure occurs is a function of the normal stress acting on that plane. The Mohr theory does not establish the nature of the relationship between the normal stress and shearing stress but leaves its determination to experimental findings. As Mohr indicated, one of the most convenient methods of showing the experimental results is by plotting the corresponding series of Mohr circles to the same set of axes. If several combinations of maximum and minimum principal stresses resulting in failure are determined experimentally and the Mohr circles are constructed as shown in Fig. 24, the critical combination of normal and shearing stresses may be determined by drawing the envelope of the circles.

It is evident that if shearing strength alone were responsible for the resistance to failure, *i.e.*, if the maximum-shearing-stress theory of failure were valid, the limiting curve would be horizontal at a distance above the  $x$  axis equal to the critical shearing

<sup>1</sup> MOHR, O., Welche Umstände bedingen die Elastizitätsgrenze und den Bruch eines Materials, *Z. V. D. I.*, p. 1524, 1900.

MOHR, O., "Abhandlungen aus dem Gebiete der Technischen Mechanik," 2d ed., W. Ernst & Sohn, Berlin, p. 192, 1914.

stress. If the maximum-normal-stress theory were valid, the limiting curve would be a vertical line, and if the resistance to failure by sliding were due entirely to friction with no true shearing strength, the limiting curve would be a straight line passing through the origin.

Tests made on marble at the University of Göttingen<sup>1</sup> and on concrete at the University of Illinois<sup>2</sup> indicate that the inter-

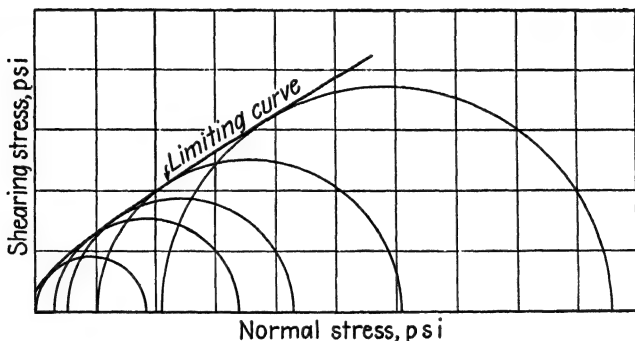


FIG. 24.—Series of Mohr circles for a material.

mediate principal stress, as well as the maximum and minimum principal stresses considered in the Mohr theory, has an appreciable effect upon the results. A concept of the mechanism of failure in a nonisotropic material was developed by Brandtzaeg in connection with the tests on concrete.<sup>3</sup>

**38. Maximum-strain-energy Theory.**—The maximum-strain-energy theory, which was developed by Beltrami,<sup>4</sup> by Huber,<sup>5</sup> and later by Haigh,<sup>6</sup> is based on the assumption that the material

<sup>1</sup> VON KÁRMÁN, T., Festigkeitversuche unter allseitigem Druck, *Mitt. Forschungsarb. Gebiete Ing.*, p. 118, 1912.

BÖKER, R., Die Mechanik der bleibenden Formänderung in kristallinisch aufgebauten Körpern, *Mitt. Forschungsarb. Gebiete Ing.*, pp. 175–176, 1915.

<sup>2</sup> RICHART, F. E., A. BRANDTZAEG, and R. L. BROWN, A Study of the Failure of Concrete under Combined Compressive Stresses, *Univ. Illinois Eng. Expt. Sta. Bull.* 185, 1928.

<sup>3</sup> BRANDTZAEG, A., Failure of a Material Composed of Non-isotropic Elements, *Kgl. Norske Videnskab. Selskabs, Skrifter*, Trondhjem, 1927.

<sup>4</sup> BELTRAMI, E., Sulle condizioni di resistenza dei corpi elastici, *Milano, Ist Lomb. Rend.*, 18, p. 704, 1885.

<sup>5</sup> HUBER, M. T., Właściwa praca odkształcenia jako miara wyteżenia materyału, *Czasopismo Techniczne*, Lwow, 1904.

<sup>6</sup> HAIGH, B. P., The Strain-energy Function and the Elastic Limit, *Engineering* London, Vol. 109, p. 158, 1920.

will fail, regardless of the combination of stress and strain involved at the point, when the value of the *strain energy per unit volume* at a point in the material reaches the maximum value of the strain energy per unit volume that the material is capable of absorbing under a condition of axial loading.

If the critical condition is taken as that corresponding to the proportional limit under axial loading, the maximum amount of strain energy per unit volume that the material is capable of absorbing in an axial tensile test is equal to

$$U_m = S_{av}\epsilon_{max} = \frac{1}{2}S_m\epsilon_m \quad (66)$$

$$= \frac{S_m^2}{2E} \quad (66a)$$

The amount of strain energy per unit volume that is absorbed in a material subjected to biaxial stress can be evaluated as

$$U = \frac{1}{2}S_u\epsilon_u + \frac{1}{2}S_v\epsilon_v \quad (67)$$

$$= \frac{1}{2}S_u \left( \frac{S_u}{E} - \frac{\mu S_v}{E} \right) + \frac{1}{2}S_v \left( \frac{S_v}{E} - \frac{\mu S_u}{E} \right) \quad (67a)$$

$$= \frac{S_u^2}{2E} + \frac{S_v^2}{2E} - \frac{2\mu S_u S_v}{2E} \quad (67b)$$

For the limiting condition of failure the strain energy per unit volume absorbed in the material, Eq. (67b), will equal the maximum energy absorbed per unit volume in an axial test, Eq. (66a), or  $U = U_m$ . Then

$$S_u^2 + S_v^2 - 2\mu S_u S_v = S_m^2 \quad (67c)$$

Equation (67c) indicates that for principal stresses of unlike sign  $S_u$  will be less than  $S_m$ , the same effect that was observed in the normal-strain and shearing-stress theories and which agrees with test results on ductile materials.

**39. Hencky-von Mises Theory.**—A theory of failure developed independently by H. Hencky<sup>1</sup> and by R. von Mises,<sup>2</sup> gives results in good agreement with test data for a number of materials. The theory is expressed in the form of an equation

$$(S_u - S_v)^2 + (S_v - S_w)^2 + (S_w - S_u)^2 = 2S_m^2 \quad (68)$$

<sup>1</sup> HENCKY, H., *Zur Theorie plastischer Deformationen . . .*, *Z. angew. Math. Mech.*, Vol. 4, p. 323, 1924; Vol. 5, p. 115, 1925.

<sup>2</sup> VON MISES, R., *Mechanik der festen Körper im plastisch-deformablen Zustand*, *Nachr. Ges. Wiss. Göttingen*, Math. physik. Klasse, p. 582, 1913.

For the condition of biaxial stresses  $S_w = 0$ , and the condition of failure becomes

$$S_u^2 - S_u S_v + S_v^2 = S_m^2 \quad (68a)$$

Equation (68a) shows a marked similarity to Eq. (67c). Hence the two theories may be expected to give rather similar results. The Hencky-von Mises theory is sometimes called the *shear-distortion* or *shear-energy* theory since each term may be interpreted as being proportional to a component of strain energy in shear.

It is apparent that the Hencky-von Mises theory is valid for the condition of hydrostatic pressure, which is not true for the other theories. As will be shown in the following article, test data indicate that it is the most accurate theory for ductile materials.

**40. Comparisons of Theories.**—The validity or usefulness of any one theory of failure can be determined only by comparing it with the results of tests on materials subjected to combined stresses. Hence, a large number of tests has been conducted on many of the common engineering materials. While the results are not entirely consistent and are not conclusive, the trend of the data indicates that when a material is in a plastic or ductile condition one theory of failure may hold, but when it is in a brittle condition a different theory of failure may give results more nearly in agreement with the test results. One of the most useful techniques<sup>1</sup> for comparing the theories with test results consists in plotting values of  $S_u/S_m = u$  as abscissae and values of  $S_v/S_m = v$  as ordinates as shown in Fig. 25c. With these axes any combination of normal stresses for a biaxial stress situation at the critical point may be represented as a point on the graph. Tensile stresses are plotted as positive and compressive stresses are plotted as negative. Thus, a point in the first quadrant indicates that both  $S_u$  and  $S_v$  are tension, a point in the second quadrant indicates that  $S_u$  is compression and  $S_v$  is tension, etc.

<sup>1</sup> HAIGH, B. P., *The Strain-energy Function and the Elastic Limit, Engineering*, London, Vol. 109, p. 148, 1920. Also reprints of British Association for the Advancement of Science, 1919-1923.

WESTERGAARD, H. M., *The Resistance of Ductile Materials to Combined Stresses in Two or Three Directions Perpendicular to One Another, J. Franklin Inst.*, May, 1920.

Point  $A$ ,  $u = 1$ , corresponds to the condition of zero stress in the  $v$  direction and a stress in the  $u$  direction equal to  $S_m$ , the strength of the material. If the point representing the stress situation were to the right of  $A$ , it would indicate that  $S_u$  was greater than  $S_m$ , and failure would be expected. Similarly, point  $B$  represents the limiting condition for a tensile stress in the  $v$  direction with  $S_u = 0$ , and  $C$  and  $D$  represent the limiting conditions for axial compressive stresses in the  $u$  and  $v$  directions

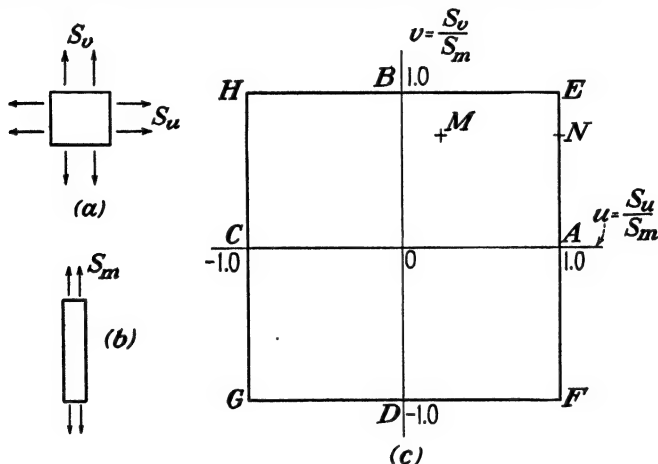


FIG. 25.—Representation of maximum-normal-stress theory of failure.

respectively. Boundaries may also be established for biaxial loading for each of the theories of failure.

**Maximum-normal-stress Theory.**—If the material is subjected to biaxial loading, as in Fig. 25a, and both principal stresses are tensile stresses less than  $S_m$ , the condition may be represented by a point such as  $M$  in the first quadrant in Fig. 25c. If  $S_u$  is increased and  $S_v$  held constant, the point will move to the right. According to the maximum-normal-stress theory, the stress in the  $u$  direction may be increased to the value  $S_m$  ( $u = 1$ ) before failure occurs. The corresponding point in Fig. 25c is  $N$ . Since failure is assumed to be independent of  $S_v$  (for  $S_v < S_m$ ), a series of points similar to  $N$  could be established for different values of  $S_v$ . The locus of these points is the line  $EAF$ . Points to the right of  $EAF$  indicate a condition of failure, and points between  $EAF$  and the  $v$  axis indicate a safe condition. Similarly, if  $S_v$  is increased with  $S_u$  constant and less than  $S_m$ ,



the locus of the points representing the limiting condition will be the line  $HBE$ . In the same manner the sides  $FDG$  and  $HCG$  are established by the limiting values of the compressive stress. Therefore, if the point that represents the stress condition in the material falls within the square  $EFGH$ , the material will not fail according to the maximum-stress theory, and if the point falls outside the square, the material will fail.

*Maximum-normal-strain Theory.*—A graphical representation for the maximum-normal-strain theory of failure similar to the representation for the maximum-normal-stress theory given in Fig. 25 may be developed by simply substituting principal strains for principal stresses and using  $\epsilon_u/\epsilon_m$  and  $\epsilon_v/\epsilon_m$  as coordinates. A square will be obtained as before. However, to obtain a direct comparison with the maximum-normal-stress theory it is desirable to express the strains in terms of stresses as was done in Eq. (64a). From Eq. (64a)

$$\frac{S_u}{S_m} = 1 + \frac{\mu S_v}{S_m} \quad (64b)$$

or

$$u = 1 + \mu v \quad (64c)$$

Equation (64c) plotted to the  $u$  and  $v$  axes in Fig. 26 gives the line  $IAJ$ , the slope of which is the reciprocal of Poisson's ratio.

Similarly, if  $S_v$  is large in comparison with  $S_u$

$$\frac{S_v}{S_m} = 1 + \frac{\mu S_u}{S_m} \quad (64d)$$

or

$$v = 1 + \mu u \quad (64e)$$

which is plotted as the line  $LBI$ . The slope of  $LBI$  is equal to Poisson's ratio.

In the same manner the other boundaries of the stress figure are established as the lines  $LCK$  and  $KDJ$ , resulting in a diamond-shaped figure. A comparison of this figure with the square that was obtained for the maximum-normal-stress theory of failure indicates that the maximum-normal-strain theory will permit somewhat higher stresses when the stresses are of like sign and somewhat lower stresses than the maximum-normal-stress theory when the stresses are of unlike sign. In other words, the maximum-normal-strain theory indicates that if a material is subjected to an axial stress, an additional orthogonal

stress of like sign may have a strengthening influence on the material, and an orthogonal stress of unlike sign may have a weakening effect.

One extreme condition in which this is true is that of a block subjected to triaxial compressive stresses. Obviously, the

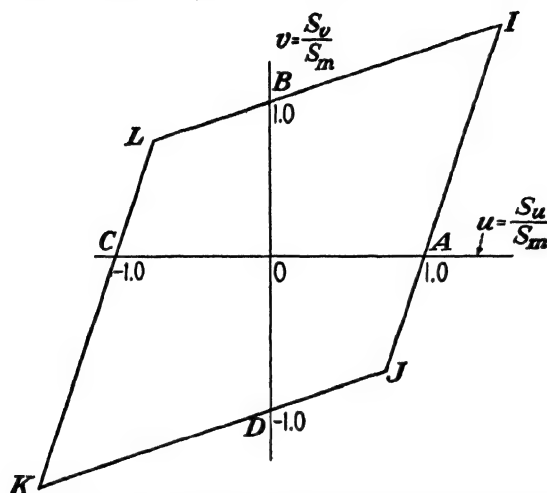


FIG. 26.—Representation of maximum-normal-strain theory of failure.

material cannot fail in the usual sense because it has no way to escape the stress.

*Maximum-shearing-stress Theory.*—The maximum-shearing-stress theory, as well as the two preceding theories, may be represented graphically since the maximum shearing stress may be evaluated in terms of the principal stresses. For the biaxial situation in which  $S_w = 0$ , there are two possible conditions depending upon whether  $S_u$  and  $S_v$  are alike or different in sign.

1. If  $S_u$  and  $S_v$  are of like sign, the maximum-shearing-stress theory reduces to the maximum-normal-stress theory as was shown in Art. 36. Therefore, the limiting stress figure will be bounded by the lines  $BEA$  and  $CGD$  in the first and third quadrants of Fig. 27.

2. If the principal stresses  $S_u$  and  $S_v$  are of unlike sign, failure will occur according to the maximum-shearing-stress theory when

$$S_u - S_v = S_m \quad (65a)$$

or

$$\frac{S_u}{S_m} - \frac{S_v}{S_m} = 1 \quad (65b)$$

giving

$$u - v = 1 \quad (65c)$$

Equation (65c) will plot as the line  $BC$  in the second quadrant of Fig. 27 and as the line  $AD$  in the fourth quadrant. Therefore, the limiting stress figure for the condition of failure by the maximum-shearing-stress theory is the six-sided figure  $BEADGCB$  of Fig. 27.

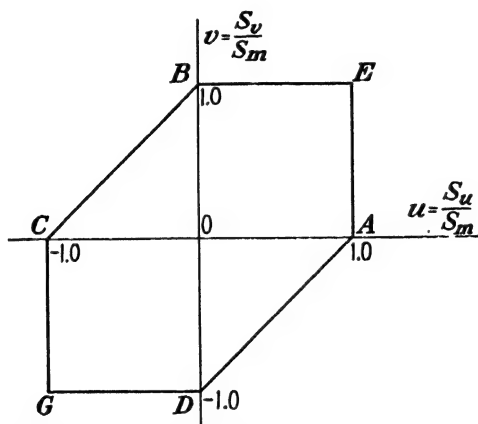


FIG. 27.—Representation of maximum-shearing-stress theory of failure.

A comparison of Fig. 27 with Figs. 25 and 26 indicates that the maximum-shearing-stress theory is equivalent to the maximum-normal-stress theory when the principal stresses are of like sign and is more conservative than either the maximum-normal-stress theory or the maximum-normal-strain theory when the principal stresses are of unlike sign.

*Maximum-strain-energy Theory.*—The equation of the limiting stress boundary for the strain-energy theory of failure may be obtained from Eq. (67c) by dividing each side by  $S_m^2$ .

$$\left(\frac{S_u}{S_m}\right)^2 + \left(\frac{S_v}{S_m}\right)^2 - 2\mu \left(\frac{S_u}{S_m}\right) \left(\frac{S_v}{S_m}\right) = 1 \quad (67d)$$

or

$$u^2 + v^2 - 2\mu uv = 1 \quad (67e)$$

The plot of Eq. (67e) will result in the ellipse indicated in Fig.

28, the relative width of the ellipse depending upon the value of Poisson's ratio. It is evident that the maximum-strain-energy theory is rather conservative for a biaxial stress condition with stresses of unlike signs but will admit higher stresses than

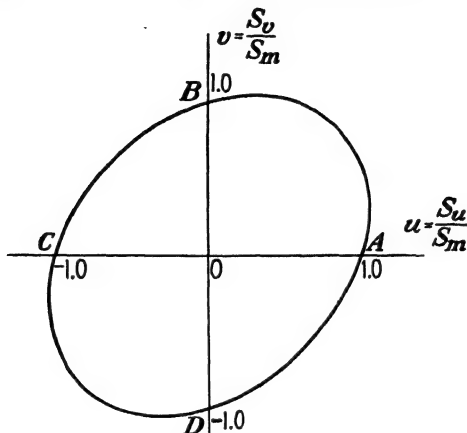


FIG. 28.—Representation of maximum-strain-energy theory of failure.

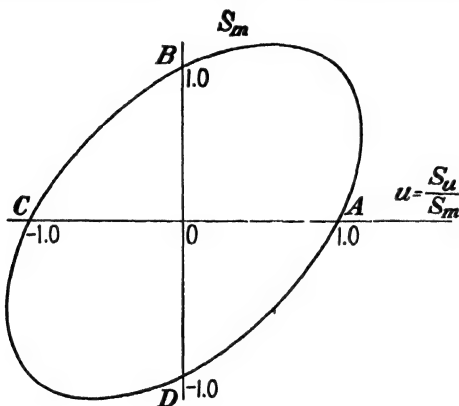


FIG. 29.—Representation of Hencky-von Mises theory of failure.

the maximum-normal-stress theory or the maximum-shearing-stress theory when the stresses are of like sign.

*Hencky-von Mises Theory.*—The stress figure for the Hencky-von Mises theory of failure is shown in Fig. 29. The equation may be derived from Eq. (68a) by dividing both sides by  $S_m^2$  giving

$$u^2 - uv + v^2 = 1 \quad (68b)$$

In Fig. 30 are plotted some examples of test data accumulated in a number of investigations,<sup>1</sup> together with the boundary curves

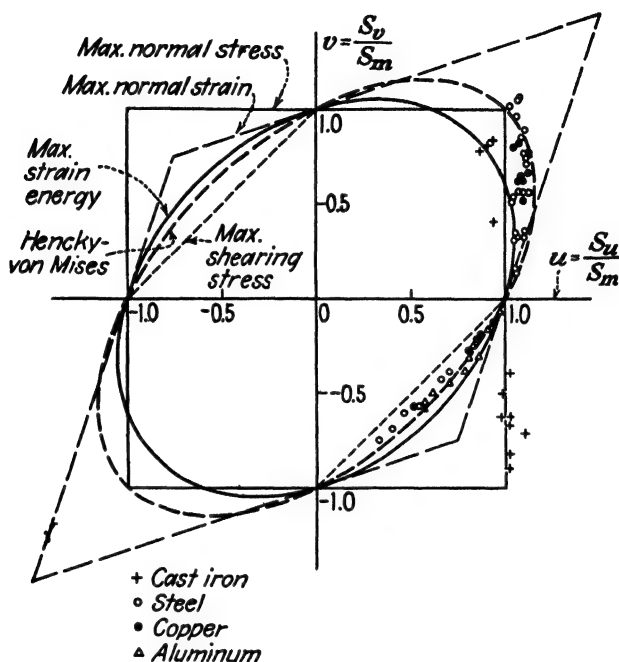


FIG. 30.—Comparison of test data from several sources with theories of failure.

for several theories of failure. The data indicate that the maximum-normal-stress theory is satisfactory for the brittle cast iron,

<sup>1</sup> Test data as follows:

Cast iron, stresses of like sign, ROS, M., and A. EICHINGER, *Versuche sur Klamung der Frage der Bruchgefahr, Proc. 2d Intern. Congr. Applied Mech.*, p. 315, 1916.

Cast iron, stresses of unlike sign, COOK, G., and T. ROBERTSON, *The Strength of Thick Hollow Cylinders under Internal Pressure, Engineering*, Vol. 92, p. 786, 1911.

Steel and copper, stresses of like sign, LODE, W., *Versuche über den Einfluss der mittleren Hauptspannung auf des Fließen der Metalle Eisen Kupfer und Nickel, Z. Physik*, Vol. 32, p. 913, 1926; and *Der Einfluss der Mittleren Hauptspannung auf das Fließen der Metalle, Mitt. Forschungsarb., V.D.I.*, No. 303, 1928.

Steel, stresses of unlike sign, ROS and EICHINGER, *loc. cit.*

Copper and aluminum, stresses of unlike sign, TAYLOR, G. I., and H. QUINNEY, *Plastic Distortion of Metals, Trans. Roy. Soc. London, Ser. A*, Vol. 23, p. 323, 1931.

while the Hencky-von Mises theory is in reasonable agreement with the test data for the ductile metals. The maximum-shearing-stress theory gives conservative results for the ductile metals and ultraconservative results for brittle materials subjected to stresses of opposite sign. The maximum-unit-strain theory is unsafe for the ductile metals. Data by other investigators support these general observations.

The trend of design practice is toward the use of the maximum-normal-stress theory for brittle materials and the Hencky-von Mises theory for ductile materials.<sup>1</sup> For many combinations of stresses there will be but little difference in the results obtained from the various theories of failure. The maximum difference occurs when the two principal stresses are of equal magnitude.

**41. Interaction Curves.**—A biaxial stress condition at a point may be due to a single load as at a point on the outside of a boiler under internal pressure, or it may be due to a pair of loads (or couples) as at a point on the outside of a shaft that is subjected to both bending and torsion. For the latter type of situation an “interaction curve” is sometimes used, especially in analyses of aircraft members, instead of a curve similar to one of the types shown in Fig. 30.

In an interaction curve, ratios of the stresses due to each of the components to the strength (with reference to that component) are plotted along the coordinate axes, instead of the ratios of the principal stresses to the strength. That is, for a tube subjected to a combination of bending and torsion, the interaction curve would be obtained by plotting along one axis the ratio of the maximum stress in bending ( $Mc/I$ ) to the strength in bending, and along the other axis, the ratio of the torsional stress ( $Tc/J$ ) to the strength in torsion. The limiting curve may be obtained from an appropriate theory of failure, or better, directly from dependable test data.

The factor of safety may be considered to be the ratio of the distance from the origin to the limiting curve divided by the distance from the origin to the point representing the stress situation, both distances measured along the same radial line.

Interaction curves are given for several combinations of

<sup>1</sup> Several design codes, including the A.S.M.E. Code for Design of Transmission Shafting and the Westinghouse Code specify the maximum-shearing-stress theory for ductile materials, insuring results on the safe side.

loading of standard shapes such as round tubes, streamline tubes, and flat panels by ANC-5, Strength of Aircraft Elements, issued by the Army-Navy-Civil Committee on Aircraft Design Criteria.

### PROBLEMS

**124.** Construct the limiting stress figure similar to Fig. 26 for the maximum-unit-strain theory of failure for values of Poisson's ratio equal to 0,  $1/4$ ,  $1/3$ , and  $1/2$ .

**125.** What will Figs. 25, 26, and 27 become if extended to represent triaxial stress by three-dimensional plotting?

**126.** What type of boundary solid will the Hencky-von Mises theory give if Fig. 29 is extended to include the triaxial loading condition?

**127.** Under what conditions will each of the theories of failure give results 10 per cent different from those obtained by the maximum-normal-stress theory?

**128.** At the critical point on the free surface of a member, one principal stress is 12,000 p.s.i. tension and the other principal stress is 8,000 p.s.i. compression. To what axial stress is this equivalent according to each of the theories of failure?

**129.** Construct a set of Mohr circles, corresponding to those shown in Fig. 24, to define the limiting curve for the condition of biaxial loading if the maximum-unit-strain theory of failure prevails. Assume the strength of the material to be 40,000 p.s.i. under the condition of axial loading.

**130.** Solve Prob. 129 using the maximum-strain-energy theory and the Hencky-von Mises theory of failure.

**131.** A structural-steel cylinder with an internal diameter of 4 ft. is to be used to store a gas under a pressure of 1,000 p.s.i. Determine the thickness of wall required using the maximum-normal-stress, maximum-normal-strain, and maximum-shearing-stress theories of failure if the limiting-stress condition corresponds to a normal stress of 20,000 p.s.i. in axial loading.

**132.** A shaft transmits 400 hp. at 200 r.p.m. and is subjected to a maximum bending moment of 8,000 ft.-lb. Determine the minimum diameter of solid structural-steel shaft that could be used if the factor of safety is to be at least 1.50 with respect to failure by slip. Solve using (a) maximum-normal-stress theory, (b) maximum-shearing-stress theory, and (c) Hencky-von Mises theory of failure.

**133.** A steel tube with an outside diameter of 3.00 in. and a wall thickness of 0.25 in. is used for the propeller shaft of an airplane engine. If under take-off conditions, the shaft transmits 2,000 hp. at 1,650 r.p.m., and the propeller develops a thrust of 8,000 lb., determine the margin of safety of the shaft based on a limiting normal stress of 60,000 p.s.i. in an axial test. Use any three theories of failure.

**134.** A 24- by 48-in. rectangular plate simply supported on all four sides is subjected to a uniformly distributed load of 100 p.s.i. normal to its area. The maximum bending moments occur at the center of the plate, the moment in the direction of the long side being equal to  $0.1017wa^2$  per unit width,

and the moment in the direction of the short side being equal to  $0.0464wa^2$  per unit width, in which  $w$  is the intensity of the load and  $a$  is the length of the short side. If the plate is to be made of aluminum alloy 17S-T, determine the minimum thickness required to prevent failure by slip. Use any three theories of failure.

**135.** The Aeronautical Board Publication ANC-5, Strength of Aircraft Elements, specifies that the stress situation in round tubes subjected to combined bending and torsion shall not exceed

$$R_b^2 + R_s^2 = 1$$

in which  $R_b$  is the ratio of the bending stress ( $Mc/I$ ) to the bending strength and  $R_s$  is the ratio of the shearing stress ( $Tc/J$ ) to the shearing strength. To which, if any, of the theories of failure discussed does the formula correspond?

**136.** The publication ANC-5 specifies

$$R_b + R_s = 1$$

as representing the limiting condition for streamline tubing subjected to bending and torsion in which  $R_b$  is the ratio of the bending stress ( $Mc/I$ ) to the bending strength, and  $R_s$  is the ratio of the shearing stress ( $Tc/J$ ) to the shearing strength. To which, if any, of the theories of failure does it correspond?

**137.** The interaction curve that ANC-5 specifies for tubes in bending, compression, and torsion satisfies the equation

$$R_c + R_b + R_s^2 = 1$$

in which  $R_c$  is the ratio of the compressive stress to the compressive strength

$R_b$  is the ratio of the bending stress ( $Mc/I$ ) to the bending strength

$R_s$  is the ratio of the shearing stress ( $Tc/J$ ) to the torsional strength

Does this correspond to any of the theories of failure considered in this chapter, and if so, to which?

**138.** A spring having an outside diameter of 5.00 in. is made of 17S-T tubing with an outside diameter of 1.00 in. and a wall thickness of 0.049 in. If the spring has a pitch of 2 in. per turn, determine the maximum load to which the spring may be subjected without permanent set. Use two acceptable theories of failure.



## CHAPTER V

### AXIAL LOADING

**42. Definition and Loading Requirements.**—An axially loaded member is one in which the resultant force on every cross section passes through the centroid of the cross section and is directed along the geometrical axis of the member. This definition

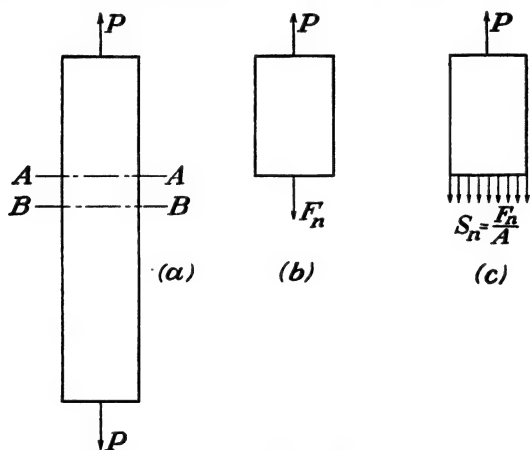


FIG. 31.—Axial loading.

imposes certain requirements upon the shape of the member and the line of action of the applied loads.

The requirements may be determined by considering a member that is assumed to be axially loaded, as the bar in Fig. 31*a*. A free-body diagram of a portion of the bar is shown in Fig. 31*b*, with  $P$  designating the applied load and  $F_n$  the resultant force developed at the cut section. By definition, the line of action of  $F_n$  passes through the centroid of the section and is directed along the axis of the member. The weight of the material is assumed to be negligible. From the equations of equilibrium it is evident that the applied load  $P$  must be equal to  $F_n$  in magnitude, opposite in sense, and collinear with  $F_n$ . Hence, the applied load must be axial. In order for the single load  $P$

to balance the force  $F_n$  developed at each cross section in the bar, the axis of the member must be a straight line.

**43. Distribution of Stress in Axially Loaded Members.**—The distribution of stress across any transverse section of an axially loaded member is usually assumed to be uniform. Actually, the distribution is not necessarily uniform but is dependent upon the characteristics of the material and upon the shape of the member. *Statics, geometry, and properties of the material* of the member must all be considered in determining the stress distribution.

If the material is homogeneous and if the member has a constant cross section, any transverse cross section, such as  $AA$  in Fig. 31a, which is plane and at right angles to the axis before the member is loaded, may be assumed to remain plane and at right angles to the axis after loading.<sup>1</sup> Then two parallel plane sections through the member, such as  $AA$  and  $BB$  in Fig. 31a, normal to the axis must remain plane and parallel after loading. If this is true, the total strain and also the unit strain are constant across any cross section. If the strain is uniform across the cross section and if the material is homogeneous, the stress must be uniformly distributed across the cross section. Then from the definition of unit stress, Fig. 5,

$$\begin{aligned} F_n &= \int_0^A S \, da \\ &= SA \end{aligned} \quad (69a)$$

From statics  $F_n = P$ , hence

$$S = \frac{P}{A} \quad (69b)$$

In addition, if the stress is uniformly distributed across the section, the resultant must act at the centroid of the cross section, which satisfies the definition of axial loading.

If the stress is not uniformly distributed across the section, Eq. (69b) gives the value of the average unit stress, and the *maximum unit stress must be greater* than the value given by Eq. (69b).

Even though the applied loads are axial and the material is

<sup>1</sup> That this assumption is not valid for a member containing a change in cross section is evident from Fig. 22. Similar distortions have been observed in rectangular bars of constant cross section as the stress approaches the ultimate strength.

homogeneous, the stress is not necessarily uniformly distributed. There are two important situations in which the stress is not uniform: one, in which the applied loads are compressive and cause buckling of the member; the other, in which the member does not have a constant cross section throughout its length.

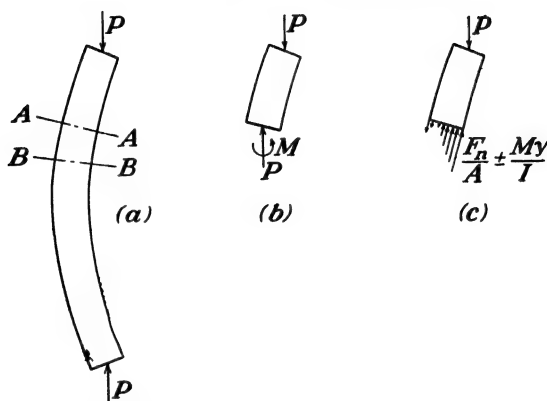


FIG. 32.—Axial compressive load causing buckling.

**44. Axial Compressive Loads.**—If a long slender member is subjected to compressive loads that are originally axial, the loads may be sufficiently large to cause buckling of the member as indicated in Fig. 32a. After buckling occurs, two adjacent plane sections such as  $AA$  and  $BB$ , even though they remain plane, do not remain parallel. Hence, the unit strain and, therefore, the unit stress, is not constant across the cross section. If the applied loads are greater than the critical buckling load for the member, the stresses may be evaluated by considering the member to be subjected to a combination of axial load and bending.

The usual design procedure for a compressive member in which buckling may occur consists in proportioning the member so that the average value of  $P/A$  for the member does not exceed the value stipulated by an appropriate column formula (Euler, Rankine, straight-line, parabolic, etc.), which has been found suitable for the given situation. Examples of typical column formulas are given in Table IV.

If the slenderness ratio  $L/r$  is less than 40, the effect of buckling may usually be neglected. Many specifications place a definite upper limit on the permissible slenderness ratio for a structural

member because of the reduced strength and stiffness of the long member. The long slender member will also have a lower natural frequency, which may make it more susceptible to damage by vibration.

TABLE IV.—TYPICAL COLUMN FORMULAS

Material	Maximum $\frac{P}{A}$ , p.s.i.	Limitations	Source	No.
Steel:				
Structural . . . . .	$\frac{18,000}{1 + \frac{1}{18,000} \left(\frac{L}{r}\right)^2}$	$60 < \frac{L}{r} < 120$	AISC	1
1025 . . . . .	$\frac{276,000,000}{\left(\frac{L}{r}\right)^2}$	$\frac{L}{r} > 124$	ANC-5	2
1025 . . . . .	$36,000 - 1.172 \left(\frac{L}{r}\right)^2$	$\frac{L}{r} < 124$	ANC-5	3
X-4130 . . . . .	$\frac{286,000,000}{\left(\frac{L}{r}\right)^2}$	$\frac{L}{r} > 86$	ANC-5	4
X-4130 . . . . .	$90,100 - 64.4 \left(\frac{L}{r}\right)^{1.5}$	$\frac{L}{r} < 86$	ANC-5	5
X-4130, heat-treated.	$165,000 - 23.78 \left(\frac{L}{r}\right)^2$	$\frac{L}{r} < 58.9$ (a)	ANC-5	6
Aluminum alloys:				
17S-T . . . . .	$\frac{103,800,000}{\left(\frac{L}{r}\right)^2}$	$\frac{L}{r} > 85.7$	ANC-5	7
17S-T . . . . .	$42,500 - 330.5 \left(\frac{L}{r}\right)$	$\frac{L}{r} < 85.7$	ANC-5	8
24S-T . . . . .	$50,000 - 421.0 \left(\frac{L}{r}\right)$	$\frac{L}{r} < 79.2$ (b)	ANC-5	9
Magnesium alloys . . .	$\frac{48,000}{1 + 0.00075 \left(\frac{L}{r}\right)^2}$	$\frac{L}{r} < 80$	Am. Mag. Corp.	10
Magnesium alloys . . .	$11,000 - 53.6 \left(\frac{L}{r}\right)$	$\frac{L}{r} < 120$	AAF, Navy	11
Wrought iron . . . . .	$12,000 - 60 \left(\frac{L}{r}\right)$		Wis. Bldg. Code	12
Cast iron . . . . .	$10,000 - 40 \left(\frac{L}{r}\right)$		Wis. Bldg. Code	13
Timber (fir, spruce) . .	$640 - 26.7 \left(\frac{L}{r}\right)$		Wis. Bldg. Code	14

NOTE:  $\frac{L}{r}$  is slenderness ratio of equivalent pin-ended column.

Formulas 1, 12, 13, 14 include factor of safety; other formulas do not.

(a) For  $\frac{L}{r} > 58.9$  use (4).

(b) For  $\frac{L}{r} > 79.2$  use (7).

The ordinary column formulas such as those given in Table IV are all based on the assumption that the column will fail as a structural unit, *i.e.*, by over-all bending or buckling rather than by localized action. Conventional rolled steel shapes such as

I beams, channels, and angles, as well as "closed" sections such as round and streamline tubing, will, in general, act as structural units, but thin-walled "open" sections or bent-up shapes such as Z sections or hat sections with outstanding legs or flanges may fail by local crippling of the thin, outstanding element.

Unsymmetrical, thin-walled open columns may also fail in torsion.

**45. Nonuniform Axially Loaded Members.**—If the axially loaded member does not have a constant cross section throughout

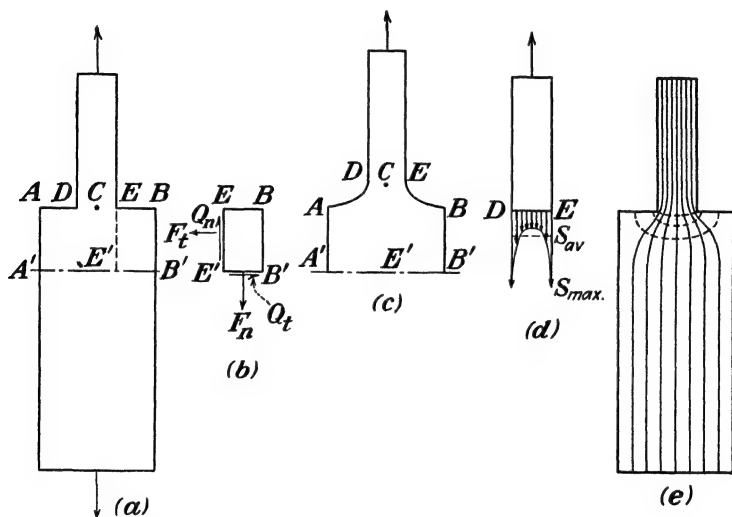


FIG. 33.—Stress concentration at a change in cross section.

its length, stresses higher than those given by Eq. (69b) will be developed near the change in cross section. For example, if a tension member contains a pair of symmetrical notches, it may still be axially loaded, but the stress is not uniformly distributed across the cross section near the notches. The nonuniform distribution of strain for this type of a member is clearly indicated in Fig. 22. The strain at the base of the notches is much higher than at other sections, and this region of high strain is a region of comparatively high stresses, for stresses below the proportional limit, at least.

The same type of irregularity in stress distribution exists for other nonuniform axially loaded members, such as a member of constant thickness that has an abrupt change in width as indi-

cated in Fig. 33a. A free-body diagram of the portion  $EBB'E'$  is shown in Fig. 33b. Obviously, the side  $EB$  can develop no tension, and  $E'B'$  is subjected to tension; hence, a shearing force  $Q_n$  must be developed on the side  $EE'$  to preserve equilibrium. This force will induce a shearing force  $Q_t$  along  $E'B'$ , which in turn must be balanced by a tensile force  $F_t$  on the side  $EE'$ . A small element at the corner  $E'$  is therefore subjected to a biaxial stress situation, and there will be developed a principal tensile stress greater than the average stress on the side  $E'B'$ . The same general situation exists at all points in the vicinity of  $E$ .

The existence of the shearing stress may also be shown by considering the geometry of the member in the vicinity of the change in cross section. If the line  $A'B'$  is assumed to be fixed, the tensile load will cause the distance  $EE'$  to increase more than  $BB'$ , with the result that the line  $ADCEB$  will assume the shape indicated in Fig. 33c. This change in shape induces shearing strains,  $\gamma_{xy}$  as shown, the magnitude of the strain increasing toward point  $E$ . The shearing strains are accompanied by shearing stresses that are a maximum near  $E$ , and the resulting principal stress is a maximum at  $E$ . The stress distribution across the reduced section  $DE$  is approximately as indicated in Fig. 33d. The maximum stress occurs at points  $D$  and  $E$ , and its magnitude is dependent upon the radius of the fillets at the change in section as well as the ratio of the widths  $AB$  and  $DE$ . Stress trajectories are indicated in Fig. 33e. The solid lines are similar to the streamlines representing the flow of fluid from a channel of one width into a channel of different width.

In certain respects the stress distribution across the smaller section near the junction is similar to the stress distribution across the end of a short compressive specimen loaded in a testing machine. Friction between the specimen and the machine prevents free lateral expansion of the specimen near the ends, resulting in a nonuniform stress distribution at the ends.

**46. Stress-concentration Factor.**—If the stress is not uniformly distributed across a section, the maximum stress must be greater than the average as evaluated by  $S = P/A$ , and it is the maximum stress that is of obvious importance to the designer. For static axial loading the ratio of the maximum stress to the

average ( $P/A$ ) stress is called the "stress-concentration factor."<sup>1</sup> It will be designated by the symbol  $K_t$  and is normally evaluated for stresses below the proportional limit. If the proportional limit is exceeded, the maximum stress is usually less than  $K_t P/A$ .

Stress-concentration factors have been evaluated for a number of different types of discontinuities by both mathematical and experimental procedures.

It is evident that the *distribution* of stress across a member cannot be determined from the equations of equilibrium applied to a free-body diagram involving the entire cross section. The conditions of equilibrium involve only the magnitude and position of the line of action of the *resultant* force developed on the section. If the geometrical behavior of the cross section is known accurately, the strain distribution may be evaluated and from it, the stress distribution. However, the geometrical behavior may not be known, in which case the mathematical procedure that has become known as "the theory of elasticity" may be used. The method<sup>2</sup> consists in writing the equations of equilibrium for a differential element of the material, instead of for the entire cross section, and integrating the resultant differential equations. The constants of integration are evaluated from the known stress conditions at the boundaries of the member. In general, the difficulties involved in solving the differential equations and applying the requisite boundary conditions limit the practical application of the method to members of relatively simple shapes. At present the more complicated shapes are effectively analyzed by experimental procedures.

The experimental methods used for evaluating stress-concentration factors include (1) strain measurements, (2) brittle-material method, (3) repeated-loading method, (4) the brittle-paint method, and (5) the photoelastic method.

<sup>1</sup> Some writers define stress-concentration factor as the ratio of the maximum stress to the average stress on the net section instead of the gross section. Hence, values of the stress-concentration factor should not be used until it is known which definition was used in evaluating the factors.

<sup>2</sup> TIMOSHENKO, S., "Theory of Elasticity," McGraw-Hill Book Company, Inc., 1934.

PRESCOTT, J., "Applied Elasticity," Longmans, Green and Company, New York, 1924.

LOVE, A. E. H., "Mathematical Theory of Elasticity," The Macmillan Company, 1906.

1. Although a value for stress concentration factor may be determined from strains measured by a conventional strainometer or strain gage, the value will usually be too low because the strainometer records the *average* strain over the gage length, and the average is less than the maximum that is desired. If the gage length of the instrument is decreased, the accuracy of the results is also decreased owing to the increased percentage of error involved in the readings. In some situations the strains may be evaluated by the Photogrid technique indicated in Art. 25 with somewhat less error than by the use of the conventional strainometer.

2. In the brittle-material method a pair of specimens is made, one having the change in cross section causing the concentration of stress, the other having a constant cross section. The two specimens are loaded to failure, and the stress-concentration factor is determined as the ratio of the ultimate loads. This procedure requires the use of a material that has a straight-line stress-strain diagram to the ultimate and assumes that the material in the two specimens is identical. Plaster of paris<sup>1</sup> has been successfully used as the brittle material, and some grades of cast iron are suitable. The method requires the use of several pairs of specimens to reduce experimental error due to the nonhomogeneity of the material.

3. The repeated-loading method, which is discussed in Art. 48, essentially produces a brittle material in the region of stress concentration. However, different materials respond in different ways, depending on the sensitivity of the material to stress concentration, and the results are of value primarily for the condition of repeated loading and for the material used in the test.

4. One of the more satisfactory techniques for evaluating stress-concentration factors consists in covering the specimen with a coating of a brittle material that will crack at a known stress. The specimen is then loaded until a crack appears at the critical section, giving directly the relationship between the load and the maximum stress, from which the stress-concentration factor may be determined. Whitewash, cement paste, and similar materials may be used as the brittle coating, and the

<sup>1</sup> SEELY, F. B., and T. J. DOLAN, Stress Concentration at Fillets, Holes, and Keyways as Found by the Plaster-model Method, *Univ. Illinois Eng. Expt. Sta. Bull.* 276, 1935.



stress at which a crack appears is determined from a control specimen. A special varnish, known as "Stresscoat," has been developed specifically for this use.<sup>1</sup>

The general method is based on the same principle as evaluating the yield point of a hot-rolled steel specimen by the "scaling" of the iron oxide or mill scale on the surface. The formation of Lüders' lines, or slip lines, has similarly been used to indicate the development of a maximum stress.<sup>2</sup>

In general, the brittle-coating method gives a lower value of the stress-concentration factor than the mathematical method or photoelastic method owing to the difficulty of detecting the cracks as they first appear.

5. The photoelastic method of evaluating stresses, which is discussed in Chap. 10, gives results in close agreement with those obtained by the theory of elasticity.

Because of their great practical importance, stress-concentration factors have been determined for several specific shapes, and representative values are shown in Figs. 34-40.

**47. Values of Stress-concentration Factor.**—In Fig. 34 are shown values of the stress-concentration factor for a transverse or a longitudinal elliptical hole in a wide plate subjected to axial tension, for a small circular hole near the edge of a wide plate subjected to tension, and for a hole reinforced by a bead. In each case the maximum stress occurs at the edge of the hole.

The value of the stress-concentration factor for the small transverse elliptical hole in a wide plate subjected to tension may be expressed in equation form as<sup>3</sup>

$$K_t = 1 + \frac{2a}{b} \quad (70)$$

in which  $2a$  is the length of the major axis and  $2b$  is the length of

<sup>1</sup> DE FOREST, A. V., GREER ELLIS, and F. B. STERN, JR., Brittle Coatings for Quantitative Strain Measurements, *J. Applied Mech.*, Vol. 9, December, 1942.

ELLIS, GREER, Practical Strain Analysis by Use of Brittle Coatings, *Proc. Soc. Exptl. Stress Analysis*, Vol. 1, No. 1, pp. 46-53, 1943.

<sup>2</sup> TIMOSHENKO, S., Stress Concentration Produced by Fillets and Holes, *Proc. 2d Intern. Congr. Applied Mech.*, Zurich, 1926.

<sup>3</sup> KOLOSOFF, G., "Dissertation," St. Petersburg, 1910.

INGLIS, C. E., Stresses in a Plate due to the Presence of Cracks and Sharp Corners, *Engineering*, Vol. 95, p. 315, 1913. Also *Trans. Inst. Naval Arch.*, Vol. 55, p. 219, 1913.

the minor axis of the ellipse. The maximum stress occurs at the end of the major axis, the axis perpendicular to the direction of the applied load. For the special case of a circular hole Eq. (70) reduces to  $K_t = 3$ . A transverse crack in a wide plate may be assumed to be an extremely narrow ellipse. For example, if

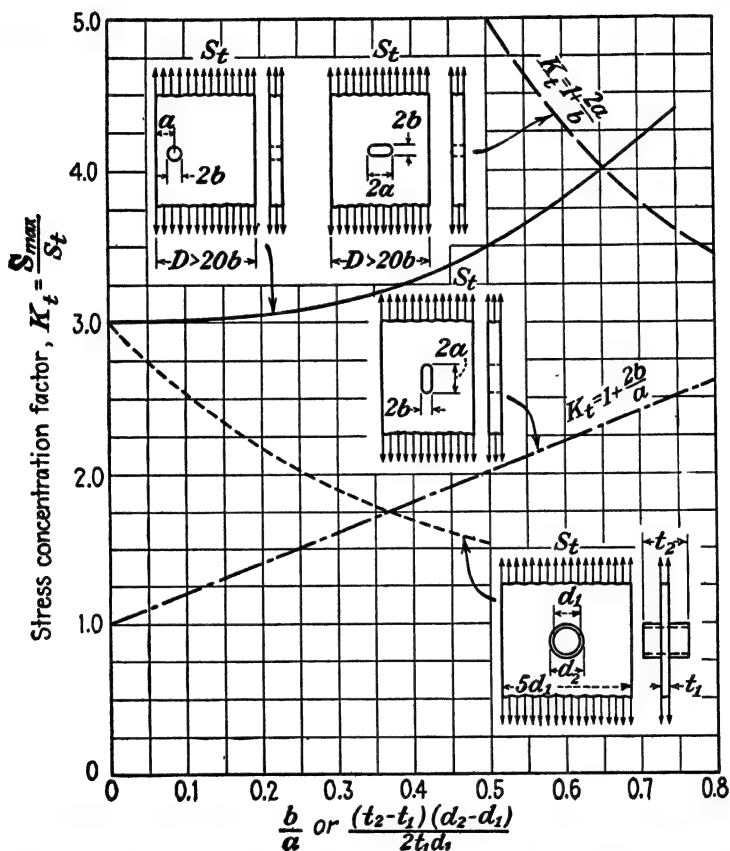


FIG. 34.—Stress-concentration factors for plates subjected to tension.

$a = 1,000b$ , the stress-concentration factor becomes equal to 2,001, indicating the high concentration of stress at the end of a transverse crack. With the high stress developed the crack will tend to extend, particularly under repeated loading. The tendency may be greatly reduced by drilling a small hole at the end of the crack, which will reduce the stress-concentration factor to approximately 3.00.

The stress at the end of the minor axis of the elliptical hole is equal to the average stress in the cross section of the plate and is compressive. If the major axis of the elliptical hole is parallel to the axis of the plate, the stress-concentration factor is

$$K_t = 1 + \frac{2b}{a} \quad (70a)$$

Durelli and Murray<sup>1</sup> have investigated the stresses in the vicinity of an elliptical hole in a plate subjected to biaxial loading, using both the Stresscoat and the photoelastic method to supplement the mathematical analysis.

The curve in Fig. 34 giving the values of the stress-concentration factor for a circular hole near the edge of a wide plate is from data by Jeffery.<sup>2</sup> As the distance  $a$  becomes large in comparison with the radius  $b$  of the hole, the value of the stress-concentration factor approaches 3.00, which agrees with the special case of the ellipse with major and minor axes equal. The maximum stress occurs at the edge of the hole nearest the edge of the plate. For values of  $a/b$  less than about 2, a compressive stress is developed at the edge of the plate.

The stress distribution in the vicinity of a small circular hole in a wide plate (theoretically of infinite width) is given by Kirsch<sup>3</sup> as

$$S_r = \frac{1}{2}S(1 - \alpha) + \frac{1}{2}S(1 - 4\alpha + 3\alpha^2) \cos 2\theta \quad (71a)$$

$$S_t = \frac{1}{2}S(1 + \alpha) - \frac{1}{2}S(1 + 3\alpha^2) \cos 2\theta \quad (71b)$$

$$S_{rt} = -\frac{1}{2}S(1 + 2\alpha - 3\alpha^2) \sin 2\theta \quad (71c)$$

in which  $S$  is the axial stress in the gross section of the plate

$S_r$  is the radial stress at the point with reference to an origin at the center of the hole

$S_t$  is the tangential stress (normal to the radial)

<sup>1</sup> DURELLI, A. J., and W. M. MURRAY, Stress Distribution around an Elliptical Discontinuity in Any Two-dimensional, Uniform and Axial, System of Combined Stress, *Proc. Soc. Exptl. Stress Analysis*, Vol. 1, No. 1, p. 19, 1943.

<sup>2</sup> JEFFERY, G. B., *Trans. Roy. Soc. London*, Ser. A, Vol. 221, p. 265, 1921.

<sup>3</sup> KIRSCH, G., *V. D. I.*, Vol. 42, p. 797, 1898.

See also TIMOSHENKO, S., "Theory of Elasticity," p. 75, McGraw-Hill Book Company, Inc., New York, 1934.

TIMOSHENKO, S., "Strength of Materials," Part II, p. 454, D. Van Nostrand Company, Inc., New York, 1930.

$S_{rt}$  is the shearing stress

$\theta$  is the angle that the radius to the point makes with the longitudinal axis of the plate

$\alpha$  is the square of the ratio of the radius of the hole to the radius of the point

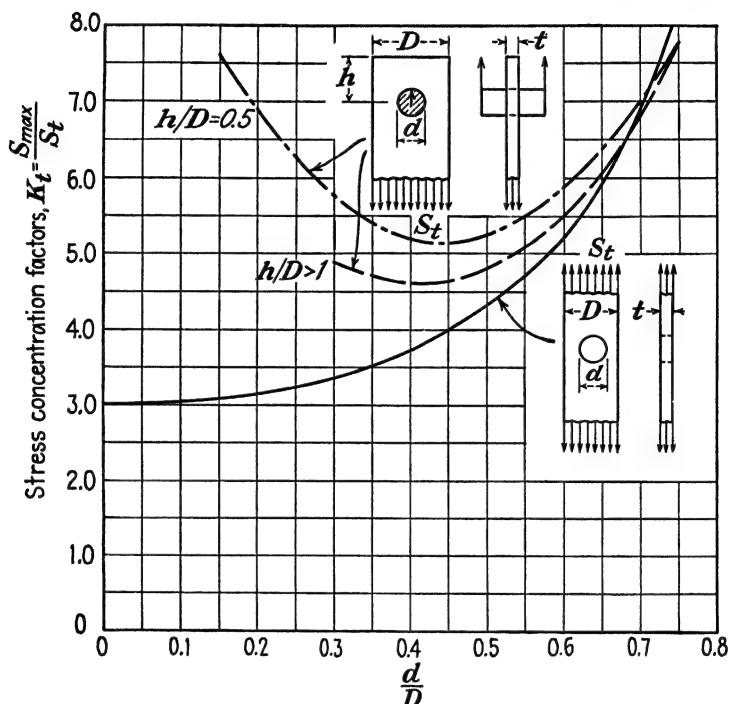


FIG. 35.—Stress-concentration factors for holes in plates in tension.

From Eq. (71b) it is evident that the maximum normal stress occurs at the edge of the hole, on the transverse diameter, where  $\theta = 90$  deg. and  $\alpha = 1.00$ . Then  $S_t = 3S$ , which gives a stress-concentration factor of 3.00, agreeing with results previously noted.

The stress concentration in the plate is a highly localized phenomenon. Hence, Eq. (71) may be applied to plates of finite width if the radius of the hole is small in comparison with the width of the plate. However, as the width of the plate approaches the diameter of the hole, the stress-concentration factor exceeds 3.00.

The stress-concentration factor for a hole in a plate of finite width subjected to tension has been determined analytically by Howland<sup>1</sup> and experimentally by Wahl and Beeuwkes<sup>2</sup> with almost identical results. Their findings are indicated in Fig. 35 and show that the stress-concentration factor increases as the size of the hole is increased. The value of the stress-concentration factor is about 4.3 for a plate having a width equal to twice the diameter of the hole. If the diameter of the hole is less than 0.3 of the width of the plate, the value of 3.00 will be less than 10 per cent in error.

The stress-concentration factor for a hole may be reduced by putting a bead around the periphery of the hole. The values of stress-concentration factor shown in Fig. 34 for this case are from a solution by Timoshenko.<sup>3</sup>

The concentration of stress due to a load applied through a pin fitting in a hole in a flat plate was studied by Frocht and Hill.<sup>4</sup> Their results are also shown in Fig. 35.

Values of the stress-concentration factor for an abrupt change in width of a plate of constant thickness subjected to axial tension are given in Fig. 36. The data<sup>5</sup> indicate that the stress-concentration factor decreases as the two widths become more nearly equal and that the factor decreases rapidly as the radius of the fillet is increased.

Figure 37 shows the effect of fillets in reducing stress concentration at the shoulder in a tensile member when the load is uniformly distributed along the flat portions of the shoulder.<sup>6</sup>

Stress-concentration factors due to grooves and notches in

<sup>1</sup> HOWLAND, R. C. J., On the Stresses in the Neighborhood of a Circular Hole in a Strip under Tension, *Trans. Roy. Soc. London*, Ser. A, Vol. 229, p. 49, 1929.

<sup>2</sup> WAHL, A. M., and R. BEEUWKES, Stress Concentration Produced by Holes and Notches, *Trans. Am. Soc. Mech. Engrs.*, Vol. 56, pp. 617-625, 1934.

<sup>3</sup> TIMOSHENKO, S., "Strength of Materials," Part II, p. 457, D. Van Nostrand Company, Inc., New York, 1930.

<sup>4</sup> FROCHT, M. M., and H. N. HILL, Stress Concentration Factors around a Central Circular Hole in a Plate Loaded through Pin in the Hole, *J. Applied Mech.*, March, 1940.

<sup>5</sup> TIMOSHENKO, S., and W. DIETZ, Stress Concentration Produced at Holes and Fillets, *Trans. Am. Soc. Mech. Engrs.*, Vol. 47, p. 199, 1925.

<sup>6</sup> HETÉNYI, M., Some Applications of Photoelasticity in Turbine-generator Design, *J. Applied Mech.*, December, 1939.

the sides of tension members have been evaluated by several investigators. The solid lines in Fig. 38 show values of the stress-concentration factor due to a pair of hyperbolic notches in a plate subjected to an axial tensile load,<sup>1,2</sup> and the dotted

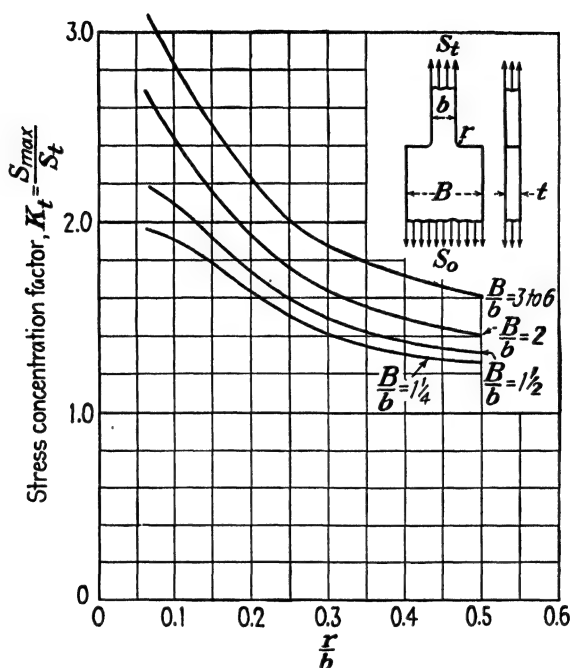


FIG. 36.—Stress-concentration factors for a change in width.

lines give values of the factor for a circular tensile member containing an hyperbolic groove. Values of the stress-concentration factor for pairs of circular notches of various depths in the edges of plates subjected to axial tension are shown in Fig. 39. A protrusion or bead on the edge of a flat plate in tension will cause concentration of stress. Values<sup>1</sup> of the factor are given in Fig. 40.

Values of the stress-concentration factor for bolts under axial

<sup>1</sup> NEUBER, H., "Kerbspannungslehre," Berlin, 1937.

<sup>2</sup> LEE, GEO. E., The Influence of Hyperbolic Notches on the Transverse Flexure of Elastic Plates, *J. Applied Mech.*, June, 1940.

load have been published by several investigators.<sup>1</sup> In the standard bolt the critical section is at the first thread inside the

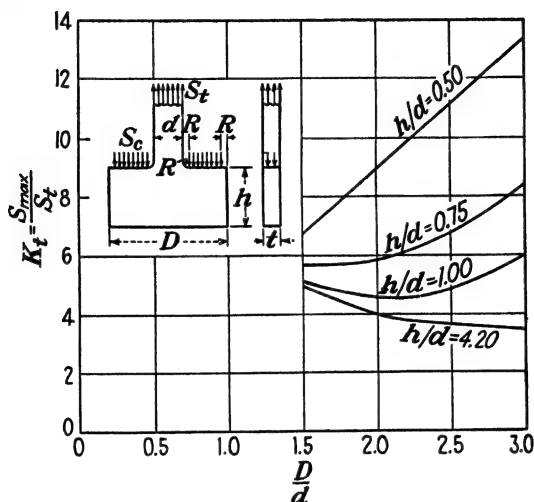


FIG. 37.—Stress-concentration factors for a shoulder.

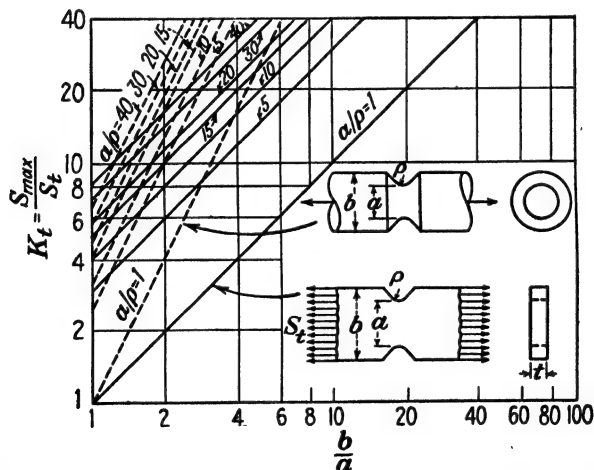


FIG. 38.—Stress-concentration factors for hyperbolic notches in tension members. nut, about 65 per cent of all failures in bolts starting at that section. The section of the bolt at the last thread and the junction of the shank and head are also regions of stress con-

<sup>1</sup> HETÉNYI, M., The Distribution of Stress in Threaded Connections, *Proc. Soc. Exptl. Stress Analysis*, Vol. 1, No. 1, p. 147, 1943.

centration. An increase in the radius of the fillet between shank and head and a reduction in the diameter of the unthreaded portion of the bolt will reduce the stress-concentration factors

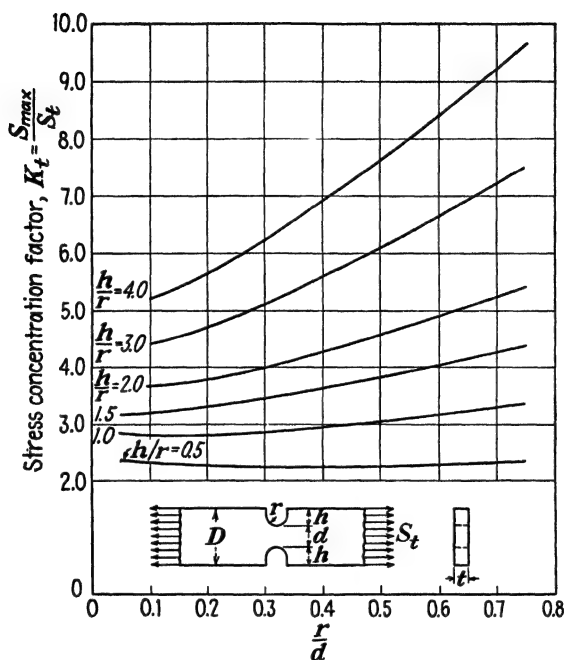


FIG. 39.—Stress-concentration factors for circular notches.

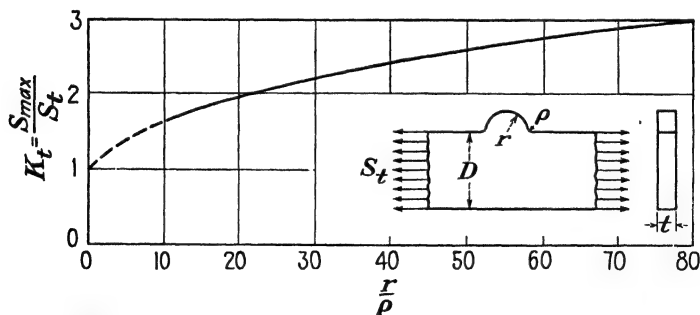


FIG. 40.—Stress-concentration factors for a protrusion on a tension member.

at the two latter sections. Stress concentration at the first thread in the nut may be reduced by using a nut having a lower modulus of elasticity than the bolt or by tapering the threads,



each modification giving a better distribution of the load transfer from bolt to nut. The stress-concentration factor for a standard Whitworth thread with a conventional nut is about 3.85. Double threads or the use of a spherical washer have no appreciable effect upon the value. Hetényi found that the use of a tapered thread reduces the stress-concentration factor to 3.10, and the use of a nut with a tapered lip results in a factor of 3.00.

**48. Stress Concentration under Repeated Loading.**—Values of the stress-concentration factor given in Art. 47 are for the condition of static loading. If the member is subjected to repeated loading, the endurance limit is taken as the criterion of strength and is used as a basis of design. Hence, in evaluating the effect of a notch, hole, scratch, or other defect in a member subjected to repeated loading it is desirable to consider the ratio of the endurance limit of a polished specimen (free from blemishes) to the endurance limit of the shape under consideration. This ratio will be called the *endurance-limit-reduction factor*<sup>1</sup> and will be designated as  $K_s$ . The factor is not a constant for a given geometrical discontinuity, such as a hole or notch, but depends upon the material because some materials are much more sensitive than others to stress raisers. This may be explained by considering the mechanism of failure by repeated loading.

At the base of a notch or crack, or in any region where stress concentration exists, relatively high stresses (above the proportional limit) may be developed at relatively low loads. Thus, a load that is not large enough to damage the member as a whole may cause localized strain hardening in the region of stress concentration. Under static loading this is not serious, but under repeated loading the brittleness, increased by each application of load, may become sufficiently great to result in the formation of a crack. When a crack forms, it produces stress concentration, which in turn causes the crack to lengthen. Extension of the crack by continued strain hardening results in a fatigue failure. It is evident that the rapidity of the process depends upon the strain-hardening characteristics of the material.

In other words, the stress-concentration factor is dependent only upon the *geometry* of the member as long as the material is homogeneous and the proportional limit is not exceeded, but

<sup>1</sup> This ratio has also been called the stress-concentration factor, although it is different from the stress-concentration factor as previously defined.

the endurance-limit-reduction factor is dependent upon both the *geometry of the member and the properties of the material*.

Even if designed notches and holes are not present, failure under repeated loading may occur due to cracks spreading from scratches and other surface irregularities. Several investigators have found that this effect is augmented by corrosion.

Moore and Henwood<sup>1</sup> report values of endurance-limit-reduction factors as obtained from tests on  $\frac{3}{8}$ -in. bolts of about 0.30 per cent carbon steel and S.A.E. 2320 steel that were subjected to axial tension varying from approximately zero to a maximum. Their results are given in Table V together with values of stress-concentration factors from photoelastic studies by Hall.<sup>2</sup> The value of 3.86 for the Whitworth thread checks the value of 3.85 reported by Hetényi,<sup>3</sup> who also used the photoelastic method.

TABLE V.—ENDURANCE LIMIT REDUCTION FACTORS FOR TWO STEELS

Thread	Endurance-limit reduction factor		Stress-concentration factor
	C. steel	S.A.F. 2320	
U. S. std. . . . .	2.84	3.85	5.62
Whitworth . . . . .	1.76	3.32	3.86
Rolled . . . . .	2.15		

The data indicate that the S.A.E. 2320 steel is definitely more sensitive to stress concentration than is the plain carbon steel, but both steels have a lower factor than that obtained photoelastically. The value of the stress-concentration factor may be considered to represent an upper limit of the endurance-limit-reduction factor for a Whitworth thread. A material that is highly sensitive to stress concentration would be expected to have a value of endurance-limit-reduction factor approaching 3.85 for a Whitworth thread. The sensitivity of the material to stress concentration might be evaluated as the ratio of the

<sup>1</sup> MOORE, H. F., and P. E. HENWOOD, The Strength of Screw Threads under Repeated Tension, *Univ. Illinois Eng. Expt. Sta. Bull.* 264, 1934.

<sup>2</sup> HALL, S. G., Determination of Stress Concentration in Screw Threads by the Photoelastic Method, *Univ. Illinois Eng. Expt. Sta. Bull.* 245, 1932.

<sup>3</sup> *Loc. cit.*

strength-reduction factor in repeated loading to the stress-concentration factor.

In general, the sensitivity of a material to stress concentration is associated with small grain size and lack of ductility. A ductile material is capable of making local adjustments to redistribute the stress in the region of stress concentration, and a brittle material is not. Hence, in the brittle material there is more tendency for a crack to form and develop into a progressive fracture. Cast iron is an important exception, exhibiting comparatively little sensitivity to stress concentration. Moore attributes this to the fact that cast iron is initially full of stress raisers, owing to the presence of graphite, which is structurally weak, so the endurance limit of the polished specimen that serves as the standard is relatively low.

If the member is subjected to bending instead of axial load, other factors may be involved, as is discussed in Chap. 8.

**49. Reduction of Stress-concentration Factor.**—In a member composed of a homogeneous material and subjected to an axial

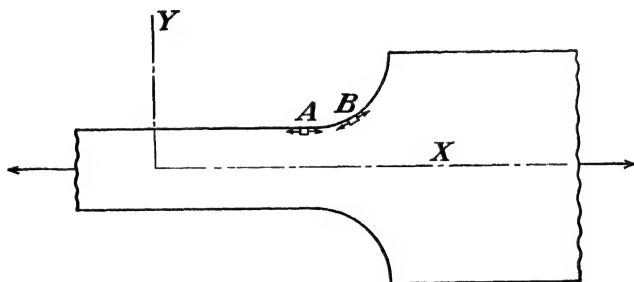


FIG. 41.—Directions of principal stresses.

static load the magnitude of the stress-concentration factor is dependent only upon the geometry of the member and the discontinuity. As the abruptness of the discontinuity is decreased, the stress-concentration factor is decreased.

This follows from the fact that the shearing stress must be zero on the boundary of the member; hence, at each point on the boundary one principal stress is parallel to the boundary, and the other principal stress is zero. For example, in Fig. 41 the directions of the maximum principal stresses at points *A* and *B* are as shown. The change in the direction of the principal stress is a function of the shearing stress and the principal stresses.

From Eq. (17), for  $S_v = 0$

$$\sin 2\theta_{uz} = \frac{2S_{xy}}{S_u} \quad (17a)$$

Since at point  $A$ ,  $S_{xy} = 0$  and  $\theta = 0$ , the change in the angle  $\theta$  between points  $A$  and  $B$  is due to the increase in the shearing stress. However, an increase in shearing stress results in an increase in the principal stress, from Eq. (11). Thus, abrupt change in the direction of the boundary resulting in an abrupt change in the direction of the principal stress produces large

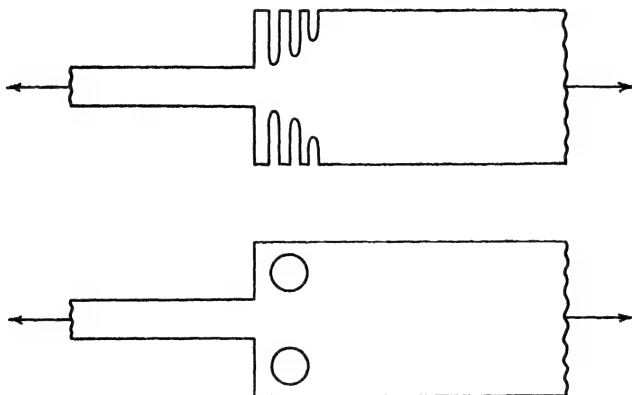


FIG. 42.—Reduction of stress concentration by removal of material.

shearing stresses, which in turn increase the principal stress. A more gradual transition in the boundary reduces the stress-concentration factor.

A gradual transition in the boundary may be attained either by adding material or by removing material. As has been noted, the stress-concentration factor at a change in width of a tension member may be reduced by increasing the radius of the fillet, which adds material. The factor may also be reduced by removing material as indicated in Fig. 42. In this case the removal of material decreases the rigidity of the “dead” material in the corner, permitting more deformation at the corner, thereby decreasing the abruptness of the transition. As another example, the stress-concentration factor at a transverse ellipse in a wide tension member may be reduced by removing enough material to make the hole circular or even elliptical with the major axis parallel to the tensile load, as shown in Fig. 43.

In general, stress concentration may be reduced by "streamlining" the discontinuity.

**50. Significance of Stress-concentration Factor.**—The values of the stress-concentration factors given in Art. 47 and shown in Figs. 34 to 40 are derived on the assumption that the proportional limit of the material is not exceeded, and they are, therefore, not valid above the proportional limit. If a stress-concentration factor indicates a value of stress in excess of the proportional limit, the interpretation of the result must depend upon the characteristics of the material when strained above the proportional limit.

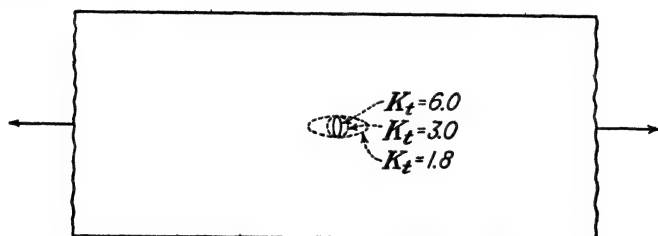


FIG. 43.—Reduction of stress concentration by enlargement of hole.

If the material is very brittle, so that its proportional limit and ultimate strength are identical and it will fracture at the proportional limit, the member may be expected to fail when the maximum stress, as evaluated from the stress-concentration factor, exceeds the proportional limit. As the stress exceeds the proportional limit at the section of stress concentration, a local fracture will develop at that point. The resulting crack will usually produce an even higher stress concentration, causing the crack to extend, thereby increasing the stress above the proportional limit progressively across the member.

If the material is ductile, however, a localized stress in excess of the proportional limit will not result in a crack. The material will deform with little or no increase in stress. Usually the local yielding will increase the stress in the adjacent material sufficiently to produce equilibrium. The localized yielding serves to reduce the effect of the stress concentration, *i.e.*, it will tend to "streamline" the discontinuity causing the high stress.

The values of stress-concentration factors given in Art. 47 were obtained for the condition of static loading. If the member is subjected to repeated loading that produces a localized stress

in excess of the endurance limit, the material will crack regardless of whether it is ductile or brittle.<sup>1</sup> As soon as a crack (with its accompanying high stress-concentration factor) has formed, failure by progressive fracture may result. That is, the crack will work across the member progressively as the material at the tip of the crack is stressed above the proportional limit.

If the member is subject to impact loading, the stresses cannot be evaluated by the ordinary techniques, and conservative practice dictates the use of stress-concentration factors for both ductile and brittle materials.

To summarize, recommended engineering practice is to use stress-concentration factors in designing members of both ductile and brittle materials subjected to impact or repeated loads and for brittle materials under static loads. For ductile materials subjected to steady loads the stress-concentration factor may be ignored except where tolerances are very small. Then an investigation of the strain due to local yielding should be made to determine whether or not excessive permanent set will result. If materials that are usually considered ductile are used under abnormal conditions such as at low temperatures, they may become brittle, necessitating the use of stress-concentration factors in design.

There is evidence to indicate that quenching may induce initial cracks in metals, or produce a condition of initial strain that will result in cracks with the application of relatively small loads. Working stresses for such materials, particularly for the condition of repeated loading, may need to be reduced appreciably to prevent progressive fracture from starting as a result of the high stresses at the tips of such cracks.

Working stresses in members containing stress raisers may be increased if the member is subjected to shot blasting, nitriding, or any of the comparable techniques designed to increase strength.

### PROBLEMS

**139.** Under the three headings of load, material, and shape of member tabulate all of the assumptions involved in the formula  $S = P/A$ .

**140.** Prove that a curved member cannot be axially loaded.

**141.** Does the formula  $S = P/A$  hold for stresses above the proportional limit? Explain.

<sup>1</sup> This may be attributed to the fact that a material which is initially ductile will become brittle (locally) under repeated loading above the proportional limit, owing to strain hardening.

**142.** Prove the statement following Eq. (69b).

**143.** A rod, each transverse cross section of which is circular, is supported at one end and hangs in a vertical position. The material of the rod weighs  $w$  p.c.f., and the rod carries an axial load  $F$  at the lower end. Derive an equation for the diameter of the rod at any section along its length if the average tensile stress is to be the same at each cross section and the weight of the rod is not negligible.

**144.** A vertical rectangular panel of height  $h$ , width  $b$ , and uniform thickness  $t$  is pinned at the top and bottom and also along the vertical sides. Along the top edge it carries a uniformly distributed vertical load, which is resisted by an equal load along the bottom edge. According to ANC-5 specifications the critical load that will cause the panel to buckle is given by

$$\frac{P}{A} = 3.6E \frac{t^2}{b^2}$$

where  $h > 2.56b$ , and  $A = bt$ .

Does this formula appear to be rational? Explain.

**145.** A plate 20 in. wide and  $\frac{1}{2}$  in. thick has a  $\frac{1}{4}$ -in. hole drilled through the  $\frac{1}{2}$ -in. thickness at the center and is subjected to an axial tensile load of 10,000 lb. Plot a graph showing the variation in the radial and tangential stresses along a diametral plane perpendicular to the axis.

**146.** An axially loaded tensile member 10 in. wide and  $\frac{3}{8}$  in. thick contains a circular hole  $\frac{1}{4}$  in. in diameter at the center. Determine, from Eq. (71b), the magnitude and the position of the line of action of the resultant force acting on one-half of the transverse section cut along a diameter perpendicular to the axis of the plate.

**147.** Using polar coordinates, plot a curve showing the variation of  $S_r$  around the edge of a small circular hole in an axially loaded plate.

**148.** Determine the magnitude and location of the maximum shearing stress in the plate of Prob. 145.

**149.** Determine the maximum axial tensile load which a 2- by  $\frac{1}{4}$ -in. strap with a  $\frac{1}{4}$ -in. hole drilled through the center will carry if the maximum tensile stress is not to exceed 24,000 p.s.i.

**150.** Determine the maximum axial tensile load that the strap in Fig. P-150 will carry if the tensile stress is not to exceed 24,000 p.s.i.

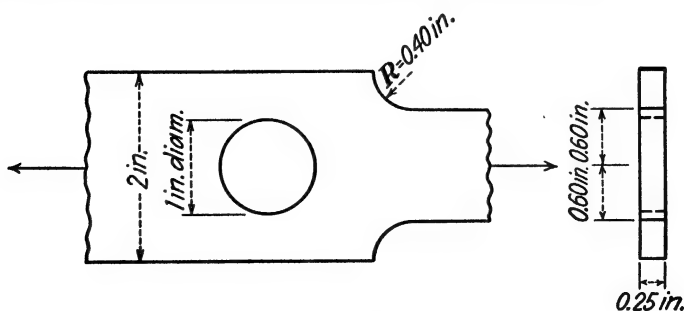


FIG. P-150.

**151.** The fitting indicated in Fig. P-151 is subjected to a static axial load of 8,000 lb. All material is structural steel.

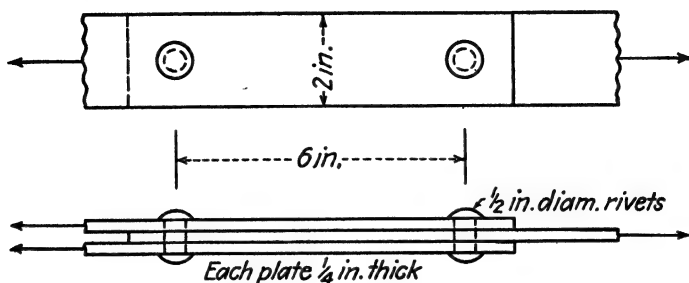


FIG. P-151.

- Determine the approximate maximum stress in the fitting and tell where it occurs.
- Determine the approximate change in distance between centers of the rivets.

**152.** A dashpot for a certain mechanism consists of a cylinder with an inside diameter of 4.00 in. and a wall thickness of 0.250 in. The cylinder contains a small hole in one side (not the end). If the maximum permissible stress in the material is 60,000 p.s.i., what is the limiting internal pressure for that cylinder? Which of the two types of construction indicated in Fig. P-152 is the stronger?

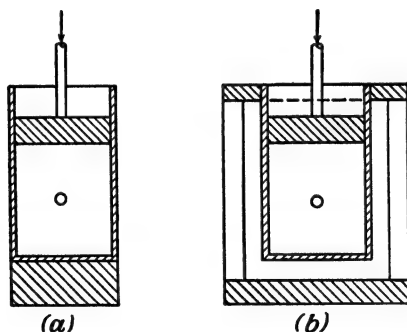


FIG. P-152.

**153.** Determine the stress-concentration factor for a small hole in a large plate subjected to equal biaxial tensile stresses.

**154.** A large shaft has a small transverse hole drilled along a diameter. Determine the stress-concentration factor for the hole when the shaft is subjected to torque.



**155.** A structural-steel plate  $\frac{3}{8}$  in. thick and 16 in. wide contains a  $\frac{1}{2}$ - by  $\frac{1}{4}$ -in. elliptical hole with the major axis normal to the longitudinal axis of the plate.

- a. Determine the maximum axial tensile load that the plate will withstand without inelastic action.
- b. Determine the maximum axial load the plate will withstand without inelastic action if the ellipse is drilled out to a  $\frac{1}{2}$ -in. diameter hole.

## CHAPTER VI

### CYLINDERS, SPHERES, AND DISKS UNDER RADIALLY SYMMETRICAL LOADS

**51. Thin-walled Pressure Vessels.**—The relationship between the internal pressure and the stresses in the walls of a thin-walled

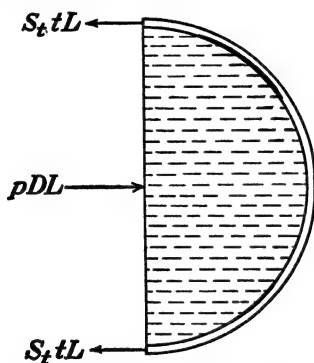


FIG. 44.—Free-body diagram of portion of thin-walled cylinder.

pressure vessel, such as a cylindrical tank, under internal fluid pressure is usually determined by considering a free-body diagram of a short length of one-half of the cylinder and fluid as indicated in Fig. 44. If the internal pressure (gage pressure) is  $p$ , the internal diameter is  $D$ , and a section of length  $L$  is selected, the resultant force developed by the fluid on the inside is  $pDL$ . This force will be resisted by the equal circumferential tensile forces developed in the walls at the top and bottom. If the wall thickness is  $t$  and if the tensile stress in the wall is *assumed* to be *uniformly distributed*, the circumferential tensile stress  $S_t$  is, from the equation of equilibrium applied to Fig. 44,

$$S_t = \frac{pD}{2t} \quad (72)$$

The longitudinal tensile stress may be found similarly from a free-body diagram of one end of the tank, and, for a cylindrical tank, equals

$$S_t = \frac{pD}{4t} \quad (72a)$$

Many tanks are built with ends that are surfaces of revolution, being sections of cones, paraboloids, or ellipsoids. The longitudinal stresses in them may be found from a free-body diagram

of a section normal to the axis of revolution as shown in Fig. 45a. If the tensile stress is uniformly distributed across the cut section, the stress at a point is

$$S_t = \frac{px}{2t \cos \theta} \quad (72b)$$

in which  $x$  is the radius to the point at which the stress is desired  
 $\theta$  is the angle that a tangent at the point makes with the axis of revolution.

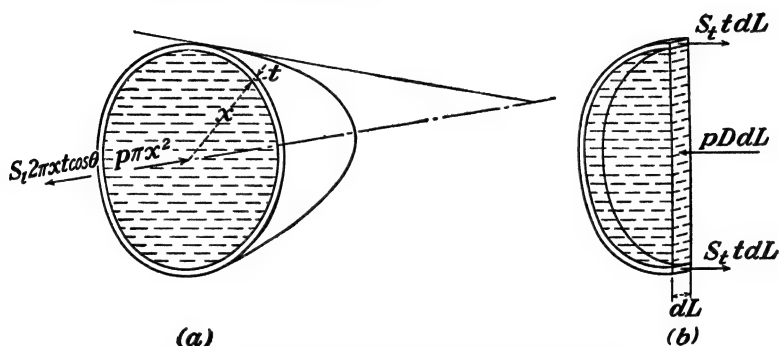


FIG. 45.—Elements of thin-walled pressure vessels.

The circumferential stress may be determined from the free-body diagram of Fig. 45b, which represents half of a thin disk cut from the diagram of Fig. 45a. If there is no abrupt change in cross section at the section, the expression for circumferential stress is identical to Eq. (72).

The general solution for stresses in thin-walled pressure vessels is given by Timoshenko.<sup>1</sup>

Equations (72), (72a), and (72b) give the average value of the tensile stress for a condition of internal pressure only. If the walls of the tank are relatively thin in comparison with the diameter of the tank, the stress is approximately uniformly distributed as assumed; but if the walls are relatively thick, or if there are abrupt changes in shape or thickness, the stress is not uniformly distributed. If the stress is not uniformly distributed, the maximum stress must be greater than that given by Eq. (72). Also, if the tank is under external pressure, buck-

<sup>1</sup> TIMOSHENKO, S., "Theory of Plates and Shells," McGraw-Hill Book Company, Inc., New York, 1940.

ling may occur which is not accounted for in Eq. (72), so the ordinary thin-wall theory is not adequate for all cylinders.

**52. Thick-walled Pressure Vessels.**—Pressure vessels are frequently required to operate under pressures of 4,000 p.s.i. or more, and a cannon, while the projectile is traveling the length of the barrel, is essentially a pressure vessel subjected to an internal pressure that may exceed 35,000 p.s.i. Under these conditions, as well as many others, the walls of the vessel must be

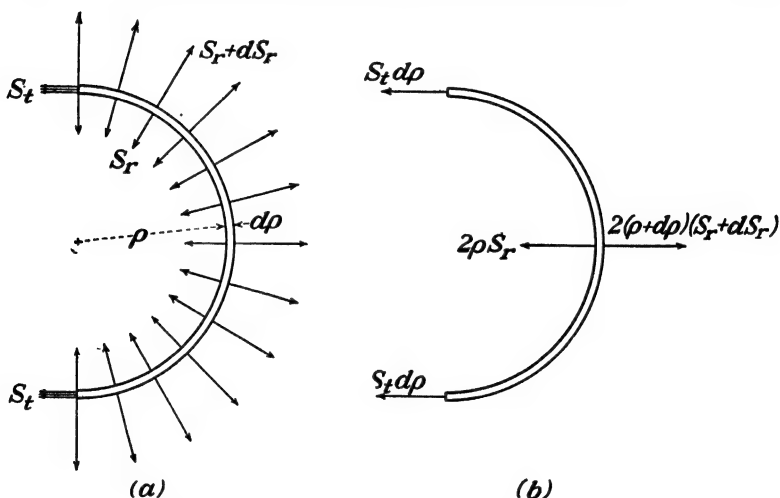


FIG. 46.—Element of wall of thick-walled cylinder.

relatively thick in comparison with the diameter, and the stress is not uniformly distributed throughout the wall.<sup>1</sup>

Since a free-body diagram and the equations of equilibrium can be used to determine only resultant forces and not the distribution of stress, it is necessary to consider the geometry of the deformed vessel and, in addition, the properties of the material. That is, the stress is dependent upon each of the three items, *statics*, *geometry*, and the *properties of the material*.

1. *Statics*.—The cylinder may be assumed to consist of a series of rings of infinitesimal thickness  $dp$ , a typical one of which (at a distance  $\rho$  from the center) is subjected to an internal normal stress  $S_r$  and an external normal stress  $S_r + dS_r$ . Since the cylinder is symmetrical, these stresses will be uniformly dis-

<sup>1</sup> The original solution to the problem was given by Lamé in "Leçons sur la théorie de l'élasticité," Paris, 1852.

tributed around the circumference of the ring as indicated in Fig. 46a. A free-body diagram of a unit length (longitudinally) of one-half of one of the rings is indicated in Fig. 46b. For convenience, all of the stresses are assumed to be tensile; negative values will therefore indicate compressive stresses. From the equation of equilibrium

$$2S_t d\rho + 2\rho S_r = 2(\rho S_r + \rho dS_r + S_r d\rho + d\rho dS_r) \quad (73a)$$

from which

$$S_t = S_r + \rho \frac{dS_r}{d\rho} \quad (73b)$$

This equation of equilibrium cannot be integrated directly because  $S_t$  and  $S_r$  are functions of  $\rho$ . Hence, supplementary information must be obtained from geometry and the properties of the material.

2. *Geometry*.—Figure 47 indicates a cross section of the thick-walled cylinder. If the pressure is uniformly distributed internally, externally, or both, and if the material is homogeneous, the displacement of any point in the cross section must be along a radial line. For example, as internal pressure is applied, an arbitrary point  $A$  in the wall will

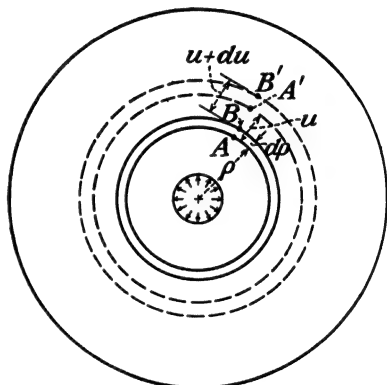


FIG. 47.—Displacements in an element of a thick-walled cylinder.

move outward along a radius  $OA$  to a new position  $A'$ , and  $B$  will move to  $B'$ . That is, the ring of which  $AB$  is the thickness will move outward to the new position  $A'B'$ . If the radius  $OA$  is called  $\rho$  and the displacement  $AA'$  is called  $u$ , the radius  $OA'$  becomes  $(\rho + u)$ . Every point at a distance  $\rho$  from the center has the same displacement, so a circle that originally had a radius  $\rho$  has a new radius  $\rho + u$  after the pressure is applied. The unit strain  $\epsilon_t$  in the direction of the tangent to the circle is, therefore

$$\begin{aligned} \epsilon_t &= \frac{2\pi(\rho + u) - 2\pi\rho}{2\pi\rho} \\ &= \frac{u}{\rho} \end{aligned} \quad (74)$$

Similarly, point  $B$  will move to  $B'$ . Since there may be a change in the thickness of the wall, the distance that  $B$  moves will not necessarily be  $u$  but will be assumed to be  $u + du$ . If  $B$  is located at a distance  $d\rho$  from  $A$ , the average unit strain between  $A$  and  $B$  (the radial unit strain) is

$$\epsilon_r = \frac{du}{d\rho} \quad (75)$$

A uniform cylinder under uniform pressure would be expected to deform in such a way that a plane section which is normal to the longitudinal axis before loading will remain plane after the pressure is applied, provided that the section is not near the end of the cylinder. If a plane section remains plane,  $\epsilon_w$  in the longitudinal ( $w$ ) direction will be a constant.

3. *Properties of the Material.*—If the properties of the material are known, the principal stresses  $S_t$  and  $S_r$  (in the tangential and radial directions) may be expressed in terms of the radial displacement  $u$  and the unit strain  $\epsilon_w$ . If the material is homogeneous and isotropic, and if the proportional limit is not exceeded, Eq. (55a) applies and

$$\begin{aligned} S_t &= \frac{E[\epsilon_t + \mu(-\epsilon_t + \epsilon_r + \epsilon_w)]}{1 - \mu - 2\mu^2} \\ &= \frac{E\left[\frac{u}{\rho} + \mu\left(\frac{-u}{\rho} + \frac{du}{d\rho} + \epsilon_w\right)\right]}{1 - \mu - 2\mu^2} \end{aligned} \quad (76a)$$

from Eqs. (74) and (75).

Also

$$S_r = \frac{E\left[\frac{du}{d\rho} + \mu\left(\frac{-du}{d\rho} + \frac{u}{\rho} + \epsilon_w\right)\right]}{1 - \mu - 2\mu^2} \quad (76b)$$

Similarly, the stress  $S_w$  in the longitudinal direction may be expressed as

$$S_w = \frac{E\left[\epsilon_w + \mu\left(-\epsilon_w + \frac{u}{\rho} + \frac{du}{d\rho}\right)\right]}{1 - \mu - 2\mu^2} \quad (76c)$$

4. *Combination.*—The results of the contributions of statics, geometry, and the properties of the material may be combined by substituting values of  $S_t$ ,  $S_r$ , and  $dS_r/d\rho$  from Eq. (76) into

Eq. (73b). The quantity  $E$  and the denominator  $(1 - \mu - 2\mu^2)$  are common to all terms so they may be canceled out. Then

$$\frac{u}{\rho} + \mu \left( \frac{-u}{\rho} + \frac{du}{d\rho} + \epsilon_w \right) = \frac{du}{d\rho} + \mu \left( \frac{-du}{d\rho} + \frac{u}{\rho} + \epsilon_w \right) + \rho \frac{d^2u}{d\rho^2} - \mu\rho \frac{d^2u}{d\rho^2} + \mu \frac{du}{d\rho} - \frac{u}{\rho} + \mu\rho \frac{d\epsilon_w}{d\rho} \quad (77a)$$

which reduces to

$$\rho \frac{d^2u}{d\rho^2} + \frac{du}{d\rho} - \frac{u}{\rho} = 0 \quad (77b)$$

or

$$\frac{d^2u}{d\rho^2} + \frac{1}{\rho} \frac{du}{d\rho} - \frac{u}{\rho^2} = 0 \quad (77c)$$

Since this equation involves only the relationship between the two variables  $u$  and  $\rho$ , it may be integrated.<sup>1</sup>

One solution of Eq. (77c) is

$$u = a\rho + \frac{b}{\rho} \quad (78)$$

in which  $a$  and  $b$  are the constants of integration. The constants may be evaluated by making use of the "boundary conditions," i.e., by substituting the known values of the radial stress at the inner and outer boundaries of the cross section. From Eq. (76b) the radial stress may be expressed in terms of  $E$ ,  $\mu$ ,  $\rho$ ,  $\epsilon_w$ ,  $a$ , and  $b$ .

$$S_r = \frac{E \left( a - \frac{b}{\rho^2} + 2\mu \frac{b}{\rho^2} + \mu\epsilon_w \right)}{1 - \mu - 2\mu^2} \quad (79)$$

At the inner boundary where  $\rho = r_1$ ,  $S_r = -p_1$  in which  $p_1$  is the magnitude of the internal pressure. The minus sign is used to convert a positive pressure to a negative (compressive)

<sup>1</sup> The integration may be performed by the standard methods of differential equations or by assuming that the solution is a polynomial. Then

$$u = c\rho^x$$

If this assumed solution is substituted in Eq. (77c) there results

$$x(x-1)c\rho^{x-2} + xc\rho^{x-2} - c\rho^{x-2} = 0$$

from which  $x = \pm 1$ , and

$$u = a\rho + b\rho^{-1}$$

stress. Then

$$-p_1 = \frac{E \left[ a - \frac{b}{r_1^2} (1 - 2\mu) + \mu \epsilon_w \right]}{1 - \mu - 2\mu^2} \quad (79a)$$

At the outer boundary where  $\rho = r_2$ ,  $S_r = -p_2$  in which  $p_2$  is the magnitude of the external pressure. From Eq. (79),

$$-p_2 = \frac{E \left[ a - \frac{b}{r_2^2} (1 - 2\mu) + \mu \epsilon_w \right]}{1 - \mu - 2\mu^2} \quad (79b)$$

The values  $a$  and  $b$  may be determined by solving Eqs. (79a) and (79b) simultaneously

$$a = \frac{(p_1 r_1^2 - p_2 r_2^2)(1 - \mu - 2\mu^2)}{E(r_2^2 - r_1^2)} - \mu \epsilon_w$$

$$b = \frac{(1 + \mu)(p_1 - p_2)r_1^2 r_2^2}{E(r_2^2 - r_1^2)}$$

Values of  $u$ ,  $S_r$ ,  $S_t$ , and  $S_w$  may be found by substituting the values of  $a$  and  $b$  in Eq. (76)

$$u = \frac{\rho^2(1 - \mu - 2\mu^2)(p_1 r_1^2 - p_2 r_2^2) + r_1^2 r_2^2(1 + \mu)(p_1 - p_2)}{E\rho(r_2^2 - r_1^2)} - \mu \rho \epsilon_w \quad (80)$$

$$S_t = \frac{p_1 r_1^2 - p_2 r_2^2 + \frac{r_1^2 r_2^2}{\rho^2} (p_1 - p_2)}{r_2^2 - r_1^2} \quad (81)$$

$$S_r = \frac{p_1 r_1^2 - p_2 r_2^2 - \frac{r_1^2 r_2^2}{\rho^2} (p_1 - p_2)}{r_2^2 - r_1^2} \quad (82)$$

$$S_w = E\epsilon_w + \frac{2\mu(p_1 r_1^2 - p_2 r_2^2)}{r_2^2 - r_1^2} \quad (83)$$

In Eqs. (80) to (83) pressures greater than atmospheric are positive, and negative stresses denote compression as before.

If Eqs. (81) and (82) are added, there results

$$S_r + S_t = \frac{2(p_1 r_1^2 - p_2 r_2^2)}{r_2^2 - r_1^2} \quad (84)$$

which indicates that  $S_t + S_r$  is constant at all points in the wall. If  $S_t$  is evaluated at the inside and at the outside of the



wall and the values are subtracted

$$\begin{aligned} S_{ii} - S_{to} &= \frac{(r_2^2 - r_1^2)(p_1 - p_2)}{r_2^2 - r_1^2} \\ &= p_1 - p_2 \end{aligned} \quad (85a)$$

Similarly

$$S_{ro} - S_{ri} = p_1 - p_2 \quad (85b)$$

Equation (83) indicates that the stress in the longitudinal direction is constant over the cross section since  $\epsilon_w$  is constant and  $\rho$  does not appear in the second term.

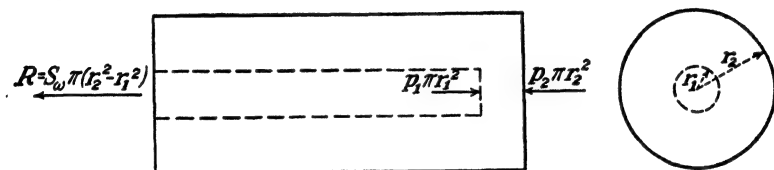


FIG. 48.—Free-body diagram of longitudinal portion of cylinder.

The longitudinal stress  $S_w$  may therefore be evaluated directly from a free-body diagram of a portion of the cylinder as indicated in Fig. 48.

From the equation of equilibrium

$$S_w \pi (r_2^2 - r_1^2) + p_2 \pi r_2^2 = p_1 \pi r_1^2 \quad (86)$$

or

$$S_w = \frac{p_1 r_1^2 - p_2 r_2^2}{r_2^2 - r_1^2} \quad (87)$$

A comparison of Eq. (87) with Eq. (84) shows that

$$S_w = \frac{1}{2}(S_i + S_r) \quad (88)$$

The unit strain in the longitudinal direction may be determined by substituting the value of  $S_w$  from Eq. (87) in Eq. (83).

$$\epsilon_w = \frac{(1 - 2\mu)(p_1 r_1^2 - p_2 r_2^2)}{E(r_2^2 - r_1^2)} \quad (89)$$

or

$$\epsilon_w = \frac{(1 - 2\mu)S_w}{E} \quad (89a)$$

$$= \frac{(1 - 2\mu)(S_i + S_r)}{2E} \quad (89b)$$

The expression for the radial displacement of any point, Eq. (80),

may be simplified somewhat by substituting the value of  $\epsilon_w$  from Eq. (89).

$$u = \frac{\rho^2(p_1 r_1^2 - p_2 r_2^2)(1 - 2\mu) + (p_1 - p_2)r_1^2 r_2^2(1 + \mu)}{E\rho(r_2^2 - r_1^2)} \quad (80a)$$

It may readily be shown that if the longitudinal stress is zero

$$u = \frac{\rho^2(p_1 r_1^2 - p_2 r_2^2)(1 - \mu) + (p_1 - p_2)r_1^2 r_2^2(1 + \mu)}{E\rho(r_2^2 - r_1^2)} \quad (80b)$$

**53. Variation of Stress in a Thick-walled Cylinder.**—Equation (81) indicates the variation in the tangential stress throughout the wall of the cylinder. The maximum stress occurs at the inside of the shell ( $\rho = r_1$ ) and is equal to

$$S_{t(\max)} = \frac{p_1 r_1^2 - p_2 r_2^2 + r_2^2(p_1 - p_2)}{r_2^2 - r_1^2} \quad (90)$$

For a cylinder subjected to internal pressure only, Eq. (90) reduces to

$$S_{t(\max)} = \frac{p_1(r_1^2 + r_2^2)}{r_2^2 - r_1^2} \quad (90a)$$

and the ratio of the maximum stress to the average stress computed by the thin-wall theory, Eq. (72), is

$$K_t = \frac{1 + (r_2/r_1)^2}{1 + \frac{r_2}{r_1}} \quad (91)$$

Values of  $K_t$ , plotted against  $r_2/r_1$ , shown in Fig. 49a indicate that the thin-wall theory gives results within 10 per cent of the thick-wall theory when  $r_2/r_1$  is less than 1.2, *i.e.*, when the wall thickness is less than 10 per cent of the inside diameter. In other words, when  $D/t$  is more than 10, the error is less than 10 per cent.

From Eq. (82) it is evident that the maximum radial stress occurs at that surface on which the pressure is the greater and is equal in magnitude to the pressure. The maximum tangential stress is always larger in magnitude than the maximum radial stress or the longitudinal stress. Figure 49b shows the variation in the tangential stress and in the radial stress throughout the wall for a cylinder with an external diameter of 8 in. and an internal diameter of 4 in. subjected to an internal pressure of

10,000 p.s.i. The average tangential stress is included for comparison. The fact that the  $S_r$  curve is a constant distance (6,670 p.s.i.) below the  $S_t$  curve agrees with Eq. (84), which states that the sum of  $S_r$  and  $S_t$  is constant. The radial stress is compressive and the tangential stress is tensile.

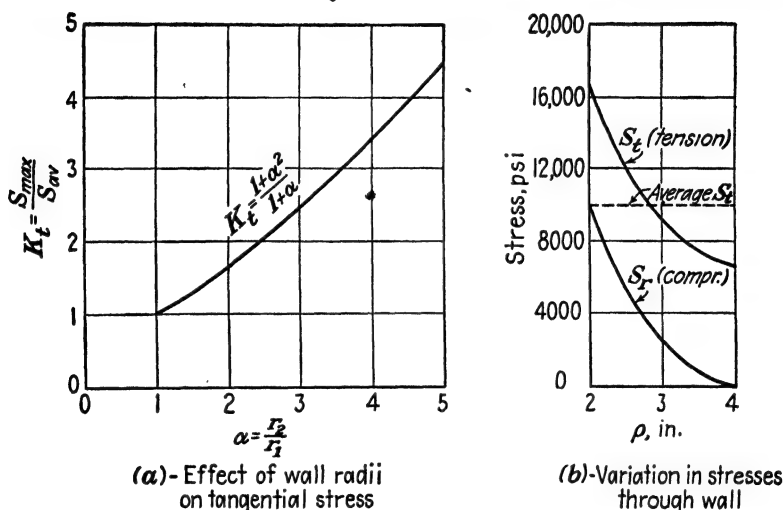


FIG. 49.—Stresses in thick-walled cylinders.

**54. Increasing the Effectiveness of the Material.**—As is evident in Fig. 49b the maximum stresses in a thick-walled cylinder under internal pressure occur at the inside surface. If the shell is designed for the maximum stress at the inside surface, the material in the rest of the wall will not be stressed to the allowable and, consequently, will not be used so effectively as it could be if the stress were uniformly distributed through the wall. The most direct method of achieving a more nearly uniform distribution of stress is to subject the material near the inside wall to an initial compressive stress when the cylinder is not loaded. Then as the pressure on the inside of the cylinder is increased the compressive stresses at the inside must be relieved before any tensile stresses can be developed. Two techniques are used commercially for developing initial compressive stresses near the inside wall. One consists in producing a permanent external pressure on the cylinder by shrinking an external cylinder or hoop on the original cylinder, or by winding the original with

wire under tension; the second involves the application of a temporary internal pressure sufficiently high to produce plastic flow, resulting in a residual compressive stress upon removal of the initial pressure.

**55. External Loading by a Shrink Fit.**—One method for producing an initial pressure on the outside of a cylinder consists in building an outer cylinder having an inside diameter slightly less than the outside diameter of the original cylinder. The outer cylinder is heated and slipped over the original cylinder. As it cools it shrinks, producing an external pressure around the outside of the inner cylinder, which develops initial compressive stresses near the inside wall of the inner cylinder. The entire assembly is effective in resisting an internal pressure and will withstand a higher internal pressure than a single cylinder having the same over-all dimensions. For a cylinder of fixed dimensions the amount of initial compressive stress is controlled by the relative thicknesses of the two cylinders and by the difference in initial diameters at the surface of contact.

*Illustrative Problem.*—A steel cylinder having an inside diameter of 5.996 in. and an outside diameter of 8.000 in. is heated and shrunk over a steel cylinder of equal length having an internal diameter of 4.000 in. and an external diameter of 6.000 in. Determine (a) the initial stresses induced in the cylinders, and (b) the resultant stresses if the assembly is subjected to an internal pressure of 30,000 p.s.i.

*Solution.*—The first step is to evaluate the radial pressure at the boundary of the two cylinders. This may be done by equating the sum of the magnitudes of the displacements of the surfaces of contact to the difference in radii. If the inner cylinder is designated  $A$ , the outer cylinder  $B$ , and the subscripts are used to designate cylinders and radii,

$$u_{A3} + u_{B3} = 0.002 \quad (a)$$

The radial displacement (for  $p = 3$  in.) of each of the cylinders may be determined from Eq. (80a). Poisson's ratio is assumed equal to 0.30,  $E = 30,000,000$  p.s.i., and the radial pressure at the surface of contact is designated as  $p_i$ . From Eq. (80b) the displacement of the outside of the inner cylinder is

$$\begin{aligned} u_{A3} &= \frac{-9p_i(9)(0.7) - p_i(4)(9)(1.3)}{30 \times 10^6(3)(5)} \\ &= -2.30(10)^{-7}p_i \end{aligned} \quad (b)$$

The minus sign indicates a displacement toward the center of the cylinder, as would be expected. For the outer cylinder, which is subjected to an internal pressure of  $p_i$ ,

$$u_{B3} = \frac{9p_i(9)(0.7) + p_i(9)(16)(1.3)}{30 \times 10^6(3)(7)} \\ = 3.87(10)^{-7}p_i \quad (c)$$

This displacement is positive, indicating that the final internal diameter of the outer cylinder is greater than it was before heating. The displacement of the inner cylinder plus the displacement of the outer cylinder must equal the 0.002-in. difference in radii of the cylinders. Hence

$$p_i = \frac{0.002}{6.17 \times 10^{-7}} \\ = 3,240 \text{ p.s.i.} \quad (d)$$

Then

$$u_{A3} = -0.000745 \text{ in.} \quad \text{and} \quad u_{B3} = 0.001255 \text{ in.} \quad (e)$$

The initial tangential stresses in the inner cylinder may be evaluated from Eq. (81) by considering the cylinder as being subjected to an external pressure of 3,240 p.s.i.

$$S_t = \frac{-3,240(9) - 3,240(4)(9)/\rho^2}{5} \quad (f)$$

At the inside  $S_{t2} = -11,660$  p.s.i., and at the outside  $S_{t3} = -8420$  p.s.i. In the outer cylinder  $S_{t3} = 11,570$  p.s.i., and at the outside  $S_{t4} = 8,330$  p.s.i.

If the entire assembly is subjected to an internal pressure of 30,000 p.s.i., the additional tangential stresses due to the internal pressure may be determined from Eq. (81) as

$$S_t = \frac{30,000(4) + 30,000(4)(16)/\rho^2}{12} \quad (g)$$

from which

$$S_{t2} = 50,000 \text{ p.s.i.}, S_{t3} = 27,800 \text{ p.s.i.}, S_{t4} = 20,000 \text{ p.s.i.} \quad (h)$$

The resultant stresses when the cylinder is under internal pressure may be found by adding the initial shrinkage stresses to the stresses due to the internal pressure. The resultant stress at the inside is only 38,340 p.s.i. tension. The maximum stress occurs at the inner surface of the outer cylinder and is 39,370 p.s.i. (if the proportional limit is not exceeded), which is about 20 per cent less than the maximum stress of 50,000 p.s.i. in a single cylinder of 4 in. inside diameter and 8 in. outside diameter. It is apparent that a slight change in the difference in radii at the surface of contact would alter the maximum stresses. For example, if the inside diameter of the outer cylinder is increased to 5.998 in. (a difference of one-half as much as before), the initial (shrinkage) stresses will be one-half as great. Then the resultant stress at the inside surface is 44,170 p.s.i., and the stress at the inside of the outer cylinder is reduced to 33,585 p.s.i. Thus a variation of only 0.002 in. in the diameter will alter the maximum stress in the outer cylinder by about 15 per cent. The resultant stress distribution for the 0.004-in. difference in diameters is the better.

Figure 50a shows the distribution of tangential shrinkage stresses (for the 0.004-in. difference in diameters) across the

cylinder and also the resultant stresses after the internal pressure of 30,000 p.s.i. is applied. The curve showing the variation of stress due to the internal pressure alone, which is the same as the stress distribution for a nonlaminated cylinder, is included for comparison. The horizontal line at 30,000 p.s.i. represents the stress distribution that would exist if all portions of the cylinder

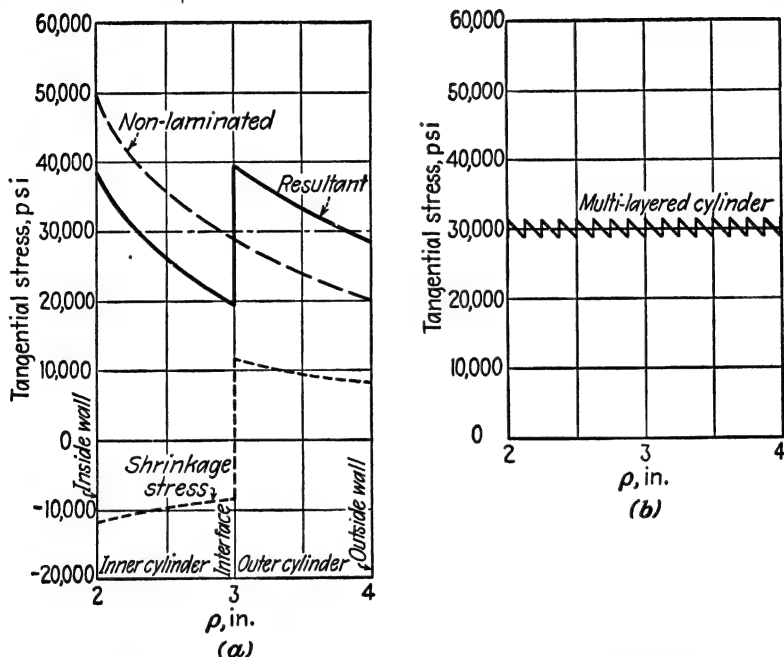


FIG. 50.—Stresses in laminated cylinders.

were equally effective in carrying load. It corresponds to a decrease of 40 per cent in maximum stress as compared with the nonlaminated cylinder.

An infinite number of laminations would be required to obtain the uniform distribution of stress, although the use of several laminations will give results closely approximating that condition as illustrated in Fig. 50b. However, the stress distribution can be balanced for only one magnitude of internal pressure.

A uniform distribution of tangential stress does not represent the optimum distribution because of the influence of the negative  $S_r$  at the critical sections in reducing the strength. For the cylinder under internal pressure a relatively low value of  $S_t$

at the inside surface is desirable since  $S_r$  is a maximum there. A comparison of the minimum values of  $S_m$  (tensile strength under axial load) that the material must be capable of developing to prevent failure by slip of the 4- by 8-in. cylinder is given in Fig. 51 for four theories of failure. The longitudinal stress is assumed to be zero, as in a cannon. Values on the left-hand

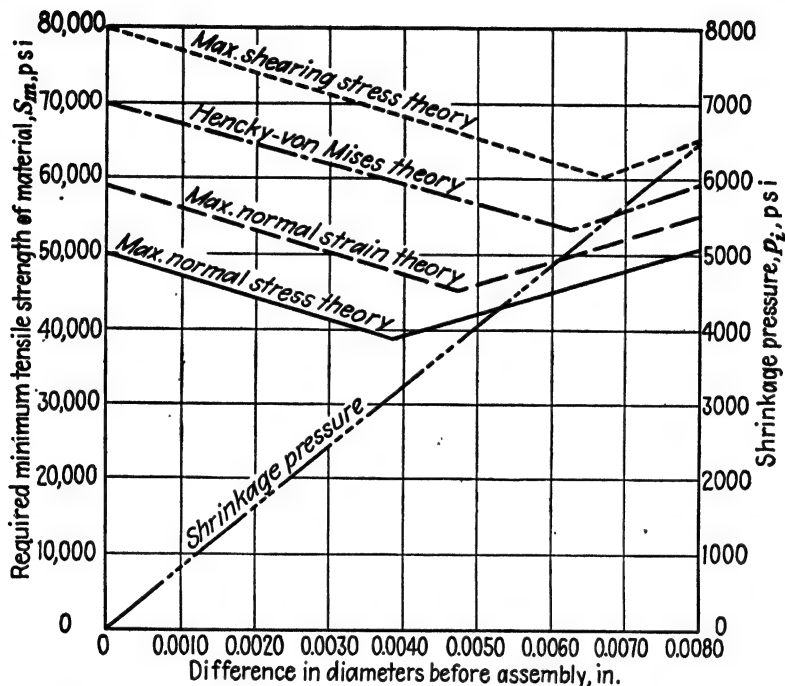


FIG. 51.—Effect of initial difference in diameters upon required strength.

border, for a difference in diameter of zero, correspond to the nonlaminated cylinder. For the cylinder made up of two component rings the optimum condition prevails when the value of the required  $S_m$  at the inside of the inner cylinder equals the required value at the inside of the outer cylinder. The amount of shrinkage necessary to produce that condition is dependent upon which theory of failure is used, as is shown in Fig. 51. Values of the initial shrinkage pressure are also shown.

Although laminated construction has been widely used in the manufacture of thick-walled cylinders, it has the disadvantage of requiring close tolerances on shaping operations. For the

cylinders in the illustrative problem a variation of 0.002 in. in the diameter of one of the surfaces may alter the stresses by 6,000 p.s.i. However, if the individual cylinders are made thinner, the tolerance is increased. Another technique that has been developed to lessen the difficulties somewhat consists in shaping the inner cylinder and then winding it with wire under tension. The wire winding has the same effect upon the inner cylinder as an external cylinder shrunk over the inner cylinder, and the stresses are more easily controlled.

*Illustrative Problem.*—Determine the stress under which a 0.10-in. square wire must be wound on a 4.00- by 6.00-in. cylinder if the maximum stress in the cylinder is not to exceed 40,000 p.s.i. under an internal pressure of 18,000 p.s.i.

*Solution.*—The loading condition for the cylinder is critical when the cylinder is resisting both the internal pressure and the external pressure due

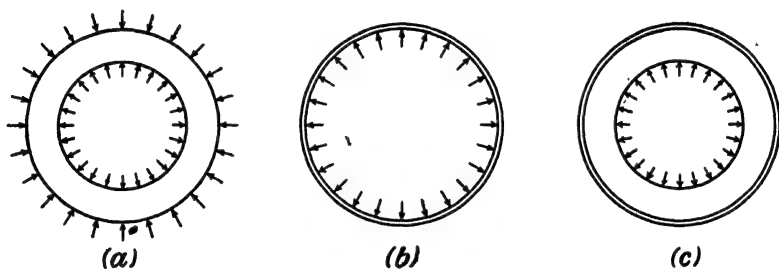


FIG. 52.—Analysis of wire-wound cylinder.

to the wire, Fig. 52a. The pressure that the wire must develop may be found from Eq. (81).

$$40,000 = \frac{18,000(4) - 9p_2 + 9(18,000 - p_2)}{9 - 4} \quad (a)$$

$$p_2 = 1,890 \text{ p.s.i.}$$

The stress developed in the wire may be found by considering it as a cylinder subjected to an internal pressure of 1,890 p.s.i., Fig. 52b,

$$S_t = \frac{1,890(9 + 9.61)}{9.61 - 9.00} \quad (b)$$

$$= 57,700 \text{ p.s.i.}$$

The stress of 57,700 p.s.i. is the sum of the stress due to the initial winding tension and the stress due to the internal pressure. The portion due to the internal pressure may be found by considering the cylinder and winding as a unit, Fig. 52c.



$$S_i = \frac{18,000(4) + \frac{4(9.61)(18,000)}{9.00}}{9.61 - 4} \quad (c)$$

$$= 25,800 \text{ p.s.i.}$$

Hence, the initial stress in the wire must be  $57,700 - 25,800$ , or  $31,900$  p.s.i.

For a number of years wire winding was used as a means of prestressing large caliber cannon, using square wire approximately 0.10 in. on a side, but this practice has been abandoned in favor of shrinking jackets and hoops on the gun tube. Plastic prestressing is used in the smaller calibers. A wire-wound gun is much more flexible than one with a preshrunk jacket and also presents more difficult repair problems.

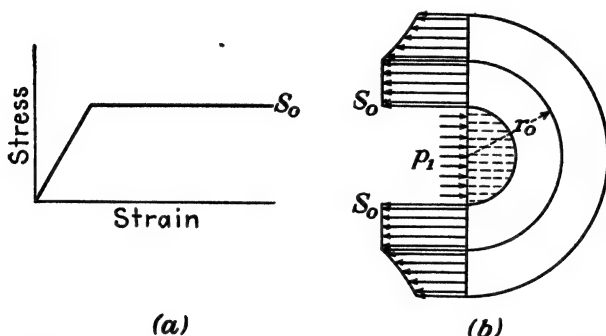


FIG. 53.—Redistribution of stress in thick-walled cylinder due to plastic action.

**56. Plastic Prestressing.**—The condition of an initial compressive stress at the inside of the cylinder when it is not under internal pressure may also be obtained by applying a preliminary internal pressure sufficiently high to stress part of the shell above the proportional limit.

As the internal pressure is increased, the proportional limit is first exceeded at the inside of the wall. With further increase in pressure there is an increase in strain, but the material near the inside cannot develop stress as rapidly as the material that is not stressed above the proportional limit. The latter must, therefore, pick up stress more rapidly than before, and the plastic area spreads outward. When the internal pressure is released, the material near the inside tends to recover the strain that was imposed during loading. However, since the stress-strain diagram upon unloading does not retrace the diagram for loading but follows a straight line parallel to the initial

tangent, the stress is reduced more than it was increased during loading, and a compressive stress near the inside surface results. For any subsequent loading the initial compressive stress near the inside wall must be overcome before any tensile stress can be developed. Hence, a greater internal pressure is required to stress the material to the proportional limit than was required in the preliminary loading. The magnitude of the initial compressive stress required and the effectiveness of the procedure

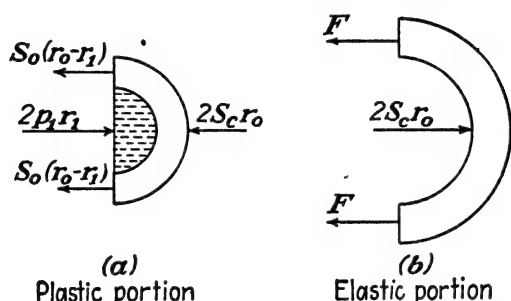


FIG. 54.—Free-body diagrams of portions of thick-walled cylinder.

depend upon the characteristics of the material and the magnitude of the prestressing pressure.

For example, if it is assumed that the stress-strain diagram for the material has the idealized shape indicated in Fig. 53a and that the geometrical behavior of the cylinder is not affected by stresses above the proportional limit, the cylinder may be assumed to consist of two concentric cylinders, as indicated in Fig. 53b, the inner one stressed to the proportional limit and the other one below the proportional limit.

If a unit length of one half of the inner cylinder is taken as a free body, as shown in Fig. 54a, the force equation of equilibrium gives

$$p_1 r_1 = S_o(r_o - r_1) + S_c r_o \quad (92)$$

in which  $S_o$  is the proportional limit of the material<sup>1</sup> and  $S_c$  is the radial stress at the surface of contact of the two cylinders.

From Eq. (92)

$$S_c = \frac{p_1 r_1 - S_o(r_o - r_1)}{r_o} \quad (92a)$$

<sup>1</sup> This will be the proportional limit under the prevailing biaxial or triaxial loading condition and not the proportional limit as determined in an axial test.

The outer cylinder may be assumed to function as a thick-walled cylinder of thickness  $r_o - r_i$  subjected to an internal pressure  $S_o$  as shown in Fig. 54b. Since the tangential stress at the inner surface of the outer cylinder must be equal to  $S_o$ , there follows from Eq. (81)

$$S_o = \frac{[p_1 r_1 - S_o(r_o - r_1)](r_o^2 + r_i^2)}{r_o(r_o^2 - r_i^2)} \quad (93)$$

Equation (93) may be solved for  $r_o$  to determine the outer boundary of the plastic area

$$r_o = \frac{S_o r_i^2 \pm r_i \sqrt{(S_o r_i)^2 - r_1(p_1 + S_o)^2}}{r_1(p_1 + S_o)} \quad (94)$$

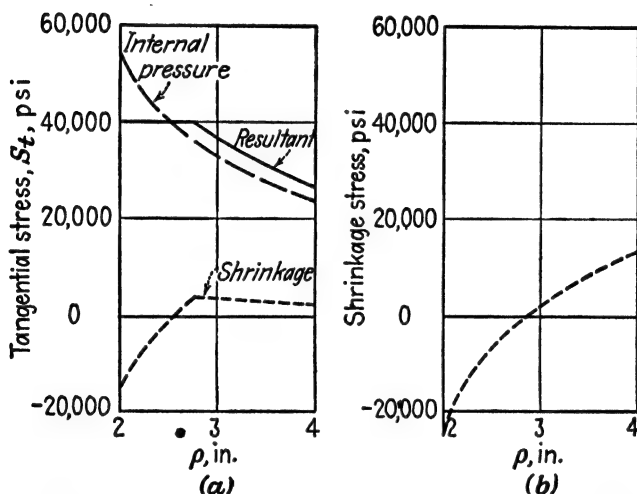


FIG. 55.—Effect of plastic prestress of (a) 35,000 p.s.i. and (b) 40,000 p.s.i.

For example, if the value of  $S_o$  for a 4- by 8-in. cylinder is 40,000 p.s.i. and the cylinder is subjected to an internal pressure of 30,000 p.s.i.,  $r_o$  is equal to 2.36 in. If the internal pressure is increased to 35,000 p.s.i.,  $r_o$  becomes 2.78 in. An internal pressure of 40,000 p.s.i. is required to extend the plastic range to the outside of the cylinder. The distribution of tangential stress corresponding to an internal pressure of 35,000 p.s.i. is given by the solid line in Fig. 55a. If the 35,000-p.s.i. pressure is applied and removed, the decrease in tangential stresses below those corresponding to the 35,000-p.s.i. pressure may be found from Eq. (81) by making  $p_1$  the decrease in pressure below 35,000

p.s.i. because the stress-strain relationship is linear for decreasing stresses. The change in stress due to the removal of the 35,000-p.s.i. pressure varies from 58,400 p.s.i. at the inside to 23,400 p.s.i. at the outside as shown by the dashed line in Fig. 55a. The resultant initial stresses induced by the prestressing are obtained by subtracting the latter stresses from those induced by the application of the pressure and are shown by the dotted line in Fig. 55a. Reapplication of the 35,000-p.s.i. internal pressure will produce the same stresses as on the original application. If a 40,000-p.s.i. prestressing pressure were used, the distribution of tangential prestress would be as indicated in Fig. 55b.

Prestressing is practiced commercially as a means of increasing the resistance of thick-walled cylinders to internal pressure. The magnitude of initial pressure required to produce a satisfactory degree of prestress is often determined experimentally, one rule being to apply sufficient pressure to produce a 4 per cent permanent increase in diameter. As is evident from Eqs. (92) and (93) an analytical solution requires a value of  $S_0$ , which is a function of  $S_c$ . Nádai<sup>1</sup> has obtained a solution by assuming that the material in the plastic state undergoes no volume change with a change in stress.

**57. Displacements Due to a Uniform Temperature Change.**—The change in dimensions of a thick cylinder due to a temperature change may be found from Eqs. (74) and (75). If the temperature change is uniform throughout the cylinder and if there are no external restraints,  $\epsilon_t$  will be constant. From Eq. (74)

$$u = \epsilon_t \rho = c \rho \Delta t \quad (95)$$

in which  $c$  is the coefficient of thermal expansion  
 $\Delta t$  is the change in temperature.

Equation (75) is also satisfied

$$\begin{aligned} \epsilon_r &= \frac{du}{d\rho} = \frac{d}{d\rho} (c \rho \Delta t) \\ &= c \Delta t = \epsilon_t \end{aligned} \quad (96)$$

<sup>1</sup> NÁDAI, A., "Plasticity," Chap. 28, McGraw-Hill Book Company, Inc., New York, 1931.

Hence, the unit strain is the same in all directions, as would be expected.

**58. Stresses in a Thick-walled Sphere.**—The stresses in a thick-walled sphere may be determined by a procedure similar to that outlined for cylinders in Art. 46. The tangential and radial stresses are found to be

$$S_t = \frac{p_1 r_1^3 - p_2 r_2^3 + \frac{r_1^3 r_2^3 (p_1 - p_2)}{\rho^3}}{r_2^3 - r_1^3} \quad (97)$$

and

$$S_r = \frac{p_1 r_1^3 - p_2 r_2^3 - \frac{r_1^3 r_2^3 (p_1 - p_2)}{\rho^3}}{r_2^3 - r_1^3} \quad (98)$$

**59. Shrink-fit Assemblies.**—The principle of shrink fitting has many applications other than pressure vessels. It is used extensively in assemblies such as bushings, bearings, crankshafts,

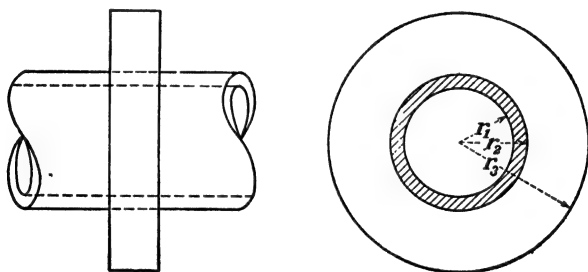


FIG. 56.—Hub and shaft assembly.

couplings, flywheels, car axles, and hub and shaft units. For the assemblies in which the component parts are cylindrical in form, as in Fig. 56, the type of analysis used in the illustrative problem of Art. 55 is applicable. A general expression for the *average* shrink pressure between a hub and hollow shaft may be developed by equating the sum of the displacements of the units at their point of contact to the difference in radii  $\Delta r$ .

If the width of the hub is relatively small, the longitudinal stress in the hub may be assumed to be zero and the radial displacement  $u$  may be found from Eq. (80b). Thus the displacement  $u_s$  of the shaft, at a distance  $r_2$  from the center is

$$u_s = \frac{-p_s r_2 [r_2^2 (1 - \mu_s) + r_1^2 (1 + \mu_s)]}{E_s (r_2^2 - r_1^2)} \quad (80c)$$

and the displacement  $u_h$  of the hub at the same radius is

$$u_h = \frac{p_i r_2 [r_2^2 (1 - \mu_h) + r_3^2 (1 + \mu_h)]}{E_h (r_3^2 - r_2^2)} \quad (80d)$$

Since the total displacement is the sum of the components  $u_s$  inward and  $u_h$  outward,

$$\Delta r = -u_s + u_h$$

and

$$p_i = \frac{\Delta r}{\frac{r_2}{E_s} \left( \frac{r_2^2 + r_1^2}{r_2^2 - r_1^2} - \mu_s \right) + \frac{r_2}{E_h} \left( \frac{r_3^2 + r_2^2}{r_3^2 - r_2^2} + \mu_h \right)} \quad (80e)$$

This is the average value of  $p_i$ . It may be shown that  $p_i$  is a maximum at the edges of the hub.

The average shrinkage pressure developed when a hub is shrunk over a solid shaft may be determined from Eq. (80e) by letting  $r_1 = 0$ .

$$p_i = \frac{\Delta r}{\frac{r_2}{E_s} (1 - \mu_s) + \frac{r_2}{E_h} \left( \frac{r_3^2 + r_2^2}{r_3^2 - r_2^2} + \mu_h \right)} \quad (80f)$$

If the solid shaft and hub are made of the same material

$$p_i = \frac{E(r_3^2 - r_2^2) \Delta r}{2r_2 r_3^2} \quad (80g)$$

With the shrinkage pressure known, the stresses in the hub and shaft may be found by Eq. (81).

Various design aspects of shrink-fit assemblies including the effect of bending or torsional loads are discussed in the literature.<sup>1</sup>

If the assembly is to rotate about a longitudinal axis the shrinkage pressure will be decreased by the centrifugal forces developed in the hub and shaft. The general stress analysis for rotating parts is outlined in the following article.

**60. Stresses in Rotating Disks of Constant Thickness.**—If a circular disk of constant thickness is rotated at a constant angular

<sup>1</sup> MARIN, J., Designing Shrink-fit Assemblies, *Machine Design*, Vol. 14 p. 68, June, 1942; p. 72, July, 1942; p. 78, August, 1942.

EKSERGIAN, R., The Design of Railway Axles and Locomotive Crank Pins, *Trans. Am. Soc. Mech. Engrs.*, Vol. 60, pp. 153-189, 1938.

HORGER, O. J., and C. W. NELSON, Design of Press and Shrink-fitted Assemblies, *Trans. Am. Soc. Mech. Engrs.*, Vol. 59, pp. 183-187, 1937.

velocity about its centroidal axis normal to the plane of the disk, stresses are developed by the centrifugal forces induced in the material. Except for the absence of stress parallel to the axis of rotation the stress situation is similar to that existing in a thick-walled cylinder under pressure. Every point in the rotating disk will tend to be displaced outward along a radial line, so Eqs. (74) and (75) apply.

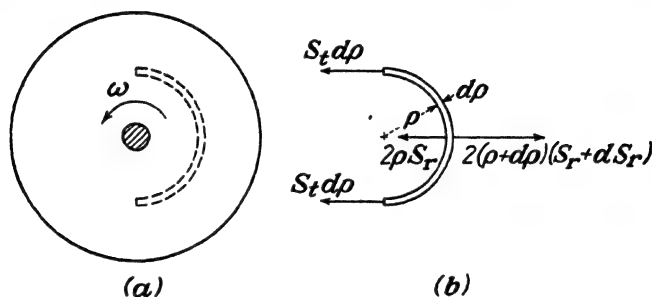


FIG. 57.—Element of a rotating disk.

The stresses may be determined by following a procedure similar to that used in the analysis of the thick-walled cylinder. An elementary half ring of unit length, radius  $\rho$ , and thickness  $d\rho$ , will be subjected to the forces indicated in the free-body diagram of Fig. 57.

The equation of motion may be written in the radial direction

$$\begin{aligned}\Sigma F_r &= M \bar{a}_r \\ &= \frac{W}{g} \omega^2 \bar{r}\end{aligned}$$

$$-2S_t d\rho - 2\rho S_r + 2(\rho + d\rho)(S_r + dS_r) = \frac{-\delta \pi \rho d\rho}{g} \omega^2 \frac{2\rho}{\pi} \quad (99)$$

in which  $\delta$  is the specific weight of the material

$\omega$  is the angular velocity.

Equation (99) will reduce to

$$-S_t + S_r + \rho \frac{dS_r}{d\rho} = -\delta \rho^2 \frac{\omega^2}{g} \quad (100)$$

If  $\omega$  is zero, that is, if the disk is not rotating, Eq. (100) reduces to Eq. (73) for the cylinder. As in that case, the equation cannot be integrated directly, but the additional information available from *geometry* and the *properties of the material* is required. The

two strains  $\epsilon_t$  and  $\epsilon_r$  may be expressed in terms of the displacement  $u$  and the stresses may be expressed in terms of the strains. Hence the stresses  $S_t$  and  $S_r$  may be expressed in terms of the radial displacement  $u$  of the elementary ring, and the resulting equation in  $\rho$  and  $u$  may be integrated. If there is no stress in the direction of the axis of rotation, Eqs. (57a) and (57b) apply, giving

$$S_r = \frac{E(\epsilon_r + \mu\epsilon_t)}{1 - \mu^2} \quad (101)$$

$$= \frac{E\left(\frac{du}{d\rho} + \mu \frac{u}{\rho}\right)}{1 - \mu^2} \quad (101a)$$

and

$$S_t = \frac{E\left(\frac{u}{\rho} + \mu \frac{du}{d\rho}\right)}{1 - \mu^2} \quad (101b)$$

If these values are substituted in Eq. (100), there results

$$\rho \frac{d^2u}{d\rho^2} + \frac{du}{d\rho} - \frac{u}{\rho} = \frac{-(1 - \mu^2)\delta\rho^2\omega^2}{Eg} \quad (102)$$

or

$$\frac{d^2u}{d\rho^2} + \frac{1}{\rho} \frac{du}{d\rho} - \frac{u}{\rho^2} = 8k\rho \quad (103)$$

in which

$$k = \frac{-(1 - \mu^2)\delta\omega^2}{8Eg} \quad (104)$$

It will be noted that if  $\omega$  is zero, that is, if the cylinder is not rotating, Eq. (103) is identical with Eq. (77c) for the thick-walled cylinder. One solution of Eq. (103) is

$$u = a\rho + \frac{b}{\rho} + k\rho^3 \quad (105)$$

in which  $a$  and  $b$  are the constants of integration as before. The values of the constants may be determined from the boundary conditions.

**61. Specific Solutions.**—Two different conditions will be investigated corresponding to two different situations at the inner boundary of the disk. The outer boundary will be assumed to be free.



1. No radial stress on the inner boundary.

2. No displacement of the inner boundary.

1. *No Radial Stress on the Inner Boundary.*—This condition approximates that existing near the center of a hollow cylinder attached to a shaft at the ends or at a section on the rim of a wheel midway between spokes.

The two boundary conditions are

$$\begin{aligned} S_r &= 0 & \text{for } \rho &= r_1 & \text{at the inner boundary} \\ S_r &= 0 & \text{for } \rho &= r_2 & \text{at the outer boundary.} \end{aligned}$$

In order to use these conditions  $S_r$  is evaluated in terms of  $a$  and  $b$  by substituting the value of  $u$  and  $du/d\rho$  from Eq. (105) into Eq. (101a)

$$S_r = \frac{E \left( a - \frac{b}{\rho^2} + 3k\rho^2 + \mu a + \mu \frac{b}{\rho^2} + \mu k\rho^2 \right)}{1 - \mu^2} \quad (106)$$

If the radial stress is zero at the outer edge ( $\rho = r_2$ ) and also at the inner boundary ( $\rho = r_1$ )

$$a = \frac{-k(3 + \mu)(r_2^2 + r_1^2)}{1 + \mu} \quad (107a)$$

and

$$b = \frac{-k(3 + \mu)r_1^2 r_2^2}{1 - \mu} \quad (107b)$$

Then the radial stress at any point may be determined by substituting the values of  $a$  and  $b$  back into Eq. (106)

$$S_r = \frac{(3 + \mu)Ek}{1 - \mu^2} \left( \frac{r_1^2 r_2^2}{\rho^2} + \rho^2 - r_1^2 - r_2^2 \right) \quad (108)$$

$$= \frac{-(3 + \mu)\delta \omega^2}{8} \frac{g}{g} \left( \frac{r_1^2 r_2^2}{\rho^2} + \rho^2 - r_1^2 - r_2^2 \right) \quad (108a)$$

The tangential stress may be found from Eqs. (101b), (105), (107a), and (107b)

$$S_t = \frac{Ek}{1 - \mu^2} \left[ \rho^2(1 + 3\mu) - (3 + \mu) \left( r_2^2 + r_1^2 + \frac{r_1^2 r_2^2}{\rho^2} \right) \right] \quad (109)$$

$$= \frac{-\delta \omega^2}{8} \frac{g}{g} \left[ \rho^2(1 + 3\mu) - (3 + \mu) \left( r_2^2 + r_1^2 + \frac{r_1^2 r_2^2}{\rho^2} \right) \right] \quad (109a)$$

The radius  $\rho_m$  at which the radial stress is a maximum may be

determined by differentiating Eq. (108a) and equating the derivative to zero. This gives

$$\rho_m = \sqrt{r_1 r_2} \quad (110)$$

Then

$$S_{r(\max)} = \frac{(3 + \mu) \delta \omega^2}{8g} (r_2 - r_1)^2 \quad (111)$$

Equation (109a) indicates that the maximum tangential stress in the disk occurs at the inside surface ( $\rho = r_1$ ). At that section

$$S_t = \frac{\delta \omega^2}{4g} [r_1^2(1 - \mu) + r_2^2(3 + \mu)] \quad (112)$$

For the limiting case in which the disk is decreased in radial thickness to a thin ring of radius  $r$

$$\begin{aligned} r_1 &= r_2 = r \\ S_r &= 0 \end{aligned} \quad (113a)$$

$$S_t = \frac{\delta r^2 \omega^2}{g} \quad (113b)$$

$$= \delta \frac{v^2}{g} \quad (113c)$$

which is the same result as that obtained by assuming a uniform distribution of tangential stress across the section.

The ratio of the maximum tangential stress to the average tangential stress is

$$K_t = \frac{r_1^2(1 - \mu) + r_2^2(3 + \mu)}{4r^2} \quad (114)$$

If the ratio of the radial thickness to the mean diameter is designated as  $\alpha$ , the value of the stress ratio  $K_t$  from Eq. (114) becomes

$$K_t = 1 + \alpha(1 + \mu) + \alpha^2 \quad (114a)$$

Values of the stress ratio plotted against  $\alpha$  in Fig. 58 indicate that the factor increases as the radial thickness of the ring increases. For the approximate formula, Eq. (113c), to give results within 10 per cent of the maximum stresses for a material having a Poisson's ratio of  $\frac{1}{3}$ , the ratio of the radial thickness to the mean diameter must not exceed 0.08. That is, the outside radius must not exceed 1.175 times the inside radius.

If the radial stress around the boundary of the disk is not zero

but is constant, (as in a shrink-fit assembly) the stresses due to the radial pressure, evaluated by Eqs. (81) and (82), may be added algebraically to the stresses determined from Eqs. (108) and (109), provided that the stresses do not exceed the proportional limit of the material.

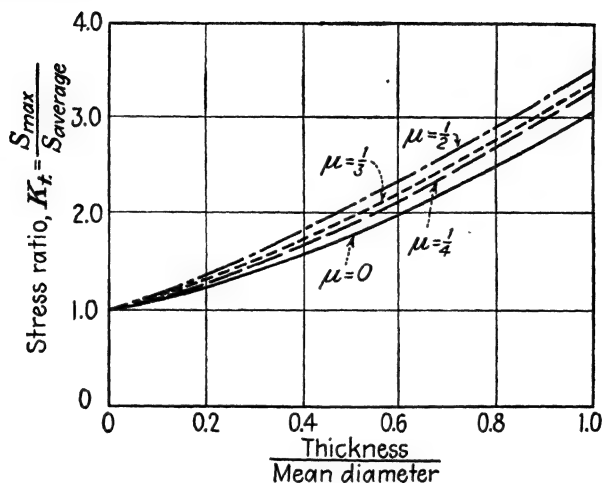


FIG. 58.—Effect of relative dimensions upon stresses in rotating disk.

2. *No Displacement of the Inner Boundary.*—If the disk is solid or is attached to a small shaft the constants of integration of Eq. (105) may be evaluated from the boundary conditions

- a. that the displacement  $u$  is zero when  $\rho = 0$ , and
- b. that  $S_r = 0$  when  $\rho = r$ , where  $r$  is the outside radius of the disk.

From the first condition Eq. (105) gives  $b = 0$ .

The second condition substituted into Eq. (106) gives

$$a = \frac{-kr^2(3 + \mu)}{1 + \mu} \quad (115)$$

Then from Eq. (101b)

$$S_t = \frac{Ek[\rho^2(1 + 3\mu) - r^2(3 + \mu)]}{1 - \mu^2} \quad (116)$$

which will be a maximum when  $\rho = 0$ . For that condition

$$S_t = \frac{-Ekr^2(3 + \mu)}{1 - \mu^2} \quad (116a)$$

The constant  $k$  may be eliminated by substituting its value from

Eq. (104). Then

$$S_t = \frac{(3 + \mu)\delta\omega^2 r^2}{8g} \quad (116b)$$

If the disk contains a very small hole through the center the maximum stress may be obtained from Eq. (112) by letting  $r_1 = 0$  and  $r_2 = r$ .

$$S_t = \frac{(3 + \mu)\delta\omega^2 r^2}{4g} \quad (112a)$$

A comparison of this with Eq. (116b) indicates that a small hole at the center of the disk results in a maximum stress twice as great as the maximum stress in a solid disk. That is, a small hole has a stress-concentration factor of 2.00.

The stress distribution around a set of six symmetrically located  $\frac{1}{2}$ -in. and  $\frac{3}{8}$ -in. holes at a distance of 1 in. from the center of a rotating disk was investigated photoelastically by Newton.<sup>1</sup> He found that the maximum stress at the holes was about 20 per cent greater than that which would be developed around a hole in a wide plate subjected to radial and tangential stresses equal to those existing at the corresponding point in a rotating disk without holes.

Equations (111), (112), (112a), (113c), and (116b) all show that the maximum stress varies directly with the specific weight of the material and the square of the speed. It is evident that for high-speed rotating machinery the strength-weight ratio is one important factor in the selection of the most suitable material.

**62. Stresses in Disks of Variable Thickness.**—The expressions developed in Arts. 60 and 61 are valid for stresses in disks of constant thickness rotating at a constant speed. Many types of rotating equipment such as turbine and supercharger units contain elements that are not disks of constant thickness. However, the stresses in some such elements are of great practical importance, because of the high temperatures or high speeds involved.

If the disk is not of constant thickness, the general differential equation for displacement, corresponding to Eq. (77c) for the disk of constant thickness, is<sup>2</sup>

<sup>1</sup> NEWTON, R. E., A Photoelastic Study of Stresses in Rotating Disks, *Trans. Am. Soc. Mech. Engrs.*, Vol. 62, p. A-57, 1940.

<sup>2</sup> STODOLA, A., "Dampf- und Gas Turbinen," 6th ed., 1924.

MORLEY, A., "Strength of Materials," 7th ed., p. 387, Longmans, Green and Company, New York, 1928.

$$\frac{d^2u}{d\rho^2} + \left(\frac{1}{\rho} + \frac{1}{b} \frac{db}{d\rho}\right) \frac{du}{d\rho} - \frac{u}{\rho} \left(\frac{1}{\rho} - \frac{\mu}{b} \frac{db}{d\rho}\right) + \frac{(1 - \mu^2)\delta\rho\omega^2}{gE} = 0 \quad (77d)$$

in which  $b$  is the thickness of the element at the radius  $\rho$ .

Equation (77d) may be integrated for special cases, such as  $b = C\rho^n$ .

The stresses in a rotating disk of variable thickness may be evaluated approximately by assuming the disk to consist of a series of disks of constant thickness. Lake<sup>1</sup> has presented another approximate method based on the assumption that the tangential strain varies inversely with the distance  $\rho$  and that the radial strain is negligible. This leads to the conclusion that the tangential stress varies inversely with  $\rho$ . If  $r_o$  indicates the radius to the point at which the stress  $S_t$  equals the average tensile stress  $S_o$  on the cross section

$$S_t = \frac{S_o r_o}{\rho} \quad (117a)$$

Also

$$S_o = \frac{\bar{r}^2 \delta \omega^2}{g} \quad (117b)$$

in which  $\bar{r}$  is the radius of gyration of the cross section.

The radius  $r_o$  may be evaluated from

$$\frac{a}{r_o} = \int_{r_1}^{r_2} \frac{b}{\rho} d\rho \quad (117c)$$

For disks of constant thickness and hyperbolically tapered ( $b \propto 1/r$ ) the method gives maximum stresses within 5 per cent of those obtained by using the standard theory if  $r_2 < 3r_1$ . Also, the error is on the safe side. The quantities  $\bar{r}$  and  $r_o$  may be determined by graphical integration or by dividing the cross section into finite increments and applying a summation process.

### PROBLEMS

**156.** A tank 4 ft. in diameter contains gas under a pressure of 200 p.s.i. Determine the thickness of structural steel necessary for the end of the tank if the end is

- a. Conical.
- b. Parabolic.
- c. Ellipsoidal.

<sup>1</sup> LAKE, G. F., A Simplified Method of Determining Hoop Stresses in Fan Rotors, *J. Applied Mech.*, Vol. 12, No. 2, p. A-65, June, 1945.

The center of the end is to project 18 in. beyond the end of the cylindrical portion, and a minimum factor of safety of 2.4 with respect to failure by slip is to be used.

**157.** Classify the assumptions involved in Eq. (72) under the headings of statics, geometry, and properties of the material.

**158.** A tank 3 ft. in diameter has a wall thickness of  $\frac{1}{4}$  in. It is constructed with a spiral joint having a lead of 6 ft. Determine the normal and shearing forces per inch of joint when the internal pressure is 200 p.s.i.

**159.** Prove that  $S_r$  is zero in a thick-walled cylinder.

**160.** Derive the equation for the tangential stress in a thick-walled cylinder, assuming that the longitudinal stress is zero.

**161.** Where will the maximum tangential stress occur in a thick-walled cylinder subjected to both internal and external pressure?

**162.** Determine the maximum allowable internal pressure to which a cylinder with an inside diameter of 8 in. and an external diameter of 12 in. may be subjected if the cylinder is to have a factor of safety of 3 with respect to failure by slip based on a proportional limit of 36,000 p.s.i. determined from an axial test. Use the maximum-shearing-stress theory of failure.

**163.** A gun with a bore of 8 in. develops a maximum internal pressure of 30,000 p.s.i. Determine the minimum outside diameter required if the maximum allowable tensile stress is (a) 45,000 p.s.i., (b) 30,000 p.s.i.

**164.** An alloy steel cylinder with an inside diameter of 4 in. and an outside diameter of 8 in. is subjected to an internal pressure of 36,000 p.s.i., which develops a bursting force of 144,000 lb. per in. of length. What percentage of the bursting force is carried by the inner half of the cylinder wall?

**165.** A gun barrel with an inside diameter of 2.96 in. and an outside diameter of 6.84 in. is made of steel having a proportional limit of 56,000 p.s.i. To what maximum internal pressure may the barrel be subjected without inelastic action occurring?

**166.** Determine the change in internal diameter of the barrel of the gun in Prob. 165 for the internal pressure of 10,000 p.s.i. Is the change in diameter significant?

**167.** Draw curves similar to Fig. 49b if the 10,000-p.s.i. pressure on the 8- by 4-in. cylinder is external instead of internal.

**168.** A cylinder with an external diameter of 8.00 in. and an internal diameter of 4.00 in. is subjected to an internal pressure of 10,000 p.s.i. and an external pressure of 60,000 p.s.i. Draw curves showing the variation in  $S_r$  and  $S_t$  throughout the wall of the cylinder.

**169.** A steel cylinder with an internal diameter of 3.00 in. and an external diameter of 4.80 in. is wound with a single layer of 0.050-in.-diameter steel wire under tensile stress of 50,000 p.s.i. Determine the maximum allowable internal pressure if the tensile stress in the cylinder is not to exceed 40,000 p.s.i. What will be the stress in the wire when the cylinder is under pressure?

**170.** Design a structural-steel cylinder having an internal diameter of 3.20 in. if it is to carry an internal pressure of 16,000 p.s.i. with a factor of safety of 2.00 with respect to failure by slip.

**171.** Design the cylinder of Prob. 170 using an external winding of 0.10-in. square wire having a yield strength of 100,000 p.s.i.

**172.** Design the cylinder of Prob. 170 using laminated construction.

**173.** A steel cylinder with an external diameter of 8 in. and an internal diameter of approximately 6 in. is shrunk over another steel cylinder having external and internal diameters of 6 in. and 4 in. respectively. The maximum tangential shrinkage stress produced in the inner cylinder is -8,000 p.s.i. Determine the maximum resultant tangential stress in the outer cylinder when an internal pressure of 20,000 p.s.i. is applied to the assembly.

**174.** A steel cylinder with an inside diameter of 4 in. was designed for a maximum tensile stress of 20,000 p.s.i. when subjected to an internal pressure of 4,000 p.s.i. The internal pressure must be increased to 8,000 p.s.i., and it is proposed to strengthen the cylinder by shrinking a steel jacket around it. Determine

- a. The maximum pressure that may be developed between the cylinder and the jacket if the maximum tensile stress in the cylinder is not to exceed 20,000 p.s.i.
- b. The outside radius of the jacket if the maximum tensile stress in the jacket is not to exceed 20,000 p.s.i.

**175.** A laminated cylinder consists of a jacket with an internal diameter of 8 in. and an external diameter of 12 in. shrunk over a tube with an internal diameter of 4 in. When an internal pressure of 24,000 p.s.i. is applied the maximum resultant tensile stress in the tube is 22,000 p.s.i. Determine the maximum  $S_r$  and  $S_t$  in the jacket when the cylinder is under the internal pressure and indicate them on a sketch.

**176.** A hollow cylinder consists of a jacket with an internal diameter of 8 in. and an external diameter of 10 in. shrunk on a tube with an internal diameter of 4 in. The initial shrinkage pressure on the surface of contact is 6,000 p.s.i. The cylinder is then subjected to an internal pressure of 24,000 p.s.i. Determine the resultant maximum tensile stresses and maximum compressive stresses in both the tube and jacket and indicate their location.

**177.** A laminated cylinder is composed of a tube having an inside diameter of 4 in. and an outside diameter of 8 in. and a sleeve having an outside diameter of 16 in. The cylinder is to be subjected to an internal pressure of 24,000 p.s.i., and it is desirable to have the maximum tensile stress in the tube equal to the maximum tensile stress in the sleeve under that condition. What will be the maximum compressive stress in the sleeve under that condition?

**178.** A homogeneous thick cylinder made of steel has an internal diameter of 4 in. and an external diameter of 8 in. If the maximum shearing stress is not to exceed 24,000 p.s.i., what is the maximum permissible internal pressure?

**179.** A structural-steel cylinder with an internal diameter of 4 in. and an external diameter of 6 in. is to be subjected to an internal pressure of 24,000 p.s.i. Using a factor of safety of 1.5 with respect to failure by slip

and the maximum-unit-strain theory of failure, design a jacket for the cylinder if the jacket is made of

a. Structural steel.

b. 17S-T aluminum alloy.

180. Solve Prob. 179 using the Hencky-von Mises theory of failure.

181. Using the maximum-strain-energy theory of failure, prepare a minimum strength curve similar to those shown in Fig. 51 for the cylinder of the illustrative problem.

182. To what temperature would a steel cylinder with an inside diameter of 3.520 in. and an external diameter of 5.200 in. need to be heated to slip it over a cylinder having an external diameter of 3.600 in.?

183. A cylinder with radii  $r_3$  and  $r_2$  is to be shrunk over a cylinder of the same material having radii  $r_2$  and  $r_1$ . Determine the required difference in  $r_2$  for the two cylinders if the maximum tensile shrinkage stress in the outer cylinder is to equal the maximum compressive shrinkage stress in the inner cylinder.

184. Derive Eq. (97) and (98).

185. A steel rod  $\frac{3}{4}$  in. in diameter and 10 in. long is rotated at 2,400 r.p.m. about an axis through one end. Determine the maximum tensile stress in the rod.

186. What is the maximum speed at which a steel disk with an external diameter of 8.00 in., a thickness of  $\frac{1}{4}$  in., and an inside diameter of 3.00 in. may be rotated if the maximum stress is not to exceed 24,000 p.s.i.?

187. Solve Prob. 186 for a solid 8.00-in. disk.

188. The disk of Prob. 186 is supported by four spokes  $\frac{1}{2}$  in. wide and  $\frac{1}{4}$  in. thick. Determine the stress in the spokes.

189. Which of the materials listed in Table II is most suitable for high-speed rotating disks?

190. A steel disk  $\frac{1}{2}$  in. thick with an outside diameter of 8.000 in. and an inside diameter of 0.998 in. is shrunk on a solid steel shaft 1.000 in. in diameter. Determine the maximum stress in the disk.

191. The disk-and-shaft unit of Prob. 190 is rotated at 10,000 r.p.m. Determine the maximum stress in the disk.

192. Develop an equation for the radial stress in a solid disk of constant thickness rotating at a constant speed.

193. Show how Eqs. (117b) and (117c) are obtained.

194. Develop an expression for the tangential stress in a solid rotating disk, the thickness of which varies directly with the square of the radius.

195. A disk with an internal radius  $r_1$ , an external radius  $r_2$ , and a thickness  $b = c/r$  rotates at a constant speed. Develop an equation for the tangential stress.

196. Derive Eq. (77d).



## CHAPTER VII

### TORSION

**63. General Considerations.**—A member is subjected to torsion if a couple is developed at each cross section of the member, the plane of the couple being normal to the axis of the member. Torsion is one of the four simple stress situations that may be produced in a member. In general, the force system acting

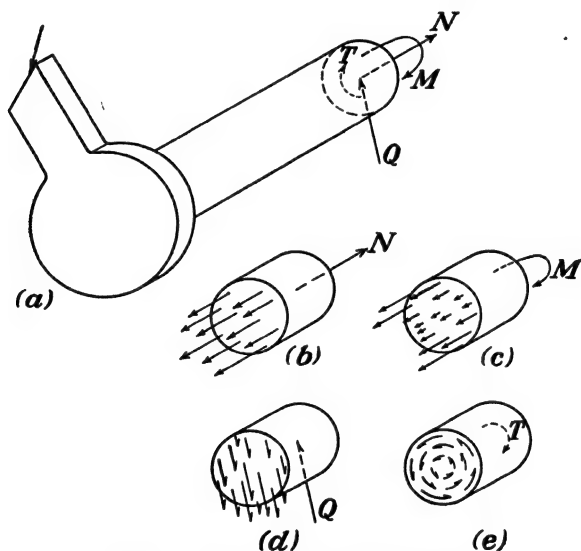


FIG. 59.—Four component force systems.

on a transverse plane may be resolved into four components as indicated in Fig. 59: (1) a force  $N$  normal to the transverse plane and acting through the centroid of the area, (2) a force  $Q$  lying in the plane and acting through the centroid of the area, (3) a couple  $M$  normal to the plane, and (4) a couple  $T$  in the plane of the area. The first force produces normal stresses, as discussed in Chap. 5, and the second force produces cross shearing and longitudinal shearing stresses, which are considered in Chap. 9.

The first couple produces flexural stresses, discussed in Chap. 8, and the second couple produces torsional stresses, to be considered in this chapter. •

The torsional couple is the principal component in a shaft; hence, the elementary formula for the evaluation of torsional stresses is developed for circular shafts. However, the torsional couple is also an important component in many members of noncircular cross section, such as airplane wings and propellers, automobile frames, and floor beams.

The well-known torsion formula  $S = Tc/J$  for the evaluation of the stresses in a shaft having a circular cross section is based on several assumptions.

1. Statics

- a. The resultant of the external forces is a couple that lies in a plane perpendicular to the longitudinal axis of the shaft.
- b. The shaft is in equilibrium.

2. Geometry

- c. The axis of the shaft is straight.
- d. The shaft is circular and free from changes in cross section.
- e. A plane section normal to the axis of the shaft before twisting remains plane after the shaft is twisted.
- f. Any diameter before twisting remains a straight line after twisting.

3. Properties of the Material

- g. The material is homogeneous and isotropic.
- h. The stresses do not exceed the proportional limit of the material.

If assumption (a) does not hold, the external forces may be resolved into the components that produce axial loading alone, bending alone, or twisting alone. Each effect may be dealt with separately and the results added if the stresses do not exceed the proportional limit of the material. If assumption (b) does not hold, as in a condition of dynamic loading, the stresses may be higher than those given by the torsion formula. If the axis of the shaft is not straight, bending may be introduced at intermediate sections along the shaft even though the loading requirement of (a) is satisfied. Assumption (d) is necessary to eliminate the necessity for considering stress concentration.

Assumption (e) is valid for a solid circular shaft or a circular tube of constant diameter and wall thickness but is not valid for other shapes. It may also be invalid near the sections at which the torque is applied. Assumption (f) may be verified experimentally. Most engineering materials are reasonably homogeneous and isotropic, so assumption (g) is acceptable. Assumption (h) places a definite upper limit on the valid range of the formula.

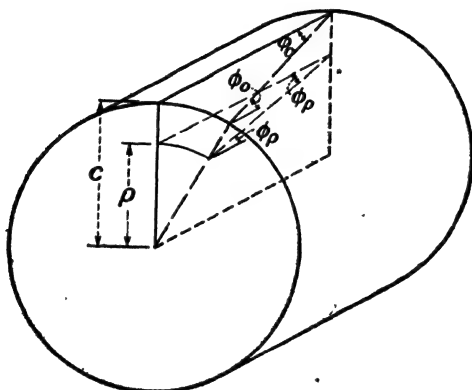


FIG. 60.—Geometry of a circular member in torsion.

If assumption (f) is valid, a section of the shaft will deform as indicated in Fig. 60, and the unit strain at any point in the cross section is proportional to the distance of the point from the center of the shaft. That is

$$\frac{(\gamma_{xy})_\rho}{(\gamma_{xy})_o} = \frac{\rho}{c} \quad (118)$$

Then from assumption (h)

$$\frac{S_\rho}{S_o} = \frac{\rho}{c} \quad (118a)$$

in which  $S_o$  is the stress at the outside of the shaft

$(\gamma_{xy})_o$  is the strain at the outside of the shaft

$S_\rho$  is the stress at any point in the cross section

$(\gamma_{xy})_\rho$  is the strain at any point in the cross section

$c$  is the radius of the shaft

$\rho$  is the radius of the point.

If the shaft is in equilibrium, assumption (b), the external torque equals the resultant torque developed by the shearing stresses, or

$$T = \int_0^A S_{\rho} \rho \, da \quad (119)$$

$$= \frac{S_o}{c} \int_0^A \rho^2 \, da \quad (119a)$$

The integral defines the polar moment of inertia  $J$ . Hence

$$T = \frac{S_o}{c} J \quad (119b)$$

That the ordinary torsion formula, Eq. (119b), does not apply to a shaft having a rectangular cross section is evident from a consideration of a few elements of the area at various portions of the cross section, as indicated in Fig. 61.

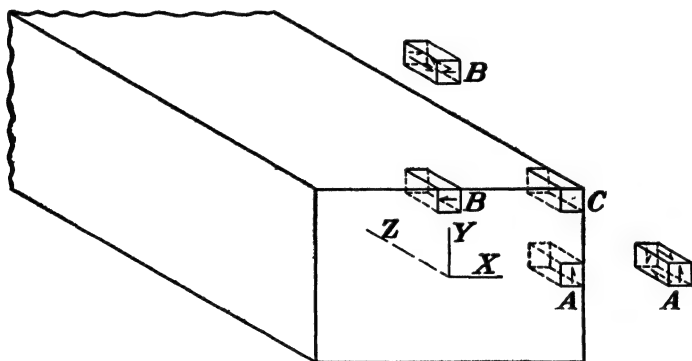


FIG. 61.—Member of rectangular cross section in torsion.

For example, there can be no vertical or horizontal shearing forces on the vertical outside face of block A, at the center of one vertical side. Consequently, the only shearing forces that can act on block A are a vertical shearing force on the front and back faces and a longitudinal shearing force on the top and bottom faces.<sup>1</sup> Similarly, block B at the top of the section can have no shear on the top face; hence, the shearing force on the front face must be horizontal. Since block C at the corner can develop no shearing force on either outside face, it follows that

<sup>1</sup> If block A were not on an axis of symmetry, a longitudinal shearing force,  $Q_{xz}$ , would be developed on the inner vertical face. However, the shearing stress,  $S_{xz}$ , must be zero at the outside.

there can be no shearing force on the front face. In other words, the shearing stress at the corner of the cross section must be zero, which is not the result that one would obtain from Eq. (119*b*). Equation (119*b*) is not valid for any section other than circular.

It is apparent that in a rectangular shaft the vertical component of the shearing stress near the vertical edges must vary from a maximum at the center of a side (at *A*) to zero at the corner (at *C*), and that the horizontal component near the top must vary from a maximum at the center (at *B*) to zero at the corners.

**64. Solutions for Noncircular Members.**—There are essentially four different procedures that may be used in the evaluation of shearing stresses in a member subjected to torsion.

1. Analytical
  - (a) Approximate
  - (b) "Exact," or Saint Venant theory
2. Experimental
  - (a) Strain measurements
  - (b) Application of analogies based on the exact theory

In the first method, the approximate distribution of shearing stress throughout the cross section is deduced from observation of strains, and the relationship between torque, and stress developed by statics for the approximate stress variation. As is indicated in Fig. 62, the shearing force acting on an element of area at any point in the cross section may be resolved into two components  $S_{xz}$  and  $S_{yz}$  parallel to the coordinate axes. Each of the components will have a moment with respect to the longitudinal axis through the origin, and the resisting moment may be evaluated as the summation of the moments of the components of the forces acting at all points in the section. From Fig. 62

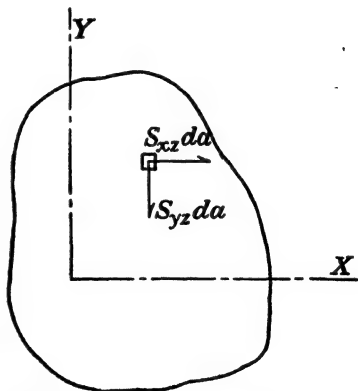


FIG. 62.—Components of shearing forces.

$$T = \int_0^4 (S_{xz}y + S_{yz}x) da \quad (120)$$

If the variation in  $S_{xz}$  and  $S_{yz}$  across the section is known or can be assumed, the relationships may be substituted in Eq. (120) and the resulting equation integrated. The method, which is illustrated in Art. 65, is limited only by the accuracy with which the stress distribution is known or can be assumed.

In the so-called "exact method," which was devised by Saint Venant,<sup>1</sup> the components of stress are determined so that they satisfy not only the equations of equilibrium as applied to a differential block at any point in the shaft but also the stress-strain relationships. The method, which is discussed in Art. 67, is limited by the mathematical difficulties involved in solving the differential equation that is developed and in satisfying the boundary conditions.



FIG. 63.—Distortion of grid lines on a rectangular member in torsion.

Experimental methods involving the use of strain-measuring devices or brittle varnish have been used in evaluating the maximum stress in members of irregular cross section subjected to torsion. One particularly useful experimental tool is the membrane analogy, which may be used to evaluate the shearing stress at any point in a cross section of a shaft, regardless of irregularities. The method is outlined in Art. 68. Other analogies include the sand-heap

analogy for evaluating torque-stress relationships above the proportional limit as described in Art. 77 and the electrical analogy for evaluating stresses in tapered shafts.

### 65. Approximate Solution for a Rectangular Cross Section.—

C. Bach<sup>2</sup> obtained an approximate solution for the stresses in a shaft having a rectangular cross section. From observation of the shearing strains developed in a rectangular bar as shown in Fig. 63, he assumed that  $S_{xz}$ , the  $x$  component of the shearing stress at any point, varies parabolically from a maximum along the  $y$  axis to zero at the outer edge along any line parallel to the  $x$  axis, as indicated in Fig. 64, and that  $S_{yz}$  varies directly as the distance from the  $x$  axis. These two assumptions may be combined and expressed mathematically as

<sup>1</sup> SAINT VENANT, B. de, *Mém. savants étrangers*, 14, 1855.

<sup>2</sup> BACH, C., and R. BAUMANN, "Elasticität und Festigkeit," 8th ed., Verlag Julius Springer, Berlin, 1924.

$$S_{xz} = S_1 \left(1 - \frac{x^2}{a^2}\right) \frac{y}{b} \quad (121a)$$

in which  $S_1$  is the shearing stress at the center of the long edge (point B). Similarly

$$S_{yz} = S_2 \left(1 - \frac{y^2}{b^2}\right) \frac{x}{a} \quad (121b)$$

in which  $S_2$  is the shearing stress at the center of the short edge

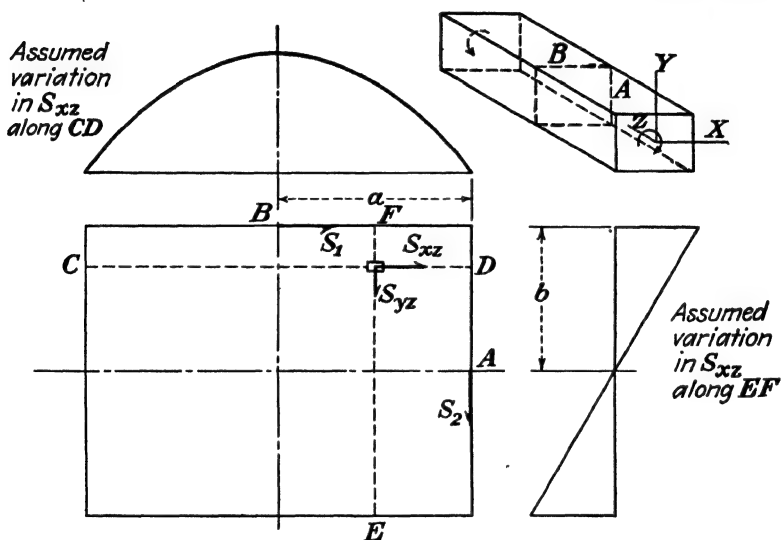


FIG. 64.—Shearing stresses in member of rectangular cross section as assumed by Bach.

(point A). If these values are substituted in Eq. (120) there results

$$T = 4 \int_0^a \int_0^b \left( S_1 \frac{y^2}{b} - S_1 \frac{x^2 y^2}{a^2 b} + S_2 \frac{x^2}{a} - S_2 \frac{x^2 y^2}{a b^2} \right) dx dy \quad (120a)$$

Bach further assumed that the stresses  $S_1$  and  $S_2$  are inversely proportional to their distances from the center of the section. This assumption is in general agreement with observation. Thus,

$$\frac{S_1}{S_2} = \frac{a}{b}$$

Then Eq. (120b) becomes, upon integration and substitution for

$S_2$ ,

$$T = \frac{16S_1ab^2}{9} \quad (120c)$$

also

$$T = \frac{16S_2a^2b}{9} \quad (120d)$$

from which

$$S_1 = \frac{9T}{16ab^2} \quad (122a)$$

$$S_2 = \frac{9T}{16a^2b} \quad (122b)$$

These equations indicate that the maximum torsional stress in a rectangular shaft occurs at the boundary nearest the center. The correctness of the assumptions concerning the stress distribution may be checked by comparing the results with those obtained from the exact theory. The value of the maximum torsional stress as obtained from the exact solution may be written in terms of Eq. (122a) as

$$S_{\max} = \frac{K_1 9T}{16ab^2} \quad (123)$$

with values of  $K$  as given in Table VI. The angle of twist in a length  $L$  may be evaluated (from the exact solution) as

$$\theta = \frac{K_1 TL}{16Gab^3} \quad (124)$$

with values of  $K_1$  as given in Table VI.  $G$  is the modulus of rigidity.

TABLE VI.—TORSION CONSTANTS FOR A RECTANGULAR BAR\*

$\frac{a}{b}$	$K$	$K_1$	$\frac{a}{b}$	$K$	$K_1$
1.0	1.068	7.14	3	0.829	3.80
1.2	1.015	6.02	4	0.788	3.56
1.5	0.962	5.10	5	0.764	3.44
2.0	0.903	4.37	10	0.712	3.21
2.5	0.861	4.02	$\infty$	0.667	3.00

\* Data from TIMOSHENKO, S., "Theory of Elasticity," p. 248, McGraw-Hill Book Company, Inc., New York.

The values of  $K$  indicate that the Bach formula, Eq. (122), gives stresses within 10 per cent of those obtained by the rigorous



solution when the length of one side of the cross section is not more than twice the length of the other side. For a long, narrow rectangle the error is larger, but Eq. (122) is on the safe side. The data also indicate that a rectangular section has a higher strength (*i.e.*, will develop more torque for the same maximum stress) than the sum of the strengths of the circular sections that can be inscribed in the rectangle. For example, a 1- by 3-in. rectangular section is stronger than three 1-in.-diameter circular sections. The rectangular section will also be more rigid. That is, the angle through which the 1- by 3-in. shaft will twist is less than one-third the angle through which a 1-in.

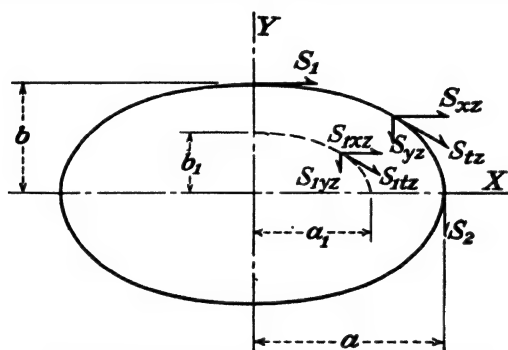


FIG. 65.—Torsional stresses in a member of elliptical cross section.

circular shaft of the same length will twist when subjected to the same torque.

**66. Torsional Stresses in an Elliptical Shaft.**—The torsional stresses in a solid elliptical shaft may be evaluated by assuming that the section is composed of a series of thin-walled elliptical tubes with no shearing stresses developed on the surfaces of contact of the tubes. In other words, the shearing stress is assumed to be tangent to the boundary of each elementary ellipse.

The direction of the shearing stress at any point in the cross section may therefore be determined from the equation of the ellipse through that point. For the section indicated in Fig. 65 the equation of any one of the component elliptical tubes is

$$\frac{x_1^2}{a_1^2} + \frac{y_1^2}{b_1^2} = 1 \quad (125)$$

The direction of the tangent to the ellipse at any point  $(x_1, y_1)$

may be found by differentiating Eq. (125).

$$\frac{dy_1}{dx_1} = \frac{-b_1^2 x_1}{a_1^2 y_1} \quad (126)$$

Since the shearing stress is assumed to be tangent to the ellipse, the relationship between the components of the shearing stress at  $(x_1, y_1)$  is

$$\frac{S_{1yz}}{S_{1xz}} = \frac{-dy_1}{dx_1} \quad (127)$$

$$= \frac{b_1^2 x_1}{a_1^2 y_1} \quad (127a)$$

A similar equation may be written for any other ellipse with major and minor axes equal to  $a_2$  and  $b_2$  or for the outside boundary with major and minor axes equal to  $a$  and  $b$ .

$$\frac{S_{yz}}{S_{xz}} = \frac{b^2 x}{a^2 y} \quad (127b)$$

in which  $S_{yz}$  and  $S_{xz}$  are the components of the stress at  $x, y$  on the boundary.

If it is assumed that each component of the shearing stress is proportional to its distance from the axis to which it is parallel

$$\frac{S_{1xz}}{y_1} = \frac{S_{xz}}{y} = \text{constant} \quad (128a)$$

and

$$\frac{S_{1yz}}{x_1} = \frac{S_{yz}}{x} = \text{constant} \quad (128b)$$

The torque may be evaluated, from Eq. (120), as

$$T = \int_0^A \left( \frac{S_{xz}}{y} y_1^2 + \frac{S_{yz}}{x} x_1^2 \right) da \quad (129a)$$

$$= \frac{S_{xz}}{y} I_x + \frac{S_{yz}}{x} I_y \quad (129b)$$

in which  $I_x$  and  $I_y$  are the moments of inertia of the area with respect to the  $x$  and  $y$  axes, respectively.

From Eq. (127b)

$$\frac{S_{yz}}{x} = \frac{b^2}{a^2} \frac{S_{xz}}{y} \quad (127b)$$

Therefore

$$T = \frac{S_{xx}}{y} \left( I_x + \frac{b^2}{a^2} I_y \right) \quad (129b)$$

$$T = \frac{S_{xx}}{y} \left( \frac{\pi ab^3}{4} + \frac{b^2}{a^2} \frac{\pi ba^3}{4} \right) \quad (129c)$$

$$= \frac{\pi S_{xx} ab^3}{2y} \quad (129d)$$

The maximum stress will occur at the end of the minor axis where  $y = b$ . Then

$$T = \frac{\pi S_1 ab^2}{2} \quad (129e)$$

$$S_1 = \frac{2T}{\pi ab^2} \quad (130a)$$

Similarly, the stress  $S_2$  at the end of the major axis is

$$S_2 = \frac{2T}{\pi a^2 b}$$

For the circle, the special case of the ellipse in which  $b = a$ , Eq. (130a) or (130b) reduces to

$$S = \frac{2T}{\pi b^3} \quad (130c)$$

which agrees with the result obtained from the ordinary theory, Eq. (119a).

The stresses computed by Eq. (130) are identical with those obtained by the exact theory.

If Eq. (130a) is written in the form of Eq. (123) for the rectangular shaft

$$S = \frac{K9T}{16ab^2} \quad (123)$$

$$K = \frac{2}{\pi} \frac{(16)}{9} \quad (123a)$$

$$= 1.13$$

A comparison of (123a) with the values of  $K$  in Table VI indicates that a given torque will produce somewhat higher stresses in an elliptical shaft than in a rectangular shaft of the same outside dimensions.

**67. The Saint Venant Theory.**—A general solution for the shearing stresses in a shaft of homogeneous, isotropic material

and constant cross section not stressed above the proportional limit was developed by Saint Venant as an extension of the work of Coulomb on torsion.

The method involves determining the solution of a differential equation that satisfies the equations of equilibrium and the stress-strain relationships at every point in the member.

1. *Statics*.—Figure 66*b* shows a free-body diagram of a differential element of the shaft in Fig. 66*a*. It is assumed that there are no normal stresses acting at any point in the shaft.

From the equation of equilibrium written in the  $z$  direction, there results

$$S_{xz} dy dz - \left( S_{xz} + \frac{\partial S_{xz}}{\partial x} dx \right) dy dz + S_{xy} dx dz - \left( S_{xy} + \frac{\partial S_{xy}}{\partial y} dy \right) dx dz = 0 \quad (131a)$$

or

$$\frac{\partial S_{xz}}{\partial x} + \frac{\partial S_{xy}}{\partial y} = 0 \quad (131b)$$

This may also be written as

$$\frac{\partial S_{xz}}{\partial x} + \frac{\partial S_{yz}}{\partial y} = 0 \quad (131c)$$

As in the case of the thick-walled cylinder, the equation of equilibrium contains too many unknowns to give the stress distribution directly. It is necessary to obtain some additional relationships from the geometry of the twisted member and the properties of the material.

2. *Geometry*.—For any given shape of cross section there exists a *center of twist* about which each point in the cross section rotates. The center of twist is, in effect, the instantaneous center of motion of the cross section. If the origin is taken at the center of twist, as shown in Fig. 67*a*, the point  $A$  (one corner of the differential element) will move along the arc  $AB$  as the shaft is twisted through the angle  $\theta$ . However, if the angle  $\theta$  is small, the point may be assumed to move along the tangent  $AB'$  to  $B'$ . The  $x$  component of the displacement is called  $u$  and the  $y$  component of the displacement is called  $v$ . Then, from similar triangles  $ACB'$  and  $AJO$ , Fig. 67*a*

$$\frac{B'C}{x} = \frac{AB'}{OA} = \theta \quad (132a)$$



Figure 67b shows the top view of the differential element and the shearing forces to which it is subjected in accordance with Fig. 66b. The shearing forces will be accompanied by displacements. The displacements of the other corners relative to  $A$  are as shown in Fig. 67c. The line  $AD$  is rotated through the angle  $DAD'$ , which may be expressed as  $\partial u/\partial z$ , indicating the rate of change of displacement  $u$  with respect to  $z$ . Similarly, the line  $FA$  is rotated to  $F'A$ , through the angle  $\partial w/\partial x$ , in which  $w$  denotes displacement in the  $z$  direction. It is evident that the shearing stresses as shown in Fig. 67b are accompanied by strains that cause relative displacements in the  $z$  direction, resulting in a warped cross section instead of a plane cross section.

The unit shearing strain  $\gamma_{xz}$  at a point  $A$  is equal to the total angle through which the two adjacent sides have been rotated with respect to each other. That is

$$\gamma_{xz} = \angle FAF' + \angle DAD' \quad (133a)$$

$$= \frac{\partial u}{\partial z} + \frac{\partial w}{\partial x} \quad (133b)$$

Similarly

$$\gamma_{yz} = \frac{\partial v}{\partial z} + \frac{\partial w}{\partial y} \quad (133c)$$

in which  $u$ ,  $v$ , and  $w$  represent displacements in the  $x$ ,  $y$ , and  $z$  directions respectively.

The shearing strain may be expressed in terms of the angle of twist by substituting the value of  $\partial u/\partial z$  from Eq. (132c) in Eq. (133b). If the shaft has a constant cross section, the rate of change of  $u$  with respect to  $z$  is simply  $\theta/L$ , or the angle of twist per unit length. Hence

$$\gamma_{xz} = \frac{-y\theta}{L} + \frac{\partial w}{\partial x} \quad (133d)$$

Equation (133d) will reduce to the familiar  $\epsilon_s = c\theta/L$  if  $\partial w/\partial x = 0$ ; i.e., if the cross section does not warp but remains a plane. In general, the cross section does not remain a plane for noncircular torsional members.

3. *Properties of the Material.*—If the stress does not exceed the proportional limit in shear

$$\gamma_{xz} = \frac{S_{xz}}{G} = \frac{-y\theta}{L} + \frac{\partial w}{\partial x} \quad (134a)$$

Similarly

$$\gamma_{yz} = \frac{S_{yz}}{G} = \frac{x\theta}{L} + \frac{\partial w}{\partial y} \quad (134b)$$

Equations (134a) and (134b) may be combined to eliminate the unknown warping  $w$  by differentiating the first with respect to  $y$  and the second with respect to  $x$  and subtracting one from the other to give

$$\frac{\partial S_{xz}}{\partial y} - \frac{\partial S_{yz}}{\partial x} = \frac{-2G\theta}{L} \quad (135)$$

4. *Combination.*—Equation (135), which comes from geometry and the properties of the material, may be combined with the equation of equilibrium, Eq. (131c), by differentiating each and adding to produce

$$\frac{\partial^2 S_{xz}}{\partial x^2} + \frac{\partial^2 S_{xz}}{\partial y^2} = 0 \quad (135a)$$

or

$$\frac{\partial^2 S_{yz}}{\partial x^2} + \frac{\partial^2 S_{yz}}{\partial y^2} = 0 \quad (135b)$$

However, a more useful combination may be made by eliminating both unknown stresses from the equations. This may be done by introducing a new quantity, called the "stress function," which is a function of  $x$  and  $y$ . It is defined by two equations, which relate it to the stresses.

$$S_{xz} = \frac{\partial \phi}{\partial y} \quad (136a)$$

$$S_{yz} = \frac{-\partial \phi}{\partial x} \quad (136b)$$

in which  $\phi$  is the stress function  $\phi(x, y)$ .

This definition of  $\phi$  satisfies the equation of equilibrium, Eq. (131c), as may be verified by substitution. If the values of the stresses from Eqs. (136a) and (136b) are substituted in Eq. (135), there results

$$\frac{\partial^2 \phi}{\partial x^2} + \frac{\partial^2 \phi}{\partial y^2} = \frac{-2G\theta}{L} \quad (136c)$$

which is the basic differential equation for a member subjected to pure torque. By substituting values of the stress from Eqs. (136a) and (136b) into Eq. (120) and integrating, it may be

shown that the torque, as well as the stresses, may be found from the stress function.

$$T = 2 \int_0^A \phi \, da \quad (137)$$

The solution of a torsion problem by the "exact" method therefore involves determining the stress function  $\phi$ . When the stress function is known, the two components of shearing stress may be evaluated by Eqs. (136a) and (136b) and the torque from Eq. (137). In addition to satisfying Eq. (136c), the stress function is equal to zero on the boundary of the cross section. This is true since from Eqs. (136a) and (136b) the slope of the function in any direction is equal to the component of the shearing stress at right angles to that direction (the directions of  $x$  and  $y$  being arbitrary). Since the component of the shearing stress normal to the boundary must be equal to zero on the boundary, the slope of the stress function in the direction of the boundary is zero (or constant) on the boundary. In many cases it therefore becomes possible to develop the stress function from the equation of the boundary.

For example, in a circular shaft of radius  $r$  the equation of the boundary is

$$r^2 - x^2 - y^2 = 0 \quad (a)$$

Hence, the stress function may take the form

$$\phi = K(r^2 - x^2 - y^2) \quad (b)$$

The constant  $K$  may be determined by substituting in the differential equation Eq. (136c).

$$-2K - 2K = \frac{-2G\theta}{L} \quad (c)$$

$$K = \frac{G\theta}{2L} \quad (d)$$

Hence, the stress function is

$$\phi = \frac{G\theta}{2L} (r^2 - x^2 - y^2) \quad (e)$$

The shearing stress may be found from Eq. (136a)

$$S_{xz} = \frac{-G\theta y}{L} \quad (f)$$



which will be a maximum at the edge  $y = r$

$$S_{xz(\max)} = -\frac{G\theta r}{L} \quad (g)$$

The torque may be determined by means of Eq. (137)

$$T = 2 \int_0^A \frac{G\theta}{2L} (r^2 - x^2 - y^2) da \quad (h)$$

$$T = \frac{G\theta}{L} (r^2 a - I_y - I_z) \quad (i)$$

$$= \frac{G\theta}{L} \left( \pi r^4 - \frac{\pi r^4}{4} - \frac{\pi r^4}{4} \right) \quad (j)$$

$$= \frac{\pi G\theta r^4}{2L} \quad (k)$$

Hence, from (g)

$$S_{xz(\max)} = \frac{2T}{\pi r^3} \quad (l)$$

which agrees with Eq. (119a).

Also, from (g) and (l)

$$\theta = \frac{2TL}{G\pi r^4} = \frac{TL}{GJ} \quad (m)$$

Saint Venant presented solutions for several specific cross sections. For example, he found that for a shaft having a cross section in the form of an equilateral triangle, the maximum stress occurs at the center of the sides and is equal to

$$S_{\max} = \frac{G\theta a}{2L} \quad (138)$$

in which  $a$  is the altitude of the triangle.

Also

$$T = \frac{Ga^4\theta}{15\sqrt{3}L} \quad (139)$$

Saint Venant showed that of all possible shapes of cross sections having a given area and not containing holes, the circular section has the maximum rigidity and the least maximum stress for a given torque.

**68. The Membrane Analogy.**—The determination of the stress function for all but a few relatively simple cross sections becomes

involved mathematically; hence, approximate mathematical solutions or experimental techniques are often relied upon for the evaluation of shearing stresses in the more complex shapes found in engineering practice. One of the most useful of the experimental tools for this purpose is the membrane analogy discovered by Prandtl, apparently first applied by Anthes and extended by Griffith and Taylor.<sup>1</sup> The analogy is based upon

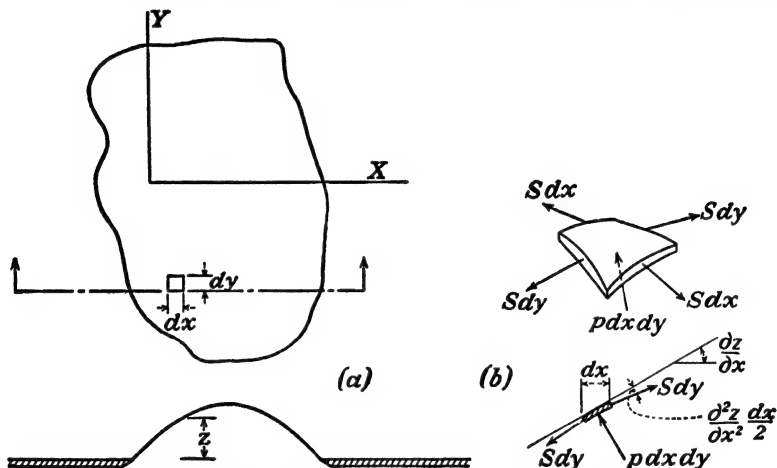


FIG. 68.—Element of a membrane under pressure.

the fact that the differential equation for the equilibrium of a membrane subjected to pressure on one side and the differential equation for a member subjected to torsion, Eq. (136c), are identical in form.

If a membrane, which has no resistance to bending, is held in a plane (the  $xy$  plane) around the edges and subjected to pressure on one side, it will stretch and deflect in the  $z$  direction as indicated in Fig. 68a. Figure 68b shows a free-body diagram of an element of area  $dx dy$  of the membrane. The differential element is subjected to the resultant pressure  $p dx dy$ , and the four forces due to the surface tension  $S$  developed in the membrane. Two of the forces  $S dy$  act on the edges parallel to the

<sup>1</sup> PRANDTL, L., *Zur Torsion von Prismatischen Stäben*, *Physik. Z.*, Vol. 4, p. 758, 1903.

ANTHES, "Doctoral Dissertation," Dresden, 1912.

GRIFFITH, A. A., and G. I. TAYLOR, *Tech. Repts., Advisory Comm. Aeronaut.* Vol. 3, p. 918, 938, London, 1917-1918.

$y$  axis, and there are two similar forces  $S dx$  acting on the edges parallel to the  $x$  axis. The surface tension  $S$  expressed in pounds per inch (or similar units) is equal in all directions. The weight of the film is neglected, and it is assumed that there are no moments on the edges of the element.

If the deflection of the center of the differential element is  $z$ , the slope (at the center) in the  $x$  direction is  $\partial z / \partial x$ , and the rate of change of slope in the  $x$  direction is  $\partial^2 z / \partial x^2$ . Then the change in slope between the center and either end of the differential element is  $\frac{\partial^2 z}{\partial x^2} \frac{dx}{2}$ . This change in slope is also the angle which either of the forces  $S dy$  makes with the tangent to the surface at the center of the element. The component of either force  $S dy$  in the direction of the resultant pressure is  $S dy \frac{\partial^2 z}{\partial x^2} \frac{dx}{2}$ , provided that the deflections are small. Similar forces are developed on the two edges parallel to the  $x$  axis. The equation of equilibrium for forces, when written in the direction of the resultant pressure, gives

$$p dx dy + \frac{S \partial^2 z}{\partial x^2} dx dy + S \frac{\partial^2 z}{\partial y^2} dx dy = 0 \quad (140a)$$

or

$$\frac{\partial^2 z}{\partial x^2} + \frac{\partial^2 z}{\partial y^2} = \frac{-p}{S} \quad (140b)$$

Equation (140b), the differential equation for the membrane, is identical in form with Eq. (136c), the differential equation for a torsional member. Hence, if

$$\frac{p}{S} = \frac{2G\theta}{L} \quad (141)$$

and if the boundary conditions are satisfied,  $z$  will equal  $\phi$ . That is, the deflection of the membrane will give the stress function. The boundary conditions can be satisfied by making the boundary of the membrane lie in a plane and having it in the shape of the cross section of the member. This requirement satisfies the condition that  $\phi$  must be equal to zero around the periphery of the member, and, in addition, the requirement that at the boundary the slope parallel to the boundary must equal zero, which is equivalent to saying that the derivative of

the stress function in the direction of the boundary must be zero. However, from Eqs. (136a) and (136b), the derivative in the direction of the boundary is equal to the component of the shearing stress perpendicular to the boundary, so the plane boundary for the membrane satisfies the condition that the shearing stress must be zero around the edge of the member.

Therefore, if a hole having the same shape as the cross section of a shaft is cut in a plate and a membrane<sup>1</sup> across the opening is subjected to pressure on one side, the slope of the surface will be proportional to the shearing stress at right angles to the direction in which the slope is measured. If Eq. (141) is satisfied, the slope will be equal to the shearing stress, otherwise a proportionality constant  $k$  must be determined. That is

$$\frac{p}{S} = k \frac{2G\theta}{L} \quad (142)$$

Then

$$\frac{\partial^2 z}{\partial x^2} + \frac{\partial^2 z}{\partial y^2} = \frac{-k2G\theta}{L} = \frac{k}{\partial x^2} \phi + \frac{k}{\partial y^2} \phi \quad (143)$$

and

$$z = k\phi \quad (144)$$

from which

$$S_{zz} = \frac{1}{k} \frac{\partial z}{\partial y} \quad (145)$$

and

$$S_{yz} = \frac{-1}{k} \frac{\partial z}{\partial x} \quad (145a)$$

The volume  $V$  enclosed between the membrane and the plane of the boundary is

$$V = \int_0^A z \, da \quad (146)$$

$$= k \int_0^A \phi \, da \quad (147)$$

However, from Eq. (137)

$$\int_0^A \phi \, da = \frac{T}{2}$$

Hence

$$V = k \frac{T}{2}$$

<sup>1</sup> A material having no weight and no resistance to bending is required. Soap solutions that form a tough film lasting for several hours are usually used as a satisfactory approximation.

That is, the volume under the membrane is proportional to the torque. In the practical application of the membrane analogy, the constant  $k$  is not found since its evaluation from Eq. (142) would necessitate the determination of  $S$ , the surface tension of the membrane. Instead, a calibration shape is usually used. This consists of a circular hole cut in the same plate as the section being studied and covered with the same membrane. Equation (145) may be written for both the cross sections, and since  $k$  is common to the two equations it may be eliminated. Similarly, a torque-volume equation for the two shapes may be obtained from Eq. (148). Since the slope-stress-torque values

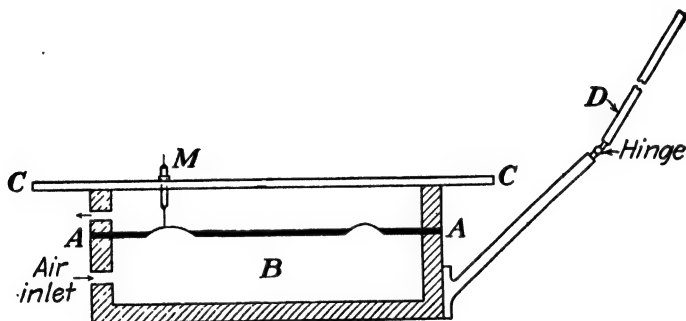


FIG. 69.—Sketch of equipment for membrane analogy.

are known for the circular shaft, they may be found for the other shape by proportions.

The techniques of evaluation of stresses by the membrane analogy have been developed by Griffith and Taylor,<sup>1</sup> by Trayer and March,<sup>2</sup> and by others.

The standard equipment consists of a box, the cross section of which is indicated in Fig. 69. The plate, containing two holes, one having the shape of the cross section being investigated, and the other circular, for calibration, is located at  $AA$ . After the membrane, usually a special soap solution, is placed across the openings, a measured volume of air is admitted to the chamber  $B$  below the plate. The glass plate  $CC$  in which is mounted a micrometer  $M$  is used to map the deflected surfaces.

<sup>1</sup> *Loc. cit.*

<sup>2</sup> TRAYER, G. W., and H. W. MARCH, The Torsion of Members Having Sections Common in Aircraft Construction, *Nat. Advisory Comm. Aeronaut. Tech. Repts.* 334, 1930.

With the micrometer set for a given reading, the glass plate is adjusted until the needle on the lower end of the micrometer contacts the soap film. Then the hinged board *D*, to which is attached a sheet of paper, is swung down until the needle on the upper end of the micrometer pierces the paper. The board is lifted, the plate adjusted to give a micrometer contact at a different point on the film, and the new point recorded on the paper. A repetition of this procedure permits the location of a series

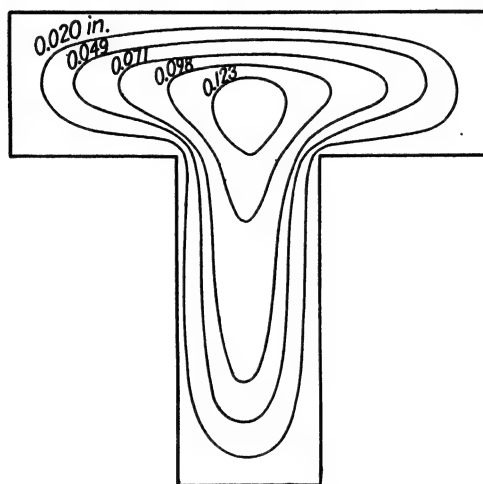


FIG. 70.—Contour lines for a T section.

of contour lines for the deflected films. A set of contour lines as determined from a T section is shown in Fig. 70.

From these lines, which are known as “lines of shearing stress,” since they give the directions of the maximum shearing stresses, the necessary slopes and volumes of the films may be obtained. The stress-torque relationships for the cross section being considered may then be determined by the application of Eqs. (145) and (148) to the cross section and to the circle, together with Eq. (119b) for the circle. It is evident that the maximum shearing stress in the T section of Fig. 70 will occur near the reentrant corners, because the slope is greatest in that region. The direction of the shearing stress is perpendicular to the direction in which the slope is measured by Eq. (145).

Slopes may also be determined by a device that projects a ray of light toward the film. The ray is adjusted until the

reflected ray coincides with the impinging ray. Since the slope of the film is normal to the ray under that condition, the slope may be evaluated by measuring the direction of the ray.

**69. Application of the Membrane Analogy.**—The practical application of the membrane analogy to the determination of torsional stresses in shafts of various cross sections may be qualitative or quantitative. The qualitative application involves the use of the analogy as a mental tool in locating the point

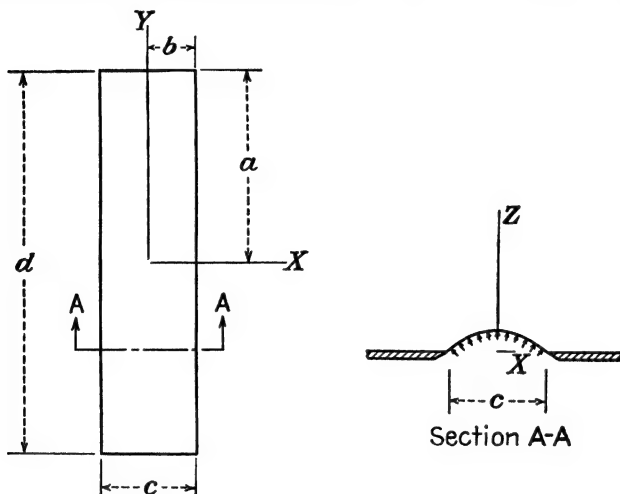


FIG. 71.—Narrow rectangular section in torsion.

of maximum stress or in making a comparison of the torque-carrying capacities of different cross sections. For example, the shape of the deflected membrane may be readily visualized with sufficient accuracy to indicate directly that a reentrant corner in a shaft is a point of high stress, or that for a given angle of twist or a given maximum stress, a square shaft will transmit but slightly more torque than the circular shaft that may be inscribed in it.

An approximate evaluation of the stresses in a member of long narrow rectangular cross section subjected to torsion follows directly from the membrane analogy. If a small distance near each end is neglected, each cross section normal to the longitudinal center line will be identical and may be represented as indicated in Fig. 71. Hence  $\partial z / \partial y$  is equal to zero, and Eq. (143), for  $k = 1$ , reduces to

$$\frac{\partial^2 z}{\partial x^2} = \frac{-2G\theta}{L} \quad (149)$$

which may be integrated directly to give

$$\frac{\partial z}{\partial x} = \frac{-2G\theta}{L} x + C_1 \quad (149a)$$

The constant of integration may be evaluated from the fact that the membrane is horizontal at the center, *i.e.*,

$$\frac{\partial z}{\partial x} = 0 \quad \text{when} \quad x = 0$$

Therefore

$$C_1 = 0$$

A second integration gives

$$z = \frac{-G\theta}{L} x^2 + C_2 \quad (149b)$$

from the boundary condition that  $z = 0$  at  $x = b$

$$C_2 = \frac{G\theta b^2}{L}$$

Therefore

$$\phi = z = \frac{G\theta}{L} (b^2 - x^2) \quad (149c)$$

The torque may be found from Eq. (137)

$$T = 2 \int_0^A \phi \, da \quad (137)$$

$$= 2 \int_{-b}^b \int_{-a}^a \frac{G\theta}{L} (b^2 - x^2) \, dx \, dy \quad (150)$$

$$= \frac{16G\theta ab^3}{3L} \quad (150a)$$

from which

$$\theta = \frac{3TL}{16Gab^3} \quad (150b)$$

The maximum shearing stress occurs at the edge  $x = b$  and is, from Eqs. (149a) and (136b),

$$S_{ys} = \frac{2G\theta b}{L} \quad (151)$$

The stress may be expressed in terms of the torque by sub-



stituting the value of  $G\theta$  from Eq. (150b)

$$S_{ys} = \frac{3T}{8ab^2} \quad (151a)$$

The maximum stress in a long narrow rectangular bar is, from Eq. (123) and Table VI,  $a/b = \infty$

$$S_{\max} = \frac{0.667(9)T}{16ab^2} \quad (151b)$$

$$= \frac{3T}{8ab^2} \quad (151c)$$

which agrees with the result obtained in Eq. (151a) by the approximate analysis. For  $a/b = 10$  the approximate analysis is about 7 per cent in error, and on the unsafe side. Equations (150b) and (151a) may be written in terms of the width  $c$  and the total depth  $d$  of the cross section as

$$\theta = \frac{3TL}{Gc^3 d} \quad (150c)$$

$$S_{ys} = \frac{3T}{c^2 d} \quad (151d)$$

**70. Hollow Sections.**—The membrane analogy may be extended to cross sections containing holes. Since there can be

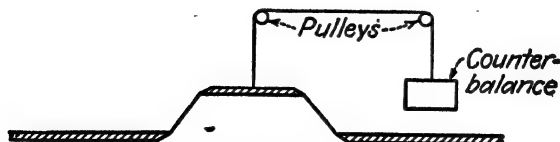
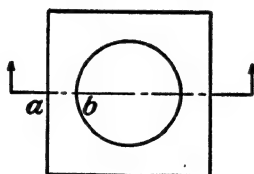


FIG. 72.—Membrane-analogy equipment for a hollow section.

no shearing stress normal to the boundary of the hole at the boundary, the slope of the membrane parallel to the boundary must be zero on the boundary. This condition may be satisfied

by attaching the membrane to a flat plate of the proper size, shape, and location to correspond with the hole. The plate must be allowed to deflect as pressure is applied, but its weight must be counterbalanced, and it must be kept level. Figure 72 indicates how the analogy might be used in determining the stresses in a square shaft containing a longitudinal circular hole.

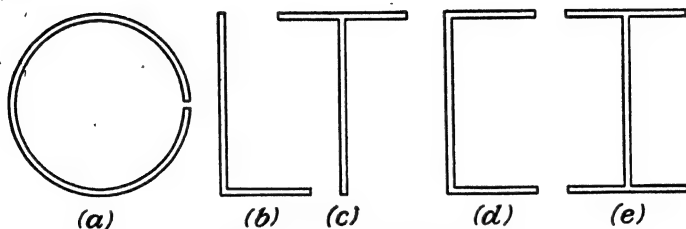


FIG. 73.—Thin-walled open sections.

**71. Torsional Stresses in Thin-walled Open Sections.**—In some types of structures, particularly in aircraft units, members having a small thickness in comparison with other dimensions may be required to transmit torque. The wall of the member may form a closed curve, in which case the cross section is known as a “closed section,” or it may form an “open section,” examples of which are shown in Fig. 73. With a given cross-sectional area and wall thickness the torsional resistance of a closed section is far different from that of an open section. From a consideration of the shape of the deflected membrane it is evident that Eq. (150c) may be extended with little error to *open thin-walled sections* such as those indicated in Fig. 73. The total torque developed by the section composed of a series of rectangles will be equal to the sum of the torques developed by each component rectangle.

$$T = T_1 + T_2 + T_3 + \cdots + T_n \quad (152)$$

However, the torque developed by each rectangle may be evaluated from Eq. (150c)

$$T = \frac{G_1 \theta_1 c_1^3 d_1}{3L_1} + \frac{G_2 \theta_2 c_2^3 d_2}{3L_2} + \cdots + \frac{G_n \theta_n c_n^3 d_n}{3L_n} \quad (152a)$$

However, if the member is homogeneous and if no secondary effects such as buckling occur,  $\theta$ ,  $G$ , and  $L$  will be equal in each

rectangle and

$$T = \frac{G\theta}{L} \sum \frac{c^3 d}{3} \quad (152b)$$

It will be noted that Eq. (152b) is similar in general form to

$$T = \frac{G\theta J}{L}$$

for a circular shaft. Hence, for convenience Eq. (152b) may be written as

$$T = \frac{G\theta J_e}{L} \quad (152c)$$

in which

$$J_e = \frac{1}{3} \Sigma c^3 d \quad (153)$$

defines an *equivalent polar moment of inertia*. Similarly

$$S_{xz} = \frac{Tc}{J_e} \quad (151e)$$

in which the term  $c$  is the total width of the rectangle in which the stress is desired.

Saint Venant showed that for the single rectangle the equivalent polar moment of inertia is given by

$$J_e = \frac{c^3 d}{3} - \alpha c^4 \quad (153a)$$

in which  $\alpha$  varies from 0.194 for  $d = c$  to 0.210 for  $d > 2.5c$ . The second term takes into account the "end effect" or decrease in volume under the membrane near the end, which was neglected in developing Eq. (153).

Lyse and Johnston<sup>1</sup> give the value of  $J_e$  for a trapezoidal cross section such as the flange of an I beam, as

$$J_e = \frac{d}{12} (c_1 + c_2)(c_1^2 + c_2^2) - \alpha_1 c_1^4 - \alpha_2 c_2^4 \quad (153b)$$

in which  $c_1$  and  $c_2$  are the thicknesses at the ends of the section  $\alpha_1$  and  $\alpha_2$  are coefficients equal to approximately 0.10.

From tests of steel I beams and H beams Lyse and Johnston found good agreement between the measured value of  $J_e$  and

<sup>1</sup> LYSE, INGE, and B. G. JOHNSTON, Structural Beams in Torsion, *Trans. Am. Soc. Civil Engrs.*, Vol. 62, p. 857, 1936.

the computed value, assuming the sections to be composed of rectangles, trapezoids, and circles (at the intersection of flange and web). Stresses as evaluated from strain measurements were found to be in agreement with

$$S_{yx} = \frac{T(c + 0.3r)}{J_x} \quad (151f)$$

in which  $r$  is the radius of the fillet at the junction of web and flange

$c$  is the thickness of the web, or minimum thickness of flange.

As would be expected, the maximum stresses occur near the junction of web and flange.

Tests of rolled channels<sup>1</sup> indicate that the value of  $J_x$ , as computed from Eq. (153), using the mean thickness of each component part for its respective  $c$ , should be increased about 10 per cent to agree with experimental results. Closer agreement with test data may be obtained by taking into account the taper of the flanges.

It is further evident from a consideration of the membrane analogy that Eq. (151d) will give reasonable values of stress in the section shown in Fig. 73a but will be correct in the other sections only at a distance of at least  $c$  from the reentrant corners. Concentration of stress will exist at the corners, the magnitude of the concentration depending upon the radius of the fillet. Timoshenko<sup>2</sup> shows that the maximum stress may be evaluated satisfactorily as

$$S_{\max} = \frac{Tc \left(1 + \frac{c}{4r}\right)}{J_x} \quad (154)$$

in which  $r$  is the radius of the fillet at the inside corner. If the radius of the fillet is small in comparison with the thickness  $c$  ( $r$  equal to approximately  $0.1c$ ) the maximum stress may be

<sup>1</sup> SEELY, F. B., W. J. PUTNAM, and W. L. SCHWALBE, The Torsional Effect of Transverse Bending Loads on Channel Beams, *Univ. Illinois Eng. Expt. Sta. Bull.* 211, 1930.

<sup>2</sup> TIMOSHENKO, S., "Theory of Elasticity," p. 258, McGraw-Hill Book Company, Inc., 1934.

evaluated as<sup>1</sup>

$$S_{\max} = \frac{1.74Tc \sqrt[3]{\frac{c}{r}}}{J_s} \quad (155)$$

Equations (154) and (155) are compared in Fig. 78.

The effect of a longitudinal slit upon the torsional resistance of a thin-walled circular tube may be made by comparing the stress and angle of twist of the section in Fig. 73a with an unslit tube of the same dimensions. If  $R$  denotes the mean radius of the tube wall and  $t$  the wall thickness of the tube, the stress developed in the open section is, from Eq. (151d),

$$S_{ts} = \frac{3T}{2Rt^2\pi} \quad (156a)$$

The torque developed in the closed tube may be evaluated by assuming the stress to be uniformly distributed.

$$\begin{aligned} T &= S_1 AR = S_1 2\pi R t R \\ S_1 &= \frac{T}{2\pi R^2 t} \end{aligned} \quad (156b)$$

Therefore, if the two tubes are subjected to the same torque, the stress in the slit tube will be greater by the ratio  $3R/t$ . The angle of twist in the slit tube is, from Eq. (150c),

$$\theta = \frac{3TL}{2\pi R G t^3} \quad (156c)$$

for the closed section

$$\begin{aligned} \theta_1 &= \frac{TL}{GJ} \\ &= \frac{TL}{2\pi R^3 t G} \end{aligned} \quad (156d)$$

The ratio of  $\theta$  to  $\theta_1$  for the same torque is  $3(R/t)^2$ .

For example, a torque of 41,000 in.-lb. is required to produce a stress of 20,000 p.s.i. in a  $3\frac{3}{4}$ -in. tube with a wall thickness of 0.095 in. (which is a standard size), but if the tube is slit, the torque required to produce the 20,000-p.s.i. stress is only 700 in.-lb. or about 1.7 per cent of the torque for the unslit tube. In the first case the stress of 20,000 p.s.i. will be accompanied

<sup>1</sup> TREFFTZ, E., *Z. fur angew. Math. Mech.*, Vol. 2, p. 263, 1922.

by a twist of 0.00314 radian per in., if the tube is aluminum alloy, while the 20,000-p.s.i. stress in the slit tube will result in a twist of 0.062 radian per in. or nearly 20 times the twist in the unslit tube.

The difference in stress distribution in the two tubes is indicated in Fig. 74. The relatively high torque in the closed cross section is due to the fact that the shearing forces are practically constant over the area and their moments add, while in the open cross section the shearing forces on the inner half oppose those in the outer half.

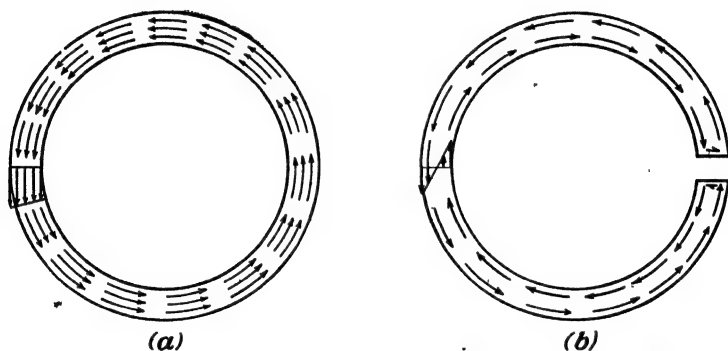


FIG. 74.—Distribution of torsional stress in closed and open sections.

**72. Torsional Stresses in Thin-walled Closed Sections.**—The evaluation of the stresses and angle of twist in the thin-walled section of circular outline follows directly from the elementary theory. An approximate solution for the torsional stresses in a thin-walled closed section having a circular or noncircular outline may be obtained by assuming that the stress is uniformly distributed across the wall of the section. The assumption is justified when the wall thickness is small in comparison with the over-all dimensions of the section. From the standpoint of the membrane analogy, the assumption is reasonable in that any radial section through the membrane, such as *ab* in Fig. 72, will be practically a straight line.

In a thin-walled section the magnitude of the shearing force per unit length of periphery of cross section is constant regardless of whether or not the wall thickness is constant. The shearing “force” per unit length of periphery is called the “shear flow” and is designated by the symbol  $q$ . It may be evaluated from

the torsional stress as  $q = S_{tz}t$ . The fact that the shear flow is constant in a thin-walled torsional member may be verified by considering a free-body diagram of a section of length  $dz$  cut from the tube as shown in Fig. 75. Under the action of the applied torque a shearing force  $Q_{tz}$  will be developed on both the front and back faces of the element. The resulting couple

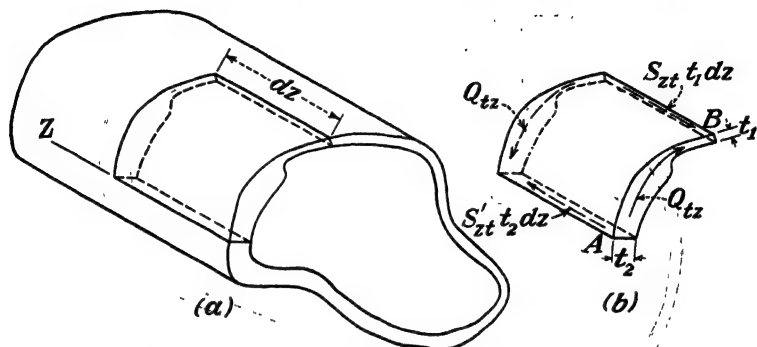


FIG. 75.—Torsion of a thin-walled closed section.

$Q_{tz} dz$  is balanced by the couple resulting from the longitudinal force  $S_{zt} t_1 dz$  and  $S'_{zt} t_2 dz$ . However, from the equation of equilibrium of forces in the  $z$  direction

$$S_{zt} t_1 dz = S'_{zt} t_2 dz$$

or

$$S_{zt} t_1 = S'_{zt} t_2$$

In addition, from a consideration of a differential block at corner  $A$  of the element, it is evident that the shearing stress  $S'_{tz}$ , developed on the face  $AB$  at  $A$  is equal to  $S'_{zt}$  and the shearing stress  $S_{tz}$ , developed on the face  $AB$  at the corner  $B$ , is equal to  $S_{zt}$ . Hence

$$S_{zt} t_1 = S'_{zt} t_2 = q = \text{constant.}$$

The torsional moment, or torque, developed by the shearing stress in the cross section ( $AB$ ) may be determined from the shear flow, as indicated in Fig. 76. The shearing force developed in a differential length  $ds$  of the wall will be  $q ds = S_{tz} ds$ .

The moment of this shearing force about any convenient  $z$  axis intersecting the cross section at point  $O$  is

$$dT = qr ds \quad (157a)$$

in which  $r$  is the moment arm of the force,

If the ends of the differential length are connected with point  $O$ , it is evident that the enclosed area  $da$  is equal to  $\frac{1}{2}r ds$ . Hence

$$dT = 2q da \quad (157b)$$

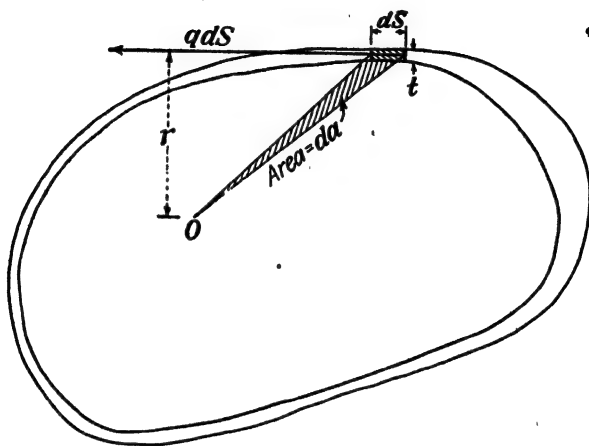


FIG. 76.—Torque in thin-walled closed section.

The total torque  $T$  developed by the entire cross section of the tube is

$$T = 2 \int_0^A q da \quad (157c)$$

However,  $q$  is constant, so

$$T = 2qA = 2S_{ts}tA \quad (157d)$$

in which  $A$  is the total area enclosed by the center line of the tube wall

$t$  is the thickness at the point where the stress  $S_{ts}$  is evaluated.

Then

$$S_{ts} = \frac{T}{2At} \quad (157e)$$

The angle of twist may be determined by equating the internal strain energy to the external work done in twisting the tube. If the stresses are below the proportional limit



$$\frac{1}{2}T\theta = \frac{S_{t,z}^2}{2G} (\text{volume}) \quad (158a)$$

$$= \int_0^s \frac{S_{t,z}^2 L ds}{2G} \quad (158b)$$

in which  $s$  is the length of the center line of the wall cross section. From Eq. (157e)

$$T\theta = \int_0^s \frac{T^2 t L ds}{4A^2 t^2 G} \quad (158c)$$

$$\theta = \frac{TL}{4A^2 G} \int_0^s \frac{ds}{t} \quad (158d)$$

$$= \frac{Lq}{2AG} \int_0^s \frac{ds}{t} \quad (158e)$$

If the tube has reentrant corners, stress concentration will occur at the corners, resulting in stresses greater than those indicated by Eq. (157e).

Thin-walled tubes subjected to torsion may fail in compression, due to local buckling as a result of the principal compressive stresses developed at an angle of 45 deg. with a transverse plane.

**73. Multicelled Thin-walled Sections.**—If the cross section of the torsional member consists of two or more thin-walled cells,



FIG. 77.—Example of a two-cell section.

as for example, in one type of airplane wing, Fig. 77, the distribution of the torque among the cells may be determined from the fact that each cell is rotated through the same angle. Hence, Eq. (158d) may be applied to each cell separately and the angles equated. In addition, the total torque is equal to the sum of the torques developed by each cell. The resulting series of simultaneous equations may be solved for the torque in each cell, and stresses determined by the application of Eq. (157e) to each cell separately. The stress in the member common to two cells is the resultant of the stress contributed by each of the cells.

If it is desired to avoid the solution using simultaneous equations the distribution of the torque among the cells of a multi-

celled torsional member may be determined by a process of successive approximation.

Baron<sup>1</sup> has outlined a systematic procedure similar to the process developed by Cross<sup>2</sup> for the analysis of flow in interconnected conduits. The analysis is based on the analogy between shear flow in a thin-walled section and the flow of a fluid or electricity in a network of conduits that is geometrically similar to the cross section of the torsional member. The shear flow entering into any joint must be equal to the shear flow "flowing" out of the joint, by statics; and the shear flow along any cell wall between joints is constant, as has been proved.

Baron has also shown that the problem may be solved by making successive corrections to a trial solution. The trial solution consists in assuming a shear flow in each closed circuit such that the total shear flow balances the external torque that the cross section must carry, and such that the angle of twist of each unit is approximately equal. The assumed distribution may violate the condition that the shear flow into a junction must equal the shear flow out of the junction. Then the "unbalanced" shear flow must be distributed among the units meeting at the junction, to satisfy Eq. (158e). The redistribution may unbalance the shear flow at other junctions, so the process is repeated at the joints in succession until the desired precision is obtained. A correct solution is obtained when Eq. (158e) and the equations of equilibrium are satisfied.

**74. Effect of End Restraint.**—The evaluation of torsional stresses considered in the preceding articles is based on the assumption that no longitudinal stresses are developed in the torsional member. This assumption is equivalent to assuming that each cross section is free to warp. If any cross section is not free to warp, as at a fixed end of a torsional member or a beam subjected to torsion, longitudinal stresses will be developed and will add to the longitudinal stresses due to bending, if any. In addition, distortion of the cross section may occur, resulting in excessive stresses. Goodier and Barton have developed an analysis for I beams,<sup>3</sup> assuming that the cross section of the web

<sup>1</sup> BARON, F. H., Torsion of Multiconnected Thin-walled Cylinders, *Trans. Am. Soc. Mech. Engrs.*, Vol. 64, p. A-72, 1942.

<sup>2</sup> CROSS, HARDY, Analysis of Flow in Networks of Conduits or Conductors, *Univ. Illinois Eng. Expt. Sta. Bull. No. 286*, 1936.

<sup>3</sup> GOODIER, J. N., and M. V. BARTON, The Effects of Web Deformation on

does not remain straight but warps, owing to bending moments developed between the flanges and web.

The effect of end restraint has been studied experimentally as well as analytically by Seely, Putnam, and Schwalbe<sup>1</sup> and by Lyse and Johnston.<sup>2</sup> Their results, as well as those of Goodier and Barton, show that the end restraint stiffens the member torsionally and that the rate of twist with respect to length  $d\theta/dz$  is not constant for some distance from the fixed end. A treatment of the problem for thin-walled cellular members is given by von Kármán and Christensen.<sup>3</sup>

**75. Stress Concentration in Torsional Members.**—Stress concentration in shafts and other torsional members may be caused by (1) irregularities in cross section, particularly reentrant corners, and (2) changes in cross section. Holes, keyways, and other irregularities are needed in shafting to transfer torque from the shaft to pulleys, gears, or other attachments, and they may cause failure under conditions of repeated loading or in a brittle material unless properly considered in design. Because of the mathematical difficulties involved in the exact solution, values of the stress-concentration factor have been obtained experimentally for the most part.

In addition to the experimental methods outlined in Art. 46 and the membrane analogy, three hydrodynamical analogies have been developed; one by Lord Kelvin,<sup>4</sup> another by Bousinesq,<sup>5</sup> and a third by Greenhill,<sup>6</sup> each for aid in evaluating the torsional stresses in members of irregular cross section. In the hydrodynamical analogy described by Greenhill, a container having the same cross section as the cross section of the shaft is partially filled with fluid (theoretically frictionless) and the container is rotated. The linear relative velocity of the fluid

---

the Torsion of I-Beams, *Trans. Am. Soc. Mech. Engrs.*, Vol. 66, p. A-35, 1944.

<sup>1</sup> *Op. cit.* p. 170

<sup>2</sup> *Op. cit.* p. 169.

<sup>3</sup> VON KÁRMÁN, T., and N. B. CHRISTENSEN, Method of Analysis for Torsion with Variable Twist, *J. Aeronaut. Sci.*, Vol. 11, p. 110, 1944.

<sup>4</sup> THOMSON, SIR WILLIAM, and P. G. TAIT, "Treatise on Natural Philosophy," Part 2, University Press, Cambridge, 1867.

<sup>5</sup> BOUSSINESQ, J., *J. math. pure appl.*, Ser. 2, Vol. 16, 1871.

<sup>6</sup> GREENHILL, A. G., Hydromechanics, "Encyclopaedia Britannica," 9th

at any point is proportional to the shearing stress at the corresponding point in the shaft. Den Hartog and McGivern<sup>1</sup> used this analogy to study stresses in square and rectangular shafts and circular shafts containing keyways.

In general, the study of stress concentration in torsional members has centered around four types of stress raisers.

1. Reentrant corners in thin-walled noncircular members.
2. Keyways in circular shafts.
3. Transverse holes in circular shafts.
4. Changes in diameter of circular shafts.

These four cases represent the important situations in which concentration of stress occurs.

1. *Reentrant Corners*.—This condition has been considered in Art. 71 and Eqs. (154) and (155), given for the evaluation of the maximum stress. They reduce to

$$K_t = 1 + \frac{c}{4r} \quad (154a)$$

and

$$K_t = 1.74 \sqrt[3]{\frac{c}{r}} \quad (155a)$$

in which  $r$  is the radius of the fillet

$c$  is the wall thickness.

Figure 78 shows values of  $K_t$  from the two formulas plotted against values of  $c/r$ .

2. *Keyways in Circular Shafts*.—Weber<sup>2</sup> showed that the maximum stress in a circular shaft containing a longitudinal semicircular groove is given by the expression

$$S_{zs} = \frac{G\theta}{L} (2r_o - r_g)$$

in which  $r_o$  is the radius of the shaft

$r_g$  is the radius of the groove.

Hence, from Eq. (g) developed in Art. 67 the stress-concentration factor is

$$K_t = 2 - \frac{r_g}{r_o}$$

<sup>1</sup> DEN HARTOG, J. P., and J. G. MCGIVERN, On the Hydrodynamical Analogy of Torsion, *Trans. Am. Soc. Mech. Engrs.*, Vol. 57, p. A-46, 1935.

<sup>2</sup> WEBER, D., *Lehre der Verdrehungsfestigkeit*, V. D. I. *Forschungsarb.*, 429, 1921.

If the shaft contains a semielliptical groove at the outside with the principal axis  $a$  in the radial direction and the other principal axis equal to  $b$ , the stress-concentration factor is

$$K_t = 1 + \frac{a}{b}$$

Hence, a narrow radial crack has a marked effect upon the strength of a shaft.

Griffith and Taylor<sup>1</sup> used the membrane analogy to evaluate the stress-concentration factor for a keyway in a hollow shaft.

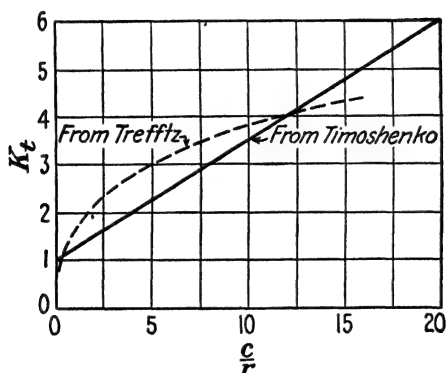


FIG. 78.—Values of stress-concentration factors for reentrant corners in thin-walled torsional members.

With this method a stress-concentration factor of 5.4 was found for a keyway 1 in. deep and 2.5 in. wide in a 10-in. by 5.8-in. hollow shaft when the radius of the fillet was 0.1 in. When the radius of the fillet was increased to 0.5 in. the stress-concentration factor was reduced to 2.1. Tests by Gough<sup>2</sup> on torsion members containing profiled keyways give a value of the endurance-limit-reduction factor of about 1.20 for Armco iron and 1.30 for 0.65 per cent carbon steel. Moore<sup>3</sup> reports a value of endurance-limit-reduction factor of 1.30 for a sled-runner

<sup>1</sup> GRIFFITH, A. A., and G. I. TAYLOR, The Use of Soap Films in Solving Torsion Problems, *Proc. Inst. Mech. Engrs. London*, p. 755, October-December, 1937.

<sup>2</sup> GOUGH, M. J., The Effect of Keyways on the Strength and Stiffness of Shafts Subjected to Torsional Stresses, *Tech. Repts. Aeronaut. Research Comm.*, p. 488, 1924-1925.

<sup>3</sup> MOORE, H. F., The Effect of Keyways on the Strength of Shafts, *Univ. Illinois Eng. Expt. Sta. Bull.* 42, 1909.

keyway in cold-rolled shafting. Tests using the brittle-material method<sup>1</sup> on plaster specimens 2 in. in diameter having milled keyways  $\frac{1}{4}$  in. deep and  $\frac{1}{2}$  in. wide gave average values of the stress-concentration factor of 1.44 for the sled-runner keyway and 1.68 for the profiled keyway.

3. *Transverse Holes in Circular Shafts.*—Seely and Dolan also investigated the effect of transverse holes upon the strength of

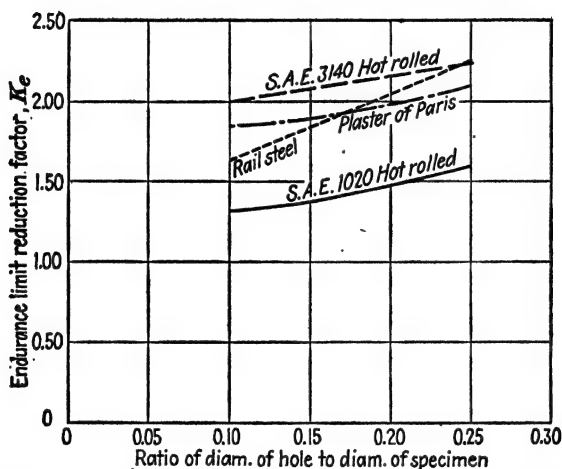


FIG. 79.—Endurance-limit-reduction factors for torsional specimens containing transverse holes.

torsional members. Two-inch diameter cylindrical plaster specimens containing transverse holes gave values of the stress-concentration factor ranging from 1.86 for a  $\frac{1}{8}$ -in. hole to 2.12 for a  $\frac{1}{2}$ -in. hole. Armbruster<sup>2</sup> found that the value of the endurance-limit-reduction factor for repeated loading of torsion specimens containing transverse holes was dependent upon the characteristics of the material. For a diameter of hole equal to 15 per cent of the diameter of the specimen his tests gave values of  $K_e$  ranging from 1.31 for a mild steel to 1.82 for a high-strength steel. Results of repeated loading tests on torsion specimens by Dolan<sup>3</sup> are indicated in Fig. 79, together with

<sup>1</sup> SEELY, F. B., and T. J. DOLAN, Stress Concentration at Fillets, Holes, and Keyways as Found by the Plaster-model Method, *Univ. Illinois Eng. Expt. Sta. Bull.* 276, 1935.

<sup>2</sup> ARMBRUSTER, E., Einfluss der Oberflächen Beschaffenheit auf den Spannungsverlauf und die Schwingungsfestigkeit, *V. D. I. Verlag.*, 1931.

<sup>3</sup> DOLAN, T. J., The Combined Effect of Corrosion and Stress Concen-

the tests by Seely and Dolan<sup>1</sup> on plaster of paris specimens. The test results show that the stronger steels are more sensitive to the stress concentration around the hole. Dolan also demonstrated that the endurance-limit-reduction factor is increased if the specimens are subjected to corrosion. The theoretical value of the stress-concentration factor at a circular hole is approximately 4. The lower values obtained in the repeated loading tests indicate the beneficial influences of local yielding in reducing the effective stress-concentration factor.

Neuber,<sup>2</sup> in investigating the effect of transverse elliptical holes in shafts, showed that the ratio of the radius of curvature at the end of the major axis of the hole to the size of the shaft is an important factor in establishing the stress-concentration factor.

4. *Change in Diameter of Circular Shafts.*—The stress concentration that occurs at a change in cross section may also be appreciable. For example, a small semicircular groove cut around the circumference of a circular shaft has a stress-concentration factor of 2.0. That is, the maximum stress at the base of the groove is twice the maximum stress in a circular shaft without the groove. The maximum stress occurs at the bottom of the groove.

The stress-concentration factor existing at a change of diameter in a stepped shaft is dependent upon the diameters of the two sections and the radius of the fillet. Values of the stress-concentration factor as determined by Jacobsen<sup>3</sup> using an electrical analogy are indicated in Fig. 80. The quantity  $D$  is the diameter of the large section,  $d$  is the diameter of the small section, and  $r$  is the radius of the fillet. The stress-concentration factor  $K_t$  is based on the maximum stress in the smaller shaft.

Values of the endurance-limit-reduction factor  $K_e$  for fillets as determined by Dolan<sup>4</sup> from repeated loading tests were

---

tration at Holes and Fillets in Steel Specimens Subjected to Reversed Torsional Stresses, *Univ. Illinois Eng. Expt. Sta. Bull.* 293, 1937.

<sup>1</sup> *Op. cit.*

<sup>2</sup> NEUBER, N., "Kerbspannungslehre," Berlin, 1937.

<sup>3</sup> JACOBSEN, L. S., Torsional-stress Concentrations in Shafts of Circular Cross Section and Variable Diameter, *Trans. Am. Soc. Mech. Engrs.*, Vol. 47, p. 619, 1925.

<sup>4</sup> *Op. cit.*, p. 180.

appreciably lower than the values of stress-concentration factor obtained by Jacobsen. In Chap. 5 it was noted that the endurance-limit-reduction factor for axial loading is less than the stress-concentration factor for the same member. The stronger S.A.E. 3140 steel indicated higher values of  $K_t$  than the weaker S.A.E. 1020 steel, which also agrees with the findings for axial loading.

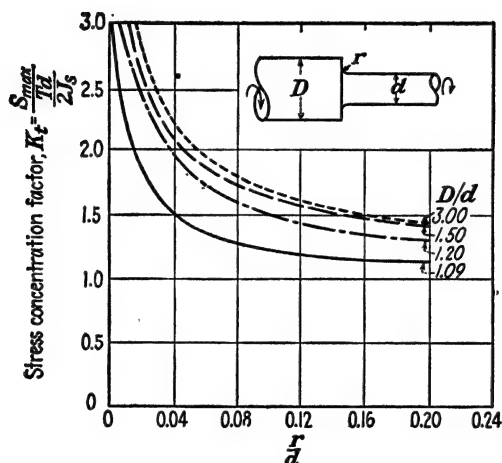


FIG. 80.—Stress-concentration factors for stepped shafts.

As was noted in connection with stress-concentration factors for axially loaded members, the factor should be taken into account in design if the material is brittle or if the member is subjected to impact or repeated loading. For ductile materials subjected to steady loading, sufficient plastic yielding can usually occur at the points of stress concentration to relieve the stresses without causing damage. However, steady loading on a shaft is not common. Resistance to fluctuating torsional stress has been investigated by Moore and Kommers<sup>1</sup> and by Smith<sup>2</sup> for 3140 steel. Their data indicate that if the specimen contains no stress raisers, the material will not fail if the *range of stress* ( $S_{\max} - S_{\min}$ ) does not exceed twice the endurance limit, provided that  $S_{\max}$  does not exceed the torsional yield strength.

<sup>1</sup> MOORE, H. F., and J. B. KOMMERS, "Fatigue of Metals," McGraw-Hill Book Company, Inc., New York, 1927.

<sup>2</sup> SMITH, J. O., The Effect of Range of Stress on the Torsional Fatigue Strength of Steel, *Univ. Illinois Eng. Expt. Sta. Bull.* 316, 1939.



However, if the specimen contains stress raisers, the allowable range of stress decreases as the maximum stress increases.

**76. Plastic Yielding in Circular Shafts.**—The equations developed thus far in this chapter are based on the assumption that the stresses do not exceed the proportional limit of the material. If the stresses do exceed the proportional limit, the maximum stresses are less and the angle of twist is greater than the values given by the formulas. However, stress may no longer be an adequate criterion of safety.

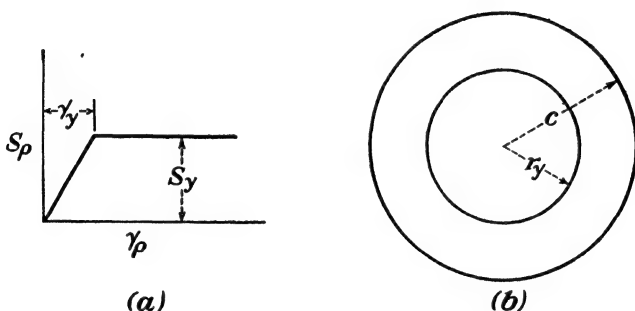


FIG. 81.—Plastic yielding in circular shafts.

The relationship between torque and the angle of twist for a circular shaft stressed above the proportional limit is dependent upon the shape of the stress-strain diagram. The stress-strain diagram for low-carbon steel in shear may be idealized as indicated in Fig. 81a for strains up to several times the elasticity. If it is assumed that a radius before twisting remains a radius after twisting, which may be verified experimentally even within the plastic range of stress, the unit strain is proportional to the distance from the center.

For values of the maximum strain not exceeding the elasticity, the conventional analysis applies. If the maximum strain exceeds the elasticity, the cross section may be considered to be composed of two portions as shown in Fig. 81b, a central circle of radius  $r_y$  to which the conventional analysis applies and an outer ring, all elements of which are stressed to the yield point in shear  $S_y$ . The torque developed by the entire cross section is

$$T = \int_0^{r_y} S_y (2\pi\rho) \rho d\rho + \int_{r_y}^c S_y (2\pi\rho) \rho d\rho \quad (159)$$

However

$$\frac{S_p}{\rho} = \frac{S_y}{r_y}$$

Hence

$$\begin{aligned} T &= \frac{2\pi S_y}{r_y} \int_0^{r_y} \rho^3 d\rho + 2\pi S_y \int_{r_y}^c \rho^2 d\rho \\ &= 2\pi S_y \frac{r_y^3}{4} + \frac{2\pi S_y}{3} (c^3 - r_y^3) \end{aligned} \quad (159b)$$

$$= \frac{\pi S_y}{6} (4c^3 - r_y^3) \quad (159c)$$

From the geometry of the shaft it is evident that

$$r_y \theta = \gamma_y L \quad (160)$$

in which  $\gamma_y$  is the elasticity. Then

$$r_y = \frac{S_y L}{G \theta} \quad (160a)$$

The radius  $r_y$  to the plastic boundary may be eliminated from Eq. (159c) by substituting its value from Eq. (160a) giving

$$T = \frac{\pi S_y}{6} \left[ 4c^3 - \left( \frac{S_y L}{G \theta} \right)^3 \right] \quad (159d)$$

as the relationship between the torque and the angle of twist.

If the material does not have a yield point as indicated in Fig. 81a, the  $T$ - $\theta$  relationship may still be developed from the stress-strain diagram. The general relationship between stress and strain may be written as

$$S_p = f(\gamma_p) \quad (161)$$

The resultant torque developed by the entire cross section is, by statics,

$$\begin{aligned} T &= \int_0^c S_p (2\pi \rho) \rho d\rho \\ &= 2\pi \int_0^c f(\gamma_p) \rho^2 d\rho \end{aligned} \quad (162)$$

From the geometry of the twisted shaft

$$\rho \theta = \gamma_p L \quad (163a)$$

so

$$\rho = \frac{\gamma_p L}{\theta} \quad (163b)$$

and

$$d\rho = \frac{L}{\theta} d\gamma_\rho \quad (163c)$$

Values of  $\rho^2$  and  $d\rho$  from Eqs. (163b) and (163c) may be substituted in Eq. (162), giving

$$T = 2\pi \int_0^{\gamma_c} f(\gamma_\rho) \frac{\gamma_\rho^2 L^2}{\theta^2} \frac{L}{\theta} d\gamma_\rho \quad (162a)$$

The limits of integration must be changed to conform to the change in variable. The upper limit becomes  $\gamma_c$ , denoting the strain at the outside of the shaft, corresponding to the upper limit of  $c$  for the variable  $\rho$  in Eq. (162). The quantities  $L$  and  $\theta$  are constant, so they may be taken outside of the integral sign giving

$$T = \frac{2\pi L^3}{\theta^3} \int_0^{\gamma_c} f(\gamma_\rho) \gamma_\rho^2 d\gamma_\rho \quad (162b)$$

As has been noted,<sup>1</sup> the integral in Eq. (162b) is the moment of inertia with respect to the stress axis of the area between the strain axis and the stress-strain diagram out to the strain  $\gamma_c$ .

The reverse problem, that of determining the stress-strain diagram for the material in shear from a torque-twist diagram of a circular bar, may be solved by multiplying both sides of Eq. (162b) by  $(c\theta/L)^3$

$$T \left( \frac{c\theta}{L} \right)^3 = 2\pi \int_0^{\gamma_c} c^3 f(\gamma_\rho) \gamma_\rho^2 d\gamma_\rho \quad (162c)$$

or

$$T \left( \frac{c\theta}{L} \right)^3 = 2\pi \int_0^{\frac{c\theta}{L}} c^3 f \left( \frac{\rho\theta}{L} \right) \left( \frac{\rho}{L} \right)^2 d \left( \frac{c}{L} \right) \quad (162d)$$

The right-hand side of Eq. (162c) is a function of the upper limit, which is equal to  $c\theta/L$ . Hence, both sides may be differentiated with respect to  $c\theta/L$  giving

$$3 \left( \frac{c\theta}{L} \right)^2 T + \left( \frac{c\theta}{L} \right)^3 \frac{dT}{d(c\theta/L)} = 2\pi S_c c^3 \left( \frac{c\theta}{L} \right)^2 \quad (163)$$

<sup>1</sup> DUGET, C., "Limite d'élasticité et résistance à la rupture," Vol. 1, p. 157, Paris, 1882.

LUDWIK, P., "Elemente der Technologischen Mechanik," Verlag Julius Springer, Berlin, 1909. NÁDAI, A., "Plasticity," p. 126, McGraw-Hill Book Company, Inc., New York, 1931.

or

$$3T + \left(\frac{c\theta}{L}\right) \frac{dT}{d(c\theta/L)} = 2\pi S_e c^3 \quad (163a)$$

Therefore, the stress at the outside is

$$S_e = \frac{3T + \left(\frac{\theta}{L}\right) \frac{dT}{d(\theta/L)}}{2\pi c^3} \quad (164)$$

The stress at the outside corresponding to a given torque may be determined from the  $T-(\theta/L)$  diagram and Eq. (164), noting that  $\frac{dT}{d(\theta/L)}$  may be evaluated as the slope of the tangent to the  $T-(\theta/L)$  curve at the given torque. The corresponding strain at the outside may be determined from Eq. (163a). At the ultimate the torque-twist diagram is horizontal, and the slope  $\frac{dT}{d(\theta/L)}$  is zero. Hence, Eq. (164) reduces to

$$S_u = \frac{3T}{2\pi c^3} \quad (164a)$$

which is  $\frac{3}{4}$  of the modulus of rupture, or the value given by the ordinary formula for the stress at the ultimate. In other words, the modulus of rupture for a circular shaft is 33 per cent greater than the true stress at the ultimate, regardless of the shape of the stress-strain diagram.

Stress-strain curves for ductile metals in pure shear have been reported by Ludwik.<sup>1</sup> The stress-strain curve in shear may be determined more directly from torque-twist data by using a thin-walled cylinder as the test specimen.

**77. The Sand-heap Analogy.**—The relative strength of cross sections of various shapes when stressed beyond the yield point may be evaluated by the sand-heap analogy, devised by Nádai.<sup>2</sup> The analogy is based on the assumption that the material has the stress-strain characteristics indicated in Fig. 81a. In the plastic region the stress is constant (equal to the yield point

<sup>1</sup> *Loc. cit.*

<sup>2</sup> NÁDAI, A., *Der Beginn des Fließvorganges in einem tordierten Stab*, *Z. angew. Math. Mech.*, Vol. 3, p. 442, 1923.

NÁDAI, A., "Plasticity," p. 132, McGraw-Hill Book Company, Inc., New York, 1931.

$S_y$ ), and the stress function, which satisfies Eq. (136c), must be such that it will have a constant slope in the plastic range. Nádai pointed out the fact that sand piled on a horizontal area having the same shape as the cross section of the shaft will satisfy the conditions for the entire cross section stressed to the yield point. The depth of the sand at any point is proportional to the stress function at that point, and the volume of sand retained on the area is proportional to the resultant torque. For example, the volume of the cone of sand retained on a circular area of radius  $c$  is equal to

$$V = \frac{1}{3}\pi c^2 h \quad (165)$$

in which  $h$  is the depth of the sand at the center. However, the slope is proportional to the stress, so

$$S_y = k \frac{h}{c} \quad (166)$$

and

$$V = \frac{1}{3}\pi c^2 \frac{c S_y}{k} \quad (165a)$$

from which

$$S_y = \frac{3kV}{\pi c^3} \quad (166a)$$

A comparison of Eqs. (166a) and (164a) gives

$$T = 2kV \quad (167)$$

The constant,  $k$ , may be evaluated from Eq. (166a)

$$k = \frac{\pi c^3 S_y}{3V} \quad (166b)$$

For evaluating the torsional resistance of an area that is partly in the plastic range and partly in the elastic range, a combination of the membrane analogy and the sand-heap analogy is useful. The sand-heap analogy may be applied to cross sections containing holes, as has been discussed by Prandtl and by Westergaard.<sup>1</sup> The analogy requires the production of a plateau corresponding to each hole in the cross section, the elevation of the plateau being equal to the product of the yield point and the shortest

<sup>1</sup> WESTERGAARD, H. M., Graphostatics of Stress Functions, *Trans. Am. Soc. Mech. Engrs.*, Vol. 56, p. 141, 1934.

distance from the hole to the outside of the member. Sadowsky<sup>1</sup> has described an experimental procedure for producing the plateau when the entire cross section has been stressed to the yield point.

Christopherson<sup>2</sup> has applied the method of finite differences to the solution of the torsion equation, Eq. (136c), and its extension into the plastic range.

### PROBLEMS

**197.** A shaft is to be made of a steel having a proportional limit in torsion of 60,000 p.s.i. If the shaft is to transmit a torque of 8,000 ft.-lb. with a factor of safety of 2.00 with respect to failure by slip, determine the weight of the shaft per foot length if it is (a) round, (b) square.

**198.** Solve Prob. 197 if the shaft is made of duralumin.

**199.** A 2,200-hp. airplane engine develops a thrust of 8,800 lb. at 2,500 r.p.m. Select a suitable material for the propeller shaft and determine the size required if the minimum factor of safety with respect to failure by slip is to be 4.

**200.** What assumption is made in Eq. (119) regarding direction of the shearing stress? Is the assumption justifiable?

**201.** Determine the maximum allowable torque and angles of twist of a 2-in. square structural-steel shaft and a 2- by 4-in. rectangular shaft of the same material if failure by slip is to be prevented.

**202.** Compare the maximum torque that a 1½- by 3-in. solid elliptical shaft will transmit with the maximum torque which a 1½-in. diameter circular shaft will transmit if the two are of the same material and if failure by slip is to be prevented.

**203.** A hollow elliptical shaft has external major and minor axes of 4 and 2 in. respectively and internal major and minor axes of 2 and 1 in. If the maximum torsional stress is not to exceed 20,000 p.s.i., determine the maximum torque that may be applied to the shaft.

**204.** Develop the stress function for an elliptical shaft and evaluate the maximum stress and the angle of twist in terms of the dimensions,  $G$  and the torque.

**205.** With the aid of the stress function developed in Prob. 204 describe the warping that occurs when an elliptical shaft is twisted.

**206.** Develop the stress function for an equilaterally triangular shaft as

$$\phi = \frac{-G\theta}{L} \left[ \frac{1}{2}(x^2 + y^2) - \frac{1}{2a}(x^3 - 3xy^2) - \frac{2a^2}{27} \right]$$

in which  $a$  is the altitude of the triangle.

The origin is at the centroid, and the  $x$  axis passes through one vertex.

<sup>1</sup> SADOWSKY, M. A., An Extension of the Sand-heap Analogy in Plastic Torsion Applicable to Cross Sections Having One or More Holes, *Trans. Am. Soc. Mech. Engrs.*, Vol. 63, p. A-166, 1941.

<sup>2</sup> CHRISTOPHERSON, D. G., A Theoretical Investigation of Plastic Torsion in an I-Beam, *Trans. Am. Soc. Mech. Engrs.*, Vol. 62, p. A-1, 1940.

**207.** With the aid of the stress function for a triangular shaft given in Prob. 206 plot a curve showing the variation in shearing stress along one edge of the cross section.

**208.** With the aid of the stress function in Prob. 206 determine the location, magnitude, and direction of the maximum shearing stress developed in a steel equilaterally triangular shaft for which  $\alpha = 2$  in. when it is twisted through an angle of 0.1 radian in a length of 10 in.

**209.** Determine the stress function for a rectangular shaft.

**210.** From Eq. (140b) what can be said regarding curvatures of the membrane? Is this conclusion valid?

**211.** Construct a set of lines of shearing stress for a torsional member having a circular cross section and a set for a member having a cross section in the form of an equilateral triangle.

**212.** The circular calibration membrane obtained in conjunction with the surface mapped in Fig. 70 had a diameter of 4 in. and center elevation of 0.280 in. The total volume displaced under the two films was 50 cc. Determine the maximum stress developed in the T section by a torque of 1,000 in.-lb. The total depth of the T section was 4 in.

**213.** Compare the torque that ten 1-in.-diameter circular rods will transmit (acting independently) with the torque that can be transmitted through a member having a rectangular cross section 1 by 10 in. The maximum stress is to be the same in both cases.

**214.** Determine the equivalent polar moment of inertia for each of the cross sections given in Fig. P-214.

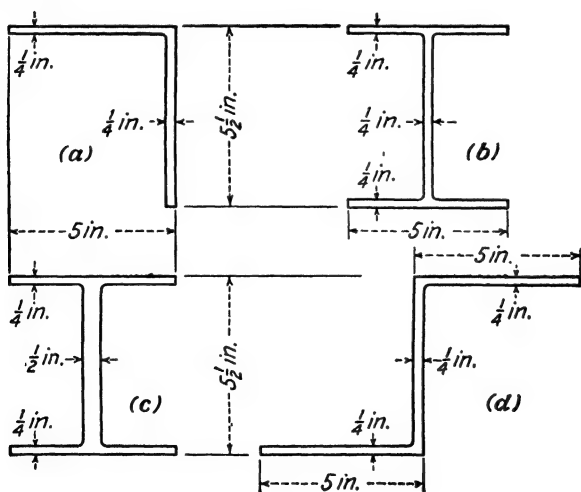


FIG. P-214.

**215.** What is the maximum torque that a standard 2- by 2- by  $\frac{1}{4}$ -in. structural-steel angle will transmit without inelastic action? Neglect stress concentration.

**216.** Determine the approximate torque to which the bulb angle in Fig. P-216 may be subjected without inelastic action. The material is 24S-T aluminum alloy.

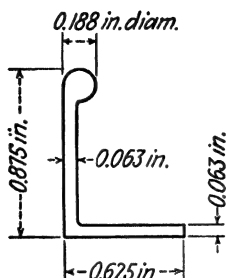


FIG. P-216.

**217.** Determine the approximate maximum allowable torque to which each of the sections in Fig. P-214 may be subjected if the maximum allowable shearing stress is 15,000 p.s.i. Determine the angle of twist in a 4-ft. length.

- Assume that the radius of all fillets is ample to prevent stress concentration.
- Assume that the radius of the fillet in (b) is  $\frac{1}{4}$  in.

The material is duralumin.

**218.** A rectangular tube with a wall thickness of 0.060 in. and outside dimensions of 4.00 in. by 2.00 in. is made of structural steel.

- Determine the maximum torque to which it may be subjected if inelastic action is to be avoided.
- Determine the maximum torque if the tube is split longitudinally.
- Determine the angle of twist in a 6-ft. length for (a) and (b).

**219.** The section shown in Fig. P-219 is subjected to a torque of 100,000 in.-lb. For what thickness of center web ( $CD$ ) will the stress in  $CD$  equal zero?

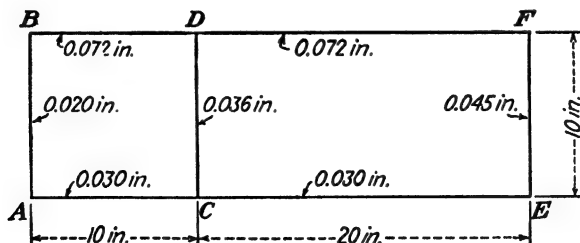


FIG. P-219.

**220.** The cross section of the wing shown in Fig. P-220 is to carry a torque of 250,000 in.-lb. Determine the maximum stress if



- a. The nose section alone is effective.
- b. The nose section is not effective due to cutouts.
- c. Both sections are effective.

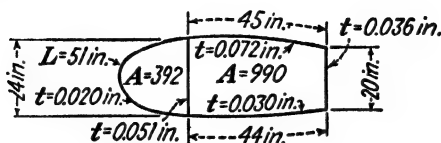


FIG. P-220.

**221.** A torsional member with a square cross section 10 in. on each side has a wall thickness of 0.120 in. If the maximum shearing stress, stress concentration neglected, is not to exceed 10,000 p.s.i., how much will the box be strengthened torsionally by subdividing it into four 5-in. square sections by inserting 0.040-in. thick webs?

**222.** A 2-in.-diameter stainless-steel shaft is turned down to a 1-in. diameter for a portion of the length. If a fillet with a 0.10-in. radius is used, to what maximum torque may the shaft be subjected?

**223.** A structural-steel shaft is designed for a torque of 10,000 ft.-lb. with a factor of safety of 2.00 with respect to failure by slip. Approximately how much permanent twist will result if the torque is accidentally increased to 26,000 ft.-lb.?

**224.** Construct the probable torque-twist diagram for a 2-in.-diameter structural-steel rod if the stress-strain diagram has the idealized shape indicated in Fig. 81a with a yield point of 24,000 p.s.i.

**225.** Develop an expression for the maximum possible torsional resistance of a bar having a rectangular cross section, assuming that the idealized stress-strain diagram indicated in Fig. 81a is valid.

**226.** Compare the maximum possible torsional resistance of a bar having a square cross section with the resistance of the rod which may be inscribed in the square.

**227.** Develop the torque-twist relationship for a circular rod made of a material having a parabolic stress-strain diagram.

## CHAPTER VIII

### FLEXURE

#### STRESSES

**78. General Considerations.**—As has been indicated previously, the force system acting at a given cross section of a member may be resolved into (1) a force normal to the section, and acting through the centroid, producing axial loading (discussed in Chap. 5); (2) a force lying in the plane of the cross section, producing cross shear (discussed in Chap. 9); (3) a couple lying in the plane of the cross section, producing torsion (discussed in Chap. 7); and (4) a couple lying in a plane normal to the plane of the cross section, producing flexure or bending (discussed in this chapter).

A state of pure flexure is said to exist if the resultant of the force system acting at each transverse cross section normal to the axis of the member is a couple lying in a plane normal to the transverse plane. The corresponding stresses developed in the member are flexural stresses.

The conventional formula for flexural stresses  $S = Mc/I$  is based on several assumptions similar to those involved in the formula for torsional stresses in circular sections.

#### 1. *Statics*

- a. The resultant of the external forces is a couple that lies in, or is perpendicular to, a plane of symmetry of the cross section.
- b. The beam is in equilibrium.

#### 2. *Geometry*

- c. The longitudinal axis of the beam is straight.
- d. The beam has a constant cross section throughout its length.
- e. A plane section that is normal to the longitudinal axis of the beam before the beam is bent remains plane after the beam is bent.
- f. The beam bends without twisting.

### 3. *Properties of the Material*

- g. The material of which the beam is composed is homogeneous and isotropic.
- h. The stresses do not exceed the proportional limit of the material.

The idealized loading conditions required by the flexure formula are essentially realized in the center portion of a beam supported at the ends and carrying two equal and symmetrically placed loads. Usually, a given section in a beam is subjected to cross shear as well as bending. That condition does not affect the values of the flexural stresses as computed by the flexure formula, but it will result in principal stresses greater than those computed by the flexure formula for most points in the cross section. In general, the maximum normal stress will be unaffected by the cross shear unless the beam is abnormally short.

However, if the bending moment is accompanied by either a normal force or a torsional moment, the maximum normal stress may be much larger than that given by the flexure formula. The derivation of the elementary flexure formula will be reviewed, following which, special cases in which assumptions (a), (c), (d), or (h) are not valid will be considered.

### 79. Derivation of Elementary Formula for Flexural Stresses.

1. *Statics*.—The usual derivation of  $Mc/I$  for the idealized case starts with assumptions (a) and (b).

If the beam is in equilibrium, the moment of the external forces must equal the resultant moment developed by the flexural stresses. The moment equation of equilibrium written with respect to the neutral axis gives

$$M = \int_0^A S_y y \, da \quad (168)$$

Equation (168) cannot be integrated directly since  $S_y$  is not constant. Its relationship to  $y$  must be determined from geometry and the material.

2. *Geometry*.—From assumption (e), which is based on observation, it follows that the total strain at any point in the section is proportional to the distance  $y$  of that point from the *neutral axis* or axis in the cross section on which the normal stresses are zero. If the axis of the beam is straight (assumption c), the unit strain is proportional to  $y$ , and

$$\frac{\epsilon_y}{\epsilon_o} = \frac{y}{c} \quad (169)$$

in which  $\epsilon_y$  is the unit strain at the point a distance  $y$  from the neutral axis

$\epsilon_o$  is the unit strain at a reference point located at a distance  $c$  from the neutral axis.

3. *Properties of the Material.*—If assumptions (g) and (h) are valid, stress is proportional to strain throughout the cross section and Eq. (169) may be written in terms of stress as

$$\frac{S_y}{S_o} = \frac{y}{c} \quad (169a)$$

in which  $S_y$  is the stress at any point

$S_o$  is the stress at the reference point at a distance  $c$  from the neutral axis.

4. *Combination.*—The variable  $S_y$  in Eq. (168) may be replaced by its equivalent, from Eq. (169a), giving

$$M = \frac{S_o}{c} \int_0^A y^2 da \quad (168a)$$

However, the integral of  $y^2 da$  is defined as the moment of inertia (with respect to the neutral axis); hence

$$M = \frac{IS_o}{c} = \frac{IS_y}{y} \quad (170)$$

The location of the neutral axis may be established by writing the force equation of equilibrium in the direction of the longitudinal axis of the beam. If there is no resultant axial load on the beam, assumption (a),

$$\int_0^A S_y da = 0 \quad (171)$$

Again  $S_y$  may be replaced by  $S_o y/c$ , from Eq. (169a), giving

$$\frac{S_o}{c} \int_0^A y da = 0 \quad (171a)$$

For this to be true the integral of  $y da$  must be equal to zero; hence, the neutral axis must be a centroidal axis, i.e., it must pass through the centroid of the cross section.

If the resultant of the external longitudinal forces is not zero

but is equal to  $F_n$ , Eq. (171a) becomes

$$\frac{S_o}{c} \int_0^A y \, da = F_n \quad (171b)$$

However, by definition of the centroid

$$\int_0^A y \, da = \bar{y}A \quad (171c)$$

in which  $\bar{y}$  is the distance from the axis of reference (the neutral axis) to the centroid.

Then

$$\frac{S_o}{c} \bar{y}A = F_n \quad (171d)$$

and

$$\bar{y} = \frac{F}{A} \frac{c}{S_o} \quad (171e)$$

$$= \frac{S_o c}{S_o} \quad (171f)$$

in which  $S_a$  is the *average* ( $F_n/A$ ) stress on the cross section.

**80. Direction of the Neutral Axis.**—In Eq. (168) it was assumed that the external moment  $M$  lies in a plane perpendicular to the neutral axis. If the plane of the external moment is not perpendicular to the neutral axis the term  $M$  in Eq. (168) must represent only that component of the moment which does lie in a plane perpendicular to the neutral axis or the cosine of the angle between the plane of the moment and a plane perpendicular to the neutral axis must be included. It is therefore necessary to determine not only the *location* of the neutral axis but also its *direction* with reference to the plane of the external moment. As is shown in the following article, the neutral axis is perpendicular to the plane of the moment if the latter contains, or is perpendicular to, an axis of symmetry of the cross section.

**81. General Solution.**—A more general solution for the stresses in a beam not subject to assumption (a) is outlined by Hardy Cross.<sup>1</sup> The development starts with the geometrical condition that a plane transverse section before bending remains plane after bending. The longitudinal displacement  $w$  of any point in the cross section can be expressed as the equation of a

<sup>1</sup> CROSS, HARDY, The Column Analogy, *Univ. Illinois Eng. Expt. Sta. Bull.* 215, 1930.

plane

$$w = a + bx + cy \quad (172)$$

in which  $a$ ,  $b$ , and  $c$  are constants

$x$  and  $y$  are coordinates of the point with reference to arbitrary  $x$  and  $y$  axes.

The equation for the total strain developed between two transverse planes will have the same form. In addition, if the beam is straight, so that the two transverse planes are parallel, and if the stresses do not exceed the proportional limit of the material, the stress at any point in the cross section may be expressed as

$$S = a' + b'x + c'y \quad (172a)$$

The three constants  $a'$ ,  $b'$ , and  $c'$  may be evaluated by writing three equations of equilibrium. From the force equation of equilibrium the external normal force  $F_n$  must equal the resultant normal force developed on the cross section. Hence

$$F_n = \int_0^A S \, da \quad (173)$$

$$= a' \int_0^A da + b' \int_0^A x \, da + c' \int_0^A y \, da \quad (173a)$$

if the  $x$  and  $y$  axes are taken as centroidal axes, Eq. (173a) reduces to

$$F_n = a'A$$

or

$$a' = \frac{F_n}{A} \quad (173b)$$

The moment equation of equilibrium, written with respect to the centroidal  $x$  axis, gives

$$M_x = \int_0^A S y \, da \quad (174)$$

$$= a' \int_0^A y \, da + b' \int_0^A xy \, da + c' \int_0^A y^2 \, da \quad (174a)$$

$$= b'P_{xy} + c'I_x \quad (174b)$$

in which  $M_x$  is the component of the external moment with respect to the  $x$  axis

$P_{xy}$  is the product of inertia with respect to the  $x$  and  $y$  axes

$I_x$  is the moment of inertia with respect to the  $x$  axis.

Similarly, the moment equation of equilibrium written with respect to the centroidal  $y$  axis gives

$$M_y = b'I_y + c'P_{xy} \quad (175)$$

The constants  $b'$  and  $c'$  may be obtained by solving Eqs. (174b) and (175) simultaneously.

$$b' = \frac{M_y I_x - M_x P_{xy}}{I_x I_y - P_{xy}^2} \quad (176)$$

$$c' = \frac{M_x I_y - M_y P_{xy}}{I_x I_y - P_{xy}^2} \quad (177)$$

The stress at any point in the cross section may be found by substituting the values of  $a'$ ,  $b'$ , and  $c'$  from Eqs. (173b), (176), and (177) back into Eq. (172a). The complexity of the resulting expression may be reduced by selecting the  $x$  and  $y$  axes so that in addition to being centroidal axes they are principal axes.<sup>1</sup> Then the product of inertia is equal to zero, and the constants  $b'$  and  $c'$  are

$$b' = \frac{M_y}{\bar{I}_y} \quad (176a)$$

$$c' = \frac{M_x}{\bar{I}_x} \quad (177a)$$

These values, together with the one for  $a'$ , given in Eq. (173b), may be substituted back into Eq. (172a) giving

$$S = \frac{F_n}{A} + \frac{M_y u}{\bar{I}_y} + \frac{M_x v}{\bar{I}_x} \quad (172b)$$

in which the subscripts  $u$  and  $v$  denote the moments of inertia or components of moments with respect to the principal axes ( $u$  and  $v$  axes) passing through the centroid of the cross section, and  $u$  and  $v$  denote the coordinates of the point with reference to the  $u$  and  $v$  axes.

<sup>1</sup> A principal axis of inertia of an area (for any point in the plane of the area) is an axis with respect to which the moment of inertia of the area is a maximum or a minimum. There is a pair of principal axes for every point in the plane of the area. The axis with respect to which the moment of inertia is a minimum is always at right angles to the axis of maximum moment of inertia. An axis of symmetry is always a principal axis. Principal axes will be denoted as  $u$  and  $v$  axes, and the moments of inertia with respect to them as  $\bar{I}_u$  and  $\bar{I}_v$ , respectively.

If the beam is subjected to pure bending  $F_n = 0$ , and if the plane of the external moment is perpendicular to one of the principal axes of the cross section (say the  $u$  axis), Eq. (172b) reduces to

$$S = \frac{M_u v}{\bar{I}_u} \quad (172c)$$

which agrees with Eq. (170). Hence, the elementary formula  $S = Mc/I$  is subject to the limitations indicated.

It will be noted that Eq. (172b) may also be developed by the principle of superposition. That is, if all stresses are below the proportional limit, the resultant normal stress at a point in a beam is equal to the sum of the normal stress and the flexural stresses produced by the bending about each of the principal centroidal axes.

Since the neutral axis is the line in the cross section on which the normal stress is zero, its position may be deduced from Eq. (172b). The equation of the neutral axis is

$$\frac{F_n}{A} + \frac{M_v u}{\bar{I}_v} + \frac{M_u v}{\bar{I}_u} = 0 \quad (178)$$

If the beam is subjected to pure flexure  $F_n = 0$ , and

$$\frac{M_v u}{\bar{I}_v} = -\frac{M_u v}{\bar{I}_u} \quad (178a)$$

The angle between the plane in which the resultant moment lies and one of the principal axes (say the  $v$  axis) may be designated as  $\beta$ , as shown in Fig. 82. The angle between the  $u$  axis and the neutral axis is designated as  $\alpha$ . Then from Eq. (178a)

$$\frac{\bar{I}_u M_v}{\bar{I}_v M_u} = -\frac{v}{u} \quad (178b)$$

$$\frac{\bar{I}_u}{\bar{I}_v} \tan \beta = -\tan \alpha \quad (178c)$$

$$\tan \alpha = \frac{-\bar{I}_u \tan \beta}{\bar{I}_v} \quad (178d)$$

The minus sign indicates that if the plane of the load lies in the first and third quadrants with respect to the  $u$  axis, the neutral axis lies in the second and fourth quadrants (and vice versa). Two conclusions may be drawn from Eq. (178d):



1. That the neutral axis is not perpendicular to the plane of the loads unless the plane of the loads is perpendicular to one of the principal axes (through the centroid). That is,  $\alpha$  will not equal zero unless  $\beta$  equals zero. The deviation of the neutral

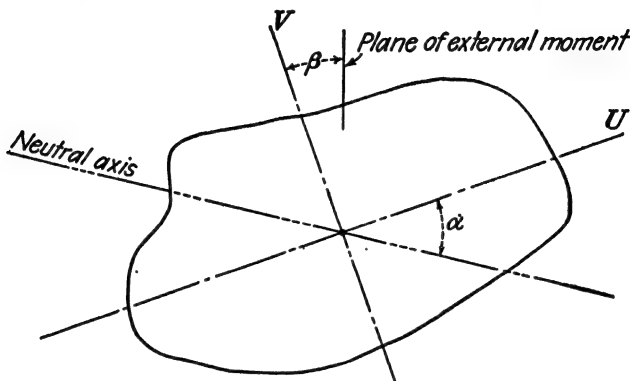


FIG. 82.—Unsymmetrical bending.

axis may be considerable. For example, for a 2- by 12-in. rectangular cross section,  $\bar{I}_u = 288 \text{ in.}^4$  and  $\bar{I}_v = 8 \text{ in.}^4$ . Then if the angle  $\beta$  is only one degree

$$\begin{aligned}\tan \alpha &= \frac{-288}{8} (0.01746) \\ &= -0.62856 \\ \alpha &= -32 \text{ deg.}\end{aligned}$$

2. That the ordinary flexure formula is not valid unless the plane of the loads is perpendicular to one of the principal axes (through the centroid). For the flexure formula  $M = IS/c$  to hold, the angles  $\alpha$  and  $\beta$  must be equal, Eq. (174a).

For this to be true, both  $\alpha$  and  $\beta$  must equal zero unless  $\bar{I}_u = \bar{I}_v$ , which is a special case. For the condition of pure bending Eq. (172b) becomes

$$S = \frac{M_v u}{\bar{I}_v} + \frac{M_u v}{\bar{I}_u} \quad (172d)$$

The quantity  $\bar{I}_v$  may be eliminated by substituting its value from Eq. (178d) giving

$$S = \frac{-M_u u \tan \alpha}{\bar{I}_u} + \frac{M_u v}{\bar{I}_u} \quad (172e)$$

$$= \frac{M_u}{\bar{I}_u} (-u \tan \alpha + v) \quad (172f)$$

$$= \frac{M_u c}{\bar{I}_u \cos \alpha} \quad (172g)$$

in which  $c$  is the distance from the neutral axis to the point under consideration.

**82. Evaluation of Stresses.**—Several procedures are available for the evaluation of stresses in a beam subjected to *unsymmetrical bending*, i.e., bending in which the plane of the moment is not perpendicular to a principal axis. If the principal centroidal axes cannot be determined readily, any convenient pair of centroidal axes may be used, the constants  $b'$  and  $c'$  determined from Eqs. (176) and (177) and the stresses evaluated from Eq. (172a). However, if the principal centroidal axes are evident by inspection, as they frequently are, or can be determined, the evaluation of stresses is somewhat simplified. Two methods are available.

*Method 1.*—The angle that the neutral axis makes with one of the principal axes may be found from Eq. (178d). With the angle  $\alpha$  known the distance  $c$  of the point from the neutral axis may be found and the stresses evaluated from Eq. (172g).

*Method 2.*—The moment may be resolved into two components  $M_u$  and  $M_v$ , each lying in a plane perpendicular to a principal axis through the centroid. The stress due to each component of the moment may be computed separately by the ordinary flexure formula  $S = Mc/I$ , and the two stresses added algebraically.

*Illustrative Problem.*—A 2- by 2- by  $\frac{1}{8}$ -in. angle with legs horizontal and vertical is used as a cantilever beam 4 ft. long. Determine the maximum flexural stress due to a vertical load of 80 lb. at the free end.

*Method 1.*—The cross section of the beam is shown in Fig. 83. One principal axis through the centroid is the axis of symmetry and is taken as the  $u$  axis. The other principal centroidal axis (the  $v$  axis) is perpendicular to the  $u$  axis. Therefore the angle  $\beta$  is equal to  $-45^\circ$ . The values of  $I_x$ ,  $I_y$ ,  $I_v$  may be obtained from a handbook as  $I_x = I_y = 0.19 \text{ in.}^4$ , and  $I_v = 0.077 \text{ in.}^4$ . Since the polar moment of inertia with respect to the longitudinal centroidal axis is constant

$$I_u + I_v = I_x + I_y \quad (a)$$

$$I_u + 0.077 = 0.19 + 0.19$$

$$I_u = 0.30 \text{ in.}^4 \quad (b)$$

from Eq. (178d)

$$\tan \alpha = \frac{-0.30(-1.000)}{0.077} = +3.90$$

and

$$\alpha = +75^{\circ}37' \quad (c)$$

The neutral axis will therefore be in the position indicated in Fig. 83. The load is in the first and third quadrants, and the neutral axis passes through the second and fourth quadrants. The maximum stress on the cross section will occur at the corner *B* because that point is at the greatest

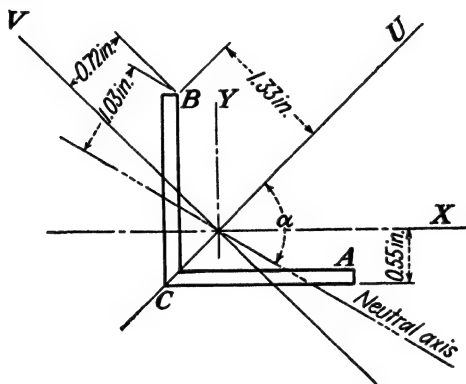


FIG. 83.—Evaluation of stresses in an angle.

distance from the neutral axis. The *c* distance from the neutral axis to *B* may be determined from the geometry of the figure as 1.03 in. Equation (172g) may be solved for the stress, giving

$$S_B = \frac{M_u c}{I_u \cos \alpha} \quad (d)$$

At the fixed end of the beam  $M = 80(48) = 3,840$  in.-lb., and

$$\begin{aligned} S_B &= \frac{3,840(0.707)(1.03)}{0.30(0.24841)} \\ &= 37,400 \text{ p.s.i.} \end{aligned} \quad (e)$$

provided that the proportional limit of the material exceeds 37,400 p.s.i. The stress will be tension for the beam in the position indicated.

*Method 2.*—The moment may be resolved into two components, each of which lies in a plane perpendicular to one of the principal centroidal axes. Each component is  $3,840(0.707) = 2,720$  in.-lb. The stress at point *B* is

$$S_B = \frac{M_u v}{I_u} + \frac{M_v u}{I_v} \quad (f)$$

$$\begin{aligned} &= \frac{2,720(1.33)}{0.30} + \frac{2,720(0.72)}{0.077} \\ &= 12,000 + 25,400 \\ &= 37,400 \text{ p.s.i.} \end{aligned} \quad (g)$$

as before.

**83. Direction of Deflection.**—The deflection of a beam that is subjected to a moment which does not lie in a plane perpendicular to a principal axis may be evaluated by resolving the load into components in the directions of the principal axes, determining the deflection due to each of the components and adding the components of deflection vectorially. If the beam has the same end condition with respect to each of the principal axes, the resultant deflection will be perpendicular to the neutral axis and *not* in the direction of the load. For example, if a cantilever beam carries at its free end a load that makes an angle  $\beta$  with the  $v$  axis, the components of deflection are

$$y_v = \frac{P \cos \beta L^3}{3E\bar{I}_u} \quad (179a)$$

$$y_u = \frac{P \sin \beta L^3}{3E\bar{I}_v} \quad (179b)$$

$$y = \frac{PL^3}{3E} \left( \frac{\cos \beta}{\bar{I}_u} + \frac{\sin \beta}{\bar{I}_v} \right) \quad (179c)$$

The direction of the deflection with respect to the  $u$  axis is

$$\tan \phi = \frac{y_v \cos \beta \bar{I}_v}{y_u \bar{I}_u \sin \beta} \quad (180a)$$

$$= \frac{\bar{I}_v}{\bar{I}_u} \frac{1}{\tan \beta} \quad (180b)$$

A comparison of Eq. (180b) with Eq. (178d) shows that

$$\tan \phi = \frac{-1}{\tan \alpha} \quad (180c)$$

Therefore,  $\phi = \alpha - 90$  deg., or the direction of the resultant deflection is perpendicular to the neutral axis.

*Illustrative Problem.*—Determine the deflection of the free end of the beam in the problem of Art. 82 if the beam is steel.

*Solution.*—The deflection in the  $v$  direction, perpendicular to the  $u$  axis, is

$$y_v = \frac{P_v L^3}{3E\bar{I}_u} \quad (a)$$

$$= \frac{80(0.707)(48)^3}{3(30)10^6(0.30)} \quad (b)$$

$$= 0.23 \text{ in.}$$

Similarly, the component of the deflection in the  $u$  direction is

$$y_u = \frac{P_u L^3}{3EI_u} \quad (c)$$

$$= \frac{80(0.707)(48)^3}{3(30)10^6(0.077)} \quad (d)$$

$$= 0.90 \text{ in.}$$

The resultant deflection is

$$y_r = y_u + y_v \quad (e)$$

$$= \sqrt{(0.90)^2 + (0.23)^2} \quad (f)$$

$$= 0.93 \text{ in.}$$

The direction of the deflection with reference to the  $u$  axis is given by

$$\tan \phi = \frac{y_v}{y_u}$$

$$= \frac{0.23}{0.90} \quad (h)$$

$$= 0.256$$

Hence

$$\phi = 14^\circ 23'$$

which is at right angles to the neutral axis. The beam will deflect as shown in Fig. 84. It will be noted that the beam has a

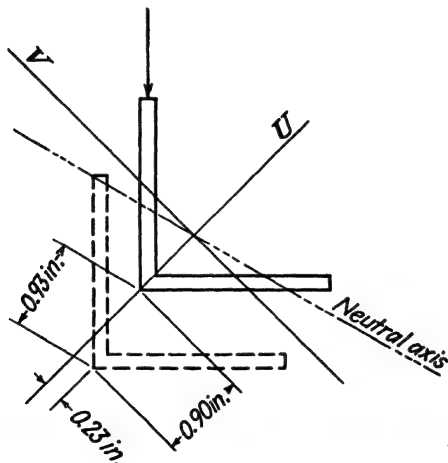


FIG. 84.—Deflection of angle used as cantilever beam with vertical load.

horizontal component of deflection as well as a vertical component even though the load is vertical.

**84. Flexural Stresses beyond the Proportional Limit.**—The flexure formula for symmetrical bending, Eq. (170), was derived on the basis of the assumption that stress and strain are pro-

portional. If the proportional limit of the material is exceeded, the formula is no longer valid. However, the relationship between the stress and the moment in a beam may be determined if the flexural stress-strain characteristics of the material in the beam may be assumed to be similar to the tensile or compressive stress-strain characteristics. Assumptions (a) to (g) as given

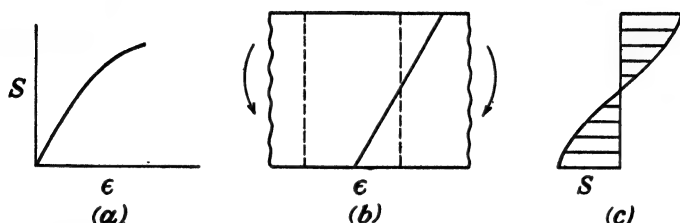


FIG. 85.—Distribution of strain and stress in a beam above the proportional limit.

in Art. 78 may still be considered valid. Assumption (e) may be verified experimentally. Instead of assumption (h), the relationship between normal stress and normal strain may be represented by the general equation

$$S = f(\epsilon) \quad (181)$$

Figure 85a illustrates a possible stress-strain relationship. Since experimental evidence shows that a plane section before bending remains plane after bending, even after plastic action is taking place, the unit strain on a cross section of a beam is proportional to the distance from the neutral axis, as shown in Fig. 85b. Hence, Eq. (169) is valid in the plastic, as well as the elastic, range of stress. The stress distribution, obtained by combining Figs. 85b and 85a, will be as shown in Fig. 85c. Since assumptions (a) and (b) are still valid, the resisting moment developed by the cross section is still given by Eq. (168)

$$M = \int_0^A S_y y \, da \quad (168)$$

$$= \int_0^A f(\epsilon_y) y \, da \quad (182)$$

If the value for  $y$  from Eq. (169) is substituted in Eq. (182), there results

$$M = \frac{c}{\epsilon_o} \int_0^A f(\epsilon_y) \epsilon_y \, da \quad (182a)$$

$$= \frac{c}{\epsilon_o} \int_{x_1}^{x_2} \int_{y_1}^{y_2} f(\epsilon_y) \epsilon_y \, dx \, dy \quad (182b)$$

The term  $dy$  may be replaced in Eq. (182b) by its equivalent obtained by differentiating Eq. (169).

$$dy = \frac{c}{\epsilon_o} d\epsilon_y \quad (169c)$$

Then

$$M = \frac{c^2}{\epsilon_o^2} \int_{x_1}^{x_2} \int_{\epsilon_1}^{\epsilon_2} f(\epsilon_y) \epsilon_y dx d\epsilon_y \quad (182c)$$

If the beam is rectangular in cross section with a width  $b$  and depth  $2c$

$$M = \frac{2bc^2}{\epsilon_o^2} \int_0^{\epsilon_o} f(\epsilon_y) \epsilon_y d\epsilon_y \quad (182d)$$

It is evident that  $\int_0^{\epsilon_o} f(\epsilon_y) \epsilon_y d\epsilon_y$  is the first moment with respect to the strain axis of the area under the portion of the stress-strain diagram between the origin and  $\epsilon_o$ . From a given stress-strain diagram either an  $M$ - $\epsilon$  diagram or an  $M$ - $S$  diagram may be constructed.

Equation (182d) may also be written as

$$M = \frac{2bc^2 A \bar{\epsilon}}{\epsilon_o^2} \quad (182e)$$

in which  $A$  is the area under the stress-strain diagram to the maximum stress (or strain) at the outside fiber  
 $\bar{\epsilon}$  is the strain at the centroid of the area  $A$ .

If the maximum stress does not exceed the proportional limit the area  $A$  will be triangular and

$$M = \frac{2bc^2 \frac{1}{2} S_o \epsilon_o \frac{2}{3} \epsilon_o}{\epsilon_o^2} \quad (182f)$$

$$= \frac{bd^2 S}{6} \quad (182g)$$

which agrees with the result obtained by the ordinary flexure formula, Eq. (170).

The location of the neutral axis may be determined from Eq. (171).

$$\int_0^A S_y da = 0 \quad (171)$$

The stress  $S_y$  may be expressed in terms of  $\epsilon$  from Eq. (181),

and  $da$  may be expressed in terms of  $dx$  and  $\epsilon_y$ . Then Eq. (171) becomes

$$\frac{c}{\epsilon_o} \int_{x_1}^{x_2} \int_{\epsilon_1}^{\epsilon_2} f(\epsilon_y) dx d\epsilon_y = 0 \quad (183)$$

if the beam is rectangular, Eq. (183) reduces to

$$\int_{\epsilon_1}^{\epsilon_2} f(\epsilon_y) d\epsilon_y = 0 \quad (183a)$$

and if the stress-strain characteristics are the same in tension and compression, the neutral axis will be at the centroid.

**85. Stress Concentration in Beams.**—In the development of the preceding formulas for flexural stresses it was assumed on

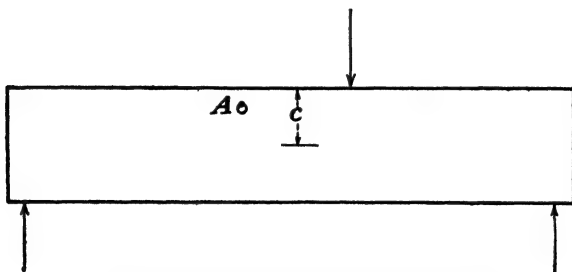


FIG. 86.—Beam containing a stress raiser.

the basis of experimental evidence that a plane section before bending remains plane after bending. This assumption is not valid at a change in cross section; hence, the flexure formula is limited to beams of constant cross section. Any deviation from the conditions upon which the flexure formula is based usually results in a maximum stress greater than that given by the flexure formula; *i.e.*, stress concentration generally occurs.

The stress-concentration factor for a region of high flexural stress may be defined in several ways, but it is most convenient to define it as the ratio of the maximum stress developed by the stress raiser to the maximum stress at that cross section computed by the flexure formula, assuming that the stress raiser is not present. For example, a comparatively high stress will exist at point *A* near the hole in the beam of Fig. 86 when the beam is bent. The stress-concentration factor is

$$K_t = \frac{S_A}{Mc/I} \quad (184)$$

in which  $I$  is computed on the basis of the gross cross section.



In general, experimental methods have been used for the evaluation of stress-concentration factors for beams because of the difficulties involved in the mathematical analysis of all but the simplest cases. The experimental methods described in Art. 46 may be applied to beams as well as to axially loaded members.

The photoelastic technique is the most sensitive and generally gives values of the stress-concentration factor practically equal to those obtained by mathematical analysis. Otherwise, the

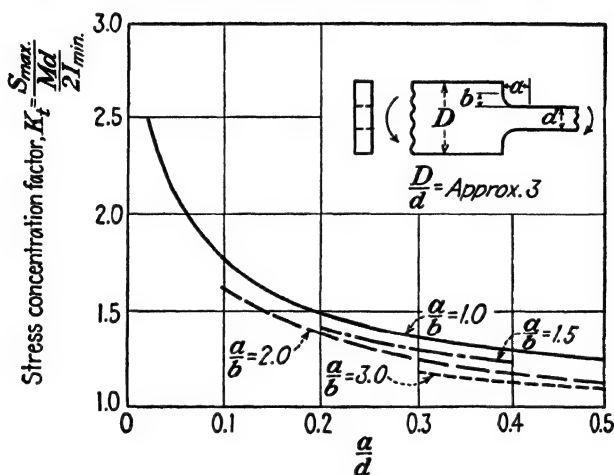


FIG. 87.—Stress-concentration factors for elliptical fillets in beams.

experimental methods tend to give values of the stress-concentration factor less than the value that is obtained by mathematical analysis because they are not affected by a slight initial yield of the material at the point of maximum stress. Thus, the values of stress-concentration factor obtained experimentally depend upon the characteristics of the material used in the test and the precision with which failure was noted. This is in accordance with the fact previously noted that the importance of the stress-concentration factor is dependent upon the characteristics of the material in the member.

Figure 87 gives values of the stress-concentration factor for a few specific cases of elliptical fillets<sup>1</sup> in beams having constant thickness but an abrupt change in depth. The curve for a

<sup>1</sup> BERKEY, DONALD C., Reducing Stress Concentration with Elliptical Fillets, *Proc. Soc. Exptl. Stress Analysis*, Vol. 1, No. 2, p. 56, 1943.

circular fillet is included for comparison. Neuber<sup>1</sup> made an analytical investigation of the effect of hyperbolic notches, grooves, and holes upon stress concentration. Figures 88 and 89 give his values of the stress-concentration factors (based on the net, or minimum, cross section) for wide members containing hyperbolic notches or grooves. In his analysis Neuber assumed the members to be of infinite width, so the stress-concentration factors must be based on the net, rather than the gross,

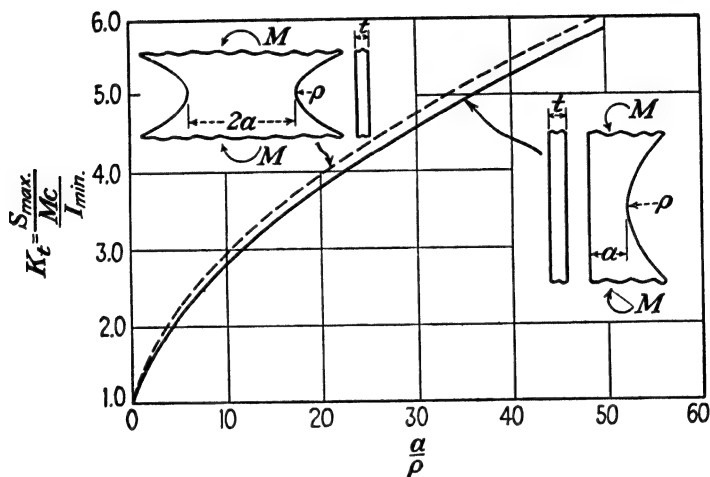


FIG. 88.—Stress-concentration factors for hyperbolic notches in flat beams.

cross section. In Fig. 90, also from Neuber's data, the stress-concentration factors for flexural stresses in a plate containing a hole are based on the stress at the edge of the hole. Values of the stress-concentration factor in Fig. 91 are from data by Frocht.<sup>2</sup>

For some cases of stress concentration the point of maximum stress is subjected to a condition of biaxial stress. For example, in a cylindrical beam containing a circumferential groove, the longitudinal stress at the base of the groove is accompanied by a circumferential stress of like sign. The magnitude of the circumferential stress is dependent upon Poisson's ratio and the magnitude of the longitudinal stress. Neuber's data (Fig.

<sup>1</sup> NEUBER, H., "Kerbspannungslehre," Berlin, 1937.

<sup>2</sup> FROCHT, M. M., Factors of Stress Concentration Photoelastically Determined, *Trans. Am. Soc. Mech. Engrs.*, Vol. 57, p. A-67, 1935.

89) show that for a range of dimensions and a Poisson's ratio of 0.30, the circumferential stress is approximately one-third of the longitudinal stress. The fact that the stress condition at the critical point is biaxial requires the use of an appropriate theory

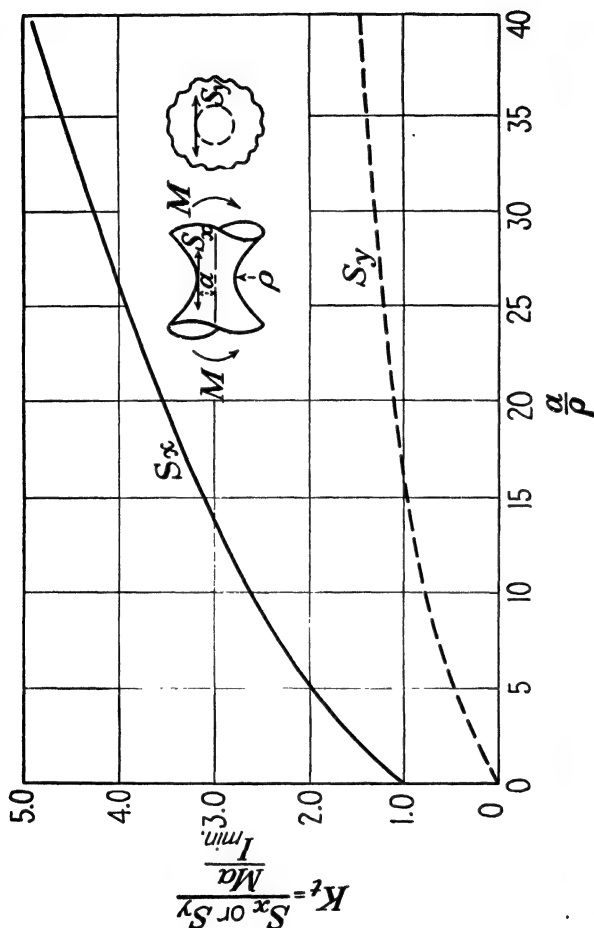


Fig. 89.—Stress-concentration factors for a circumferential hyperbolic notch in a beam.

of failure in making strength calculations. The tendency of the circumferential stress is to strengthen the material or to reduce the effect of the stress concentration.

The ratio of the static strength of the member without the stress raiser to the static strength of the member containing the notch, groove, or hole may be called the *strength-reduction*

factor and will be designated as  $K_s$ . If the stress situation at the critical point is axial,  $K_s$  equals  $K_t$ ; if a biaxial stress situation with stresses of like sign exists,  $K_s$  is less than  $K_t$ ; but if the biaxial stresses are of unlike sign,  $K_s$  is greater than  $K_t$ .

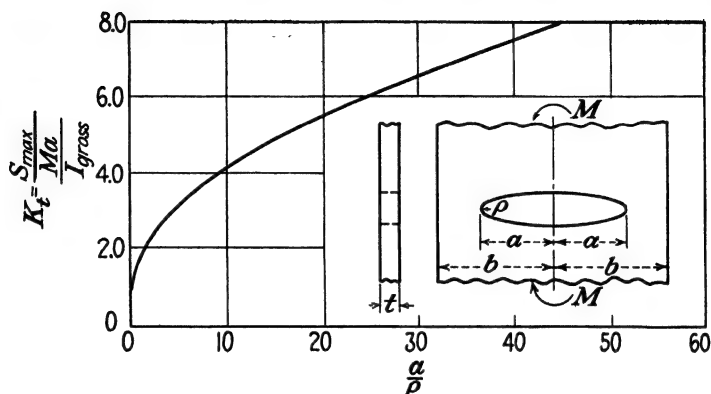


FIG. 90.—Stress-concentration factors for a hole in a beam.

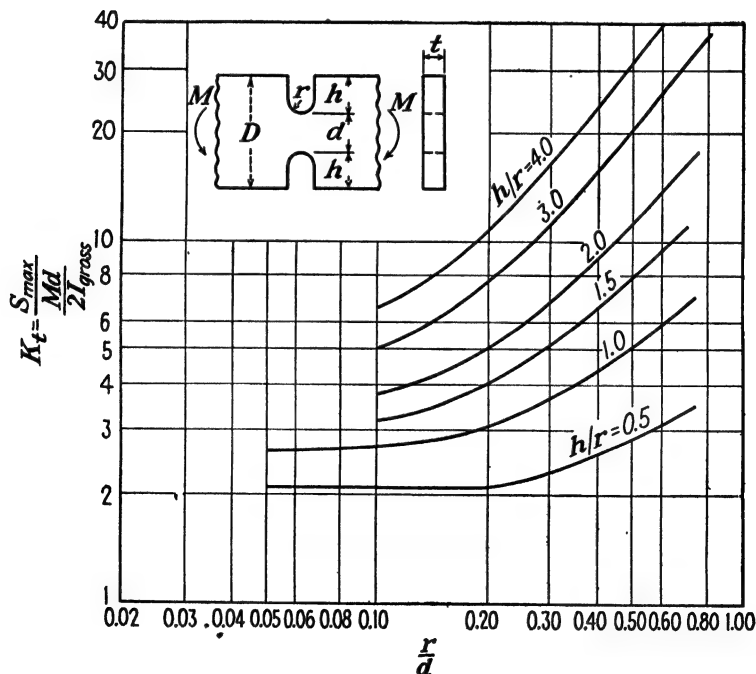


FIG. 91.—Stress-concentration factors for notches in beams.

TABLE VII.—ENDURANCE-LIMIT-REDUCTION FACTORS DETERMINED FROM ROUND SPECIMENS IN REVERSED BENDING\*

Material	Treatment	60° notch, $\frac{\rho}{h} = 0.40$	60° notch, $\frac{\rho}{h} = 0.50$	Square notch	Trans- verse hole $\frac{d}{D} =$ 0.10
S.A.E. 1020 steel	Rolled		1.41	1.17	
S.A.E. 1045 steel	Cold drawn Normalized Quenched and tempered				2.53 1.60 3.15
S.A.E. 2330 steel	Drawn at 1100°F.	2.55			
S.A.E. 3140 steel	Hot rolled Quenched and tempered				2.06 2.90
S.A.E. 4130 steel	Normalized Drawn at 650°F.	1.70 2.15			
S.A.E. 4140 steel			2.15		
Stainless steel			2.42		
Ni-Cr steel	Annealed Cold drawn	1.20 1.43			
Gray cast iron				1.18	
Moly. cast iron				1.41	
Mall. cast iron				1.52	
Wrought iron				1.47	
Brass			2.00		
Al alloy 17S-T			1.25		
Al alloy 24S-T		2.00			

AVERAGE VALUES OF  $K_s$  FOR LOW-CARBON STEEL IN REVERSED BENDING

Nonuniformity	Factor	Nonuniformity	Factor
Square corner.....	2.0	Concentric groove	
Sharp V-thread.....	3.0		
Whitworth thread.....	2.0	$\frac{\rho}{D} = 0.1$	2.0
U.S. standard thread.....	2.5	$\frac{\rho}{D} = 0.5$	1.6
Lathe finish.....	1.2	$\frac{\rho}{D} = 1.0$	1.2
Grinding wheel finish.....	1.05	$\frac{\rho}{D} = 2.0$	1.1

$\rho$ —radius at bottom of notch or groove.

$D$ —diameter of specimen.

$h$ —depth of notch.

$d$ —diameter of hole.

\* Data from

*Proc. Am. Soc. Test. Mat.*, 1934–1941.

SEELY, F. B., "Advanced Mechanics of Materials," John Wiley & Sons, Inc., New York, 1932.

TIMOSHENKO, S., "Theory of Elasticity," McGraw-Hill Book Company, Inc., New York, 1934.

The numerical relationship between  $K_s$  and  $K_t$  is dependent not only upon the geometry of the stress raiser, which controls the relative magnitudes of the biaxial stresses, but also upon which theory of failure is presumed to apply.

A number of determinations of the endurance-limit-reduction factor  $K_s$  have been made for flexural members. Some of them are shown in Table VII. As would be expected, the values of  $K_s$  are lower than the corresponding values of  $K_t$  and depend upon the material as well as upon the geometry of the stress raiser.

**86. Beams of Two Materials.**—In some types of construction beams composed of two or more materials, fabricated to act as a unit, are desirable. For example, in a reinforced concrete beam the steel provides the necessary resistance to tension that the concrete lacks, while the concrete supplies other desirable characteristics. The two materials act together as a unit, so that in a beam of constant cross section a transverse plane section may be assumed to remain plane during bending. The total strain is proportional to the distance from the neutral axis, and if the beam is straight, the unit strain is proportional

to the distance from the neutral axis. Hence, Eq. (169) applies, and the distribution of unit strain is as indicated in Fig. 92*b*. However, because of the difference in moduli of elasticity of the two materials the stress will not be proportional to the distance from the neutral axis. In addition, the concrete on the tension side of the neutral axis is assumed to develop no stress because of the low tensile strength of concrete. As a result, the distribution of stress throughout the depth of the reinforced-con-

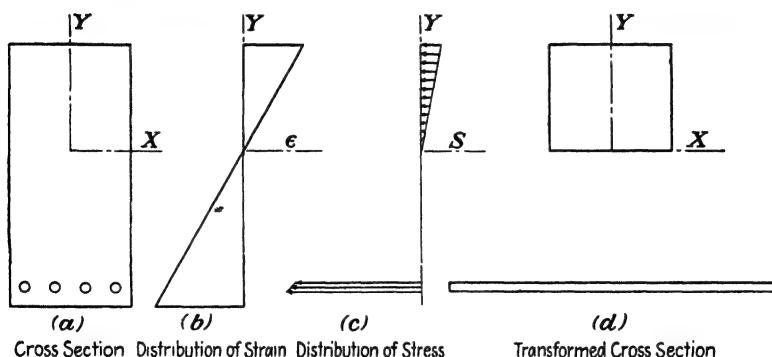


FIG. 92.—Beam of two materials.

crete beam is about as indicated in Fig. 92*c* if the stresses do not exceed the proportional limit.

The expression for stress in the stiffer material at a distance  $y$  from the neutral axis may be developed from the geometrical condition of Eq. (169) by multiplying numerator and denominator of the left-hand side by  $E'$ , the modulus of elasticity of the stiffer material.

$$\frac{\epsilon_y E'}{\epsilon_o E'} = \frac{y}{c} \quad (185)$$

or

$$\frac{\epsilon_y E'}{\epsilon_o n E} = \frac{y}{c} \quad (185a)$$

in which  $n$  is the ratio of the moduli of elasticity  $n = E'/E$ . Then

$$S'_y = \frac{n S_o y}{c} \quad (185b)$$

If the plane of the moment is perpendicular to the neutral axis the moment equation of equilibrium with respect to the neutral

axis, Eq. (168) gives

$$M = \int_0^A S_y y \, da + \int_0^{A'} S'_y y \, da' \quad (186)$$

$$= \frac{S_o}{c} \int_0^A y^2 \, da + \frac{S_o}{c} \int_0^{A'} y^2 (n \, da') \quad (186a)$$

It is evident that the two integrals in Eq. (185a) may be combined into a single integral if the portion of the area occupied by the stiffer material is imagined to be replaced by an area  $n$  times as great (but at the same distance from the neutral axis) of the less stiff material. The imaginary cross section in which the stiffer material is replaced by a greater area of the less stiff material is known as the *transformed cross section* and is illustrated in Fig. 92(d) for the reinforced-concrete beam. Then Eq. (186a) will reduce to

$$M = \frac{S_o I_t}{c} \quad (186b)$$

in which  $S_o$  is the stress in the less stiff material

$I_t$  is the moment of inertia of the transformed cross section with respect to the neutral axis.

The stress in the stiffer material may be found from Eq. (185b), i.e., it is  $n$  times the stress in the less stiff material at the same distance from the neutral axis.

The position of the neutral axis of the transformed cross section may be located by the same procedure that was used for the ordinary beam—the resultant of the normal forces acting on the cross section equals the external normal force. If the cross section is subjected to pure bending and the neutral axis is, or is perpendicular to, an axis of symmetry

$$\int_0^A S_y \, da + \int_0^{A'} S'_y \, da' = 0 \quad (187a)$$

$$\int_0^A y \, da + \int_0^{A'} y (n \, da') = 0 \quad (187b)$$

If the transformed cross section is used, Eq. (187b) reduces to

$$\int_0^{A_t} y \, da = 0 \quad (187c)$$

Hence, the neutral axis passes through the centroid of the transformed cross section.



**87. Curved Beams.**—The general flexure formula, Eq. (172b), was derived on the assumption that the beam is straight. If the longitudinal axis of the beam is curved, and if a plane section before bending remains plane after bending, the unit strain will not be proportional to the distance from the neutral surface as in the straight beam. For example, if a short length, Fig. 93a, of the curved beam indicated in Fig. 93b is cut by radial

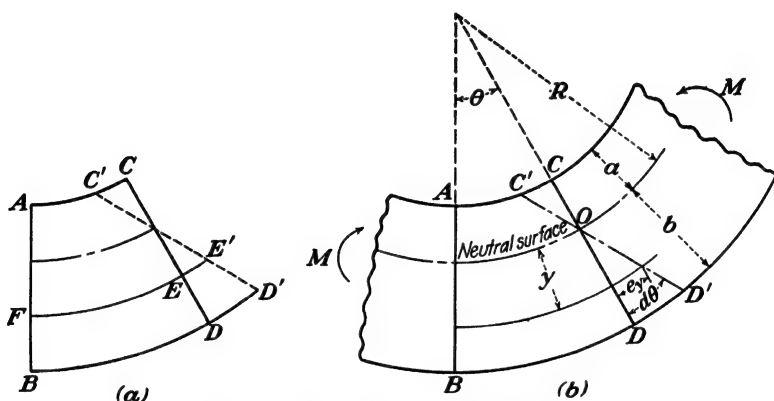


FIG. 93.—Geometry of a curved beam.

planes, the plane ends  $AB$  and  $CD$  are assumed to remain plane, and  $CD$  may be regarded as shifting to  $C'D'$  with respect to  $AB$  when the beam is bent. The total strains  $CC'$  and  $EE'$  at equal distances from the neutral axis are equal, but the unit strain along  $CC'$  is greater than along  $EE'$  because the gage length  $AC$  on the inside is less than the corresponding length  $FE$  on the outside. Consequently, the unit stress is higher on the inside than on the outside and in order to equalize the total tensile and total compressive forces, the neutral axis shifts from the centroid of the cross section toward the inside. It is evident that the ordinary straight-beam theory is not valid for a curved beam.

Two methods for evaluating stresses in curved beams will be developed. The first is the Winkler-Bach theory,<sup>1</sup> the second,

<sup>1</sup> WINKLER, E., *Form-Änderung und Festigkeit gekrümmter Körper*, *Zivilingenieur*, Vol. 4, p. 232, 1858.

WINKLER, E., "Die Lehre von der Elastizität und Festigkeit," Prague, 1867.

discussed in Art. 91, is a procedure based on the transformed cross section. The two methods give identical results, and both assume that the curvature is restricted to one plane, the plane of the external moment.

**88. Winkler-Bach Theory for Curved Beams.**—Equation (168)

$$M = \int_0^A S_y y \, da \quad (168)$$

is valid for the curved beam as well as for a straight beam. However, it cannot be integrated unless a relationship can be established between  $S_y$  and  $y$ . The necessary relationship may be obtained from *geometry* and the *properties of the material*. In Fig. 93b the radial section  $CD$  is assumed to rotate to the position  $C'D'$  with respect to the radial section  $AB$  with the neutral axis at an unknown location  $O$ . The original angle between the sections  $AB$  and  $CD$  is designated as  $\theta$ . When the beam is subjected to a pure moment, section  $CD$  rotates with respect to  $AB$  through the angle  $d\theta$  to the new position  $C'D'$ . As long as a plane radial section before bending remains plane after bending, which may be verified experimentally, the *total strain*  $e_y$  on any fiber at a distance  $y$  from the neutral axis is proportional to the distance  $y$

$$\frac{e_y}{e_b} = \frac{y}{b} \quad (188)$$

The unit strain  $\epsilon_y$  is equal to the total strain  $e_y$  divided by the length over which the strain occurs, which is  $(R + y)\theta$ ,

$$\epsilon_y = \frac{(R + b)y\epsilon_b}{(R + y)b} \quad (189)$$

in which  $R$  is the distance from the center of curvature to the neutral axis.

If the material is homogeneous and if the proportional limit is not exceeded, the stress at a distance  $y$  from the neutral axis is

$$S_y = \frac{(R + b)yS_b}{(R + y)b} \quad (190)$$

The force acting on a differential area  $da$  at a distance  $y$  from the neutral axis is  $dF = S_y da$ . If a condition of pure flexure prevails, the force equation of equilibrium gives

$$\int_0^F dF = \int_0^A \frac{(R + b)yS_b}{(R + y)b} da = 0 \quad (191)$$

The quantities  $(R + b)$ ,  $b$ , and  $S_b$  are constant, so Eq. (191) may be written

$$\frac{(R + b)S_b}{b} \int_0^A \frac{y da}{R + y} = 0 \quad (191a)$$

or

$$\int_0^A \frac{y da}{R + y} = 0 \quad (191b)$$

Equation (191b) determines the location of the neutral axis. The evaluation of the integral for specific cross sections is discussed in Art. 89. From Eq. (190) and the moment equation of equilibrium with respect to the neutral axis

$$M = \int^A S_y y da \quad (168)$$

there results

$$M = \frac{(R + b)S_b}{b} \int_0^A \frac{y^2 da}{R + y} \quad (192)$$

Equation (192) may also be written as

$$M = \frac{(R + b)S_b}{b} \int_0^A \left( y - \frac{Ry}{R + y} \right) da \quad (192a)$$

$$= \frac{(R + b)S_b}{b} \int_0^A y da - \frac{(R + b)S_b R}{b} \int_0^A \frac{y da}{R + y} \quad (192b)$$

However, from Eq. (191b) the second term is zero. Hence

$$M = \frac{(R + b)S_b}{b} \int_0^A y da \quad (192c)$$

$$= \frac{(R + b)S_b}{b} A \bar{y} \quad (192d)$$

or

$$S_b = \frac{Mb}{(R + b)A \bar{y}} \quad (193)$$

$$= \frac{Mb}{R_o A \bar{y}} \quad (193a)$$

in which  $R_o$  is the radius of curvature at a distance  $b$  from the neutral axis. From Eqs. (193a) and (190) it follows that, in general,

$$S_y = \frac{My}{(R + y)A \bar{y}} \quad (193b)$$

In Eqs. (193a) and (193b) the denominator corresponds to the moment of inertia in the ordinary flexure formula. It is evident that the denominator decreases for points toward the inside surface of the beam and increases for points toward the outside surface. Hence, from the neutral axis to the inside the stress increases more rapidly than the normal linear variation, and from the neutral surface outward the stress increases less rapidly than the normal linear distribution. The stress variation is as indicated in Fig. 94.

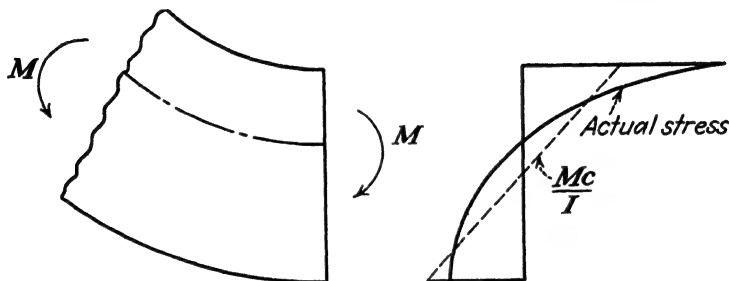


FIG. 94.—Stress variation in a curved beam.

**89. Location of Neutral Axis in Curved Beams.**—The determination of the location of the neutral axis in a curved beam involves the solution of Eq. (191b) for  $y$ . This operation corresponds to the solution of

$$\int_0^A y \, da = 0$$

for the straight beam. From Eq. (191b) it is evident that the location of the neutral axis is dependent not only upon the shape of the cross section, as in the straight beam, but also upon the radius of curvature of the neutral surface at the section under consideration. Just as in the case of the centroid, the integral in Eq. (191b) must be evaluated separately for each different shape of cross section.

For a rectangular cross section of thickness  $t$  and depth (radially) of  $a + b$  (Fig. 93), Eq. (191b) becomes

$$\therefore \quad t \int_{-a}^b \frac{y \, dy}{R + y} = 0 \quad (191c)$$

This integrates to (dropping  $t$ )

$$b - a + R \log \left( \frac{R + b}{R - a} \right) = 0 \quad (194)$$

which may also be written as

$$\frac{d}{R} = \log \left( \frac{R_o}{R_i} \right) \quad (194a)$$

in which  $d$  is the depth of the section ( $a + b$ )

$R_o$  is the radius of the outer surface ( $R + b$ )

$R_i$  is the radius of the inner surface ( $R - a$ ).

Then

$$R = \frac{d}{\log (R_o/R_i)} \quad (194b)$$

in which  $R$  is the unknown radius of the neutral surface. With  $R$  known, the distance  $a$  or  $b$  may be determined from  $R_i$  or  $R_o$ , locating the neutral axis.

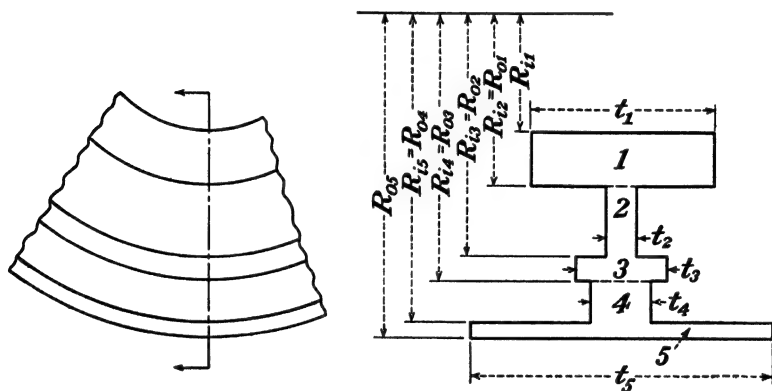


FIG. 95.—Subdivision of cross section of curved beam.

If the cross section of the curved beam consists of a series of rectangles with sides parallel and perpendicular to the plane of the loads, as indicated in Fig. 95, the radius of the neutral axis may be determined as

$$R = \frac{A}{\log [(R_{o1}/R_{i1})^{t_1} (R_{o2}/R_{i2})^{t_2} (R_{o3}/R_{i3})^{t_3} \dots (R_{on}/R_{in})^{t_n}]} \quad (194c)$$

in which  $A$  is the total area of the cross section

$t_1, t_2, t_3 \dots t_n$  is the width of the successive rectangles  
 $R_{o1}, R_{o2}, R_{o3} \dots R_{on}$  is the outside radius of the successive rectangles

$R_{i1}, R_{i2}, R_{i3} \dots R_{in}$  is the inside radius of the successive rectangles.

**90. Modification of Stress Formula.**—The formula for stress in a curved beam, Eq. (193b), may be modified to the form

$$S_o = \frac{K_o M c_o}{I} \quad (193c)$$

and

$$S_i = \frac{K_i M c_i}{I} \quad (193d)$$

in which  $I$  is the moment of inertia of the cross section with respect to the centroidal axis

$c_o$  is the distance from the centroidal axis to the outside

$c_i$  is the distance from the centroidal axis to the inside

$K_o$  and  $K_i$  are correction factors.

$$K_o = \frac{I}{R_o A \bar{y}} \quad (194a)$$

$$= \frac{k^2}{R_o \bar{y}} \quad (194b)$$

$$K_i = \frac{I}{R_i A \bar{y}} \quad (194c)$$

$$= \frac{k^2}{R_i \bar{y}} \quad (194d)$$

Values of  $K_o$  and  $K_i$  for beams of rectangular and elliptical cross sections are given in Fig. 96 for a range of values of  $R/c$  in which  $R$  is the radius of the neutral surface.

For values of  $R/c$  greater than 10, the stresses as computed by the ordinary flexure formula will be within 10 per cent of the values given by the curved-beam theory.

**91. Stresses in Curved Beams by the Transformed Cross Section.**—Application of the Winkler-Bach theory to beams having cross sections other than those considered in Art. 90 becomes involved owing to the difficulty of locating the neutral axis by Eq. (191b). Hardy Cross<sup>1</sup> has described the use of the transformed cross section in evaluating stresses in a curved beam having any cross section.

The transformed cross section is developed by dividing the width  $x$  of the beam at each point by the radius of curvature

<sup>1</sup> *Op. cit.*, p. 195.

at that point. Thus

$$x' = \frac{x}{R + y} \quad (195)$$

$$da' = x' dy \quad (196)$$

$$= \frac{da}{R + y} \quad (196a)$$

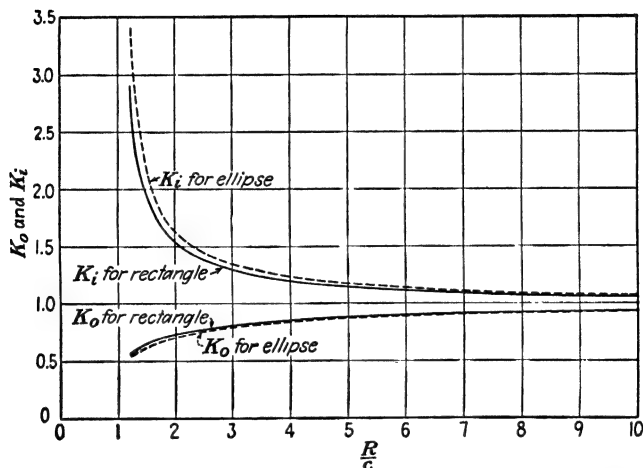


FIG. 96.—Values of  $K_o$  and  $K_i$  for stresses in curved beams.

In addition, the flexural stress  $S'_y$  at any point in the transformed cross section is

$$S'_y = (R + y)S_y \quad (197)$$

Hence, from Eq. (190)

$$S'_y = \frac{(R + b)yS_b}{b} \quad (197a)$$

$$= y \frac{S'_b}{b} \quad (197b)$$

which is the same linear stress distribution that occurs in a straight beam. It follows that the neutral axis of the curved beam passes through the *centroid* of the *transformed cross section* and that the stresses in the transformed cross section may be determined from

$$S'_y = \frac{M'y'}{\bar{I}'} \quad (197c)$$

in which  $M'$  is the moment of the external loads with respect to the neutral axis of the transformed cross section

$y'$  is the ordinate of the point under consideration with reference to the neutral axis of the transformed cross section

$I'$  is the moment of inertia of the transformed cross section with respect to the neutral axis.

The stresses in the original cross section are obtained from Eqs. (197c) and (197). It may be shown by a procedure parallel to that followed in Art. 81 that the general flexural-stress equation, Eq. (172b), applies to the transformed cross section if a combination of axial loading and unsymmetrical bending exists.

The centroid of the transformed cross section may be located by taking moments about the center of curvature. By definition

$$R' = \frac{\int (R + y) da'}{\int da'} \quad (198)$$

$$= \frac{A}{A'} \quad (198a)$$

in which  $R'$  is the radius of the centroid of the transformed cross section

$A'$  is the area of the transformed cross section

$A$  is the area of the original cross section.

Equation (198a) locates the neutral axis of the curved beam if there is no resultant normal force acting on the cross section.

The moment of inertia of the transformed cross section with respect to an axis through the center of curvature of the beam is, by definition

$$I_o = \int (R + y)^2 da' \quad (198b)$$

$$= \int (R + y) da \quad (198c)$$

$$= RA \quad (198d)$$

in which  $R$  is the radius of the centroid of the original area  $A$ .

From the parallel-axis theorem, the moment of inertia of the transformed cross section with respect to its centroidal axis is

$$I' = I_o - A'(R')^2 \quad (198e)$$

$$= RA - \frac{A^2}{A'} \quad (198f)$$

$$= A \left( R - \frac{A}{A'} \right) \quad (198g)$$

Hence, all of the required properties of the transformed cross section may be determined from its area and the area and location of the centroid of the original cross section.



## DEFLECTIONS

**92. General Considerations.**—The deflection of a beam is entirely a matter of geometry. The strains that occur over any differential length cause, or are caused by, a relative rotation of the transverse planes at each end of the length. Each rotation is accompanied by a change in slope, resulting in a relative transverse displacement of the two ends of the differential length. The relative deflection of one end of a finite length with respect to the other is the algebraic sum of the relative displacements throughout the finite length.

Because of the importance of being able to predict the deflection of a flexural member, several tools have been developed for the purpose of evaluating deflection in terms of the loads or moments and the properties of the beam. Five of the most important are

1. Double integration.
2. Area moments.
3. Conjugate beam.
4. Castigliano's theorem.
5. Virtual work.

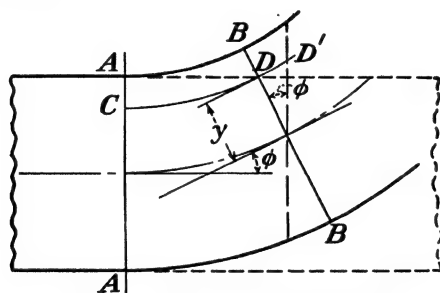


FIG. 97.—Geometry of a bent beam.

Each represents a slightly different interpretation of the relationships that may be developed from a consideration of the statics, geometry, and properties of the material of the beam.

Figure 97 represents a portion of a bent beam. The two transverse sections  $AA$  and  $BB$ , which were originally parallel and a distance  $\Delta x$  apart, remain straight but rotate with respect to each other when the beam is bent. The change in angle of section  $BB$  relative to  $AA$  is designated as  $\phi$ . That is,  $\phi$  is the slope of the beam at section  $BB$ , since  $AA$  is assumed to

remain fixed. Therefore, if the deflection of  $BB$  relative to  $AA$  is designated as  $\Delta y$

$$\phi = \frac{\Delta y}{\Delta x} = \frac{dy}{dx} \quad (199)$$

$$y = \int_A^B \phi \, dx \quad (199a)$$

From Fig. 97 and the assumption that a plane section before bending remains plane after bending, it is evident that the unit strain at a distance  $y$  from the neutral axis is

$$\epsilon_y = \frac{DD'}{CD'} \quad (200)$$

$$= \frac{\phi y}{\Delta x} \quad (200a)$$

If the stresses do not exceed the proportional limit

$$S_y = \frac{E\phi y}{\Delta x} \quad (200b)$$

and if the flexure formula is valid

$$\frac{M}{I} = \frac{E\phi}{\Delta x} \quad (200c)$$

Hence, the total angle change occurring between two sections  $A$  and  $B$  is

$$\phi = \int_A^B \frac{M \, dx}{EI} \quad (200d)$$

which may be combined with Eq. (199) to give

$$\frac{d^2y}{dx^2} = \frac{M}{EI} \quad (201)$$

Equation (201) is the basic differential equation for the deflection of a beam due to flexure. It is subject to all of the limitations of the flexure formula and, in addition, is limited to small deflections.

**93. Double Integration.**—The double-integration procedure consists in substituting the general expression for the moment at any point in the beam into Eq. (201) and integrating. If the moment is a function of  $x$  and not of  $y$ , the integration may proceed directly. The resultant expression for  $y$  will contain two constants of integration, which may be evaluated from

known conditions of slope or deflection at given points on the beam. The procedure is described in detail in most textbooks in elementary mechanics of materials.

If the beam is subjected to axial loading as well as transverse loads, the moment is a function of the deflection  $y$  as well as  $x$ , and the integration of Eq. (201) becomes somewhat more involved.

**94. Area Moments.**—In 1869 Greene<sup>1</sup> published two theorems pertaining to beams.

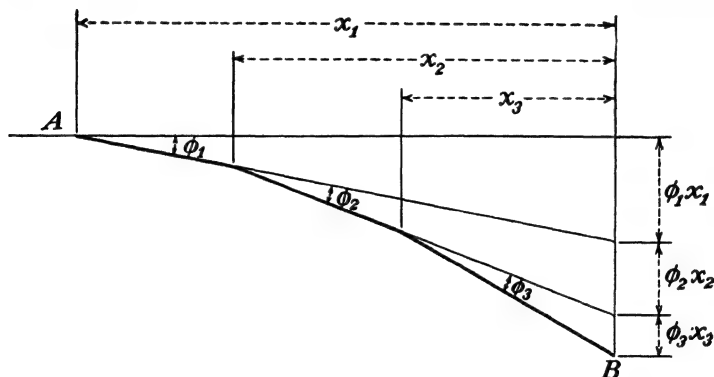


FIG. 98.—Deflection of a line due to angle changes.

1. The rotation at point  $B$  relative to point  $A$  is equal to the area of the  $M/EI$  diagram between  $A$  and  $B$ .

2. The deflection of point  $B$  with respect to a tangent at point  $A$  is equal to the moment, with respect to an axis at  $B$ , of the area of the  $M/EI$  diagram between  $A$  and  $B$ .

The first theorem follows directly from Eq. (200d). The validity of the second may be shown from the construction in Fig. 98. The line  $AB$  is bent at several points, and the deflection of point  $B$  from a tangent at  $A$  is

$$y = \sum_A^B \phi_i x_i \quad (202)$$

If the angle changes,  $\phi_i$ , are due to moment, they may be evaluated in terms of the moment from Eq. (200d). Hence

$$y = \int_A^B \frac{Mx}{EI} dx \quad (202a)$$

<sup>1</sup> GREENE, C. E., *Michigan Technic*, 1869.

It is evident that the right-hand side of Eq. (202a) is equal to the moment, about  $B$ , of the area under the  $M/EI$  diagram between  $A$  and  $B$ , thus proving the second theorem.

Mohr<sup>1</sup> showed by means of force and string polygons that the deflection at any point in a simple beam may be found by treating the  $M/EI$  diagram of the beam as a load on a second simple beam of the same span as the first. The moment at any point in the second beam is equal to the deflection at the corresponding point in the original beam. This may also be shown by expressing the loading on a beam in terms of the moment. From statics

$$w = \frac{dV}{dx} \quad (203)$$

$$V = \frac{dM}{dx} \quad (203a)$$

Therefore

$$\frac{d^2M}{dx^2} = w \quad (203b)$$

A comparison of Eq. (203b) with Eq. (201) shows the analogy between load and moment.

Greene's theorems are particularly useful for cantilever beams, while Mohr's method is better adapted to simply supported beams. The area-moment procedure is generally considered preferable to double integration when the deflection at a single point is wanted, when the beam carries a number of concentrated loads, or when the moment of inertia of the beam varies. The double-integration procedure has the advantage of giving the equation of the elastic curve instead of the deflection at a single point.

**95. Conjugate Beams.**—Müller-Breslau<sup>2</sup> and Westergaard<sup>3</sup> have generalized the area-moment procedure, making it applicable for any condition of support. In each case the  $M/EI$  diagram for the original beam is imagined to be the load on a second beam, known as the "conjugate beam," having the same

<sup>1</sup> MOHR, O., *Beitrag zur Theorie der Holz-und Eisenconstruktionen*, *Z. Arch. Ing.-Ver. Hanover*, 1868.

<sup>2</sup> MÜLLER-BRESLAU, H., *Beitrag zur Theorie des Fachwerks*, *Z. Arch.- und Ing.-Ver. Hanover*, Vol. 31, 1885.

<sup>3</sup> WESTERGAARD, H. M., *Deflection of Beams by the Conjugate Beam Method*, *J. Western Soc. Engineers*, Vol. 26, 1921.

span as the original beam. It follows from Eqs. (203b) and (201) that moments in the conjugate beam are equal to deflections in the original beam and from Eqs. (199) and (203a) that the shear in the conjugate beam is equal to the slope of the original beam at the corresponding point.

The conditions that the supports of the conjugate beam must satisfy are established.

1. A simple support on the original beam (at which there may be slope but no deflection) requires shear, but no moment, at the corresponding point on the conjugate beam. Hence, the conjugate beam must be pinned at that point.

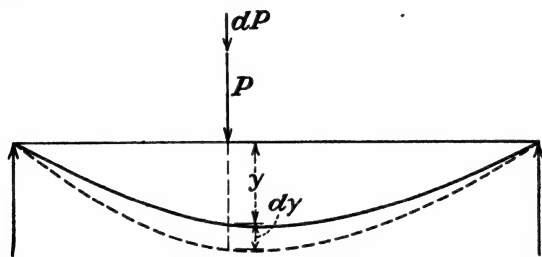


FIG. 99.—Beam for development of Castigliano's theorem.

2. A fixed end on the original beam (at which there is zero slope and zero deflection) requires zero shear and zero moment at the corresponding point on the conjugate beam. This requirement is satisfied by a free end.

3. A free end on the original beam (at which there is both slope and deflection) must be matched by a fixed end, with both shear and moment, on the conjugate beam.

Other conditions may be established in like manner. The idea of the conjugate beam may be extended to frames and other structures in which the primary cause of distortion is bending.

**96. Castigliano's Theorem.**—Castigliano's theorem states that if several forces act upon a structure, the displacement of the structure in the direction of one of the forces is equal to the partial derivative of the total internal strain energy of the structure with respect to that force.

$$\frac{\partial U}{\partial P} = y \quad (204)$$

The theorem may be derived as follows. If a force  $P$  is applied to a member such as the beam in Fig. 99, the work done by the

force on the beam for stresses below the proportional limit is

$$U = \frac{1}{2}Py \quad (205)$$

in which  $y$  is the deflection (in the direction of the force) of the point at which the force is applied. If an additional force  $dP$  is applied at the same point, the increment of deflection is  $dy$  and the additional work  $dU$  is

$$dU = P dy + \frac{1}{2} dP dy \quad (205a)$$

The total work done on the beam is, from Eqs. (205) and (205a),

$$U + dU = \frac{1}{2}Py + P dy + \frac{1}{2}dP dy \quad (205b)$$

However, if the two forces  $P$  and  $dP$  are applied at the same time the total work is

$$\begin{aligned} U + dU &= \frac{1}{2}(P + dP)(y + dy) \\ &= \frac{1}{2}Py + \frac{1}{2}P dy + \frac{1}{2}dP y + \frac{1}{2}dP dy \end{aligned} \quad (205c)$$

Since the total work done must be independent of the order of application of the forces, the value of the total work from Eq. (205) equals that given in Eq. (205c). Hence,

$$\frac{1}{2}Py + P dy + \frac{1}{2}dP dy = \frac{1}{2}Py + \frac{1}{2}P dy + \frac{1}{2}y dP + \frac{1}{2}dP dy \quad (205d)$$

from which

$$P dy = y dP \quad (205e)$$

However,  $P dy$  may be expressed in terms of  $dU$ , from Eq. (205a), neglecting differentials of the second order

$$dU = P dy$$

If  $dU$  is substituted for  $P dy$  in Eq. (205e), there results

$$dU = y dP$$

and

$$\frac{dU}{dP} = y \quad (205f)$$

If several forces are involved, the deflection in the direction of one of the forces is equal to the partial derivative of the work with respect to that particular force, and Eq. (205f) reduces to the form given in the statement of the theorem, Eq. (204).

The use of Castigliano's theorem requires the evaluation of the work or strain energy in the beam. For the condition of

pure flexure, the work is done in bending the beam. The work done by a moment or couple is equal to one-half the couple times the angle of twist.

$$U = \frac{1}{2} M \phi \quad (206)$$

However,  $\phi$  may be evaluated in terms of the moment from Eq. (200d). Then

$$U = \int_A^B \frac{M^2 dx}{2EI} \quad (206a)$$

$$y = \frac{\partial}{\partial P} \int_A^B \frac{M^2 dx}{2EI} \quad (204a)$$

If no concentrated load acts at the point where the deflection is desired, a "dummy load" may be placed at the point, included in the moment and the strain energy, and finally equated to zero after the strain energy is differentiated.

Castigliano's theorem may be extended to evaluate displacements due to torsion and to axial loading.

**97. Virtual Work.**—The process known as virtual work or single integration may be developed from Eq. (204a) by performing the differentiation before the integration.

$$y = \int_A^B \frac{M(\partial M / \partial P) dx}{EI} \quad (204b)$$

The quantity  $\partial M / \partial P$  is the rate of change of moment at any point due to a change in the load  $P$  at the point where the deflection is desired. It is therefore equal to the moment due to a unit load at the point where the deflection is desired, but the moment due to a unit load is a function of  $x$ . Hence, if the origin is at the point the deflection of which is to be determined, Eq. (204b) reduces to Eq. (202a), which may be integrated directly if the moment is constant or is a function of  $x$ .

The process, which was described by Clark Maxwell in 1864 and by Otto Mohr in 1874, is sometimes called the Maxwell-Mohr method.

**98. Comparison of Methods.**—Each of the procedures outlined and others that have been developed have their advantages and disadvantages. The mathematical operations involved in some are identical with operations involved in others. In those cases the distinction is only one of interpretation of the individual steps, and the apparent advantage of one method over another

may lie solely in the relative degrees of familiarity that the user has with the various processes. However, one real difference exists: the double-integration procedure gives the equation of the elastic curve; the other processes here outlined give only the deflection at a *point*, although they may be manipulated to give the equation of the elastic curve.

No single problem can give a fair comparison of methods. The following simple illustrative problem is included only to

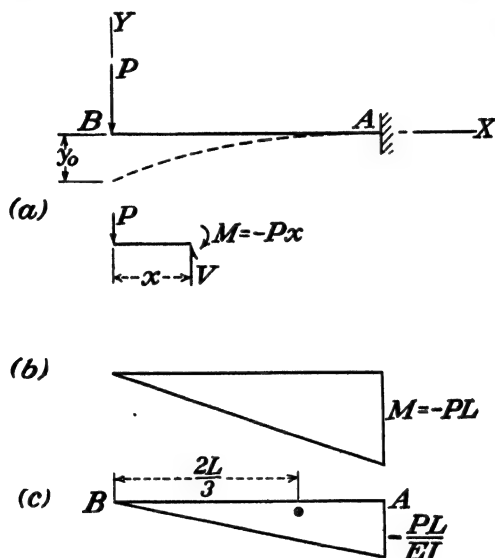


FIG. 100.—Deflection of a beam.

indicate the procedure to be followed in each case and is not intended to be used in comparing the relative difficulty of the methods.

*Illustrative Problem.*—Determine by each of the procedures outlined the deflection at the end of a uniform cantilever beam carrying a concentrated load at the end

*Solution.*—Regardless of the procedure to be used, the first step is to make a sketch, indicating pertinent dimensions and showing the axes. A suitable sketch is indicated in Fig. 100a. A free-body diagram of a portion of the beam is drawn for aid in evaluating the moment at a distance  $x$  from the origin.

1. *Double Integration.*—The moment at a distance  $x$  from the origin is evaluated as  $-Px$ . This value may be substituted directly into Eq. (201) and integrated.



$$EI \frac{d^2y}{dx^2} = -Px$$

$$EI \frac{dy}{dx} = -\frac{Px^2}{2} + C_1$$

The constant of integration may be evaluated from the condition that the slope is zero at the fixed end ( $x = L$ ).

$$C_1 = \frac{PL^2}{2}$$

A second integration gives

$$EIy = -\frac{Px^3}{6} + \frac{PL^2x}{2} + C_2$$

When  $x = L$ ,  $y = 0$ . Hence

$$C_2 = \frac{-PL^3}{3}$$

The equation of the elastic curve is, therefore

$$y = \frac{P}{EI} \left( \frac{-x^3}{6} + \frac{L^2x}{2} - \frac{L^3}{3} \right)$$

The deflection at the free end  $x = 0$  is

$$y = \frac{-PL^3}{3EI}$$

The negative sign indicates a downward deflection.

2. *Area Moments*.—The moment diagram, as shown in Fig. 100b, may be sketched directly from the loading diagram of Fig. 100a, and since the beam has a uniform cross section, the  $M/EI$  diagram will be as shown in Fig. 100c.

From Greene's second theorem the moment of the diagram about point  $B$  (the free end) gives the deflection of  $B$  from a tangent at  $A$ . Since the tangent at  $A$  remains horizontal, this is the desired deflection.

$$y = \frac{1}{2} \left( \frac{-PL}{EI} \right) L \left( \frac{2L}{3} \right)$$

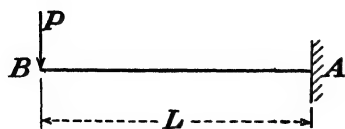
$$= \frac{-PL^3}{3EI}$$

3. *Conjugate Beam*.—The original beam is indicated in Fig. 101a, and the conjugate beam, loaded with the  $M/EI$  diagram, is shown in Fig. 101b. In accordance with the discussion in Art. 95 the free end of the beam becomes a fixed end in the conjugate beam, and vice versa. The deflection of  $B$  is equal to the moment at  $B'$ , hence

$$y = \frac{1}{2} \left( \frac{-PL}{EI} \right) L \left( \frac{2L}{3} \right)$$

$$= \frac{-PL^3}{3EI}$$

4. *Castigliano's Theorem*.—The strain energy in the beam is found from Eq. (206a) and the expression for the moment at any point in the beam.

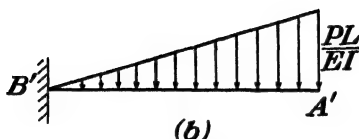


(a)

$$U = \int_0^L \frac{(-Px)^2 dx}{2EI} \\ = \frac{P^2 L^3}{6EI}$$

Then from Eq. (204a)

$$y = \frac{PL^3}{3EI}$$



(b)

The deflection is in the direction of the force with respect to which the derivative was taken—downward.

FIG. 101.—Conjugate beam.

5. *Virtual Work*.—From Eq. (202a) and the fact that  $M = -Px$

$$y = \int_0^L \frac{-Px^2 dx}{EI} \\ = \frac{-PL^3}{3EI}$$

### PROBLEMS

**228.** A rectangular cantilever beam 3 in. wide and 8 in. deep carries a concentrated load of 600 lb. at a point 4 ft from the fixed end. The line of action of the load is perpendicular to the longitudinal axis of the beam and lies in a plane making an angle  $\beta$  with the vertical. Plot a curve showing the variation in maximum stresses with  $\beta$ .

**229.** A hollow rectangular beam is made up of 0.040-in.-thick duralumin sheet. The over-all depth of the beam is 12 in., and the width is 24 in. Determine the maximum bending moment that the beam can resist without the stress exceeding 20,000 p.s.i., if the plane of the moment is (a) horizontal, (b) inclined 5 deg. with the horizontal.

**230.** A rectangular timber beam of constant cross section is to be used as a 16-ft. cantilever. The beam is to carry an inclined uniform load of 50 lb. per ft. over its entire length, the plane of the loads making an angle of 30 deg. with the bottom of the beam. If the maximum flexural stress is not to exceed 1,000 p.s.i., and if the beam is to have a minimum weight, determine the optimum dimensions of the cross section.

**231.** A beam 2 in. wide and 12 in. deep is designed to carry a vertical load. In construction the beam is inclined one degree. Determine the percentage difference that the inclination makes in the maximum stress.

**232.** A 2- by 2- by  $\frac{1}{4}$ -in. structural aluminum angle is used as a cantilever beam. Determine the maximum load that may be applied 10 ft. from the fixed end if the maximum flexural stress is not to exceed 20,000 p.s.i. The load is applied parallel to one of the legs of the angle.  $A = 0.94 \text{ in.}^2$ ,  $\bar{x} = \bar{y} = 0.58 \text{ in.}$ ,  $k_{min} = 0.39 \text{ in.}$ ,  $k_{xx} = k_{yy} = 0.60 \text{ in.}$

**233.** The Z section shown in Fig. P-233 is to be used as a simply supported beam on a span of 6 ft., and is to carry a concentrated load of 1,200 lb. in the direction of the  $y$  axis at a distance of 2 ft. from one end. Determine the

direction of the neutral axis and the magnitude of the maximum stress.  
 $A = 5.27 \text{ in.}^2$ ,  $k_{xx} = 1.91 \text{ in.}$ ,  $k_{yy} = 1.29 \text{ in.}$ ,  $k_{zz} = 0.73 \text{ in.}$

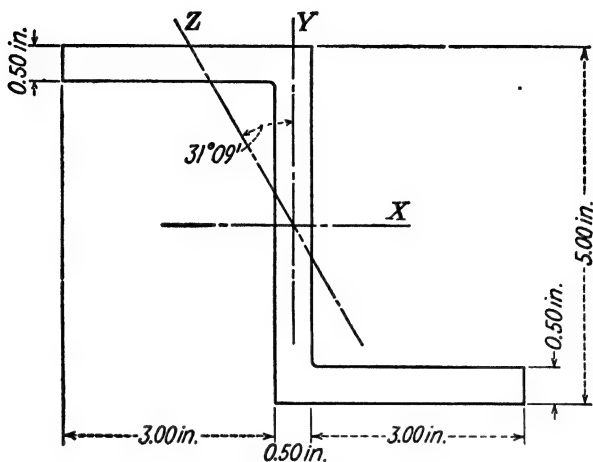


FIG. P-233.

**234.** A beam 6 in. wide and 12 in. deep carries a 2,400-lb. load at the center of a 10-ft. span. The load lies in a vertical plane, but its line of action makes an angle of 30 deg. with the vertical. Determine the flexural stresses at each corner of a section 4 ft. from the left end. Locate the neutral axis.

**235.** Solve Prob. 234 if the beam carries an additional load of 800 lb. in a transverse plane 7 ft. from the left end. The line of action makes an angle of 45 deg. with the vertical, its horizontal component opposing the horizontal component of the 2,400-lb. load.

**236.** A cantilever beam 96 in. long is 12 in. deep and 6 in. wide. Determine the minimum force applied at the end in a plane normal to the longitudinal axis that will cause a maximum flexural stress of 2,400 p.s.i. in the beam.

**237.** A steel member 1 by 2 in. in cross section is used as a beam 6 ft. long. At each end the beam is supported by a bearing perpendicular to the 2-in. faces. The bearing permits rotation about an axis parallel to the 1-in. faces and may be assumed to prevent any rotation about an axis parallel to the 2-in. faces. The beam carries at mid-span a transverse load of 400 lb. The line of action of the load passes through the centroid of the cross section and makes an angle of 30 deg. with the 2-in. faces. Determine the maximum stress and deflection of the beam.

**238.** Determine the magnitude of the moment required to produce a maximum unit strain of (a) 0.001 and (b) 0.002 in a 1-in. square steel rod if the material has a stress-strain diagram similar to that shown in Fig. 85a, and a proportional limit of 39,000 p.s.i.

**239.** A  $\frac{1}{4}$ -in. thick steel strap changes in depth from  $\frac{3}{4}$  to 2 in. What minimum radius of fillet should be used if the maximum stress is not to exceed 1,200 p.s.i. under a moment of 188 in.-lb.?

**240.** A circular steel member contains a circumferential groove which reduces its diameter to 2 in. The radius at the bottom of the groove is  $\frac{1}{8}$  in. If the maximum allowable stress for the material under conditions of axial loading is 24,000 p.s.i., determine the maximum moment to which the member may be subjected according to the maximum-shearing-stress theory of failure.

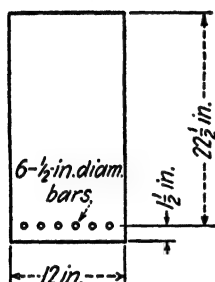


FIG. P-242.

**241.** Determine  $K_t$  for the member of Prob. 240 according to the Hencky-von Mises theory of failure.

**242.** Determine the maximum stresses in the steel and in the concrete of the beam of Fig. P-242 due to a bending moment of 40,000 ft.-lb.

**243.** Design a suitable cross section for a reinforced concrete beam which is to develop a resisting moment of +240,000 in.-lb. with a maximum allowable stress of 20,000 p.s.i. in the steel and 800 p.s.i. in the concrete. The width is to be one-half of the depth of the steel from the top of the beam.

**244.** Develop the relationship between the moment and the stresses in a beam of rectangular cross section if the modulus of elasticity in compression is  $n$  times the modulus in tension. Assume that all stresses are below the proportional limit.

**245.** Develop the relationship between the moment and the stresses in a beam of rectangular cross section if the stress-strain relationship is  $S = K\epsilon^{\frac{1}{2}}$  in both tension and compression.

**246.** Determine the maximum stress developed in the press of Fig. P-246 due to a load of 75,000 lb.

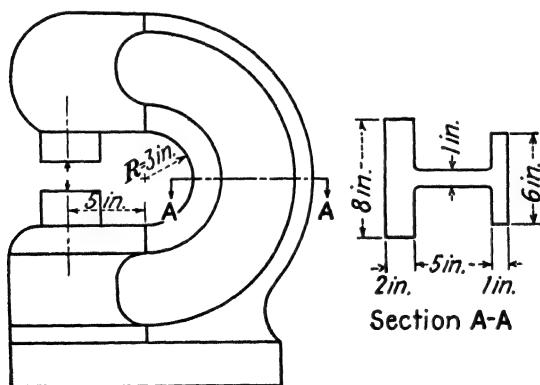


FIG. P-246.

**247.** A 1-in.-diameter steel rod is bent into an arc having an inside radius of  $2\frac{1}{2}$  in. To what maximum moment may the rod be subjected if the stress is not to exceed 20,000 p.s.i.?

**248.** A curved member of rectangular cross section  $\frac{1}{2}$  in. thick and 2 in. deep has an inside radius of 3 in. Locate the neutral axis and plot a curve showing the distribution of stress throughout the 2-in. depth if the member is subjected to a moment of 3,000 in.-lb.

**249.** Derive a general expression for the location of the neutral axis of a curved beam of circular cross section.

**250.** A curved beam of trapezoidal cross section has two sides perpendicular to the radius to the center of curvature. Derive a general expression for the location of the neutral axis.

**251.** Are Eqs. (198a), (198d), and (198g) correct dimensionally? Explain.

**252.** A beam of constant cross section and length  $L$  is fixed at the left end and is supported on a spring at the right end. The beam carries a uniform load of  $q$  lb. per ft., and the modulus of the spring is  $k$  lb. per in. Determine the equation for the elastic curve of the beam.

**253.** What must be the modulus of the spring in Prob. 252 if the deflection of the beam at the middle is the same as it is at the right end?

**254.** Determine the elastic-curve equation for a beam carrying no load but subjected to equal moments at the ends. Why is this not the equation of a circle?

**255.** A beam fixed at both ends carries a concentrated load at one of the third-points. Draw the moment diagram and determine the maximum deflection, using an appropriate method.

**256.** An inverted-L frame is fixed at the lower end of the vertical member and carries a uniform load of  $q$  lb. per ft. on the horizontal member. The moments of inertia of the vertical and horizontal members are  $I_v$  and  $I_h$  respectively. Determine the deflection of the outer end of the horizontal member.

**257.** A temporary framed dam is supported by vertical 6-in. I beams at 12.5 lb. per ft., which are embedded in concrete at the base and are free at the top. The beams are placed 6 ft. o.c. and extend 10 ft. above their fixed bases. Determine the deflection of the top of the beams when the water level is even with the top. Use Castigliano's theorem.

**258.** Determine the deflection of the top of the beams of Prob. 257 when the water depth is 8 ft.

**259.** A 1-in.-diameter rod is bent into the form of a quarter circle with a 10-in. radius. One end is securely fixed with the rod held in a horizontal plane, and a vertical load  $P$  is applied to the free end. Using Castigliano's theorem, determine the vertical component of deflection of the free end.

**260.** A cantilever beam of length  $L$  carries a uniform load of  $q$  lb. per ft. on the outer half. Determine the deflection of the free end using any appropriate method.

**261.** Show how Castigliano's theorem may be used for developing the equation of the elastic curve of a simple beam carrying a uniform load.

**262.** Can Prob. 261 be solved by virtual work?

## CHAPTER IX

### CROSS SHEAR

**99. General Considerations.**—In the preceding chapters there have been discussed methods for the evaluation of stresses in members when the resultant force system is (a) an axial force, which produces direct tension or compression; (b) a couple lying in a plane perpendicular to the transverse plane, producing flexural stresses; and (c) a couple lying in the transverse plane, producing torsional stresses. The purpose of this chapter is to consider the stresses developed in a member by a force lying in a plane perpendicular to the longitudinal axis of the member. The force will be called a cross-shearing force, and the stresses developed will be called cross-shearing stresses or longitudinal-shearing stresses, depending upon whether reference is being made to the stress on a transverse plane or a longitudinal plane.

Cross-shearing forces are always accompanied by bending moments, producing flexural stresses as well as cross-shearing stresses. In addition, twisting, accompanied by torsional stresses, will be produced by cross shear unless the resultant shearing force passes through a specific point in the cross section, known as the "shear center." This condition is analogous to that of axial loading in which the resultant force must pass through the centroid of the section to prevent (or reduce the possibility of) bending. However, the shear center is not necessarily at the centroid of the cross section, as will be shown in Art. 102.

Cross shear is important in beams or other members subjected to transverse loads. For the general case of a horizontal beam carrying vertical loads, the magnitude of the cross-shearing force at any cross section is equal to the ordinate to the shear diagram at that section. The cross-shearing force induces shearing stresses on the vertical transverse plane on which it acts and, in addition, on horizontal planes. At any point in the member the magnitudes of the shearing stresses on the two perpendicular planes are equal.

**100. Evaluation of Stresses Due to Cross Shear.**—The commonly used formula for the evaluation of cross shearing stresses (subject to the same limitations as  $Mc/I$ , since the latter is used in the development) is

$$S_s = \frac{V}{It} \bar{y}a' = \frac{VQ}{It} \quad (207a)$$

in which  $S_s$  is the shearing stress

$V$  is the total vertical shear (from the shear diagram)

$I$  is the moment of inertia of the entire cross section

$t$  is the thickness (or width) at the elevation at which the stress is desired

$Q$  is the moment (with respect to the neutral axis) of the area of the cross section on one side of the section on which the shearing stress is desired.

Equation (207a) may be derived by evaluating the stress at a representative point in the cross section of a member subjected

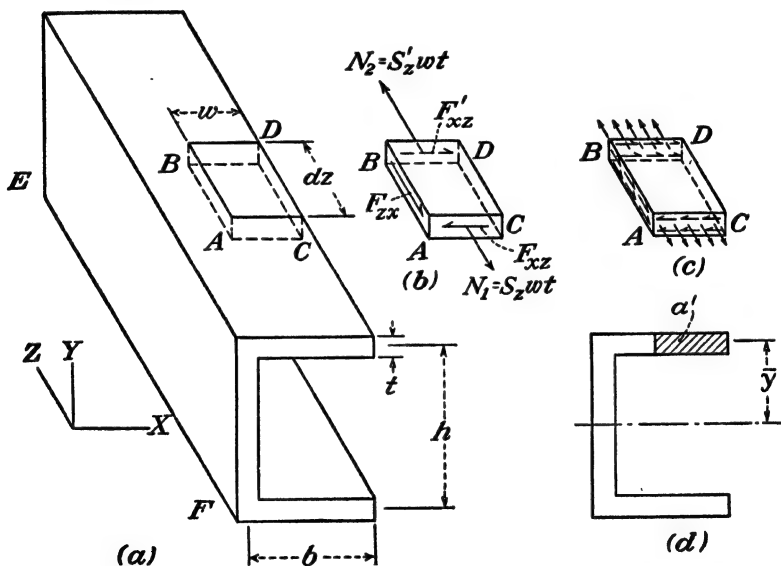


FIG. 102.—Cross shear in flanges of a channel.

to cross shear, such as the channel of Fig. 102a. The channel is assumed to be fixed at  $E$  and to be carrying a vertical concentrated load at the free end  $F$ . The  $z$  axis is in the longitudinal direction, the  $x$  axis is horizontal, and the  $y$  axis is vertical.

To evaluate the cross shearing stress in the upper flange at point *A*, for example, a free-body diagram, Fig. 102*b*, is drawn of the element *ABDC* selected so that the desired shearing stress will be acting on one face (*AC*) of the element. The element has a length *dz* and a width *w*.

As is indicated in Fig. 102*b* a tensile force  $N_1$  is developed on the outer end (*AC*) of the element due to the flexural stress, and a similar force  $N_2$  is developed on the inner end. The force  $N_2$  is greater than  $N_1$  because the moment, and hence the flexural stress, is greater at the inner end. To preserve equilibrium in the longitudinal direction, a shearing force  $F_{xz}$  must be developed on the vertical cut side (*AB*) of the element. No shearing force can act on the free side *CD*.

From the moment equation of equilibrium with respect to a *y* axis, it is evident that the shearing force  $F_{xz}$  will induce the equal and opposite shearing forces  $F_{xz}$  and  $F'_{xz}$  on the ends of the element. From the force equation of equilibrium written in the direction of the length of the beam

$$F_{xz} = N_2 - N_1 \quad (208a)$$

or

$$\begin{aligned} S_{xz}t \, dz &= S'_s wt - S_s wt \\ &= (S'_s - S_s)a' \end{aligned} \quad (208b)$$

in which  $a'$  is the area over which the forces  $N_1$  and  $N_2$  are distributed

$S_s$  and  $S'_s$  are the average values of the flexural stress produced by  $N_1$  and  $N_2$ .

However, if the flexure formula applies,  $S_s$  and  $S'_s$  may be evaluated in terms of the moments at the respective sections, and

$$S_{xz}t \, dz = (M' - M) \frac{\bar{y}}{I} a' \quad (208c)$$

or

$$S_{xz} = \frac{(M' - M)}{dz} \frac{a' \bar{y}}{It} \quad (208d)$$

in which  $M' - M$  is the difference between the bending moment at the two ends of the element

$\bar{y}$  is the distance from the neutral axis to the centroid of the area on which the forces  $N_1$  and  $N_2$  act.



However

$$V = \frac{dM}{dz} \quad (203a)$$

$$= \frac{M' - M}{dz} \quad (203c)$$

in which  $V$  is the total vertical shear at the section under consideration. So

$$S_{xz} = \frac{Va'y}{It} \quad (207)$$

$$= \frac{VQ}{It} \quad (207a)$$

As derived, Eq. (207a) gives the value of the horizontal shearing stress acting in the vertical longitudinal plane  $AB$  of Fig. 102.

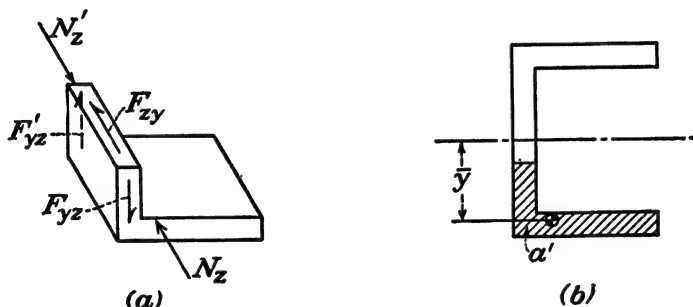


FIG. 103.—Cross shear in web of a channel.

However, because  $S_{xz} = S_{zx}$  at a point, it also gives the value of  $S_{zx}$  at point  $A$  or  $B$ , i.e., the horizontal shearing stress acting in a vertical transverse plane  $AC$  or  $BD$ . The value of the shearing stress, as given by Eq. (207a), is the *average* value throughout the thickness  $t$ . If the section is not of constant thickness, the maximum stress will exceed the value given by Eq. (207a).

The magnitude of the horizontal shearing stress ( $S_{xy}$ ) on a horizontal longitudinal plane, such as a plane through the web, may be found by a similar procedure using the free-body diagram indicated in Fig. 103. It is evident that the expression for  $S_{xy}$  will be identical in form with the expression for  $S_{xz}$ , Eq. (207a), with  $Q$  equal to the first moment of the L-shaped area outside the cut section, and  $t$  equal to the thickness of the web. The vertical shearing stress  $S_{yz}$  in the vertical transverse plane is equal to  $S_{xy}$  at any point.

Hence, all four shearing stresses  $S_{xz} = S_{zx}$  and  $S_{yz} = S_{zy}$  are found by Eq. (207a), with  $Q = a'\bar{y}$ , in which the area  $a'$  is determined by cutting the cross section at the point where the stress is desired, making the cut at right angles to the desired component of stress  $S_{xz}$  or  $S_{yz}$ . The section on either side of the cut may be used for evaluating  $Q$ .

Further consideration of Eq. (207a) shows that the vertical cross-shearing stress  $S_{yz}$  in the flanges will be small because  $Q$

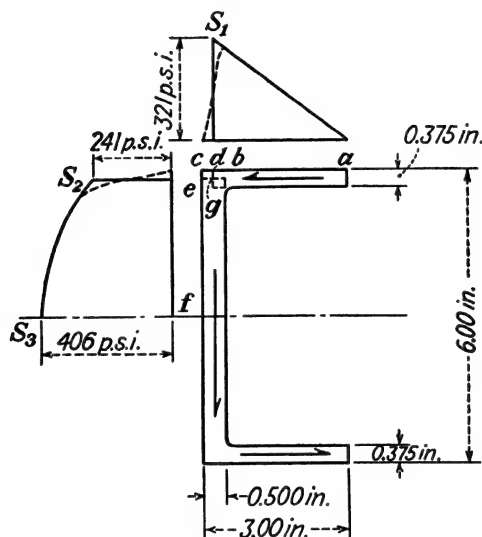


FIG. 104.—Distribution of cross shearing stress in an idealized channel.

is small and  $t$  (in this case the width  $b$  of the flange) is large in comparison with the thickness of the web. Also,  $S_{xz}$  will be zero in the web. Thus, the only cross shearing stresses of consequence in any portion of the cross section are those acting parallel to the boundary of that portion of the cross section.

The distribution of shearing stress due to a cross shear of 1,000 lb. acting on a specific channel is as indicated in Fig. 104. The shearing stress is, of course, zero at the outside of the flange, point  $a$ , and increases directly as the distance from  $a$ , since the only variable in Eq. (207) is the width  $w$  of the area  $a'$ . Beyond  $b$ , the intersection of the flange and web, the horizontal component of the shearing stress decreases to zero at the outer edge  $c$  while the vertical component of the shearing stress increases.

The vertical component of shearing stress in the web is zero at the top  $d$  and increases rapidly to  $e$ , the intersection of the web and bottom of the flange. From  $e$  to  $f$  on the horizontal axis of symmetry, the vertical component of shearing stress increases parabolically because both  $\bar{y}$  and  $a'$  in Eq. (207) vary.

For convenience, the shearing stress in the flange is usually considered to vary linearly from zero to a maximum at  $g$ , the intersection of the center lines of the flange and web. The vertical component of shearing stress is assumed to vary parabolically from  $g$  to  $f$ . If proper fillets are provided, these assumptions are on the safe side, as is the additional assumption that there is no vertical component of shearing stress in the flange. The values of the shearing stresses shown in Fig. 104 are calculated as follows:

$$\begin{aligned} S_1 &= \frac{1,000(0.375)(2.75)(2.8125)}{24.05(0.375)} \\ &= 321 \text{ p.s.i.} \\ S_2 &= \frac{1,000(0.375)(2.75)(2.8125)}{24.05(0.500)} \\ &= 241 \text{ p.s.i.} \end{aligned}$$

The shearing stress at the neutral axis is

$$\begin{aligned} S_3 &= \frac{1,000[0.375(2.50)(2.8125) + 3(0.500)(1.50)]}{24.05(0.500)} \\ &= 406 \text{ p.s.i.} \end{aligned}$$

The values of shearing stress calculated by Eq. (207) are approximate in that they are based on the assumption that the shearing stress is uniformly distributed across the thickness of the cut section. In a section composed of rectangular elements the assumption is reasonable except in the vicinity of the junction of the elements. There stress concentration may be expected. For example, in the channel of Fig. 104 the shearing stress cannot be uniformly distributed on a diagonal section extending from the corner  $c$  to the reentrant corner. Since the stress must be zero at  $c$ , it must be greater than the average at another point on the cut section. The magnitude of the stress concentration at a reentrant corner may be reduced by increasing the radius of the fillet.

At any point on the boundary of the cross section of the beam the resultant shearing stress must be parallel to the boundary,

as, for example, on the curved portions of the I beam of Fig. 105a or the circular section of Fig. 105b. On the vertical center line of the member, the resultant shearing stress must be vertical (for bending about a horizontal neutral axis), and on any transverse section that cuts the curved boundary such as *aa* the magnitude and direction of the resultant shearing stresses vary from point to point. For those sections Eq. (207) gives only the average value of the vertical component of the shearing stress.

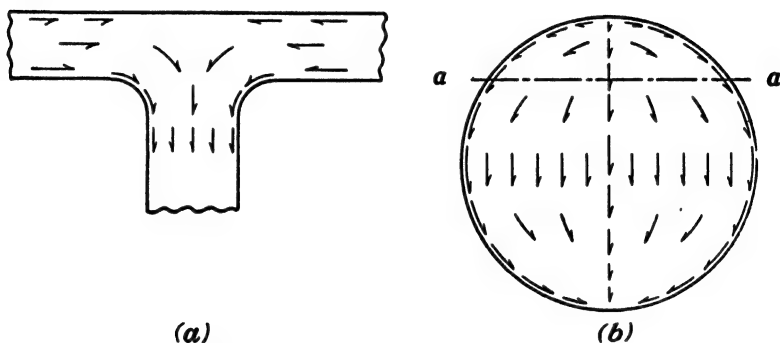


FIG. 105.—Directions of cross shearing stresses.

**101. Bending without Twisting.**—Throughout the preceding discussion the assumption has been made that the flexure formula applies and that the beam does not twist. The stipulation of no twisting involves a definite limitation upon the position of the line of action of the external loads (or plane of the external moments). For example, in the channel of Fig. 104, the shearing stresses in the upper flange are to the left and will produce a resultant shearing force to the left as shown in Fig. 106a. The shearing force in the web will be down, and the shearing force in the lower flange is to the right. The two horizontal shearing forces are equal and their magnitude may be determined as the average shearing stress multiplied by the area over which it acts, or the area under the shearing-stress diagram, Fig. 104, times the thickness.

$$\begin{aligned}
 H &= \frac{1}{2}(321)(2.75)(0.375) \\
 &= 165 \text{ lb.}
 \end{aligned}$$

The vertical shearing force *V* is equal to the area under the parabolic portion of the shearing-stress diagram, Fig. 104,

multiplied by the thickness.

$$\begin{aligned} V &= 241(5.625)(0.500) + \frac{2}{3}(165)(5.625)(0.500) \\ &= 987 \text{ lb.} \end{aligned}$$

The difference between  $V$  and the external shear of 1,000 lb. due to the applied load of 1,000 lb. is the vertical shear carried by the flange. Therefore, the assumption that the web carries all of the vertical shear is about 1.3 per cent in error. The

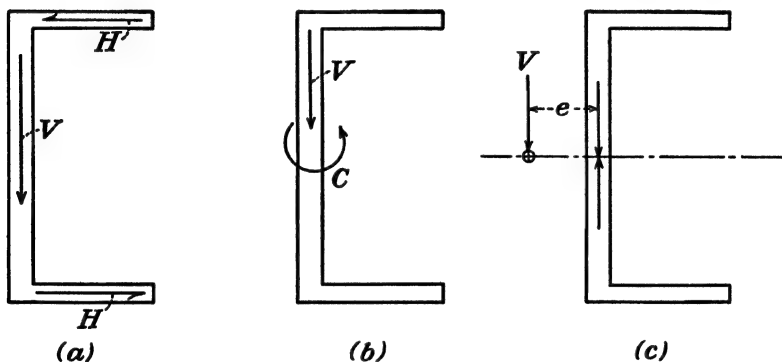


FIG. 106.—Resultant shear on cross section of a channel.

horizontal forces in the flanges form a couple having a magnitude of

$$\begin{aligned} C &= 165(5.625) \\ &= 926 \text{ in.-lb.} \end{aligned}$$

Therefore, the three forces of Fig. 106a may be represented by a force and a couple as shown in Fig. 106b, or the force  $V$  and the couple  $C$  may be replaced by their resultant, a single force  $V$  as shown in Fig. 106c. The line of action of the resultant force  $V$  will be at a distance  $e$  from the center of the web. The distance  $e$  may be found by the principle of moments.

$$e = \frac{926}{1,000} = 0.926 \text{ in.}$$

If the beam is to bend without twisting, the external load  $P$  must be applied in the same plane as the resultant shearing force  $V$ . If the load  $P$  were applied along the center line of the web, for example, it, together with the force  $V$ , would produce a torsional couple that would twist the beam. Then the value of

the maximum shearing stress exceeds that calculated using Eq. (207a) because of the presence of torsional shearing stresses that will add to the cross-shearing stresses at some points. In addition, the maximum normal stresses will exceed those calculated from  $Mc/I$  if the beam is restrained from twisting.

The intersection of the line of action of the resultant shearing force determined using Eq. (207a) with the neutral axis locates the *shear center* or point through which the plane of the loads must pass if the beam is to bend without twisting. The locus of the shear centers along the beam is called the *bending axis* of the beam. If the beam is to bend without twisting, the plane of the external moment must contain the bending axis.

**102. The Shear Center.**—Since a combination of bending and twisting produces unnecessarily large stresses in a beam as well

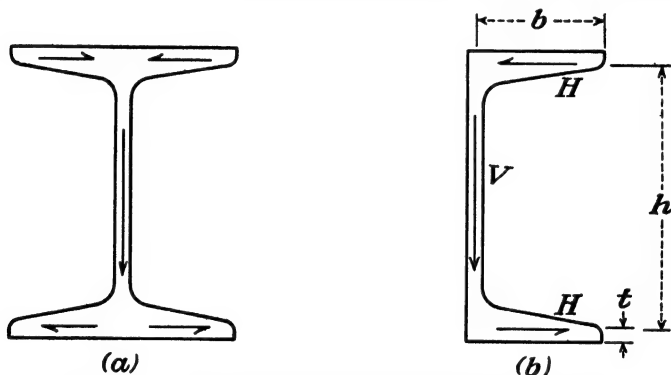


FIG. 107.—Cross shearing forces in I beam and channel.

as undesirable (in most cases) distortion of the beam, the location of the shear center of any cross section is of practical importance. The location of the shear center of a beam may be determined by assuming that the flexure formula is valid and determining the location of the resultant shearing force developed on the cross section, as was done for the channel in Art. 101. The point of intersection of the line of action of the resultant shearing force with the neutral axis of the cross section is the shear center.

For convenience, the beam may be assumed to be loaded as a cantilever and the load assumed to lie in a plane perpendicular to one of the centroidal principal axes of the cross section. If the load does not lie in such a plane, it may be resolved into two components, each of which lies in such planes, and, the two com-

ponents may be treated separately. The principal centroidal axis to which the component of the load is perpendicular becomes the neutral axis.

If the cross section has an axis of symmetry, the shear center will lie on the axis of symmetry, and if there are two axes of symmetry, the shear center will lie at the intersection of the axes, which is the centroid.

Horizontal shearing forces may be developed in the cross section of a beam having two axes of symmetry, such as the I beam of Fig. 107a. However, they are balanced and do not cause the beam to twist when loaded through the centroid. The channel of Fig. 107b will twist when loaded through the centroid because the shearing forces are not balanced.

**103. Shear Center of a Channel.**—The approximate location of the shear center of a channel, Fig. 107b, may be determined by the procedure outlined. The force  $V$  may be assumed to act along the center line of the web, and  $H$  may be assumed to act along the center line of the flange. The horizontal shearing forces  $H$  may be evaluated as the average cross-shearing stress in the flange, from Eq. (207a), multiplied by the area.

$$H = \frac{\frac{1}{2} V a_f \frac{h}{2} a_f}{\left[ 2a_f \left( \frac{h}{2} \right)^2 + \frac{a_w h^2}{12} \right] t} \quad (209a)$$

$$= \frac{V b a_f}{2h \left( a_f + \frac{a_w}{6} \right)} \quad (209b)$$

in which  $a_f$  is the area of one flange

$a_w$  is the area of the web.

The distance  $e$  from the center line of the web to the location of the resultant is found by the principle of moments.

$$e = \frac{Hh}{V} \quad (209c)$$

$$= \frac{\frac{1}{2} b}{1 + \frac{a_w}{6a_f}} \quad (209d)$$

Equation (209d) indicates that  $e = 0$  for  $a_f = 0$ , and  $e$  increases as the ratio  $a_w/a_f$  decreases. In the extreme case of  $a_w/a_f = 0$ ,

$e = \frac{1}{2}b$ . That is, the shear center is at the intersection of the center line of the flange with the neutral axis.

**104. Shear Flow.**—In some problems, particularly those dealing with thin-webbed beams subjected to both bending and torsion, it is more convenient to work with the magnitude of the shearing force per inch of length along the perimeter of the cross section than with the average stress. As was pointed out in

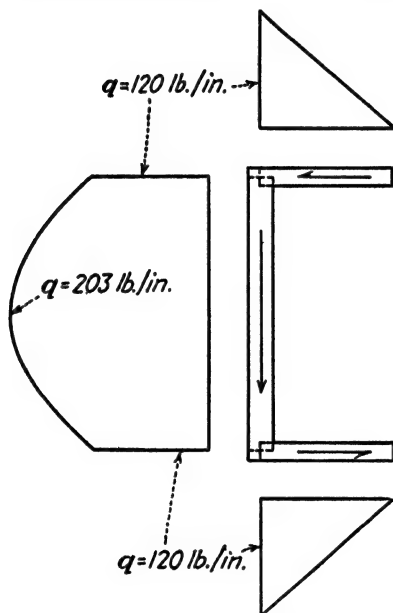


FIG. 108.—Shear flow in a channel.

Art. 72, the magnitude of the shearing force per unit length is called the “shear flow.” It is equal to the average shearing stress on a section multiplied by the thickness of the section. If the beam is subjected to bending only, the shear flow may be found by multiplying each side of Eq. (207a) by the thickness  $t$ .

$$q = S_t = \frac{VQ}{I} \quad (210)$$

in which  $q$  is the shear flow.

The shear flow is usually expressed in pounds per inch. Along a section of constant thickness the shear-flow is distributed in the same way as the average shearing stress. The shear-flow



diagram for the channel of Fig. 104 is shown in Fig. 108. The value of the shear flow at point  $g$  is, from Eq. (210),

$$\begin{aligned} q_1 &= \frac{1,000(0.375)(2.75)(2.8125)}{24.05} \\ &= 120 \text{ lb. per in.} \end{aligned}$$

The shearing stress  $S_1$  in the flange is

$$S_1 = \frac{q_1}{t_1} = \frac{120}{0.375} = 321 \text{ p.s.i.}$$

which agrees with the value given in Fig. 104. The shearing stress  $S_2$  in the web is

$$S_2 = \frac{q_1}{t_1} = \frac{120}{0.500} = 240 \text{ p.s.i.}$$

**105. Shearing Stresses and Shear Center in Thin-webbed Beams.**—Unless the span is unusually short, a beam of light-weight construction is generally a beam with relatively heavy flanges at a maximum distance apart (to be more effective in resisting bending) connected by a relatively thin web. With such construction and with the load applied so that the neutral axis is perpendicular to the line joining the centroids of the flanges, the flanges will carry comparatively little shear, and the web will offer practically no bending resistance, so the shear flow will be virtually constant throughout the web. That is, for a beam consisting of two flanges connected by a thin web the value of  $Q$  in Eq. (210) is the  $Q$  of the flange plus the  $Q$  of the web, but the latter is negligible because of less area and a smaller moment arm. Therefore,  $Q$  is the same for any point in the web, and since  $V$  and  $I$  are constant,  $q$  is constant throughout the web. Thus, the shear flow throughout the web is equal to the total vertical shear divided by the depth of the beam. If the web is straight and at right angles to the neutral axis, the maximum shearing stress is approximately equal to the average shearing stress obtained by dividing the total vertical shear by the area of the web. The shear center will be at the centroid.

If the two flanges are connected by a thin curved web, as illustrated in Fig. 109a, the shear center will not be at the centroid. The location of the shear center may be determined by the

standard procedure outlined in Art. 102. If the bending resistance of the web is negligible, it is apparent that one centroidal principal axis will pass through the centroids of the flanges along the line  $AB$ . The plane of the loads will therefore be assumed to include the line  $AB$ , and the neutral axis will be perpendicular to  $AB$ . Since the bending resistance of the web is negligible, the shear flow is constant throughout the web and is equal to  $V/h$ . Also, the resultant shearing force developed in the web must be equal to  $V$  and must be parallel to  $AB$  to preserve equilibrium.

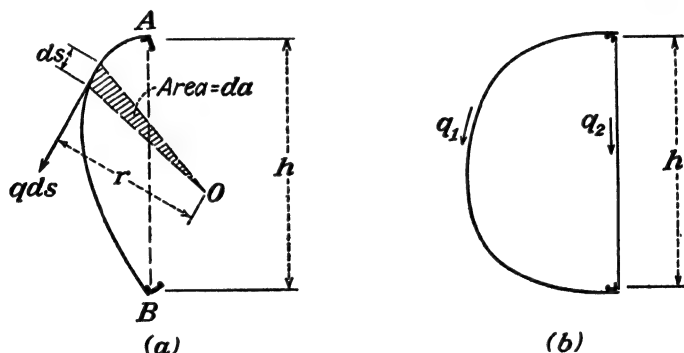


FIG. 109.—Shear flow in thin-webbed beams.

The position of the line of action of the resultant shearing force may be found by taking moments of the shear flow with respect to some convenient axis such as one through the point  $O$ . The resultant force developed on a length  $ds$  of the web is  $q ds$  and its line of action is tangent to the web. The moment of the force with respect to the point  $O$  is

$$dM = qr ds \quad (211)$$

However

$$r ds = 2 da \quad (211a)$$

in which  $da$  is the area enclosed by lines from  $O$  to the ends of the element. Then

$$dM = 2q da \quad (211b)$$

and since  $q$  is constant, the total moment developed by the cross shear is

$$M = 2qA \quad (211c)$$

in which  $A$  is the area enclosed by the web and the lines  $OA$  and  $OB$ .

By the principle of moments

$$qhe = 2qA \quad (211d)$$

in which  $e$  is the distance between the point  $O$  and the line of action of the resultant shearing force,  $qh$ . Then

$$e = \frac{2A}{h} \quad (211e)$$

Therefore, the shear center will be located on the neutral axis at a distance  $e$  (measured perpendicular to  $AB$ ) from the point  $O$ .

If the thin-webbed beam has a closed cross section, as, for example, that indicated in Fig. 109b, the shear flow will usually be different in the two webs but will be constant throughout each web. The total vertical shear will be

$$V = q_1h + q_2h \quad (212)$$

$$= h(q_1 + q_2) \quad (212a)$$

in which  $q_1$  and  $q_2$  are the values of shear flow in webs 1 and 2 respectively. As before, a moment equation may be written. For the beam shown in Fig. 109b a center of moments on web 2 will be convenient.

$$M = Ve = 2q_1A \quad (213)$$

A third equation may be obtained from the condition that the beam is to bend without twisting. The angle of twist from Eq. (158d) is

$$\theta = \frac{TsL}{4A^2tG} \quad (158d)$$

However

$$T = 2Aq$$

Hence

$$\frac{2Aq_1s_1L}{4A^2t_1G} = \frac{2Aq_2s_2L}{4A^2t_2G} \quad (214)$$

or

$$\frac{q_1s_1}{t_1} = \frac{q_2s_2}{t_2} \quad (214a)$$

Equations (212a), (213), and (214a) may be solved simultaneously for  $e$ , giving

$$e = \frac{2q_1 A}{V} \quad (215)$$

$$= \frac{2A}{h \left( 1 + \frac{s_1 t_2}{s_2 t_1} \right)} \quad (215a)$$

A comparison of Eqs. (215a) and (211e) indicates the effect of the second web in moving the shear center nearer to the centroid of the cross section.

If the cross section of the beam consists of several closed sections, the shear flow may be found by writing a series of equations similar to Eq. (214), which together with Eqs. (212a) and (213) provide sufficient information to permit solving for the unknowns. Sections composed of several cells may also be solved by successive approximation methods similar to those used in torsion.

If the resultant external shearing force does not pass through the shear center, it may be resolved into a force through the shear center producing cross-shearing stresses and a couple producing torsional-shearing stresses. The resultant shearing stress at any point will be the algebraic sum of the two, provided that the proportional limit is not exceeded or that buckling or other structural failure does not occur.

**106. Secondary Effects.**—The shearing stresses in thin-walled beams may be sufficiently great to produce compressive stresses

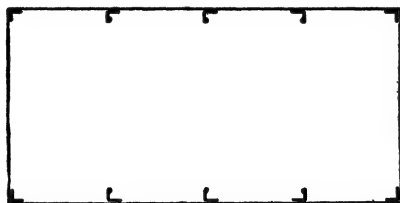


FIG. 110.—Beam with multiple flange units.

(at 45 deg. with the maximum shearing stresses) in excess of the critical buckling stress, resulting in undesirable distortion if not collapse. Buckling stresses are considered in Chap. 11. In most cases, stiffeners may be provided to prevent buckling.

A phenomenon encountered in multiple-flange beams similar to the one indicated in Fig. 110 is called "shear lag." It results in an uneven distribution of flexural stress throughout the flange elements and is due to the shearing deformation developed in the thin sheet connecting the flange elements. The shear flow, shearing stress, and shearing strain in the sheet are higher near the web than remote from the web. The unequal shearing deformation causes the section remote from the web to "lag" as the beam is bent. The result is that a plane section does not remain plane, the flange units near the web are overstressed, and those remote from the web are understressed. The same effect may occur in a wide-flanged I beam.

### PROBLEMS

**263.** A timber beam 4 in. wide and 8 in. deep carries a uniformly distributed load on an 8-ft. span. What must be the ratio of shearing strength to flexural strength for the beam to be equally strong in shear and bending? What is an average value of the ratio for structural timber?

**264.** A symmetrical hollow timber beam has outside dimensions of 6 by 12 in., inside dimensions of 4 by 8 in., and is simply supported on a 12-ft. span. It carries a 3,000-lb. load 4 ft. from the left end. Plot a curve showing the variation in shearing stress throughout the depth at a section 2 ft. from the left end.

**265.** Make a diagram showing the distribution of the shearing stresses due to a load of 1,000 lb. in a channel similar to that of Fig. 104, but with all dimensions doubled.

**266.** Determine the distribution of shearing stress throughout the cantilever beam indicated in Fig. P-266 if it carries a load of 1,000 lb. at the end. All sections are 0.05 in. thick.

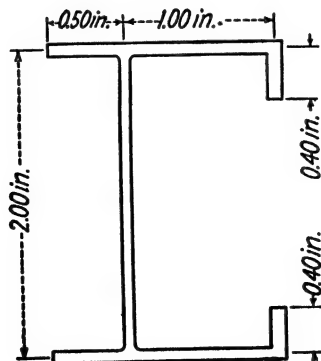


FIG. P-266.

**267.** A beam having the cross section shown in Fig. P-267 is subjected to a total vertical shear of 1,000 lb. Make a sketch showing the distribution of shearing stress throughout the beam.

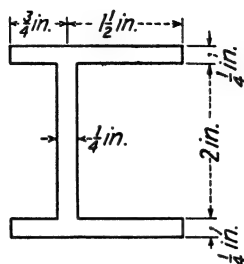


FIG. P-267.

**268.** A beam having a cross section in the form of a cross as shown in Fig. P-268 is subjected to a vertical load of 1,000 lb. Draw a diagram showing the approximate distribution of shearing stress in the beam.

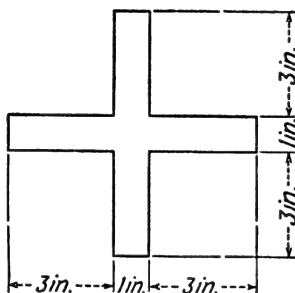


FIG. P-268.

**269.** Locate the shear center of a 6- by 6- by 1-in. angle.

**270.** Locate the shear center of a 12-in., 40-lb. channel.

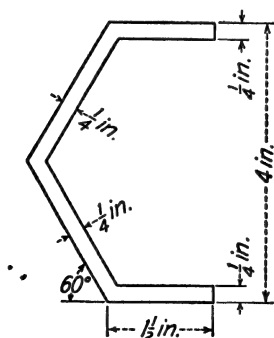


FIG. P-273.

**271.** Determine the location of the shear center of the cross section indicated in Fig. P-266.

**272.** Locate the shear center of the Z section shown in Fig. P-233.

**273.** Where is the shear center of the section shown in Fig. P-273?

**274.** Locate the shear center of a half ring having a mean radius  $R$  and a wall thickness  $t$ .

**275.** Draw the shear-flow diagram and locate the shear center of the beam shown in Fig. P-267.

**276.** A symmetrical thin-webbed beam has two flanges of area  $a$  and their centroids are a distance  $h$  apart. Develop an expression for the percentage error involved in computing the maximum cross-shearing stress as  $V/t h$ .

**277.** Construct the shear-flow diagrams and locate the shear center of each of the built-up beams indicated in Fig. P-277. Assume that the sheet carries only shear and that the angles carry only direct stress.

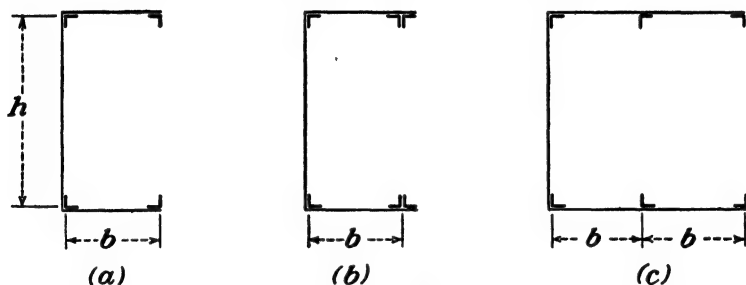


FIG. P-277.

**278.** Solve Prob. 277 assuming that the sheet can resist tension as well as shear but will buckle in compression.

**279.** Locate the shear center of the airplane wing section shown in Fig. P-220.

**280.** A horizontal cantilever beam 6 ft. long is formed from 0.040-in. sheet metal to produce a hollow rectangular cross section with a mean width of 2 in. and a mean depth of 4 in. The seam that runs the full length of the beam is located at the center of the bottom face and is not welded or connected in any way. The beam carries a vertical load of 100 lb., applied through a bracket at the free end in such a way that the line of action of the load is along the center line of one of the vertical sides. Determine the maximum shearing stress developed on a cross section 3 ft. from the load and indicate its location and direction on a sketch. Neglect stress concentration.

**281.** A tube with an outside diameter of 4 in. and a wall thickness of 0.065 in. has a thin longitudinal slit in the wall throughout its length. It is subjected to a cross-shearing force of 100 lb., the line of action of the force passing through the center of the circle and being perpendicular to the diameter through the slit. Determine the maximum shearing stress developed by the 100-lb. force.

## CHAPTER X

### INTRODUCTION TO PHOTOELASTIC ANALYSIS

**107. The Photoelastic Method.**—One of the important experimental methods that have been devised to aid in the determination of stresses in members of complex shape is the photoelastic method. It is based on the effect that the stresses in certain transparent materials have upon a ray of light passed through the member. The photoelastic method provides a rapid qualitative picture of the stress distribution in a member, as well as providing quantitative information from which the stresses may be evaluated. It is particularly useful in investigating the effect of stress concentration. Because of the adaptability of the photoelastic method to engineering problems it has received much attention in the literature, and several books<sup>1</sup> have been written describing the theory and techniques of application. The purpose of this chapter is to offer a preview of the subject rather than a complete treatment.

**108. Analytical Representation of Light.**—Light travels through air and other media along straight paths called "rays." In a given medium the velocity of a ray of light is constant and is independent of the color. In a vacuum the speed of light is  $983.571 \times 10^6$  f.p.s. (186,284 m.p.s.)

A number of phenomena associated with light may be explained by assuming that a ray of light is propagated as a series of transverse waves, which may lie in any or all planes containing the ray. The nature of any of the waves is such that the lateral displacement of any point plotted against time gives a sine, or cosine, curve and may be expressed in equation form as

$$y = a \sin \omega t \quad (216)$$

in which  $y$  is the displacement at any time  $t$

$a$  is the amplitude, or maximum displacement of the point from its mean position.

<sup>1</sup> COKER, E. G., and L. N. G. FILON, "Photo-elasticity," Cambridge University Press, London 1931.

FROCHT, M. M., "Photoelasticity," John Wiley & Sons, Inc., New York, 1941.



If the amplitude is not zero at zero time, the equation may be written as

$$y = a \sin \omega(t - t_o) \quad (216a)$$

in which  $t_o$  is the time at which the amplitude becomes zero.

A graphical representation of the wave is given in Fig. 111b. The quantity  $\omega$  in Eq. (216) may be interpreted by considering the sine curve as being generated by a point moving with constant angular velocity  $\omega$  on a circular path with radius  $a$  as indicated in Fig. 111a. One cycle is completed for each com-

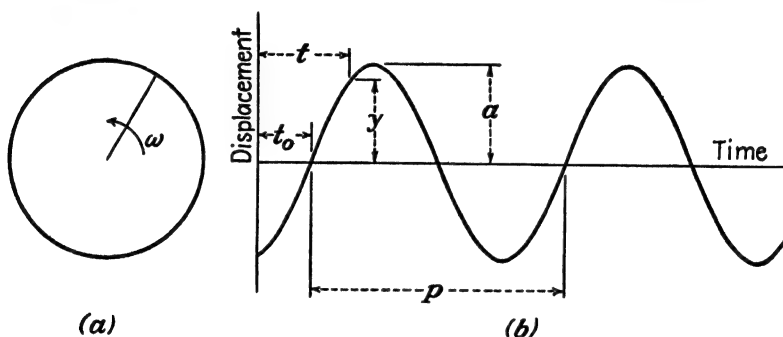


FIG. 111.—Analytical representation of light.

plete revolution of the point; i.e., for the angle  $\omega t$  equal to  $2\pi$  radians. The time required for one complete cycle or vibration is the *period*  $p$ , and the distance that the light travels in that time interval is the *wave length*  $\lambda$ . The number of cycles completed per unit time is the *frequency*  $f$ . From the definitions it is evident that

$$p = \frac{1}{f} \quad (217)$$

$$v = f\lambda \quad (217a)$$

in which  $v$  is the velocity of light.

The intensity of the light is proportional to the square of the amplitude of vibration, and the color is dependent upon the frequency. The frequency is independent of the medium through which the ray is propagated, but the velocity is dependent upon the medium. Therefore, the wave length varies with the medium. The wave length of the visible spectrum in air

ranges from 4,000 Å for violet<sup>1</sup> to about 7,000 Å for red light. White light is a mixture of other colors in definite proportions.

**109. Polarized Light.**—If the vibrations of a light ray are restricted to one plane, the ray is said to be plane polarized. Light may also be produced in which the wave motion is helical with a constant amplitude and a uniformly varying direction of polarization. The light is then said to be circularly polarized.

Several methods are available for converting a ray of light into a plane-polarized ray.

1. Reflection from a plane surface. All rays except those vibrating in one plane are absorbed. The “glare” reflected from a water surface, roadway, or table top is plane-polarized light.

2. Transmission through a stack of properly oriented glass plates.

3. Transmission through a Nicol prism, consisting of a pair of crystals of Iceland spar (calcite) properly cut and cemented together.

4. Transmission through a Polaroid<sup>2</sup> element. This is the most satisfactory method of polarization for photoelastic purposes because it provides a large field with comparatively little loss of light intensity. About 45 per cent of the incident light is transmitted.

The direction of the intersection of the plane of the polarizing element with the plane in which the vibrations of polarized light occur is known as the “axis of polarization.” If a horizontal light ray is passed through a polarizing element having a horizontal axis of polarization the ray that emerges will be vibrating in a horizontal plane only. If the ray is then passed through a second polarizing element having a vertical axis of polarization no ray will emerge from the second unit. If the second unit is rotated slightly a component of the ray with a decreased amplitude will emerge, and if the rotation is continued until the axes of polarization of the two elements are parallel, all<sup>3</sup> of the light that passes the first element will be transmitted through the second element.

<sup>1</sup> The unit Å, called the Angstrom unit, equals  $1 \times 10^{-10}$  meters.

<sup>2</sup> Polaroid is the trade name for a unit consisting of a film of properly oriented crystals cemented between two glass plates.

<sup>3</sup> Assuming that no light is lost in transmission through the element. Actually the efficiency of a Polaroid element is about 90 per cent.

**110. Refraction of Polarized Light.**—Certain noncrystalline transparent materials, including glass and a number of plastics,<sup>1</sup> when stressed will resolve an incident polarized light ray into two component rays, one in the direction of each of the principal stresses. Such materials are said to be double refracting. The velocities of the component rays through the material depend upon the magnitudes of the principal stresses, the change in velocity being proportional to the stress.

The resolution of a plane-polarized ray is indicated in Fig. 112*a*. The original plane-polarized ray, which may be assumed to enter the model beam of Fig. 112*b* at the point *M* is traveling

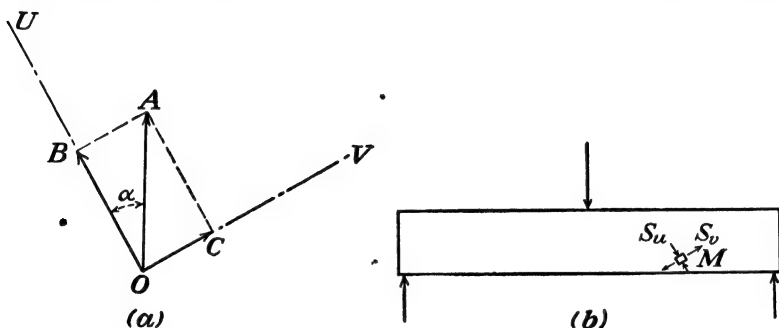


FIG. 112.—Resolution of a plane-polarized ray.

along a path perpendicular to the plane of the paper and may be represented by the vector *OA* in Fig. 112*a*. The direction of *OA* is vertical, indicating the direction of the axis of polarization, and the length *OA* represents the amplitude. As the ray enters the beam that is stressed, the direction of the principal stresses being the *u* and *v* directions, the ray *OA* will be resolved into the component rays *OB* and *OC* in the *u* and *v* directions as indicated. Since the length *OA* represents the amplitude of the entering ray, the amplitudes of the two component rays will be determined as the lengths *OB* and *OC*.

$$OB = OA \cos \alpha$$

$$OC = OA \sin \alpha$$

The displacement *y* of the original plane-polarized ray is, from

<sup>1</sup> The most satisfactory material for photoelastic purposes appears to be Bakelite BT 61-893. It is optically sensitive and is easily shaped. Other materials have been used with good results.

Eq. (216),

$$y = a \sin \omega t \quad (216)$$

Hence, the equation for the displacement  $u$  of the component in the  $u$  direction at any time  $t$  is

$$u = a \cos \alpha \sin \omega t \quad (216a)$$

and in the  $v$  direction

$$v = a \sin \alpha \sin \omega t \quad (216b)$$

while the rays are traveling through the material. If the thickness of the material is  $d$ , the time required for the  $u$  component of the ray to travel through the material is

$$t_u = \frac{d}{V_u} \quad (218a)$$

in which  $V_u$  is the velocity of the  $u$  component of the ray.

The component in the  $v$  direction will emerge at a different time because it will travel at a different velocity, the velocity being dependent upon the stress. The time required for it to travel through the material is

$$t_v = \frac{d}{V_v} \quad (218b)$$

The equations for the displacement of the component rays upon emergence from the stressed material are

$$u = a \cos \alpha \sin \omega(t - t_u) \quad (219a)$$

$$v = a \sin \alpha \sin \omega(t - t_v) \quad (219b)$$

The retardation, or time lag, of one component with respect to the other is

$$t_v - t_u = \frac{d}{V_v} - \frac{d}{V_u} \quad (220)$$

$$= \frac{(V_u - V_v)}{V_u V_v} d \quad (220a)$$

$$= \left[ \frac{(V_u - V) - (V_v - V)}{V_u V_v} \right] d \quad (220b)$$

Since  $V_u V_v$  is approximately constant (approximately  $V^2$ ), and since the change in velocity is proportional to the principal stress, the retardation is approximately proportional to the difference between the two principal stresses. That is

$$t_v - t_u = C(S_u - S_v) \quad (220c)$$

If the component rays emerging from the stressed material are passed through a second polarizing element (called "an analyzer") having its axis of polarization at right angles to the axis of the original polarizer, each of the component rays  $OB$  and  $OC$  will be resolved into two components as indicated in Fig. 113.

The rays  $OB'$  and  $OC'$  will be transmitted, and the components  $OB''$  and  $OC''$  normal to them are extinguished. The amplitudes

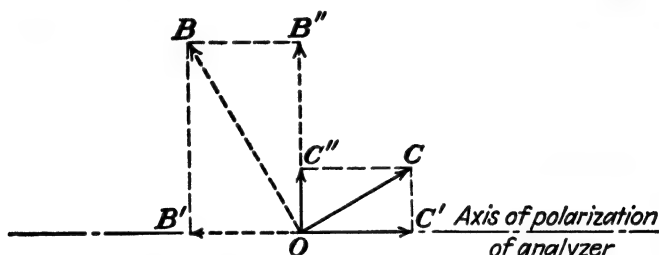


FIG. 113.—Resolution of double-refracted ray by analyzer.

of the rays that emerge from the second polarizer are

$$\begin{aligned} OB' &= OB \sin \alpha \\ &= a \cos \alpha \sin \alpha \\ &= \frac{a}{2} \sin 2\alpha \end{aligned} \quad (221a)$$

$$\begin{aligned} OC' &= OC \cos \alpha \\ &= a \sin \alpha \cos \alpha \\ &= \frac{a}{2} \sin 2\alpha \end{aligned} \quad (221b)$$

Therefore the two rays  $OB'$  and  $OC'$  that emerge from the analyzer have the same amplitude, and their equations are

$$u' = \frac{1}{2}a \sin 2\alpha \sin \omega(t - t_u) \quad (219c)$$

$$v' = \frac{1}{2}a \sin 2\alpha \sin \omega(t - t_v) \quad (219d)$$

However, they are not necessarily in phase because of the difference in the time required for the two components to travel through the material. The resultant ray will be the vector difference of the component rays. Its equation may therefore be written as

$$r' = \frac{1}{2}a \sin 2\alpha \sin \omega(t - t_u) - \frac{1}{2}a \sin 2\alpha \sin \omega(t - t_v) \quad (222)$$

$$= \frac{1}{2}a \sin 2\alpha [\sin \omega(t - t_u) - \sin \omega(t - t_v)] \quad (222a)$$

If  $t_u = t_v$ , the two component rays  $OB'$  and  $OC'$  emerge 180 deg. out of phase as shown in Fig. 114a, and there will be no resultant light. If the component rays are partially out of phase as shown in Fig. 114b, their resultant will be a vector of the same frequency, but of only slightly larger amplitude than either one of the components. That is, the transmitted light is weaker than the original light. If the retardation is such that the component rays are in phase, a vector of maximum amplitude is developed as shown in Fig. 114c. The amplitude of the resultant

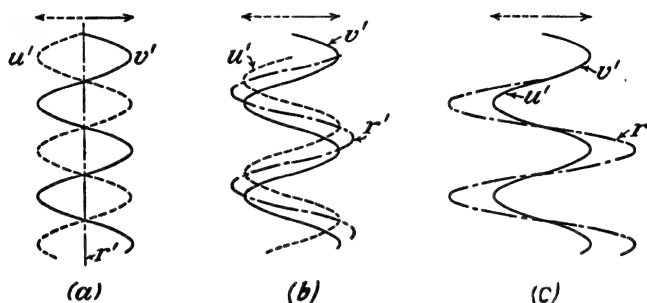


FIG. 114.—Effect of relative retardation on resultant ray.

ray will become zero (there will be no transmitted light) under two conditions.

1. When  $\alpha = 0$ ,  $\sin 2\alpha = 0$ . This corresponds to the condition of the plane of polarization coinciding with the direction of one of the principal stresses. Only one component ray will emerge from the specimen, and it will be annihilated by the analyzer.

2. The amplitude of the resultant ray will also be zero when

$$\sin \omega(t - t_u) = \sin \omega(t - t_v) \quad (223)$$

This condition is satisfied when

$$\omega(t - t_u) = \omega(t - t_v) + 2n\pi \quad (223a)$$

in which  $n$  is any integer. Then

$$\omega(t_v - t_u) = 2n\pi \quad (223b)$$

However, the quantity  $t_v - t_u$  was evaluated in terms of the principal stresses in Eq. (220c), hence

$$\omega C(S_u - S_v) = 2n\pi \quad (224)$$

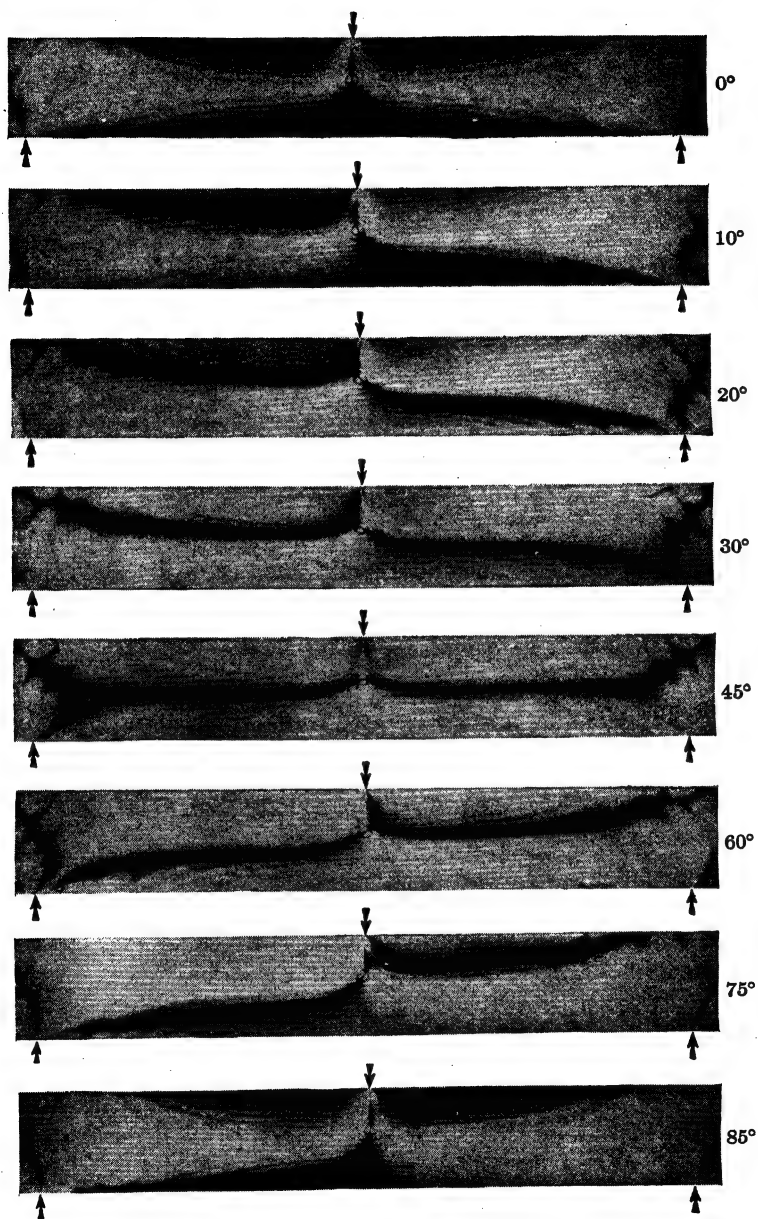


FIG. 115.—Isoelincs for a beam carrying a concentrated load. (*Reproduced by permission from Photoelasticity, by Max M. Frocht, John Wiley & Sons, Inc., New York.*)

from which

$$S_u - S_v = \frac{2n\pi}{\omega C} \quad (224a)$$

or from the relationship between principal stresses and maximum shearing stress, Eq. (20),

$$S_{ij} = \frac{n\pi}{\omega C} \quad (224b)$$

$$= \frac{n\pi V_u V_v}{\omega d} \quad (224c)$$

$$S_{ij} = \frac{nK}{d} \quad (224d)$$

in which  $K$  is a constant for the material,<sup>1</sup> called the "fringe value."

Then

$$S_u - S_v = \frac{2nK}{d} \quad (225)$$

From the first condition it is apparent that if the light source is made sufficiently large to illuminate the entire specimen, a black spot will appear on the projected image of the beam at every point for which the directions of the principal stresses coincide with the directions of the axes of polarization. The locus of these points is a line, known as an "isoclinic." If desired, the isoclinics may be eliminated from the image by using circularly polarized light. Figure 115 shows a series of isoclinics obtained from a beam carrying a concentrated load.

From the second condition, it is apparent that no light will be transmitted whenever the stresses are such that Eqs. (224d) or (225) are satisfied for an integral value of  $n$ . Therefore, a set of black points will be formed on the image for each integral value of  $n$ . The loci of the points are lines, known as "fringes," and the number  $n$  is the fringe order; hence, the black line corresponding to an  $n$  of 1 is called the "first-order fringe," the line corresponding to an  $n$  of 2 is the "second-order fringe," etc. The fringes are unaffected by the use of circularly polarized light. A set of fringes for the beam of Fig. 115 is shown in Fig. 116. The twelfth-order fringe is at the bottom of the beam under the load.

<sup>1</sup> For bakelite BT 61-893,  $K$  is approximately 43 lb. per in.



If plane-polarized white light is used instead of monochromatic light, the isoclinics still appear as black lines, but the black fringes are replaced by colored bands going through the spectrum in regular sequences, each spectrum replacing a fringe. Each

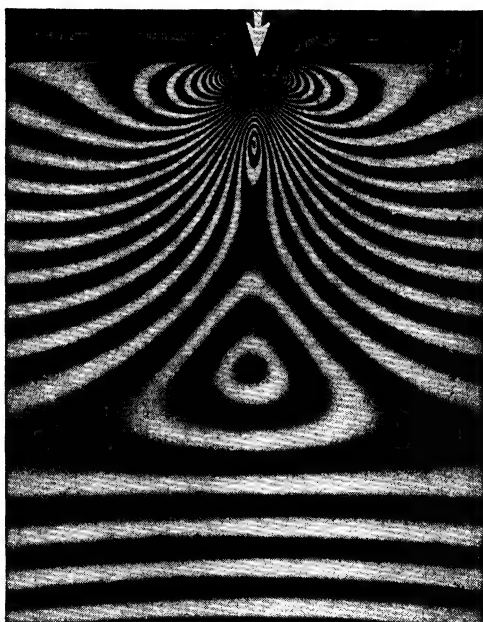
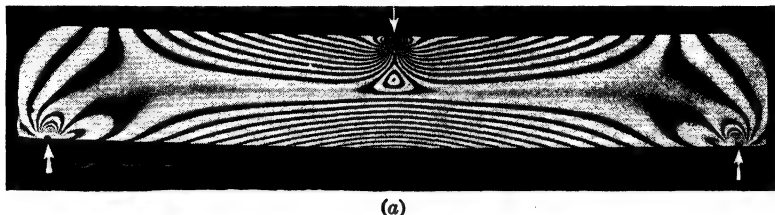


FIG. 116.—Fringe pattern for a beam carrying a concentrated load. (a) Isochromatics for entire beam; (b) enlargement of center portion. (Reproduced by permission from "Photoelasticity," by Max M. Frocht, John Wiley & Sons, Inc., New York.)

line of a single color is called an "isochromatic." The appearance of the isochromatics is due to the fact that the amount of refraction varies with the wave length (color) of the light. The white light is therefore broken up into its component colors in passing through the model and various colors are annihilated

at various stress levels. The colored bands may be used as well as the black and white bands in making a stress analysis. Current practice favors the use of a monochromatic light source, with its resulting black and monochromatic bands, because of the difficulty of matching colors for readings in the rainbow pattern. Test results<sup>1</sup> verify the theoretical conclusion that stress values for successive fringes of a given color are multiples of the first fringe value. It is also shown that the stress values corresponding to the first yellow fringe are  $\frac{1}{3}$  of the values for the first green fringe, and values for the first red fringe are  $\frac{2}{3}$  of the values for the first green fringe.

**111. Application to Stress Analysis.**—The experimental setup requires the following items in the order indicated.

1. Light source (monochromatic light preferable).
2. Polarizer.
3. Quarter-wave plate (unless isoclinics are desired).
4. Transparent model.
5. Quarter-wave plate.
6. Analyzer (axis of polarization normal to polarizer).
7. Screen or camera.

The model, carefully prepared from a suitable material and annealed to remove initial strains induced by shaping, is placed in a frame by means of which loads may be applied as desired.

At a given point in the model for a given load two observations may be made.

1. The directions of the principal stresses. The directions are obtained by loading the model, removing the quarter-wave plates and rotating the polarizer and analyzer together until a black spot appears at the point. The directions of the principal stresses then correspond to the directions of the axes of polarization of the polarizer and analyzer.

2. The magnitude of the maximum shearing stress or the algebraic difference between the principal stresses. Before load is applied to the model its image will present a uniform appearance. As load is applied slowly a band or fringe will appear at the point or area of maximum shearing stress, and will gradually move as the load is increased. Presently there will appear a second band, the second-order fringe, corresponding

<sup>1</sup> For example, FROCHT, M. M., "Photoelasticity," p. 169, John Wiley & Sons, Inc., New York, 1941.

to double the shearing stress of the first-order fringe. Further increases in load will develop higher orders of fringes, the low-order fringes moving across the specimen in sequence. The relationship between the fringes and the stress depends upon the properties of the material of which the model is constructed as indicated in Eq. (224). It is evident that a direct evaluation of the maximum shearing stress would require the values of  $n$ , the fringe order;  $\omega$ , which is dependent upon the color of the light;  $V_u$  and  $V_v$ , the velocities of the rays in the model; and  $d$ , the thickness of the model. Practically, it is easier to use a calibration strip of the same material and the same thickness loaded in such a way that the shearing stress corresponding to a given fringe order may be calculated directly.

**112. Evaluation of Principal Stresses.**—As is evident from Eq. (225), the fringe value at a given point will permit the evaluation of the differences of the principal stresses but will not permit the direct evaluation of either principal stress unless one of them is known. If the point under consideration is at a free boundary of the member, one principal stress is zero, and the other may be evaluated directly. Also, if the point is at a boundary on which a pressure or load of known intensity is applied without shear, that pressure must equal one of the principal stresses.

However, if the point is on the interior, some additional information must be obtained that will yield a value of one of the principal stresses or the magnitude of their sum.

One of the techniques that may be used is that of shear differences,<sup>1</sup> which is based on the equation of equilibrium of a small block of the material. For example, the block *A* cut from the beam indicated in Fig. 117*a* will be subjected to normal and shearing forces as shown in Fig. 117*b*.

The equation of equilibrium written in the  $y$  direction gives

$$(S_y + dS_y)t dx - S_y t dx + (S_{xy} + dS_{xy})t dy - S_x t dy = 0 \quad (226)$$

or

$$dS_y dx + dS_{xy} dy = 0 \quad (226a)$$

If Eq. (226*a*) is divided through by  $dx$  and integrated, there results

$$S_{y_0} - S_{y_1} = \int_{y_0}^{y_1} \frac{dS_{xy}}{dx} dy \quad (226b)$$

<sup>1</sup> FROCHT, M. M., "Photoelasticity," John Wiley & Sons, Inc., New York, 1941.

in which  $S_{y_0}$  is the stress at an elevation  $y_0$

$S_{y_1}$  is the stress at an elevation  $y_1$ .

or

$$S_{y_0} - S_{y_1} = \sum_{y_0}^{y_1} \frac{dS_{xy}}{dx} \Delta y \quad (226c)$$

That is, the difference between the normal stresses on two parallel planes is equal to the rate of change of the shearing stress at right angles to the planes multiplied by the distance between the planes.

To evaluate the normal stresses using Eq. (226c) a straight line is drawn across the member through the point at which the stress

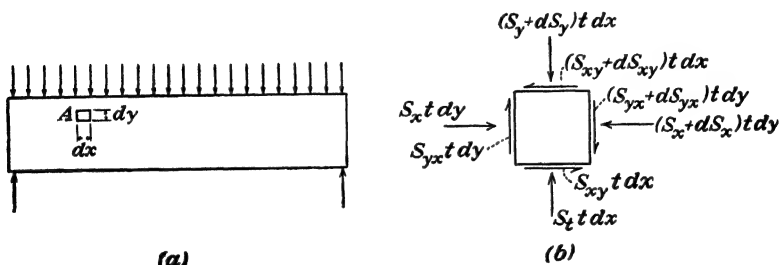


Fig. 117.—Components of stress in a beam.

is desired. That line defines the  $y$  direction. The line is divided into an appropriate number of segments, each having a length  $\Delta y$ . Next, the shearing stress  $S_{xy}$  is evaluated at a short distance on each side of the end of each of the segments with the aid of Eq. (17)

$$\begin{aligned} S_{xy} &= \frac{1}{2}(S_u - S_v) \sin 2\theta \\ &= S_{ij} \sin 2\theta \end{aligned} \quad (17)$$

The angle  $\theta$  may be determined from the isoclinics, and  $S_{ij}$  may be evaluated from Eq. (224d). From these values of  $S_{xy}$  the quantity  $dS_{xy}/dx$  may be determined at the end of each of the segments. Then beginning at one boundary where  $S_{y_0}$  is known, successive values of  $S_{y_1}$  may be evaluated at the end of each of the segments from Eq. (226c).

An equation similar to Eq. (226c) may be obtained by writing the equation of equilibrium in the  $x$  direction for the free-body diagram of Fig. 117b.

$$S_{x_0} - S_{x_1} = \sum_{x_0}^{x_1} \frac{dS_{xy}}{dy} \Delta x \quad (226d)$$

Thus, a complete analysis of the stress situation in a body may be obtained from a photoelastic model.

**113. Extension to Triaxial Stress Situations.**—The analysis as outlined is applicable to biaxial stress situations. If any stresses exist in the planes parallel to the incident light rays, the image will be blurred. However, as a result of an observation by Maxwell<sup>1</sup> and the later research of several other investigators it has been found that if a model of a suitable material is subjected to a three-dimensional stress while at an elevated temperature and the stress is maintained while the specimen is slowly cooled, the stress pattern will be “frozen” in the material. The specimen may then be cut into thin slices, which are investigated individually by the usual photoelastic technique. Extensive investigation has shown that the slicing has no appreciable effect upon the stress pattern.

Weller<sup>2</sup> has described an alternate process for the analysis of triaxial stress situations making use of the polarization phenomena accompanying the “scattering” of a light ray as it passes through a transparent model under stress. A modified polariscope is used, the model replacing either the polarizer or the analyzer.

### PROBLEMS

**282.** The material fringe value of a  $\frac{1}{4}$ -in.-thick by  $\frac{1}{2}$ -in.-wide tension specimen is 43 lb. per in. How much axial load is required to produce the third-order fringe in the center portion of the specimen?

**283.** A model beam 0.200 in. wide by 1.200 in. deep is made of bakelite BT 61-893. The beam has a span of 9.00 in. and carries a load of 14.4 lb. at each of the third points. Sketch the probable fringe pattern for the center one inch of the beam.

**284.** A model beam 0.832 in. deep and 0.250 in. wide carries a load of 100 lb. at the center of a 3.00-in. span. If the load produces 12 fringes at the bottom of the beam what is the fringe value of the material?

**285.** A beam 0.675 in. deep and 0.250 in. wide is built of a material having a fringe value of 43 lb. per in. If the beam carries a 150-lb. load at the

<sup>1</sup> MAXWELL, J. C., *Trans. Roy. Soc. Edinburgh*, Vol. 20, p. 87, 1850.

<sup>2</sup> WELLER, R., *J. Applied Phys.*, Vol. 10, p. 266, 1939; *Nat. Advisory Comm. Aeronaut. Tech. Note* 737, 1939.

center of a 3.00-in. span, at what points should the tenth-order fringe intersect the top and bottom surfaces?

**286.** A beam 1.000 in. deep and 0.250 in. wide is made of Bakelite having a fringe constant of 72 lb. per in. It is fixed at one end and carries a 24-lb. load at a distance of 4.00 in. from the fixed end. Sketch the position of the isochromatics in the center 2 in. of the beam, indicating dimensions and fringe orders.

**287.** Sketch the 45-deg. isoclinic and the 30-deg. isoclinic for the center 2 in. of the beam of Prob. 286.

**288.** Under what circumstances, if any, will the isochromatic lines be equally spaced in a beam?

**289.** A bakelite beam, for which  $K = 40$  lb. per in., is simply supported on a 6-in. span and carries a concentrated load of 25.6 lb. 2 in. from the left end. Section *A* is taken at the center of the span, and section *B* 2 in. to the right of *A*. The width of the beam is 0.20 in., and the depth is 0.80 in.

- a.* Make a sketch showing the position of all isochromatics between *A* and *B*. Indicate distances.
- b.* Indicate the position of the 30-deg. isoclinic between *A* and *B*, showing in which half of the beam it occurs and its inclination, if any.

**290.** A full-size photoelastic model of a thick-walled cylinder with an internal diameter of 2 in. and an external diameter of 6 in. is subjected to internal and external pressure sufficient to produce a third-order fringe at the inside surface. The polaroid elements are set with their axes of polarization at 45 deg. with the horizontal.

- a.* Show the position of the first-order and second-order isochromatics on a sketch and indicate pertinent dimensions.
- b.* On a second sketch show the position of the isoclinics, if any.

**291.** A bakelite beam  $\frac{1}{4}$  in. thick and 2 in. deep is loaded to simulate a cantilever beam 12 in. long with a load at the free end. The load lies in a vertical plane but is directed downward at an angle of 60 deg. with the axis of the beam. The fourth-order fringe intersects the top edge of the beam 4 in. from the fixed end. Where does the third-order fringe intersect the top surface?

## CHAPTER XI

### COMPRESSIVE LOADS AND BUCKLING

**114. General Considerations.**—In addition to the topics considered thus far, which, in general, have dealt with the prediction of inelastic action in members acting as structural units, the designer is confronted with a series of problems of somewhat different type. One of these is the evaluation of stresses in the vicinity of concentrated loads. The flexure formula, for example, makes no allowance for the localized stress that is present in the vicinity of a concentrated load on a beam or near the supports.

In addition to failure by slip, considered in the preceding chapters, a member may fail by buckling, a phenomenon usually associated with thin-walled members or slender columns. If the critical load for the member is exceeded, over-all bending or buckling may occur, materially lowering the capacity of the member for resisting load and resulting in structural failure or a redistribution of load to other members, if any, in the structure. This type of failure is far different from that in which slip occurs. In the latter case the member is practically always capable of resisting an increased load with little damage other than permanent set. Buckling may occur at a stress well below the proportional limit of the material and usually results in large distortions.

A third group of design problems consists in the prediction and prevention of localized failures by buckling or "crippling." Even though the structural member is designed to resist buckling as a unit, the action may occur in a small portion or short length of the member. As has been mentioned, this type of failure may be critical in thin-walled torsional or flexural members such as those widely used in modern aircraft construction.

Although all of these effects are associated directly or indirectly with compressive loads, the stress situation is not one of simple axial loading but rather a combination of types considered in previous chapters. Since these cases involve stress situations

more complex than those discussed in the preceding chapters, their complete solutions involve the use of the theory of elasticity or theory of elastic stability. However, a treatment of advanced mechanics of materials would be incomplete without consideration of some of the results that have been obtained analytically and experimentally.

### CONCENTRATED LOADS

**115. Point Loads.**—An analytical solution<sup>1</sup> has been developed for the stresses due to a concentrated vertical force acting on the horizontal top surface of a large volume of material, as indicated

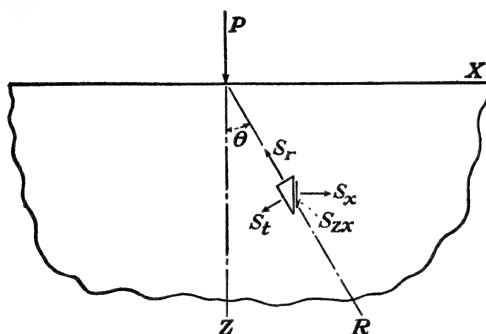


FIG. 118.—Stresses due to a point load.

in Fig. 118. The stresses are distributed symmetrically with respect to the  $z$  axis and may be evaluated in terms of the coordinates  $x$  and  $z$  and the radius  $R$ , which is  $(x^2 + z^2)^{1/2}$

$$S_x = \frac{P}{2\pi} \left[ \frac{1 - 2\mu}{x^2} \left( 1 - \frac{z}{R} \right) - \frac{3x^2z}{R^5} \right] \quad (227a)$$

$$S_z = \frac{-3Pz^3}{2\pi R^5} \quad (227b)$$

$$S_t = \frac{P(1 - 2\mu)}{2\pi} \left( \frac{z}{R^3} + \frac{z}{x^2R} - \frac{1}{x^2} \right) \quad (227c)$$

$$S_{xz} = \frac{-3Pxz^2}{2\pi R^5} \quad (227d)$$

$$S_r = \frac{-3Pz^2}{2\pi R^4} \quad (227e)$$

These equations may also be written in terms of the angle  $\theta$ , which the radius makes with the  $z$  axis. For example, Eq.

<sup>1</sup> BOUSSINESQ, J., "Application des potentiels . . .," Paris, 1885.



(227e) becomes

$$S_r = \frac{-3P \cos^2 \theta}{2\pi R^2} \quad (227f)$$

which indicates that the radial stress varies inversely as the square of the distance from the point of application of the load.

The formulas indicate an infinite stress directly under the load. However, the point load itself cannot exist; a concentrated load is actually distributed over a finite area instead of acting at a point. Equations (227) therefore give results on the safe side. If the area over which the load is distributed is known, stresses may be evaluated by integration.

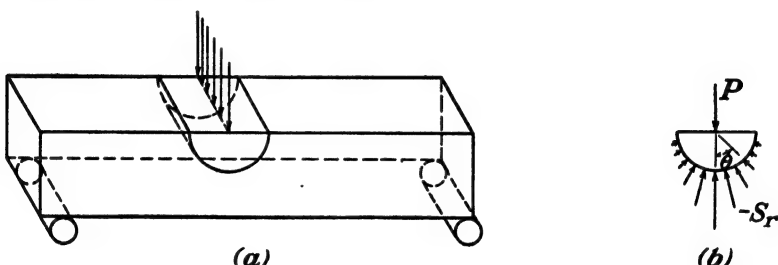


FIG. 119.—Stresses due to a line load.

Although the equations are developed for a semiinfinite elastic solid, they may be applied with reasonable accuracy to points near the load in a finite solid.

**116. Line Loads.**—If the concentrated load is distributed along a line, as across the top surface of the beam in Fig. 119a, the stresses may be determined by an application<sup>1</sup> of the general solution of the preceding article. The stresses are evaluated as

$$S_r = \frac{-2P \cos \theta}{\pi R} \quad (228a)$$

$$S_t = S_{rt} = 0 \quad (228b)$$

These results indicate that if a free-body diagram consisting of a half cylinder were removed from the beam, as indicated in Fig. 119b, it would be held in equilibrium by the radial stresses alone. Equation (228a) satisfies this condition. Other stresses

<sup>1</sup> FLAMANT, Sur la répartition des pressions den un solide rectangulaire chargé transversalement. *Acad. Sci. Comptes rendus*, Vol. 114, p. 1465, 1892.

are

$$S_z = \frac{-2P \cos^4 \theta}{\pi z} \quad (228c)$$

$$S_x = \frac{-2P \sin^2 \theta \cos^2 \theta}{\pi z} \quad (228d)$$

$$S_{yz} = \frac{-2P \sin \theta \cos^3 \theta}{\pi z} \quad (228e)$$

**117. Distributed Loads.**—If the load acting on the surface of the semiinfinite elastic solid is distributed over a circular area of radius  $a$ , the vertical component of stress is

$$S_z = \frac{-P}{\pi a^2} \left( 1 - \frac{z^3}{R^3} \right) \quad (229)$$

the maximum deflection occurs under the center of the load and is

$$w = \frac{2P(1 - \mu^2)}{\pi a E} \quad (230)$$

The maximum shearing stress occurs at  $z = 0.638a$  and is equal to one-third of the intensity of the uniform load.

**118. Contact Stresses.**—The problem of the stresses developed on the surface of contact between two elastic bodies has received the attention of many investigators. An analytical solution was published by Hertz,<sup>1</sup> showing that the pressure distribution between elastic bodies in contact is ellipsoidal. That is, the deformations that occur in the bodies are such that in the general case the area of contact is elliptical. The pressure distribution over the elliptical area is symmetrical, diminishing to zero at the edges, forming a semiellipsoid. The volume under the ellipsoid is equal to the total load transmitted from one solid to the other. The elliptical area of contact is dependent upon the shapes of the two surfaces of contact, the moduli of elasticity of the materials involved, and the magnitude of the compressive load. The semiaxes  $a$  and  $b$  of the elliptical area may be found from

$$a = m \sqrt[3]{\frac{3P \left( \frac{1 - \mu_1^2}{E_1} + \frac{1 - \mu_2^2}{E_2} \right)}{4(A + B)}} \quad (231a)$$

$$b = n \sqrt[3]{\frac{3P \left( \frac{1 - \mu_1^2}{E_1} + \frac{1 - \mu_2^2}{E_2} \right)}{4(A + B)}} \quad (231b)$$

<sup>1</sup> HERTZ, H. R., *Crelle's Journal*, Vol. 92, 1881; HERTZ, H. R., "Gesammelte Werke," Vol. 1, J. A. Barth, Leipzig, 1895.

in which  $\mu$  and  $E$  are the values of Poisson's ratio and modulus of elasticity of the two materials

$A + B$  is a constant, determined from

$$A + B = \frac{1}{2} \left( \frac{1}{R_1} + \frac{1}{R'_1} + \frac{1}{R_2} + \frac{1}{R'_2} \right) \quad (231c)$$

in which the  $R$  terms are the principal radii of curvature of the two surfaces

$m$  and  $n$  are constants, values of which are given in Table VIII.

The constants are functions of an angle  $\theta$  defined by

$$\cos \theta = \frac{B - A}{A + B} \quad (231d)$$

Values of  $A + B$  are determined from Eq. (231c) and values of  $B - A$  from Eq. (231e)

$B - A =$

$$\frac{1}{2} \sqrt{\left( \frac{1}{R_1} - \frac{1}{R'_1} \right)^2 + \left( \frac{1}{R_2} - \frac{1}{R'_2} \right)^2 + 2 \left( \frac{1}{R_1} - \frac{1}{R'_1} \right) \left( \frac{1}{R_2} - \frac{1}{R'_2} \right) \cos 2\psi} \quad (231e)$$

in which  $\psi$  is the angle between the two planes (normal to the plane of contact) containing the principal radii of curvature.

TABLE VIII.—VALUES OF CONSTANTS  $m$  AND  $n^*$

$\theta$	30°	35°	40°	45°	50°	55°	60°	65°	70°	75°	80°	85°	90°
$m$	2.731	2.397	2.136	1.926	1.754	1.611	1.486	1.378	1.284	1.202	1.128	1.061	1.000
$n$	0.493	0.530	0.567	0.604	0.641	0.678	0.717	0.759	0.802	0.846	0.839	0.944	1.000

\* From WHITTEMORE, H. L., and S. N. PETRENKO, *U. S. Bur. Standards Tech. Paper No. 201*, 1921.

With the size of the ellipse determined, the pressure distribution and the maximum pressure may be evaluated. The latter is

$$S_c = \frac{3P}{2\pi ab} \quad (231f)$$

The maximum shearing stress is developed a short distance below the surface of contact and is equal to approximately one-third of  $S_c$ . Numerous analytical and experimental investiga-

tions<sup>1</sup> have been made with reference to many of the practical problems related to this topic.

### GENERAL BUCKLING

**119. Buckling of a Bar under Axial Compression.**—If a long slender bar of constant cross section is subjected to a pair of axial compressive loads and the loads are increased sufficiently, the bar will buckle or bend, as indicated in Fig. 120a. The minimum load that will cause buckling to occur is called the

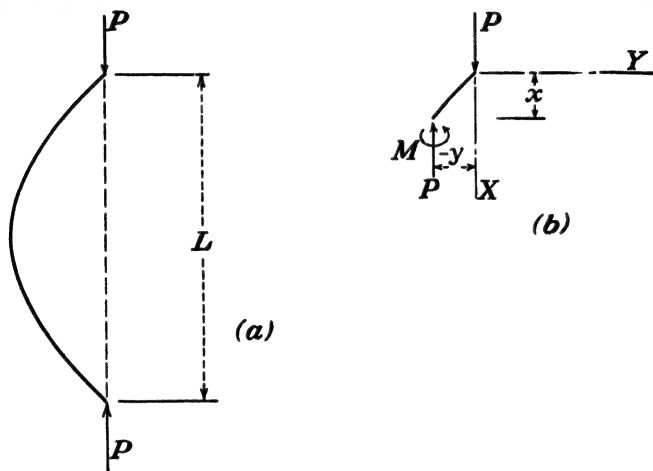


FIG. 120.—Deflection of a strut under axial compression.

critical load,  $P_{cr}$ . It may be found by considering a portion of the bar as a free-body diagram, as shown in Fig. 120b, and applying the equations of equilibrium together with the beam equation.

From the free-body diagram it is evident that a force  $P$  and a moment  $M$  are required to hold the portion of the bar in equilibrium. For small deflections the differential equation of the beam, Eq. (201), is valid

$$\frac{d^2y}{dx^2} = \frac{M}{EI} \quad (201)$$

<sup>1</sup> WILSON, W. M., Tests on the Bearing Value of Large Rollers, *Univ. Illinois Eng. Expt. Sta. Bull.* 162, 1927.

THOMAS, H. R., and V. A. HOERSCH, Stresses due to the Pressure of One Elastic Solid on Another, *Univ. Illinois Eng. Expt. Sta. Bull.* 212, 1930.

or

$$EI \frac{d^2 y}{dx^2} = -Py \quad (232a)$$

One solution of this type of differential equation is a trigonometric function, and since there are two constants of integration involved, one form in which the solution may be written is

$$y = A \sin kx + B \cos kx \quad (232b)$$

The value of the constant  $k$  may be determined by substituting the solution back into Eq. (232a)

$$EI(-k^2 A \sin kx - k^2 B \cos kx) = -P(A \sin kx + B \cos kx) \quad (232c)$$

Hence

$$k = \sqrt{\frac{P}{EI}} \quad (233)$$

The coefficients  $A$  and  $B$  are established by the end conditions. If the rod is supported so that no deflection occurs at the origin, Eq. (232b) shows that  $B = 0$ . The deflection is also zero at the other end where  $x = L$ . Therefore

$$0 = A \sin \sqrt{\frac{PL^2}{EI}} \quad (232d)$$

Equation (232d) indicates that the angle  $\sqrt{PL^2/EI}$  must be a multiple of  $\pi$ . Thus

$$\sqrt{\frac{PL^2}{EI}} = n\pi \quad (234)$$

or

$$P = \frac{n^2 \pi^2 EI}{L^2} \quad (234a)$$

Therefore, the smallest value of the load that will cause the bar to buckle is

$$P_{cr} = \frac{\pi^2 EI}{L^2} \quad (234b)$$

For this condition, the deflection at the center  $x = L/2$  is from Eq. (232b)

$$y_c = A \sin \sqrt{\frac{P}{EI}} \frac{L}{2} \quad (232e)$$

$$= A \sin \frac{\pi}{2} \quad (232f)$$

$$= A \quad (232g)$$

Values of  $n$  different from unity, in Eq. (234a), correspond to different modes of buckling. Equation (234b) is frequently rewritten by dividing each side by the area, giving the well-known Euler formula<sup>1</sup>

$$\left(\frac{P}{A}\right)_{cr} = \frac{\pi^2 E}{(L/r)^2} \quad (234c)$$

in which  $(P/A)_{cr}$  is the critical value of  $P/A$ , or lowest load per unit area that will cause buckling

$r$  is the radius of gyration with respect to the axis about which buckling will occur (the least  $r$ , if the rod is equally restrained in all directions).

In addition to all of the assumptions inherent in the use of the differential equation of the beam, two end conditions have been assumed.

1. The applied load is axial.
2. No restraining moments are developed at the ends.

If the applied load is not axial, it may be resolved into an axial load and a moment, so both conditions reduce to the assumption that there is no moment at the ends. If a moment does exist, it may easily be shown that the critical load may be expressed in the form

$$\left(\frac{P}{A}\right)_{cr} = \alpha \frac{\pi^2 E}{(L/r)^2} \quad (234d)$$

in which  $\alpha$  varies from a value of unity for a pinned end with no resistance to rotation to a value of 4 for an end that is completely restrained. The degree of restraint actually existing in a column or strut depends upon the amount of rotation that will be developed at the end. Some rotation will always occur, and the upper limit of  $\alpha$  is usually assumed to be 2.00. In some cases it has been found desirable to incorporate  $\alpha$  into the length term. For example, ANC-5 Handbook, Strength of Aircraft Elements, expresses the column formula in a form equivalent to

$$\left(\frac{P}{A}\right)_{cr} = \frac{\pi^2 E}{(L'/r)^2} \quad (234e)$$

in which  $L' = L/\sqrt{\alpha}$

<sup>1</sup> EULER, L., *De curvis elasticis*, in "Methodus inveniendi lineas curvas maximi minimive proprietate gaudentes," Lausanne, 1744.

It will be noted that the left-hand side of the Euler formula becomes infinity when the slenderness ratio  $L/r$  is equal to zero. However, the Euler formula is not valid for small values of the slenderness ratio because of its inherent limitation that stresses must be below the proportional limit. For values of the slenderness ratio below the range in which the Euler formula does apply, a number of formulas have been developed empirically and semi-empirically. A number of these are given in Table IV, and since they receive considerable attention in elementary courses, they will not be discussed here.

**120. Beam-columns.**—In many situations struts, or axially loaded members, may be subjected to lateral loads that cause

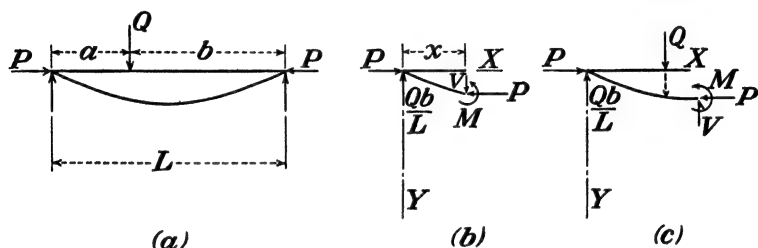


FIG. 121.—A beam-column.

bending or tend to promote buckling. This type of member has become known as a "beam-column." Since the relationships among load, moment, and deflection are not identical with those in either a beam or a column, a simple case of a beam-column carrying one concentrated lateral load will be considered. Results for other combinations of loading may be developed similarly.

The member is loaded as shown in Fig. 121a. It will be assumed that the lateral load produces bending about the principal axis that has a minimum radius of gyration and that there is no end restraint. From the free-body diagram of Figs. 121b and 121c it is evident that two equations are necessary for evaluating the moment. If the deflections are assumed to be small, the basic differential equation of the beam applies, and

$$0 \leq x \leq a \quad EI \frac{d^2y}{dx^2} = -Py - Qx + \frac{Qax}{L} \quad (235)$$

$$a \leq x \leq L \quad EI \frac{d^2y}{dx^2} = -Py - Qa + \frac{Qax}{L} \quad (236)$$

The negative sign is introduced because the  $y$  axis is selected in the direction of the deflection. A general solution for equations of this type may be written as

$$y = A \sin kx + B \cos kx + Cx \quad (237)$$

The subscript 1 will be used to designate the terms applying to the left of the load, and the subscript 2 to the right of the load. From Eq. (235)

$$EI(-A_1 k^2 \sin kx - B_1 k^2 \cos kx) = P(-A_1 \sin kx - B_1 \cos kx - C_1 x) - Qx + \frac{Qax}{L} \quad (235a)$$

It follows that

$$k = \sqrt{\frac{P}{EI}} \quad (237a)$$

$$C_1 = \frac{Q}{P} \left( \frac{a}{L} - 1 \right) \quad (237b)$$

The general solution substituted back into Eq. (236) verifies Eq. (237a) and also gives

$$C_2 x = \frac{Qa}{P} \left( \frac{x}{L} - 1 \right) \quad (237c)$$

The constants  $A_1$ ,  $A_2$ ,  $B_1$ , and  $B_2$  may be evaluated from the boundary conditions.

Since  $y = 0$  when  $x = 0$ ,  $B_1 = 0$ , and from  $y = 0$  when  $x = L$

$$A_2 \sin kL + B_2 \cos kL = 0 \quad (238a)$$

or

$$B_2 = -A_2 \tan kL \quad (238b)$$

Two other boundary conditions are that the slope and deflection as given by the two portions of the beam-column must be equal at the load.

Hence

$$A_1 k \cos ka + \frac{Q}{P} \left( \frac{a}{L} - 1 \right) = A_2 k \cos ka + A_2 k \tan kL \sin ka + \frac{Qa}{PL} \quad (239)$$



and

$$A_1 \sin ka + \frac{Qa}{P} \left( \frac{a}{L} - 1 \right) = A_2 \sin ka - A_2 \tan kL \cos ka + \frac{Qa}{P} \left( \frac{a}{L} - 1 \right) \quad (240)$$

from which

$$A_1 = \frac{Q \sin k(L - a)}{Pk \sin kL} \quad (238c)$$

$$A_2 = \frac{-Q \sin ka}{Pk \tan kL} \quad (238d)$$

By substituting the values of the constants into Eq. (237) the elastic curve is found to be

$$0 \leq x \leq a \quad y_1 = \frac{Q \sin k(L - a) \sin kx}{Pk \sin kL} + \frac{Qx}{P} \left( \frac{a}{L} - 1 \right) \quad (241)$$

$$a \leq x \leq L \quad y_2 = \frac{Q \sin ka \sin k(L - x)}{Pk \sin kL} + \frac{Qa}{P} \left( \frac{x}{L} - 1 \right) \quad (242)$$

Values of deflection, slope, moment, and stresses at any point may be obtained from Eqs. (241) and (242). The maximum deflection  $y_m$  will occur at the load when the load is at the center of the span

$$y_m = \frac{Q \tan \frac{kL}{2}}{2Pk} - \frac{QL}{4P} \quad (241a)$$

Timoshenko<sup>1</sup> shows that Eq. (241a) can be simplified by making the substitution

$$\frac{kL}{2} = u \quad (243a)$$

However

$$P = k^2 EI \quad (243b)$$

$$= \frac{4u^2 EI}{L^2} \quad (243c)$$

which gives

$$y_m = \frac{QL^3 \tan u}{16u^3 EI} - \frac{QL^3}{16u^2 EI} \quad (241b)$$

$$= \frac{QL^3}{48EI} \left[ \frac{3(\tan u - u)}{u^3} \right] \quad (241c)$$

<sup>1</sup> TIMOSHENKO, S., "Theory of Elastic Stability," McGraw-Hill Book Company, Inc., New York, 1936.

The term "outside of the brackets" is the deflection due to the lateral load acting alone, so the term "inside of the brackets" represents a multiplication factor due to the influence of the thrust.

The maximum bending moment at  $x = L/2$  when  $a = L/2$  is

$$M_{\max} = \frac{QL}{4} \left( \frac{\tan u}{u} \right) \quad (244)$$

As before, the term "in brackets" is a multiplying factor indicating the influence of the thrust. The quantity  $u$  may also be expressed as a function of the ratio of the axial load to the critical

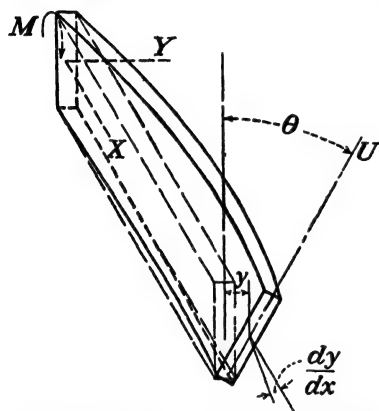


FIG. 122.—Lateral buckling of a thin strip.

axial load, *i.e.*, the load from the Euler formula if there were no lateral load. If the axial thrust is equal to one-half of the critical thrust, for example, the multiplication factor for deflection is equal to 1.967, and the factor for moment is equal to 1.812. As the value of the axial load approaches the critical value the magnitude of both magnification factors approaches infinity.

### 121. Buckling of Strips by End Moments.—

If a strip of constant (rectangular) cross section is subjected to end moments about a longitudinal axis it will twist, and the stresses and angle of twist may be found as described in Chap. 7. If it is subjected to end moments about the long principal axis of the cross section it will bend laterally, and the stresses and deflections may be found by the methods of Chap. 8. However, if it is subjected to end moments with respect to the short principal axis of the cross section, as indicated in Fig. 122, lateral buckling may occur for a value of the moment much lower than the critical moment determined from a consideration of the ordinary flexure formula. The value of the critical moment  $M_{cr}$ , or moment that will cause lateral buckling to occur, is of importance in thin-walled flexural members.

The critical moment may be evaluated by starting with a

free-body diagram of a portion of the strip, as indicated in Fig. 122. It is evident from the geometry of the figure that the centroid of the cut section has undergone a lateral displacement  $y$  and that the cross section has rotated through an angle  $\theta$  with reference to the original position.

If the value of the external moment is designated as  $M$ , the component of moment tending to produce bending with reference to the  $u$  axis of the cross section is

$$M_u = M\theta \quad (245)$$

It is this moment which is responsible for the lateral displacement  $y$ ; hence

$$EI_u = \frac{d^2y}{dx^2} = -M\theta \quad (245a)$$

provided that the assumptions involved in the flexure formula are valid and that only small deflections are involved.

The twist of the section is due to the torsional component of the moment, which is

$$T = M \frac{dy}{dx} \quad (246)$$

However, it was shown in Chap. 7 that the torque may be expressed in terms of the angle of twist as

$$T = \frac{J_s G \theta}{L} = J_s G \frac{d\theta}{dx} \quad (246a)$$

so

$$J_s G \frac{d\theta}{dx} = M \frac{dy}{dx} \quad (246b)$$

Equations (245a) and (246b) may be combined by differentiating the latter with respect to  $x$  and eliminating  $d^2y/dx^2$  between them. This procedure eliminates the variable  $y$ , giving an equation in terms of the two variables  $\theta$  and  $x$

$$\frac{d^2\theta}{dx^2} + \frac{M^2\theta}{EI_u J_s G} = 0 \quad (246c)$$

Equation (246c) is a differential equation of the same type as the one developed in the derivation of the Euler formula, so the solution may be written in the form

$$\theta = A \cos kx + B \sin kx \quad (246d)$$

If the strip does not buckle at the end,  $\theta = 0$  for  $x = 0$ . Hence,  $A = 0$ . To evaluate  $k$  the remaining term of the general solution is substituted back into Eq. (246c). This gives

$$k = \sqrt{\frac{M^2}{EI_w J_e G}} \quad (247)$$

In addition, the twist is zero at the other end of the strip where  $x = L$ . So

$$0 = B \sin kL \quad (248a)$$

or

$$kL = n\pi \quad (248b)$$

If Eqs. (247) and (248b) are combined to eliminate  $k$ , there results

$$M = \frac{n\pi \sqrt{EI_w J_e G}}{L} \quad (248c)$$

Hence,  $M_{cr}$  or the *least value* of  $M$  that will satisfy the conditions is

$$M_{cr} = \frac{\pi \sqrt{EI_w J_e G}}{L} \quad (248d)$$

It is apparent that the resistance of a member to this type of buckling is increased by using a stiffer material, by increasing the torsional rigidity, by increasing the moment of inertia with respect to the axis of least moment, and by decreasing the free length. For a steel member of thickness  $t$  and depth  $d$  Eq. (248d) reduces to

$$M_{cr} = \frac{9.90 \times 10^6 t^3 d}{L} \quad (248c)$$

In addition to the end conditions that were assumed, Eq. (248d) is subject to all of the limitations involved in the elementary flexure theory and torsion theory for slender rectangular cross sections. Among the assumptions most likely to be violated is that of stresses not exceeding the proportional limit. If stresses do exceed the proportional limit, the result may be expected to be localized failure, rather than general buckling.

Timoshenko<sup>1</sup> shows that if Eq. (248d) is extended to I beams, it gives values that are too low, because of the increased effect of the restraint to warping in an I beam. It has been noted

<sup>1</sup> *Op. cit.* p. 279.

that resistance to warping increases the torsional rigidity of a member.

**122. Buckling of Sheets and Panels.**—A flat rectangular sheet of constant thickness, subjected to distributed compressive loads along two opposite sides and unsupported along the other two sides as indicated in Fig. 123a, may be treated as an Euler column if the height is sufficiently large in comparison

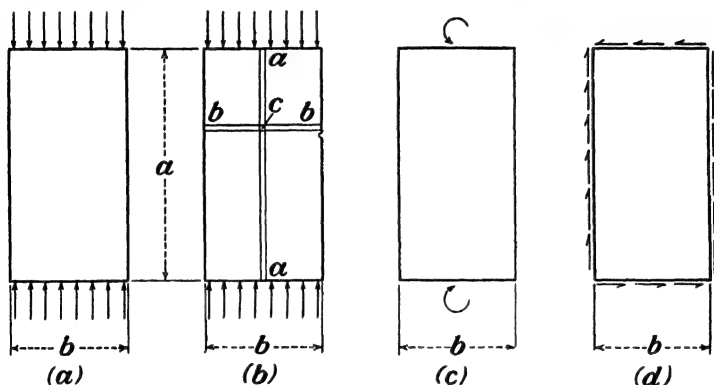


FIG. 123.—Panels with edge loads.

with the thickness to put the slenderness ratio in the Euler range. Hence, from Eq. (234c),

$$\left(\frac{P}{A}\right)_{cr} = \frac{\pi^2 E}{(a/r)^2} \quad (234f)$$

$$= \frac{\pi^2 E}{\sqrt{12}} \left(\frac{t}{a}\right)^2 \quad (234g)$$

$$= 2.85 E \left(\frac{t}{a}\right)^2 \quad (249)$$

if the top and bottom edges are pinned. The sheet will buckle in the form of a sine curve, and the critical unit load is independent of the width  $b$  of the sheet.

However, if the sheet is pinned around all four edges to form a panel, the critical unit load is no longer independent of the width  $b$  and is increased in magnitude. The panel in effect consists of a series of parallel vertical columns such as  $aa$  in Fig. 123b, each of which tends to buckle as the sheet of Fig. 123a. However, these columns are restrained from buckling by a series of transverse strips such as  $bb$ . These transverse strips

are prevented from deflecting at their ends, and hence, develop moments that decrease the tendency of the vertical strips to deflect, thereby increasing the critical load for the panel. It is evident that the restraint offered by the horizontal strips increases as the width  $b$  is decreased.

One approach to the analysis of the panel consists in considering each rectangular element of panel, such as  $c$ , as a free-body diagram and applying the equations of equilibrium. In addition to the equations of equilibrium, the geometry of the deflected panel and the properties of the material must be considered. The resulting relationships may be combined to form a differential equation, known as the "plate equation"

$$\frac{\partial^4 w}{\partial x^4} + 2 \frac{\partial^4 w}{\partial x^2 \partial y^2} + \frac{\partial^4 w}{\partial y^4} = \frac{12(1 - \mu^2)q}{Et^3} \quad (250)$$

in which  $w$  is the deflection perpendicular to the  $xy$  plane, the plane of the panel

$q$  is the unit load acting normal to the panel.

This equation is somewhat analogous to the torsion equation, Eq. (136c), in that a solution that satisfies the boundary conditions may be used to evaluate stresses, moments, slopes, etc. The details of the derivation and application of the plate equation are discussed thoroughly in the literature of theory of elasticity.<sup>1</sup>

The results of analyses show that the critical unit load for a rectangular panel with pinned edges on all four sides may be expressed in a form rather similar to Eq. (249) for the sheet.

$$\left(\frac{P}{A}\right)_{cr} = KE \left(\frac{t}{b}\right)^2 \quad (249a)$$

This formula is valid not only for the panel subjected to compression as shown in Fig. 123b but also for bending and shear, as shown in Figs. 123c and 123d. Values of  $K$  for Eq. (249a) are given in Fig. 124 for compressive and shearing loads

<sup>1</sup> TIMOSHENKO, S., "Theory of Plates and Shells," McGraw-Hill Book Company, Inc., New York, 1940.

TIMOSHENKO, S., "Theory of Elastic Stability," McGraw-Hill Book Company, Inc., New York, 1936.

LOVE, A. E. H., "Mathematical Theory of Elasticity," University Press, Cambridge, 1906.

PRESCOTT, J., "Applied Elasticity," Longmans, Green and Company, London, 1924.

and in Fig. 125 for bending moments. The curves as shown for bending and compression are the lower envelopes of a series of parabolic curves similar to those visible at the left end. Each curve corresponds to a mode of buckling. For example, the first curve of the compression set for all four edges pinned has

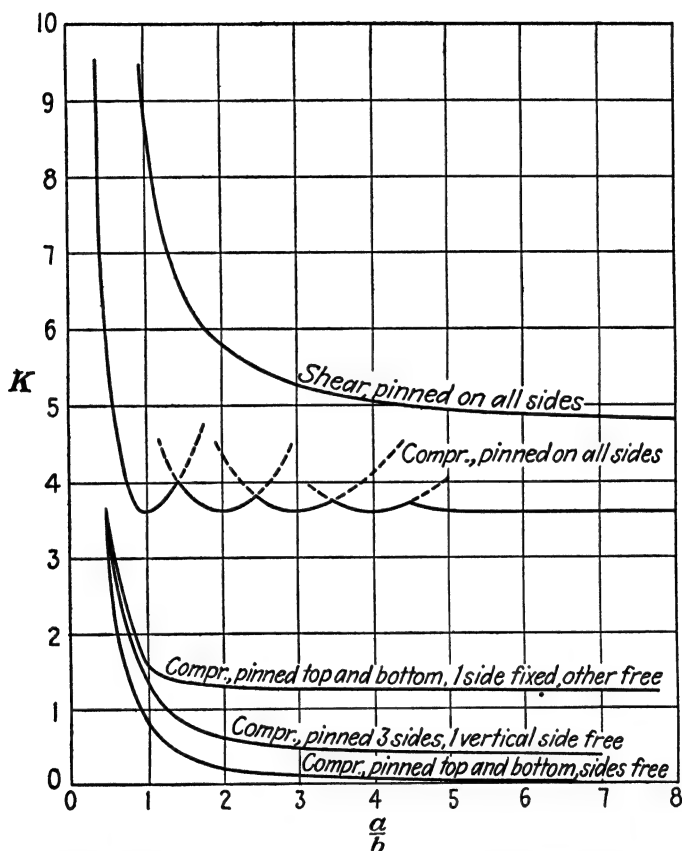


FIG. 124.—Values of  $K$  for panels in compression or shear.

its lowest point at  $a/b = 1$  and corresponds to the panel buckling with a single loop in each direction. At a value of  $a/b = \sqrt{2}$ , this curve is intersected by another curve with vertex at  $a/b = 2$ , corresponding to the panel buckling in such a way that two loops are formed in the direction parallel to the long sides and one loop in the transverse direction.

The effect of altering the edge conditions is also indicated in Fig. 124.

**123. Curved Panels in Shear.**—Analysis supplemented by test data shows that the critical shearing stress for a curved panel

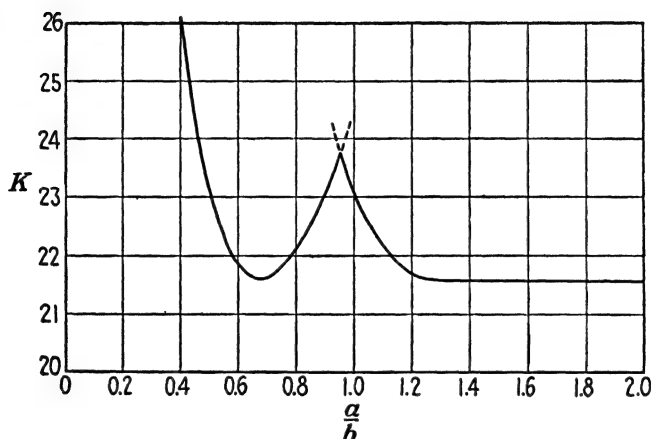


FIG. 125.—Values of  $K$  for panel in flexure.

that is a portion of a cylinder may be evaluated as

$$S_{cr} = KE \left( \frac{t}{b} \right)^2 + K_1 E \frac{t}{R} \quad (249b)$$

in which  $t$  is the thickness of the sheet

$b$  is the arc length of the curved sides

$R$  is the radius of curvature of the panel

$K$  is the same coefficient as in Eq. (249a)

$K_1$  is a coefficient equal to 0.10.

Since the first term of Eq. (249b) is identical with the right-hand side of Eq. (249a), it is evident that the second term represents the stiffening effect of the curvature.

### LOCALIZED BUCKLING

**124. Thin-walled Cylinders in Axial Compression.**—If a thin-walled cylinder or tube is subjected to a pair of axial compressive loads, it may buckle as a unit at the critical load as given by the Euler formula (if the slenderness ratio is high), or it may fail by localized buckling as indicated in the short cylinder of Fig.



126. Analytical investigations<sup>1</sup> have shown that the general expression for the critical unit load may be put in either of the forms

$$\left(\frac{P}{A}\right)_{cr} = KE \left(\frac{t}{R}\right) \quad (250)$$

$$= \frac{K_1 E}{(D/t)} \quad (250a)$$

in which  $K$  and  $K_1$  are coefficients

$t$  is the thickness of the material

$D$  is the diameter of the cylinder

$R$  is the radius of the cylinder.

The equations are independent of the slenderness ratio or the length, since it is assumed that the length is large in comparison with other dimensions. The theoretical value of  $K$  varies from 0.414 to 0.643, depending upon the type of curve assumed in the analysis. A number of experimental investigations have been made<sup>2</sup> on cylinders in compression to evaluate  $K$  or  $K_1$ . The results indicate that the theoretical values of  $K$  are high and that  $K$  is a function of  $D/t$ . For high values of  $D/t$ , the actual value of  $K$  is only about 0.06, or 15 per cent of the lower theoretical  $K$ .

An empirical equation for the critical unit load, as developed by Kanemitsu and Nojima,<sup>3</sup> is

$$\left(\frac{P}{A}\right)_{cr} = E \left[ 9 \left(\frac{t}{R}\right)^{1.6} + 0.16 \left(\frac{t}{L}\right)^{1.3} \right] \quad (250b)$$

<sup>1</sup> TIMOSHENKO, S., "Theory of Elastic Stability," McGraw-Hill Book Company, Inc., 1936.

SOUTHWELL, R. V., On the General Theory of Elastic Stability, *Trans. Roy. Soc. London*, Ser. A, Vol. 213, 1914.

DEAN, W. R., On the Theory of Elastic Stability, *Proc. Roy. Soc. London*, Ser. A, Vol. 107, p. 734.

<sup>2</sup> WILSON, W. M., and N. M. NEWMARK, The Strength of Thin Cylindrical Shells as Columns, *Univ. Illinois Eng. Expt. Sta. Bull.* 225, 1933.

DONNELL, L. H., A New Theory for the Buckling of Thin Cylinders under Axial Compression and Bending, *Trans. Am. Soc. Mech. Engrs.*, Vol. 56, p. 795, 1934.

LUNDQUIST, E. E., Strength Tests of Thin-walled Duralumin Cylinders in Compression, *Nat. Advisory Comm. Aeronaut. Tech. Rept.* 473, 1933.

<sup>3</sup> KANEMITSU, S., and H. NOJIMA, Axial Compression Tests of Thin Circular Cylinders, Thesis, Calif. Inst. Tech., 1939.

The equation was developed from a large number of test results of several investigators and includes data from steel, brass, and duralumin cylinders. The equation gives satisfactory results for values of  $D/t$  between 1,000 and 6,000 and values of  $L/D$  between 0.05 and 1.25.



FIG. 126.—Localized buckling in thin-walled cylinder in compression.

### 125. Thin-walled Cylinders under Uniform External Pressure.

In Chap. 6 it was noted that the usual formulas for evaluation of stresses in thin-walled cylinders due to internal pressure are not valid for predicting the external pressure under which the cylinder will collapse because of the possibility of buckling occurring in the cylinder wall. Analyses to determine the critical pressure have been made by several investigators using the methods of the theory of elasticity. The results may be expressed in the form

$$P_{cr} = KE \left( \frac{t}{D} \right)^3 \quad (251)$$

in which  $P_{cr}$  is the critical external pressure, or difference between external and internal pressures

$K$  is a coefficient

$E$  is the modulus of elasticity of the cylinder wall

$t$  is the thickness of the cylinder wall

$D$  is the mean diameter of the cylinder.

The coefficient  $K$  is a function of  $L/D$ ,  $D/t$ , and the end condition of the cylinder walls. Sturm<sup>1</sup> gives values of  $K$  for external pressure on the sides and on the sides and ends for the edges pinned or fixed. For a given  $D/t$  ratio values of  $K$  plotted as a function of  $L/R$  give a series of curves somewhat similar to those given in Fig. 124. The curves become asymptotic to  $K = 2.2$  for high values of  $L/R$  (100 or more). Sturm's results indicate a value of  $K$  of approximately  $50(L/R)^{-1.35}$  for small values of  $L/R$  and for  $D/t = 20$ . The magnitude of  $K$  increases with an increase in the value of  $D/t$ .

Tests made on extruded and on welded cylinders of aluminum alloy 3S gave results in good agreement with the theory.

**126. Thin-walled Cylinders in Torsion.**—In a cylinder subjected to torsion, principal stresses (one tensile and one compressive) are developed at 45 deg. with the maximum shearing stress. If the walls of the cylinder are thin, the compressive stresses may cause buckling in the form of waves that spiral around the tube throughout its length. The number and angle of the waves depend upon the dimensions of the cylinder. Figure 127 shows a photograph of a duralumin tube which failed by buckling before twisting in two.

Thin-walled cylinders in torsion have been investigated by Schwerin<sup>2</sup> and by Donnell,<sup>3</sup> who showed that the magnitude of the critical torsional stress may be evaluated by one of two formulas depending upon whether the tube is classified as *long* or *short*.

1. *Long Cylinders.*—If the value of the quantity  $\frac{1}{\sqrt{1 - \mu^2}} \frac{L^2 t}{D^3}$  is greater than 6.0, the cylinder is classified as a long cylinder

<sup>1</sup> STURM, R. G., A Study of the Collapsing Pressure of Thin-walled Cylinders, *Univ. Illinois Eng. Expt. Sta. Bull.* 329, 1941.

<sup>2</sup> SCHWERIN, E., Torsional Stability of Thin-walled Tubes, *Proc. 1st Intern. Cong. Applied Mech.*, p. 255, Delft, 1924.

<sup>3</sup> DONNELL, L. H., Stability of Thin-walled Tubes under Torsion, *Nat. Advisory Comm. Aeronaut. Tech. Rept. No.* 479.

and the critical shearing stress is given by Eq. (252a)

$$S_{cr} = 0.70E \left( \frac{t}{D} \right)^{3/4} \quad (252a)$$

2. *Short Cylinders*.—If the value of the quantity  $\frac{1}{\sqrt{1-\mu^2}} \frac{L^2 t}{D^3}$  is equal to 6.0 or less, the critical shearing stress for a tube with pinned edges is

$$S_{cr} = \frac{0.75E(t/D)^{3/4}}{\sqrt{L/D}} \quad (252b)$$

If the edges of the tube are fixed, a coefficient of 0.80 instead of 0.75 may be used.



FIG. 127.—Buckling of a thin-walled tube subjected to torsion.

**127. Thin-walled Cylinders in Bending.**—For cylinders subjected to pure bending, Lundquist<sup>1</sup> has shown that the modulus of rupture may be evaluated by

$$S_{cr} = KE \left( \frac{t}{D} \right) \quad (253)$$

which is the same form as Eq. (250) for axial compression. The value of  $K$  is from 30 to 80 per cent higher than the corresponding  $K$  for compression.

**128. Noncircular Closed Sections in Axial Compression.**—The buckling of thin-walled closed rectangular sections has been investigated by Lundquist<sup>2</sup> who developed the expression for

<sup>1</sup> LUNDQUIST, E. E., Strength Tests of Thin-walled Duralumin Cylinders in Pure Bending, *Nat. Advisory Comm. Aeronaut. Tech. Note*, No. 479.

<sup>2</sup> LUNDQUIST, E. E., Local Instability of Symmetrical Rectangular Tubes under Axial Compression, *Nat. Advisory Comm. Aeronaut. Tech. Note* No. 686.

the critical unit load as

$$\left(\frac{P}{A}\right)_{cr} = \frac{K\pi^2 E}{12(1 - \mu^2)} \left(\frac{t_a}{a}\right)^2 \quad (254)$$

in which  $a$  is the long side of the rectangular cross section

$t_a$  is the thickness of the long side

$K$  is a coefficient depending upon the ratio of the sides and the ratio of the wall thicknesses.

Representative values of  $K$  are given in Fig. 128. A square section of constant wall thickness, for example, has a value of

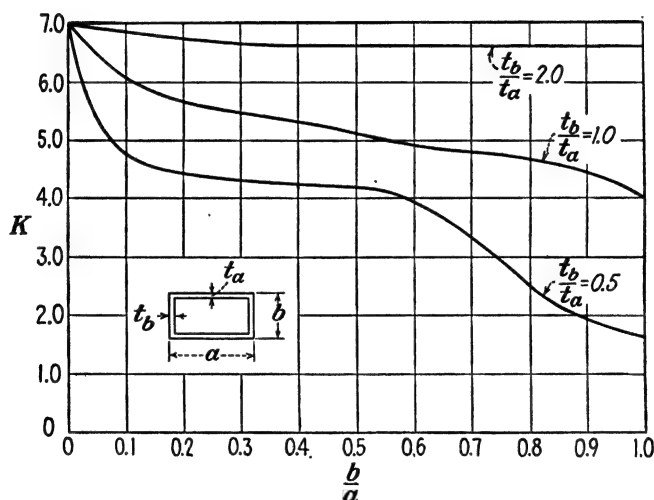


FIG. 128.—Values of  $K$  for rectangular tubes in compression.

$K$  of 4.00. Hence, the allowable unit load for  $\mu = 0.30$  is

$$\left(\frac{P}{A}\right)_{cr} = 3.62E \left(\frac{t}{a}\right)^2 \quad (254a)$$

This result agrees with that obtained using Eq. (249a) and Fig. 124 for the flat panel pinned on all four sides. That is, the effect of an adjacent side in the square tube is to provide a pinned edge.

**129. Noncircular Open Sections in Axial Compression.**—Although no general solution is available for evaluating the load that will cause localized buckling of a thin-walled open section in axial compression, an estimate can be made, based on the

results of the preceding article, if the cross section is made up of straight-line segments. The critical load may be found for each segment separately by treating it as a flat panel with pinned or free edges, depending upon whether or not there are adjacent segments. The total load that the section will carry may be taken as the sum of the loads of the segments.

For example, an angle with equal legs will carry twice as much load as that computed from Eq. (249a) and Fig. 124 for a flat panel having dimensions equal to those of one leg of the angle and assumed to be simply supported on three sides and free on the fourth. Similarly, a channel may be assumed to consist of three elements: one panel supported on all four sides, corresponding to the web; and two panels, supported on three sides and free on the fourth, corresponding to the flanges.

#### TORSIONAL INSTABILITY OF COLUMNS

**130. Torsional Failure.**—Two types of column failures have been considered thus far; one, general buckling in which the column bends as a unit, deflecting in a direction normal to the axis about which the moment of inertia is a minimum (assuming equal end restraint in all directions); and second, localized failure in which a relatively small portion of the column crushes, fails in compression, or buckles. Thin-walled open sections are subject to failure by torsion, in which the axial compressive load causes the center portion of the column to rotate with respect to the ends. The critical stress depends upon the torsional rigidity of the cross section and is sufficiently high for closed sections that this type of failure need not be considered for them.

Under the action of the compressive load some bending of the column will normally occur. Since the bending moment depends upon the deflection, it varies along the column, reaching a maximum value at the center for a uniform cross section. However, a variation in moment is accompanied by cross shear, since  $V = dM/dx$ . The shearing force may also be evaluated from the load on the column and the slope at the given section. The cross shearing forces thus developed are distributed throughout the cross section, as described in Chap. 9.

For example, if a channel is used as a column and loaded eccentrically as indicated in Fig. 129a, the channel will tend to

bend about the  $x$  axis, or axis of symmetry. As shown in Fig. 129*b* the force system acting on a cross section at some distance from the end may be resolved into a normal force  $F_n$ , a cross shearing force  $Q$ , and a moment  $M$ . The cross-shearing force is directed along the  $y$  axis of Fig. 129*a*. Owing to the difference in moment between two sections a short distance apart, shearing forces are developed on the cross section as shown. However, the resultant of these three shearing forces in the flanges and

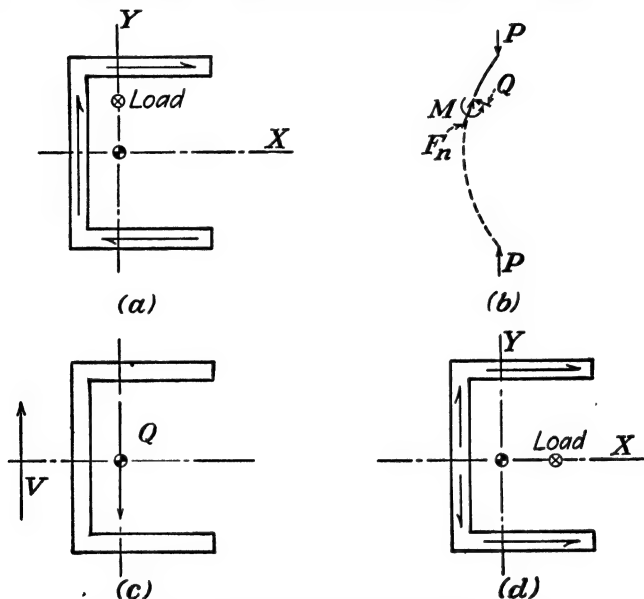


FIG. 129.—Shearing forces in open-section columns.

web must pass through the shear center. Hence, the resultant shearing force that acts through the shear center, and the cross-shearing force  $Q$  that acts along the  $y$  axis produce a couple as shown in Fig. 129*c*. This couple tends to twist the column, and if the torsional resistance is sufficiently low, torsional instability will result.

If the column is eccentrically loaded along the  $x$  axis, as shown in Fig. 129*d*, so that bending about a  $y$  axis occurs, the resultant of the shearing forces will still pass through the shear center but will be acting along the  $x$  axis. In addition, the cross-shearing force  $Q$  will be acting along the  $x$  axis, so that no couple will be produced and no twist will occur.

**131. Critical Stress for Torsional Instability.**—Analyses to determine the critical stress have been presented by Wagner,<sup>1</sup> by Lundquist and Fligg,<sup>2</sup> and by others. The results may be expressed as

$$\left(\frac{P}{A}\right)_{cr} = \frac{1}{I_p} \left[ GJ_e + \frac{\pi^2}{L^2} EC_{BT} \right] \quad (255)$$

in which  $I_p$  is the polar moment of inertia of the cross section with respect to the axis of rotation (normally the shear center)

$C_{BT}$  is the so-called torsion-bending constant.

The torsion-bending constant is a property of the cross section and is defined by

$$C_{BT} = \int_0^A w^2 da - \frac{1}{A} \left( \int_0^A w da \right)^2 \quad (256)$$

in which  $w$  is the circumferential warping, which may be evaluated from

$$w = \int_0^u r du \quad (256a)$$

in which  $du$  is a differential length of wall cross section

$r$  is the radius arm of  $du$ .

The torsion bending constant  $C_{BT}$  is evaluated with respect to the shear center, or center of rotation. For a thin-walled channel it is equal to

$$C_{BT} = \frac{at^2}{12} [c^2(a + 6b) + 2b^2(b + 3c)] \quad (257)$$

in which  $a$  is the distance between flanges

$t$  is the wall thickness

$b$  is the flange width

$c$  is the distance from center of rotation to the center of the web.

Lundquist and Fligg also discuss the torsional stability of open sections when used as stiffeners for sheets. The effect of the attached sheet is to move the center of rotation and may materially affect the torsional rigidity.

<sup>1</sup> WAGNER, H., Torsion and Buckling of Open Sections, *Nat. Advisory Comm. Aeronaut. Tech. Mem.* 807, 1936.

<sup>2</sup> LUNDQUIST, E. E., and C. M. FLIGG, A Theory for Primary Failure of Straight Centrally Loaded Columns, *Nat. Advisory Comm. Aeronaut. Tech. Rept.* 582, 1936.



## PROBLEMS

**292.** Determine the principal stresses developed at a point a distance  $R$  from a point load acting perpendicular to the plane surface of an infinite half solid.

**293.** Verify the fact that Eq. (228a) satisfies the equilibrium condition for the free-body diagram of Fig. 119b.

**294.** A beam 6 in. wide and 12 in. deep carries a 4,800-lb. load at the center of an 8-ft. span. Determine the principal stresses and the maximum shearing stress at a point 2 in. below the top of the beam and 1 in. to the right of the center. Assume the load to be a line load across the width of the beam.

**295.** A load of 1,000 lb. is transmitted through a  $\frac{1}{2}$ -in.-diameter ball bearing operating in a race 4 in. in diameter. Determine the maximum stress developed.

**296.** A telescoping strut is composed of a 1-in. steel tube  $\frac{1}{8}$  in. thick which slides inside a  $1\frac{1}{4}$ -in. steel tube 0.120 in. thick. When locked in the extended position, play at the connection permits a lateral center deflection of 0.10 in. Determine the maximum permissible axial load. Each tube has an effective length of 36 in. when extended.

**297.** A beam-column carries a uniform load over its entire length. Develop the equation of the elastic curve.

**298.** Plot curves showing the variation in the multiplication factors for deflection and moment in a beam-column, Eqs. (241c) and (244), with the ratio of the axial load to the critical axial load.

**299.** Show what differences, if any, would result in the development of Art. 120 if the  $y$  axis were taken in the direction opposite to the deflection.

**300.** Verify Eq. (244).

**301.** In the development of the expression for the critical buckling moment in a strip, Art. 121, both the torsion theory for rectangular members and the flexure theory were used. Can all of the assumptions involved in each be valid simultaneously? Discuss briefly.

**302.** Compare the relative effectiveness of steel and duralumin strip in resisting buckling due to end moments on the basis of (a) equal dimensions, and (b) equal weights.

**303.** How much will the use of a high-strength steel instead of structural steel increase the resistance of a thin-walled member to buckling?

**304.** A duralumin panel 0.040 in. thick is 4 ft. high and 2 ft. wide and is pinned on all four edges.

a. Determine the maximum compressive load that it will support.

b. Determine the maximum compressive load that could be supported by the same amount of material fabricated into a circular rod 4 ft. long.

**305.** Determine the approximate load that the duralumin panel of Prob. 304 would carry if it were fabricated into a cylinder 4 ft. long.

**306.** Determine the maximum axial load that any standard size of tin can would be expected to carry.

**307.** A long structural-steel tube 12 in. in diameter has a wall thickness of 0.072 in. Determine

- a. The maximum safe internal pressure.
- b. The maximum safe external pressure.

**308.** Determine the maximum torque that a 2-in. by 0.058-in. duralumin tube will transmit if it is

- a. 24 in. long.
- b. 48 in. long.

**309.** A rectangular tube 6 ft. long is fabricated from 0.040 in. thick duralumin sheet and has a cross section 2 by 4 in. Determine the axial compressive load which it would be expected to carry if it is fabricated as

- a. An open section with a longitudinal slit at one corner.
- b. An open section with a longitudinal slit down the middle of one of the 4-in. sides.
- c. A closed section.

## ANSWERS TO PROBLEMS

3.  $\frac{1}{2}WL(1 + \sqrt{1 + 4haE/WL})$  below proportional limit
5. 17.4
32.  $\theta_{zn} = 30 \text{ deg.}, 70 \text{ deg.}$
42.  $S_u = 6,830 \text{ p.s.i.}, S_v = -4,830 \text{ p.s.i.}, S_{ij} = 5,830 \text{ p.s.i.}, \theta_{zu} = -15.5 \text{ deg.}$
45.  $S_u = -6,250 \text{ p.s.i.}, S_v = 10,250 \text{ p.s.i.}, S_{ij} = 8,250 \text{ p.s.i.}, \theta_{zu} = -7.0 \text{ deg.}$
51. (a)  $S_{ij} = 9,250 \text{ p.s.i.}, (b) S_{ij} = 9,000 \text{ p.s.i.}$
52.  $S_u = 9,110 \text{ p.s.i.}, S_v = -9,110 \text{ p.s.i.}, S_{ij} = 9,110 \text{ p.s.i.}$
73. (a) 0.0002875, (b) 0.0004125
75. 0.000379, -0.000179, -7.0 deg.
83.  $\epsilon_u = 0.00112, \epsilon_v = -0.00039, \theta_{zu} = -16.3 \text{ deg.}$
101. Change in volume is 0.0024 cu. in.
106. (a) (b) (c) 0.50
107.  $E\epsilon_z = 0.743S_z$  for  $\mu = 0.30$
114.  $E = 2.67G$
121.  $S_u = 33,470 \text{ p.s.i.}, S_v = -1,650 \text{ p.s.i.}$
122.  $S_u = 14,400 \text{ p.s.i.}, S_v = 2,400 \text{ p.s.i.}, S_{ij} = 7,200 \text{ p.s.i.}$
131. 1.20 in., 1.04 in., 1.26 in.
132. (a) 3.66 in., (b) 3.93 in., (c) 3.83 in.
135. Maximum shearing stress
143.  $d = d_o e^{\frac{wy}{2S}}$
150. 2,780 lb.
153. 2.0
163. (a) 17.90 in.
165. 26,100 p.s.i.
175.  $S_r = 6,750 \text{ p.s.i.}$
190. 30,500 p.s.i.
197. (a) 17.2 lb. per ft., (b) 20.7 lb. per ft.
201. Square, 33,400 in.-lb., 0.00124L; Rectangular, 78,800 in.-lb., 0.000898L
204.  $S = 2a^2bG\theta/(a^2 + b^2)$
214. (a) 0.0534 in.<sup>4</sup>
215. 3,440 in.-lb.
218. (a) 18,700 in.-lb., (b) 282 in.-lb.
231. 10.5 per cent
236. 1,610 lb.,  $\theta = 63.8 \text{ deg.}$
239. 0.15 in.
247. 1,750 in.-lb.
264. Maximum = 420 p.s.i.
271.  $e = 0.37 \text{ in.}$
280. 15,990 p.s.i.
282. 64.5 lb.
285. 0.435 in. from end
289. Second-order fringe intersects top and bottom midway between A and B.



## AUTHOR INDEX

### A

Anthes, 160  
Armbruster, E., 180

### B

Bach, C., 148  
Baron, F. H., 176  
Barton, M. V., 176  
Baumann, R., 148  
Beeuwkes, R., 99  
Beltrami, E., 75  
Bergman, E. O., 66  
Berkey, D. C., 207  
Böker, R., 75  
Boussinesq, J., 177, 270  
Brandtzaeg, A., 75  
Brewer, G. A., 50  
Brown, R. L., 75

### C

Christensen, N. B., 177  
Christopherston, D. G., 188  
Coker, E. G., 254  
Cook, G., 83  
Cornell, K., 50  
Cross, Hardy, 176, 195, 220

### D

de Forest, A. V., 95  
Den Hartog, J. P., 178  
Dietz, W., 99  
Dolan, T. J., 94, 180  
Donnell, L. H., 287, 289  
Duguet, C., 185  
Durelli, A. J., 97

### E

Eichinger, A., 83  
Eksergian, R., 132

Ellis, Greer, 95  
Englis, C. E., 95  
Euler, L., 276

### F

Filon, L. N. G., 254  
Flamant, 271  
Fligg, C. M., 294  
Föppl, A., 36  
Föppl, L., 36  
Frocht, M. M., 99, 208, 254, 264, 265

### G

Gilkey, H. J., 60  
Glasco, R. B., 50  
Goodier, J. N., 176  
Gough, M. J., 179  
Greene, C. E., 225  
Greenhill, A. G., 177  
Griffith, A. A., 160, 179  
Guest, J. J., 73

### H

Haigh, B. P., 75, 77  
Hall, S. G., 104  
Hanson, H. M., 52  
Harding, J. F., 50  
Harger, O. J., 132  
Hencky, H., 76  
Henwood, P. E., 104  
Hertz, H. R., 272  
Hetényi, M., 99, 101  
Hill, H. N., 99  
Hoersch, V. A., 274  
Hoskins, E. E., 28  
Howland, R. C. J., 99  
Huber, M. T., 75

- |   |   |
|---|---|
| <p style="text-align: center;">J</p> <p>Jacobsen, L. S., 181</p> <p>Jeffery, G. B., 97</p> <p>Johnston, B. G., 169</p> <p style="text-align: center;">K</p> <p>Kanemitsu, S., 287</p> <p>Kirsch, G., 97</p> <p>Kolosoff, G., 95</p> <p>Kommers, J. B., 182</p> <p style="text-align: center;">L</p> <p>Lake, G. F., 139</p> <p>Lamé, 114</p> <p>Lee, Geo. E., 100</p> <p>Lode, W., 83</p> <p>Love, A. E. H., 93, 284</p> <p>Ludwik, P., 185</p> <p>Lundquist, E. E., 287, 290, 294</p> <p>Lyse, Inge, 169</p> <p style="text-align: center;">M</p> <p>McGivern, J. G., 178</p> <p>March, H. W., 163</p> <p>Marin, J., 132</p> <p>Martens, A., 50</p> <p>Maxwell, J. C., 267</p> <p>Mehaffey, W. R., 48</p> <p>Meier, J. H., 48</p> <p>Mohr, O., 33, 36, 74, 226</p> <p>Moore, H. F., 104, 178, 182</p> <p>Morley, A., 138</p> <p>Müller-Breslau, H., 226</p> <p>Murphy, Glenn, 52, 60</p> <p>Murray, W. M., 48, 97</p> <p style="text-align: center;">N</p> <p>Nádai, A., 130, 186</p> <p>Navier, C. L., 72, 73</p> <p>Nelson, C. W., 132</p> <p>Neuber, H., 100, 181, 208</p> <p>Newmark, N. M., 287</p> | <p>Newton, R. E., 138</p> <p>Nojima, H., 287</p> <p style="text-align: center;">O</p> <p>O'Haven, C. P., 50</p> <p>Oleson, R. C., 48</p> <p>Osgood, W. R., 66</p> <p style="text-align: center;">P</p> <p>Prandtl, L., 160</p> <p>Prescott, J., 93, 284</p> <p>Putnam, W. J., 170</p> <p style="text-align: center;">Q</p> <p>Quinney, H., 83</p> <p style="text-align: center;">R</p> <p>Richart, F. E., 75</p> <p>Robertson, T., 83</p> <p>Ros, M., 83</p> <p style="text-align: center;">S</p> <p>Sadowsky, M. A., 188</p> <p>Saint Venant, B., 72, 148</p> <p>Scherin, E., 289</p> <p>Schwalbe, W. L., 170</p> <p>Seely, F. B., 94, 170, 180, 212</p> <p>Smith, J. O., 10, 182</p> <p>Soderberg, C. R., 10</p> <p>Southwell, R. V., 287</p> <p>Stern, F. B., Jr., 95</p> <p>Stodola, A., 138</p> <p>Sturm, R. G., 289</p> <p style="text-align: center;">T</p> <p>Tait, P. G., 177</p> <p>Talbot, Arthur Newell, 60</p> <p>Taylor, G. I., 83, 160, 179</p> <p>Thomas, H. R., 271</p> <p>Thomson, Sir William, 177</p> |
|---|---|

Timoshenko, S., 93, 95, 97, 113, 150,  
170, 212, 279, 282, 284, 287

Trayer, G. W., 163

Treffitz, E., 171

Tuckerman, L. B., 50

## V

von Kármán, F., 75, 177

von Mises, R., 76

## W

Wagner, H., 294

Wahl, A. M., 99

Weber, D., 178

Weller, R., 267

Westergaard, H. M., 36, 52, 77, 187,  
226

Wilson, W. M., 274, 287

Winkler, E., 215





# SUBJECT INDEX

## A

- Allowable working stress, 2
- Aluminum alloy columns, 90
- Aluminum alloys, 13, 14
- Analogy, electrical, 181
  - hydrodynamical, 177
  - membrane, 159
  - sand-heap, 186
  - soap-film, 159
- Area moments, 225
- Assumptions in elementary flexure,
  - formula for, 192
  - in elementary torsion, formula for, 144
- Axes, principal, 197
- Axis of polarization, 256

## B

- Bach formula for torsion, 150
- Bakelite, 257
- Bead, reduction of stress-concentration, factor by, 99
- Beam-columns, 277
- Beams, curved, 215
  - deflections of, 223
  - flexural stresses in, 195
  - plastic yielding in, 203
  - beyond proportional limit, 203
  - shearing stresses in, 237
  - of two materials, 212
- Bending without twisting, 242
- Bending axis, 244
- Bolts, stress concentration in, 101
- Brass, 14
- Buckling, general, 269
  - localized, 286

## C

- Cast iron columns, 90
- Castigliano's theorem, 227
- Channel, shearing stresses in, 237
- Circle of stress, 8
- Circular members, torsion in, 145
- Column formulas, 90
- Columns, buckling of, 274
  - torsional instability of, 292
- Concrete, 13, 14
- Conjugate beam, 226
- Copper, 13, 14
- Creep, 4
- Creep limit, 11, 14
- Crippling, 269
- Cross shear, 236
- Cylinders, plastic action in, 128
  - prestressed, 127
  - thick-walled, 114
  - thin-walled in compression, 286
  - thin-walled under external pressure, 288
  - thin-walled in torsion, 289
  - wire-wound, 126

## D

- Deflection, direction of, 202
  - magnitude of, 223
- Deformation, of beams, 193, 215
  - of cylinders, 115
  - excessive elastic, 3
  - of torsion members, 145, 154
- Design, factors involved in, 19
- Design problem, 1
- Dilatation, cubic, 63
- Disks, stresses in, 132
- Double integration, 224

Ductility, effect of, upon stress concentration, 105

Duralumin, 13, 14

## E

Elasticity, 11

modulus of, 12, 14

Electric strain gage, 50

Electrical analogy, 181

Endurance limit, 7, 9, 14

Endurance-limit-reduction factor, 103, 105, 211

Equivalent static load, 6

Euler formula, 276

Extensometers, 49

## F

Factor of safety, 11

Failure, criteria of, 7

resistance to, 7

significance and types, 3

theories of, 70

Filletts, reduction of stress concentration by, 105, 181, 207

Fir, 13, 14

Flexural deflections, 223

stress, 192

in curved beams, 215

derivations of elementary formula for, 192

general solution for, 195

beyond proportional limit, 203

Fluctuating stress in torsion, 182

Fracture, 3, 4

Fringe value, 262

## G

Geometry, of cylinders, 115

of I beams, 193, 215

of torsional members, 145, 154

Gerber theory, 10

Goodman theory, 10

Grooves, stress concentration due to, 100

## H

Hardness, 15

Holes, stress concentration factors for, 95, 180

Hollow sections, torsional stresses in, 167

Huggenberger, tensometer, 79

Hydrodynamical analogy, 177

## I

Impact, 6

Interaction curves, 84

Isochromatics, 263

Isoclinics, 36, 261-262

## J

Johnson's apparent elastic limit, 11

## K

Keyways, stress concentration in, 178

## L

Lamé theory, 114

Light, properties of, 255

representation of, 254

Limit loads, 11

Lines of shearing stress, 164

Load factor, 6

Loading, axial, requirements of, 87

types of, 5

Loads, concentrated, 269

dynamic, 6

repeated, 6

static, 5

Lüders' lines, 95

## M

Magnesium alloy columns, 90

Magnesium alloys, 13, 14

Margin of safety, 12

Maxwell-Mohr method, 229

Membrane analogy, 159  
 application of, 165  
 Mirror tensometer, 49  
 Models, 51  
     of brittle material, 94  
     photoelastic, 264  
 Modulus of elasticity, 60  
 Mohr circle, 33, 75  
 Mohr-Land circle, 34  
 Moment of inertia, equivalent polar,  
     in torsion, 169  
 Multicelled sections in torsion, 175

N

Neutral axis, in curved beams, 218  
     position of, 195  
 Nickel, 13, 14  
 Nicol prism, 256  
 Noncircular members, torsion in, 147  
 Notches, stress concentration due to,  
     210

O

Oak, 13, 14  
 Optical lever, 50

P

Panels, buckling of, 283  
     curved, 286  
 Pascal's law, 23  
 Percentage elongation, 8, 14  
 Photoelastic analysis, 254  
 Photogrid, 50  
 Pin, stress concentration due to, 99  
 Plastic yielding, in beams, 203  
     in torsion, 183  
 Poisson's ratio, 12, 14, 15, 60  
 Polarized light, 256  
 Polaroid, 256  
 Pressure vessels, stresses in thick-  
     walled, 114  
     stresses in thin-walled, 112  
 Principal axis of inertia, 197  
 Principal strains, 41  
     graphical evaluation of, 51

Principal stresses, 24  
     effect of, upon polarized light, 257  
     evaluation of, from photoelastic  
         analysis, 265  
         from strains, 64  
 Product of inertia, 197  
 Proportional limit, 11  
 Protrusion, stress concentration due  
     to, 100

R

Rectangular section, torsion in, 148,  
     165  
 Reentrant corners, stress concen-  
     tration due to, 178  
 Resilience, modulus of, 7, 11  
 Resolution of force systems, 143  
 Rolled sections, torsional stresses in,  
     169  
 Rosettes, types of, 64

S

Safety, factor of, 11  
 Saint Venant theory for torsion, 153  
 Sand-heap analogy, 186  
 Scratch extensometer, 50  
 Shafts, plastic yielding in, 183  
 Shear center, 244  
     of thin-webbed beam, 249  
 Shear flow, in flexure, 246  
     in torsion, 172  
 Shear lag, 250  
 Shearing forces in columns, 293  
 Shearing stresses, in beams, 236  
     due to cross shear, 236  
     maximum, 25, 32  
 Sheets, buckling of, 283  
 Shrink fit, 122  
 Shrink-fit assemblies, 131  
 Slip, 3, 4  
 Soap-film analogy, 159  
 Soderberg theory, 10  
 Sphere, stresses in thick-walled, 131  
 Stainless steel, 13, 14  
 Steel columns, 90  
 Stiffness, 12

Straight-line theory, 10

Strain gages, 49

Strains, axial, 39

equipment for measuring, 49

evaluation of, 40

identification of axes, 42

at a point, 38

principal, 41

evaluation of, 47

shearing, 39, 43

Strength, elastic, 7, 10

shearing, 14

tensile, 14

ultimate, 7, 8

Strength-reduction factor, 209

Stress, distribution of, in laminated

cylinders, 124

normal on any plane, 23

shearing on any plane, 23

significance of, 2

Stress analysis by photoelasticity,

264

Stress concentration, in axially

loaded members, 91

in beams, 206

in torsion, 177

Stress contours, 37

Stress function for torsion, 157

Stress trajectories, 36

Stress-concentration factor, 94

effect of size of hole, 99

reduction of, 105-106

significance of, 107

Stresses, on any plane, 30

contact, 272

designation of, 21

due to a point load, 270

flexural, 192

fluctuating, 9

graphical evaluation of, 27

identification of directions, 27

at a point, 20

in rotating discs, 132

shrinkage, 131

triaxial, 35

Stress-strain diagrams, 13

Stress-strain relationships, 59

Strips, buckling of, 280

## T

Theories of failure, 70

comparison of, 77, 83

Coulomb, 73

Guest, 73

Hencky-von Mises, 76, 82

internal friction, 74

maximum-normal-strain, 72, 79

maximum-normal-stress, 72, 78

maximum-shearing-stress, 73, 80

maximum-strain-energy, 75, 81

Mohr, 74

Rankine, 72

Saint Venant, 72

shear-distortion, 77

Thermal expansion, 12

Thick-walled cylinder, displacements

in, 115

temperature strains in, 130

variation of stresses in, 120

Thin-walled open sections, torsional

stresses in, 168

Thin-webbed beams, shearing

stresses in, 247

Timber columns, 90

Torque-twist diagram, 184

Torsion, 143

in columns, 292

of rectangular section, 148

Torsional contour lines, 14

Torsional members, stress concen-

tration in, 177

Torsional stresses, effect of end

restraint upon, 176

in elliptical shaft, 151

in slit tubes, 171

in thin-walled closed sections,

172

Torsion-bending constant, 294

Toughness, modulus of, 7, 8

Transformed cross section, 214,

220

Triaxial stress, 267

Tubes, effect of slit upon torsional

stresses in, 171

Twist, angle of, in thin-walled closed

section, 174

**U****Unsymmetrical bending, 195-200****V****Virtual work, 229****W****Weight, 14, 15****Winkler-Bach theory, 216****Wrought iron, 14****Wrought iron columns, 90****Y****Yield point, 11****Yield strength, 11****Z****Zinc alloys, 14**















